Evaluation of phytochemicals with immunomodulatory activity for graft-versus-host disease prophylaxis

By

Dievya Dilip Gohil

Enrolment No. LIFE09201604014

Tata Memorial Centre-Advanced Centre for Treatment Research and Education in Cancer, Navi Mumbai

A thesis submitted to the
Board of Studies in Life Sciences

In partial fulfillment of requirements
for the Degree of
DOCTOR OF PHILOSOPHY
of
HOMI BHABHA NATIONAL INSTITUTE

August, 2023

Homi Bhabha National Institute

Recommendations of the Viva Voce Committee

As members of the Viva Voce Committee, we certify that we have read the dissertation prepared by Ms. **Dievya Dilip Gohil** entitled "**Evaluation of phytochemicals with immunomodulatory activity for graft-versus-host disease prophylaxis**" and recommend that it may be accepted as fulfilling the thesis requirement for the award of Degree of Doctor of Philosophy.

Chairperson- Dr. Santosh Kumar Sandur — Date 4/12/2023

Guide/Convener- Dr. Vikram Gota — Date 04/12/2023

External Examiner- Dr. Suresh Rayala — Date 04-12-2023

Member- Dr. Navin Khattry — Date 5/12/23

Member- Dr. Deepak Sharma — Date 04/12/2023

Member- Dr. Syed Hasan — Date 04/12/2023

Final approval and acceptance of this thesis is contingent upon the candidate's submission of the final copies of the thesis to HBNI.

I hereby certify that I have read this thesis prepared under my direction and recommend that it may be accepted as fulfilling the thesis requirement.

Date: 04/12/23
Place: Navi Mumbai

Dr. Vikram Gota
Guide

STATEMENT BY AUTHOR

This dissertation has been submitted in partial fulfillment of requirements for an advanced degree at Homi Bhabha National Institute (HBNI) and is deposited in the Library to be made available to borrowers under rules of the HBNI.

Brief quotations from this dissertation are allowable without special permission, provided that accurate acknowledgement of source is made. Requests for permission for extended quotation from or reproduction of this manuscript in whole or in part may be granted by the Competent Authority of HBNI when in his or her judgment the proposed use of the material is in the interests of scholarship. In all other instances, however, permission must be obtained from the author.

Dievya Dilip Gohil

DECLARATION

I, hereby declare that the investigation presented in the thesis has been carried out by me. The work is original and has not been submitted earlier as a whole or in part for a degree / diploma at this or any other Institution / University.

Dievya Dilip Gohil

List of Publications arising from the thesis

Journal

1. "Acute and sub-acute oral toxicity assessment of 5-hydroxy-1,4-naphthoquinone in mice," Dievya Gohil, Girish Ch. Panigrahi, Saurabh Kumar Gupta, Khushboo A. Gandhi, Poonam Gera, Preeti Chavan, Deepak Sharma, Santosh Sandur & Vikram Gota, Drug and Chemical Toxicology, 2023, 46:4, 795-808.
2. "Prevention of acute graft-versus-host-disease by Withaferin a via suppression of AKT/mTOR pathway," Miten Mehta, Dievya Gohil, Navin Khattry, Rajiv Kumar, Santosh Sandur, Deepak Sharma, Rahul Checker, Beamon Agarwal, Dhruv Jha, Anuradha Majumdar, Vikram Gota, International Immunopharmacology, 2020, Volume 84, 106575.
3. "Safety, toxicity and pharmacokinetic assessment of oral Withaferin-A in mice," Gupta SK, Jadhav S, Gohil D, Panigrahi GC, Kaushal RK, Gandhi K, Patil A, Chavan P, Gota V, Toxicology Reports, 2022, 18;9:1204-1212.
4. "Withaferin-A alleviates acute graft versus host disease without compromising graft versus leukemia effect, Kumar Gupta S, Gohil D, Dutta D, Panigrahi GC, Gupta P, Dalvi K, Khanka T, Yadav S, Kumar Kaushal R, Chichra A, Punatar S, Gokarn A, Mirgh S, Jindal N, Nayak L, Tembhare PR, Khizer Hasan S, Kumar Sandur S, Hingorani L, Khattry N, Gota V, International Immunopharmacology. 2023121:110437.

Conferences

1. Poster presentation at the 48th Annual meeting of European Society for Blood and Marrow Transplantation (EBMT), March 2022.

2. Oral presentation at 5th IUPHAR World Conference on the Pharmacology of Natural Products, held from 4th - 7th Dec, 2019, at ICMR - National Institute of Nutrition, Hyderabad.

3. Poster presentation at Immunocon 2019, 46th Annual Conference of Indian Immunology Society, 14th -16th November, DAE Convention Centre, BARC, Mumbai.

4. Indo-US Cytometry Symposium & Workshop on Advanced Flow Cytometry and Applications, 15th-17th Feb, 2018, NIRRH, Mumbai.

Awards

WCP-Young scientist award winner at 5th IUPHAR World Conference on the Pharmacology of Natural Products, held from 4th - 7th Dec, 2019, at ICMR - National Institute of Nutrition, Hyderabad.

Dievya Dilip Gohil

ACKNOWLEDGEMENTS

I am fortunate to have performed my graduate work at a research institute as collaborative as the Advanced Centre for Treatment Research and Education in Cancer (ACTREC); therefore, there are many people to thank for their part in my success.

I would first like to thank my guide and advisor, **Dr. Vikram Gota**, Professor, Department of Clinical Pharmacology, ACTREC, for accepting me as his first graduate student and for providing me with the opportunity to undertake this work. I am grateful for his guidance and the opportunities he has afforded me. His pragmatic and problem-solving qualities were immensely helpful in moving my project forward. Under his mentorship I have learned that there is nothing called as failure, but only the opportunity to improve. His kindness and encouragement at the time when my project seemed to have hit a roadblock have been the best support and source of motivation to continue. Dr. Vikram is also exceptionally generous and would frequently take his students on outings to let us know that our work is appreciated, always encouraging us to have a work-life balance. I will remember my time in the lab and these outings very fondly. I could not imagine having a better advisor and mentor.

I express sincere thanks to my doctoral advisory committee chairman, **Dr. Santosh Kumar Sandur,** Professor and Head of Department, RBHSD, BARC, for his supervision, support, and valuable suggestions at various stages of the work that granted me the capability to proceed successfully. He has not only supervised my work but also provided an opportunity to me to get trained at his laboratory

I offer my humble thanks to my subject expert and doctoral advisory committee member, **Dr. Navin Khattry**, Deputy Director, CRC, and ACTREC. His knowledge of the subject has been instrumental in initiating and shaping the course of this study. I thank him for recommending my work for presentation at the 48th Asia-Pacific Blood and Marrow Transplantation Meeting and providing travel grant support.

I am thankful to my subject expert and doctoral advisory committee members, **Dr. Deepak Sharma,** Professor and Head of the Department, LLRRS, BARC. He has given me superb scientific guidance, demonstrated a sincere interest in my work, and has personally provided training for various techniques that I have learned during my PhD tenure. His invaluable insights, timely inputs, and constructive criticism were helpful in shaping my work in the best possible way.

I am thankful to my subject expert and doctoral advisory committee member **Dr. Syed Hasan**, Associate Professor ACTREC, for his constant encouragement, insightful comments, and the hard questions that facilitated me to widen my research from various perspectives. Moreover, his laboratory has always provided resourceful support during times of need.

This work would have been impossible without the support of **Dr. Jayant Goda,** Professor Radiation Oncology ACTREC. His knowledge of radiation biology has helped us design and execute our animal experiments with much precision and ease. His support and generosity in providing his laboratory for tissue culture and animal radiation has been indispensable for this work. I express my sincere gratitude for the support.

ACTREC has been a great workplace with a scenic landscape and updated academic and scientific infrastructure, which has been possible because of **Dr. Sudeep Gupta (Director, ACTREC) and Dr. S.V. Chiplunkar (Ex-Directors, ACTREC), Dr. Prasanna Venkatraman (Deputy-Director, CRI) and Dr. Navin Khattry (Deputy-Director, CRC)**. I thank you for your efforts, especially **Dr. V. Prasanna**, for being kind and approachable by students. I also thank ACTREC for fellowship and project funding. I am extremely indebted to all the faculty members of the CRI ACTREC for their constant and continuous support.

I would like to thank the faculty of the Clinical Pharmacology Department, **Dr. Manjunath Nookala, and Anand Patil**, for their support.

I wish to express my profound gratitude to **Dr. Khushboo Gandhi,** a post-doctoral fellow, Clinician Scientist Lab, and ex-member of our lab**,** for her constant guidance and assistance in the planning and execution of my thesis experiments. She has always been there to talk if something is bothering me about my experiments or life. She is and will always be someone I can count on. My heartfelt gratitude to you.

I would like to acknowledge **Dr. Miten Mehta**, who played a major role in initiating and conducting the groundwork for this study. I am thankful to **Murari Gurjar** and **Bharati Sriyan** for always being there and helping me navigate all administrative duties in the laboratory. Dr. Yalla Durgarao for his guidance and support during the writing of this thesis. My colleagues and graduate students of the lab **Saurabh Gupta, Girish Panigrahi, Megha Garg, Aishwarya, and Amisha**. It was fun to share research problems with each other, and I will remember the lab outings with you. I would like to thank all other members of the clinical pharmacology lab, who are too numerous to name. However, I would like to

mention **Shraddha, Madhvi, Aditi, Ashish, Sharath, Akshay, Anupama, Arshiya, Renita, and Soumika** for making the lab environment friendly and lively.

I would like to express my sincere gratitude to the faculty and lab members of **the Radiation Biology and Health Sciences Division (RBHSD), BARC**, especially **Dr. Rahul Checker and Dr. Raghavendra Patwardhan**, for providing training and guidance during my work at BARC. Their mentorship helped me improve my experimental planning and execution. Special mention to **Dr. Raghavendra Patwardhan** for providing me with the opportunity to work on the mitocurcumin project. I have learned a lot working closely with you. I would like to thank **Dr. Dharmendra, Dr. Jayakumar, Debojyoti, Binita Mam, and Deepak Katholeji and Naiduji** for their constant support. **Vaitashi Purohit** for being the best labmate and friend at BARC, **Archita Rai** for being a supportive friend and always showing her interest and enthusiasm towards my work.

This research work would not have been possible without the help and expertise of many administrative staff at the CRI ACTREC. I would like to thank **Mr. Uday Dandekar, Mr. Anish**, and all the other CIR staff members. I would like to make a special mention for **Ms. Shyamal, Mr. Ravi and Mr. Prashant**, central facility- **Flow Cytometry, CRI ACTREC** for their support and dedication towards the research work of every graduate student. Thank you for patiently acquiring not less than a thousand samples brought in by me during my tenure and providing your expertise where necessary. **Ms. Vaishali, Ms. Tanuja, Mr. Mithilesh (Imaging facility).** A special thanks to the members of Laboratory Animal Facility (LAF), ACTREC, **Dr. A. Ingle, and Dr. Rahul Thorat**, and other supportive staff, especially **Mr**. **Mahesh, Mr. Sada, Mr.Ravi, Mr. Makrand, Mr.Shashi, Mr. Sandeep,** for taking care of the animals and meeting the experimental requirements on time. **Mr. Munnoli, Ms. Swati and Ms. Mughda** (Library), **Ms. Aparna Bagwe, Ms. Ojaswini** and **Ms. Prema** (SCOPE) for their assistance. **Mrs. Sharvari** for her assistance during all academic submissions and procedures.

The inspiration for conducting research was instilled in me during my post-graduation at the Biochemistry Department of Maharaja Sayajirao University, Vadodara. I am also grateful to Professors **Dr. Shashikant Acharya and Dr. Savita Gupta** for sharing their knowledge and expertise during my master's program. The members of the MESCRL lab, especially **Dr. Abhay Srivastav**, inspired and encouraged me to pursue my doctoral studies and played an integral role in my research training. I am sincerely grateful to my Professors at Department of Biotechnology Jai Hind College-Dr. Archana Ashtekar, Dr.Kruti Pandya,

Nissey Ma'am, and Dr. Suchita, their training and lessons have built a strong foundation of the subject which has styed with me all throughout my journey.

The PhD journey would not have been memorable without my dearest friends, especially Abhilash and Nirja, who have been there for me at every difficult and happy time. Asim Purna, Mayuri, Sanket, Pooja, Souvik, Sayoni, Sumit and Shruti who have shared this journey with me. A special mention is given to my best friends, Dev and Jheel, who are like a family to me. My friends who have known me even before I began my PhD, Raj, Hetali, Ishita, Sarang, Mehek, Pooja, Ankit, Vidhi, Nirvi, Chitrini, Snehal, Ayush and Karmin. My MSc. roomies and girl gang Shruti, Kalyani Poonam and Kajal for being my strength. My childhood friends Divya and Preya and most importantly Trinkle who is my soul sister.

My life and all its achievements have been a gift from my parents Dilip and Bharati Gohil. Hard work always pays off and keep trying till you get there, are the best advices I have received from them. There are no words that can express my gratitude to my parents for all they have done for me. My siblings Vaishali, Bharat, Shivani and Sachin are my strength and are always proud of my work. A special shout out to my brothers for driving me to work during peak months of COVID-19. My deepest gratitude to my father and mother-in law Bharat and Rita Makwana for making this achievement possible. They have extended their unconditional support to me and are very proud of all my achievements. I am blessed to have to have received a new family that loves me just as a daughter. I thank my sister and brother-in-law Bhakti and Bhavik Shah for understanding my work commitments and being extremely encouraging and supportive. I am grateful to my nieces Manvi and Maitri, for all their love. I love you both a lot. I am thankful to my extended family members, Sheela and Jagdish Makwana, Nileshbhai, Bhavana Bhabhi, Manisha Bhabhi, Parikshitbhai and Pari for their encouraging words and support. Additionally, I owe my talents to two very important people Mr. Raju and Mrs. Rohini Rajput. They are my Gurus and I owe all my achievements to their teachings.

I am unable to find words to express my gratitude to Viraaj, my husband, who has received the worst of my behavior and has yet overlooked all my faults and chose to see the best in me. He has been my pillar of strength and has always believed in me. I am truly blessed to have you as my life partner. Thank you for your unconditional love.

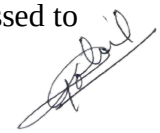

Dievya Gohil

DEDICATION

This Thesis work is dedicated to my husband, Viraaj, who has been a constant source of support and encouragement during the challenges of graduate school and life. I am truly grateful for having you in my life. To my parents, Dilip and Bharati, whose good examples have taught me to work hard for things that I aspire to achieve. To my gurus, Mrs. Rohini and Mr. Raju Rajput, for shaping me into the person I am today. This work is dedicated to my family and friends, who have supported me throughout this process. I would like to dedicate this work to all the mice that made my research possible. I am grateful for their sacrifice and contributions to my work.

Summary

Acute graft-versus-host disease (GVHD) is a major cause of non-relapse mortality after allogeneic hematopoietic stem cell transplantation (allo-HSCT). Current prophylactic regimens show limited clinical success and are associated with severe toxicities, development of steroid-refractory GVHD, increased incidence of infections, and relapse. Furthermore, it is now well-established that immunosuppression is not the best strategy for acute GVHD prophylaxis. Thus, the development of novel strategies/pharmacological agents that can modulate donor immune response in favor of antitumor immunity while suppressing allogeneic immune response is an unmet need in the field of allo-HSCT. The present study aimed to identify and develop phytopharmaceuticals with immunomodulatory activity for prophylaxis of acute GVHD.

In the present study, we screened a library of 140 phytochemicals and identified four compounds with potential immunomodulatory activity. These compounds were further subjected to secondary screening, resulting in the identification of 5-hydroxy-1,4-naphthoquinone (5NQ) or juglone as the lead molecule. The lead molecule was further evaluated for its immunomodulatory activities in vitro and in vivo, and its efficacy as a GVHD prophylactic agent was evaluated in a murine allo-HSCT model.

5-hydroxy-1,4-naphthoquinone (5NQ) or juglone, is a redox-active phytochemical found in walnuts, and has shown potent anti-inflammatory effects in various disease models, such as colitis and inflammatory bowel disease. However, its effects on T cell-mediated adaptive immune responses remain largely unknown. Considering the overlapping mediators of inflammation in GVHD and the aforementioned conditions, we investigated the use of juglone as a prophylactic agent.

The immunomodulatory activity and mechanism of action of 5NQ were studied in vitro using murine splenic leukocytes. The oral acute and subacute toxicity of 5NQ was assessed in mice

to establish a safe dosing regimen for preclinical efficacy studies. The GVHD prophylactic efficacy of orally administered 5NQ was evaluated using a murine model of allo-HSCT based on MHC-I mismatch. Finally, the efficacy of oral 5NQ in maintaining the GVL activity of the graft was evaluated in a murine model of allo-HSCT supplemented with leukemia cells.

Our data showed that 5NQ treatment inhibited mitogen-induced activation, proliferation, and cytokine secretion in murine leukocytes in vitro. In addition, 5NQ treatment inhibited the activation of antigen-presenting cells by downregulating MHC-II expression following mitogenic stimulation in vitro and in vivo. Furthermore, treatment with 5NQ led to an increase in the expression of aCD95 (Fas) and CD152 (CTLA4), which are indicative of the anergic and exhaustive state of activated $CD4^+$ T cells in both in vitro and in vivo studies. Furthermore, our in vivo studies showed that oral administration of 5NQ significantly reduced the mortality and morbidity associated with GVHD while preserving graft-versus-leukemia activity. The 5NQ mediated alleviation of GVHD and maintenance of GVL activity in transplanted mice can be attributed to the observed decrease in the number of $CD4^+$ and $CD8^+$ naïve T-cells and an increase in $CD4^+$ and $CD8^+$ central memory T cells. Moreover, the oral administration of 5NQ prevented GVHD development by inhibiting pro-inflammatory cytokines (IFNγ and TNF), promoting anti-inflammatory cytokines (IL-10 and IL-7A), and decreasing the counts of cytotoxic T cells ($CD8^+$ granzyme B^+). Additionally, oral administration of 5NQ did not affect hematopoietic stem cell recovery or donor cell engraftment in the transplanted mice. Our mechanistic studies revealed that 5NQ upregulated Nrf-2/HO1 antioxidant response signaling in leukocytes by modulating cellular redox status.

In conclusion, our study demonstrated that the prophylactic effect of 5NQ is due to its ability to modulate inflammatory innate and adaptive immune responses. Furthermore, our toxicity and efficacy studies provided a suitable dosage for oral administration of 5NQ, which can be used to devise a clinically relevant dose for human application.

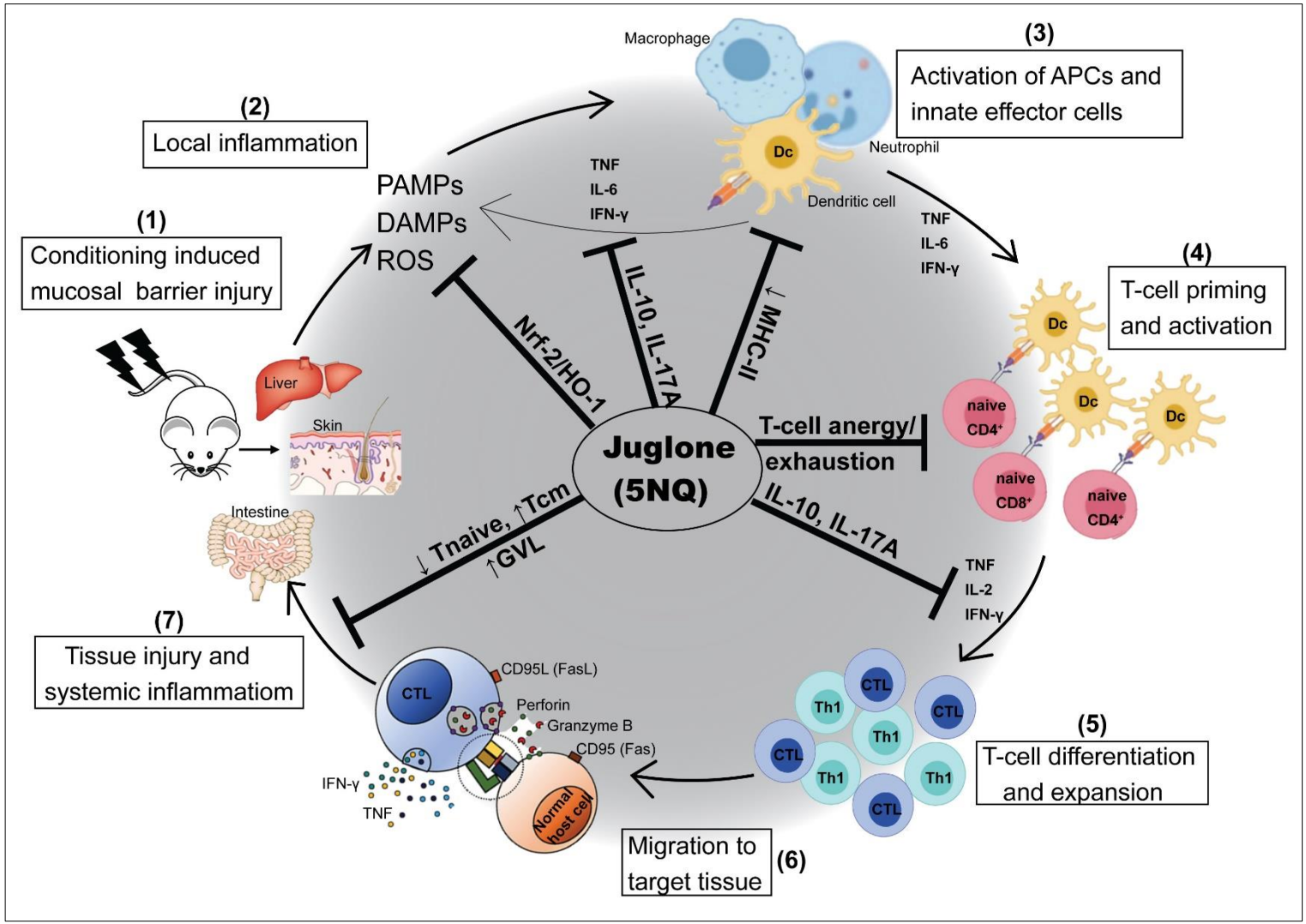

Graphical Abstract: The lead molecule juglone, exhibited immunomodulatory activity by upregulation of antioxidant response signalling, inhibiting proinflammatory cytokines, promoting anti-inflammatory cytokines, inhibiting the activation of dendritic cells and $CD4^+$ T cells, inhibiting lymphocyte proliferation, and inducing exhaustion of $CD4^+$ T cells and promoting central memory T cells, thereby preventing GVHD development while preserving GVL activity in murine model of allo-HSCT

TABLE OF CONTENTS

List of Figures

LIST OF TABLES

ABBREVIATIONS

5-hydroxy-1,4-naphthoquinone (5NQ) or Juglone

Allogeneic hematopoietic stem cell transplantation (allo-HSCT)

Antigen presenting cells (APCs)

Benchmark dose modelling (BMD)s

Benchmark response (BMR)

Bone marrow transplant (BM-HSCT)

Carboxyfluorescein succinimidyl ester (CFSE)

Carboxymethyl cellulose (CMC)

Central memory cells (Tcm)

Cherlythrine chloride (CC)

Concanavalin A (Con A)

Cyclosporine (CSA)

Cytometric Bead Array (CBA)

Cytotoxic T-lymphocyte–associated antigen 4 (CTLA-4, CD152),

Demethylzeylasteral (DMZ)

Effector memory cells (Tem)

Gastro-intestinal (GI)

Glutathione (GSH)

Graft versus leukemia (GVL)

Graft-versus-host disease (GVHD)

Granulocyte colony stimulating factor (G-CSF)

Hematopoietic stem cell transplantation (HSCT)

Hematopoietic stem cells (hscs)

Heme oxygenase1 (HO1)

Histocompatibility antigen (HA)

Homoharringtonine (HH),

Human leukocyte antigen (HLA)

Interferon (IFN),

Interleukin (IL)

Janus associated kinase (JAK)

Killer Ig-like receptors (KIR)

Lipopolysaccharide (LPS)

Lowest observed-adverse-effect level (LOAEL)

Major histocompatibility complex (MHC)

Matched related donor (MRD)

Matched unrelated donor (MURD)

Median fluorescence intensity (MFI)

Methotrexate (MTX),

Mycophenolate mofetil (MMF)

Myeloablative conditioning (MAC)

Myeloid-derived suppressor cells (mdscs)

N-acetyl-cysteine (NAC)

Naïve T cells (Tn)

Naphthoquinone (NQ)

No observed-adverse-effect level (NOAEL)

Nod-like receptors (NOD)

Peripheral blood stem cell transplant (PB-HSCT)

Pin-1 (prolyl isomerase)

Point of departure dose (POD)

Programmed death 1 (PD)

Propidium iodide (PI)

Quality of life (QOL)

Reactive oxygen species (ROS)

Reduced intensity conditioning (RIC)

Reference dose (rfd)

Retinoic acid-inducible gene-I (RIG-I)

T cell receptor (TCR)

Tacrolimus (TAC)

Toll-like receptors (TLR)

Triptolide (TP)

Tumor growth factor (TGF)

Tumor necrosis factor (TNF)

Umbilical cord blood transplant (UCB-HSCT)

Homi Bhabha National Institute

SYNOPSIS OF Ph. D. THESIS

1. **Name of the Student: Mrs. Dievya Dilip Gohil**
2. **Name of the Constituent Institution: Advanced Centre for Treatment, Research and Education in Cancer, Tata Memorial Centre**
3. **Enrolment No.: LIFE09201604014**
4. **Title of the Thesis: Evaluation of phytochemicals with immunomodulatory activity for graft versus host disease (GVHD) prophylaxis**
5. **OGCE: Held on 13th September, 2017**
6. **Review Period and Date of Meeting: 8th August, 2016- 21st December 2020**

SYNOPSIS

Introduction

Allogeneic hematopoietic stem cell transplantation (allo-HSCT) is the major curative option for various hematological malignancies[1,2]. It involves transplanting hematopoietic stem cells from either an HLA-matched family member or HLA matched unrelated donor. The patient undergoes myeloablative treatment before transplantation to facilitate engraftment and is maintained on immunosuppressants to avoid graft rejection post-transplantation[3]. One of the major benefits of allo-HSCT is the decrease in relapse rates of leukemia in patients due to the graft versus leukemia effect (GVL)[4,5]. However, 40-60% of the patients undergoing allo-HSCT develop a life-threatening complication called acute graft versus host disease (GVHD); which results in host organ damage due to immune reaction elicited by graft against the host tissues. GVHD accounts for 15-30% of deaths following allo-HSCT[6].

Immune cells such as T cells, B cells, Natural killer cells, and their secretory molecules (chemokine and cytokines) play an important role in maintaining the GVL effect through various mechanisms. These include recognition of leukemia cells; complement-mediated lysis and Antibody-Dependent Cellular

Cytotoxicity (ADCC) of leukemia cells[7]. On the other hand, similar set of immune cells and secretory factors are responsible for the development of GVHD. Conditioning with chemo or radiotherapy causes host tissue damage resulting in inflammation and the release of pro-inflammatory cytokines. This increases the capacity of antigen-presenting cells (APCs) to present host antigens to donor T-cells leading to their activation, proliferation, and differentiation. The activated T-cells cause increased release of inflammatory cytokines and promote migration of T-cells to secondary lymphoid organs and target tissues like skin, liver, gut, etc. These activated T-cells cause inflammation-mediated cell death of host tissue and induce apoptosis of host cells via granzyme B and perforin-mediated pathways. Thus, GVHD leads to host tissue damage to an extent of organ failure resulting in death[8].

Large studies have established the role of T-cells in the development of GVHD. Therefore, current prophylactic regimens target the T-cells of the graft via calcineurin inhibitors (cyclosporine A), in combination with anti-thymocyte globulin or anti-metabolites[8,9]. Corticosteroids form the first line of treatment for GVHD, nonetheless, 30-50% of patients acquire steroid resistance, for which no second-line treatment is available and these patients have a poor prognosis with a high mortality rate of 60-80%. Moreover, secondary infections due to prolonged immunosuppression and cumulative toxicities of the treatments add to the burden of non-relapse mortality post-allogeneic transplantation[10]. Until 2020, there was no FDA-approved drug for the management of GVHD, giving it an orphan disease status. However, the recent approval of ruxolitinib for the treatment of steroid-refractory GVHD makes it the only FDA-approved drug for the management of GVHD[11].

Rationale

Although the depletion or targeting of T-cells results in the elimination of GVHD; there is an increased risk of leukemia relapse due to the loss of the GVL effect. Despite the current medical advances in the field of transplantation, prevention of GVHD while maintaining the GVL effects of the graft remains a major unsolved challenge in clinics. Therefore, the development of novel pharmacological agents that prevent GVHD while preserving the GVL effect of the graft, is necessary for effective transplant outcomes.

Aim

Screening and development of novel agents for GVHD prophylaxis using a phytochemical drug library.

Objectives and Results

1. Screening of phytochemical drug library for immunomodulatory compounds.

a. Primary screening: One hundred and thirty-six compounds from the phytochemical library (obtained from Target Mol, USA) were evaluated for their inhibitory effect on IL-2 secretion by ELISA and anti-proliferative effect on murine splenic lymphocytes using CFSE dye dilution assay. All the compounds were screened for their immunomodulatory action at the concentration of 10μM for 2hrs following which they were stimulated with mitogen Concanavalin A (ConA, 2.5μg/ml), and incubated for 72 hrs. Post incubation the cells were acquired on a flow cytometer to determine the percent daughter cells. Nine compounds inhibited both cell proliferation and IL-2 secretion and were considered hit compounds. Of these nine compounds, two known immunosuppressive compounds 10-hydroxycamptothecin (1D2) and cyclosporin A (2A3), and five other compounds, namely- Triptolide (2C5), Demethylzeylasteral (2E6), Homoharringtonine (2E10), Chelerythrine chloride (2F2) and 5-hydroxy-1,4-naphthoquinone (2F5) were identified and selected for secondary screening experiments. Cyclosporin A (CA) was used as a positive control in the secondary screening experiment.

b. Secondary screening: Secondary screening aimed to identify compounds that inhibited proliferation at the least toxic dose. The compounds were therefore evaluated for time and dose-dependent toxicity and inhibition of proliferation, by propidium iodide assay and CFSE proliferation assay respectively. Following drug concentrations and time points were used for secondary screening-

c. Concentrations: 0.1, 0.25, 0.5, 1, 2.5, 5, and 10μM.

Time points for proliferation assay: 2 h and 4 h

Time points for viability assay: 4 h and 24 h

d. Immunomodulatory effect of 5NQ on lymphocytes in vitro: Based on the secondary screening, 5-hydroxy-1,4-naphthoquinone (5NQ) or Juglone was selected as the lead compound as it exhibited immunosuppression without toxicity to lymphocytes. We evaluated the immunomodulatory effect of 5NQ on murine splenic lymphocytes in vitro. First, we studied the time and dose-dependent effect of 5NQ treatment on the proliferation and toxicity of lymphocytes. Transient treatment with 5NQ for 4 h

inhibited mitogen (ConA and LPS - lipopolysaccharide) induced proliferation of lymphocytes in a dose-dependent manner. Transient treatment with 1μM 5NQ for 4 h caused inhibition of proliferation without affecting viability as evinced by the viability assay and this dose was used for subsequent experiments. Second, transient treatment of lymphocytes with 5NQ suppressed ConA-induced secretion of cytokines IL-2, IL-4, IL-6, IFN-γ, TNF, IL-17A, and IL-10 and restored the Th1/Th2 cytokine imbalance induced by ConA stimulation. We further studied the effect on the activation of antigen-presenting cells (APC) and $CD4^+$ T-cells and found that transient treatment of lymphocytes with 5NQ suppressed the expression of MHC-II on $CD11b^-$ dendritic cells, $CD11b^+$ $Ly6c^{lo}$ macrophages, and $CD11b^+$ $Ly6c^{hi}$ monocytes and suppressed the expression of CD69 and CD25 in $CD4^+$ T cells. Additionally, we observed an increase in the expression of CD95 (Fas) in $CD4^+$ T cells following the 5NQ treatment. Further, we found that transient treatment with 5NQ did not increase the number of $CD4^+$ Tregs in vitro. Lastly, we evaluated the effect of transient treatment with 5NQ on the anti-leukemic activity of lymphocytes using an in vitro model of mixed lymphocyte reaction, but with murine leukemia cell lines as stimulator cells. We observed that 5NQ-treated lymphocytes exhibited comparable anti-leukemic activity as their vehicle-treated counterparts.

2. Evaluation of anti-GVHD potential of the lead compound using a murine model of GVHD.

a. <u>Prophylactic efficacy of ex vivo treated lymphocytes using murine model of allo-HSCT:</u> First, we adopted the ex-vivo lymphocyte treatment approach to evaluate the anti-GVHD potential of 5NQ using a murine model of allogenic transplantation based on complete MHC-I mismatch[12]. Accordingly, female BALB/c mice ($H2K^d$- recipient) were given 6.5 Gy total body irradiation (TBI) and rested for 24 h followed by intravenous infusion of 5 x 10^6 bone marrow cells and transiently treated 15 x 10^6 splenocytes with vehicle or 5NQ (1μM). The recipients transplanted with ex vivo 5NQ treated lymphocytes showed complete protection from GVHD-associated symptoms resulting in significant improvement in survival of these mice compared to recipients transplanted with ex vivo vehicle-treated lymphocytes. However, upon evaluation of peripheral blood to ascertain engraftment, we observed that donor cells were absent in recipient mice that received 5NQ treated lymphocytes, whereas, recipients that received vehicle-treated graft showed complete donor chimerism. This

indicated that ex vivo treatment of donor graft with 5NQ affects the engraftment of the donor cells and hence is not a feasible approach for use in clinics. We, therefore, decided to administer 5NQ orally to evaluate its GVHD prophylactic efficacy.

b. Acute and sub-acute oral toxicity of 5NQ: Literature study revealed limited information regarding oral LD_{50} of 5NQ and hence to establish a safe dose for oral administration of 5NQ, we carried out acute and sub-acute oral toxicity study of 5NQ in BALB/c mice according to the OECD guideline 423 and 407 respectively[13,14]. We further carried out dose-response relationship modeling, known as benchmark dose modeling (BMD)[15–17] for survival, hematological and biochemical parameters to determine a point of departure dose for single and repeated administration of 5NQ and identify serum biomarkers sensitive to 5NQ treatment. Our acute toxicity data showed no mortality in mice administered with a single oral dose of 50 mg/kg 5NQ. However, toxicity-induced changes were observed at microscopic levels as evinced by histopathological findings. BMD modeling of the survival response in an acute toxicity study established a point of departure dose of 118 mg/kg for single oral administration of 5NQ. This dose can be deemed equivalent to the LD_{50} dose for single oral administration of 5NQ[18].

   In our sub-acute toxicity study, BALB/c mice (N =10) were daily administered with vehicle (5% DMSO in 0.5% carboxymethyl cellulose), or 5, 15, or 50 mg/kg 5NQ in vehicle, for 28 days. Animals administered vehicle and 5 mg/kg 5NQ did not show toxicity-related mortality. Moreover, these animals scored lower on the clinical scoring chart and did not show any toxicity-related weight loss. BMD analysis of the dose-survival response in the sub-acute toxicity studied established a point of departure dose of 1.74 mg/kg. Evaluation of hematological parameters showed no abnormalities, whereas analysis of biochemical parameters showed altered liver and renal function markers. Notably, we observed a dose-dependent change in aspartate aminotransferase (AST), total bilirubin (TB), and blood urea nitrogen (BUN), however, BMD analysis of these parameters showed that AST was the most sensitive marker to 5NQ-related toxicity[18]. The point of departure dose established in the toxicity study was used as a reference dose to evaluate the efficacy of 5NQ in pre-clinical settings.

c. Prophylactic efficacy of oral administration of 5NQ in murine model of allo-HSCT: To identify the efficacious dosage of 5NQ, a dose standardization study was carried out. We established that alternate day administration of 2.5 or 5 mg/kg 5NQ for 15 days after transplantation provided a survival benefit to the transplanted mice. We further validated our findings in a larger cohort of animals (N=12) and found that oral administration of 5mg/kg 5NQ significantly improved the survival of transplanted animals and protected from GVHD-associated clinical symptoms and weight loss. Moreover, histopathological evaluation of the intestine, liver, and skin showed that animals treated with 5NQ showed lower pathological scores for GVHD-associated tissue damage. Lastly, oral administration of 5NQ did not hamper the engraftment of donor cells as evinced by the evaluation of peripheral blood for donor chimerism.

d. Effect of oral administration of 5NQ on innate and adaptive immune responses in vivo: Evaluation of serum cytokines revealed that oral administration of 5NQ caused a decrease in levels of pro-inflammatory cytokines IFN-γ and TNF, and an increase in levels of anti-inflammatory cytokines IL-10 and IL-17A. Evaluation of splenic dendritic cells showed that 5NQ treatment caused a decrease in the activation of splenic dendritic cells as evinced by a decrease in MHC-II expression on these cells. Additionally, we observed a significant decrease in $CD4^+$ T cell counts and a decrease in the CD4/CD8 ratio in splenic lymphocytes of recipient mice compared with that in vehicle-treated mice. We further observed that $CD4^+CD25^+$ activated T cells showed an increase in the surface expression of CD152 (CTLA4), indicating an increase in the exhausted/anergic T-cell subset in the lymphocytes of recipient mice treated with 5 mg/kg 5NQ orally compared to vehicle-treated mice. Additionally, we observed a decrease in $CD62^{hi}CD44^{lo}$ naïve $CD4^+$ and $CD8^+$ T-cells along with increase in $CD62^{hi}CD44^{hi}$ central memory $CD4^+$ and $CD8^+$ T-cells. Additionally, there was no difference in expression of CD152 on $CD8^+$ cells from vehicle and 5NQ-treated mice. Lastly, we did not observe significant differences in $CD4^+CD25^{hi}FoxP3^+$ T-regulatory (Treg) cells in the lymphocytes of 5NQ-treated mice as compared to those of vehicle-treated mice.

3. Understanding the molecular mechanism of immunomodulatory action of the lead compound *in vitro*

a. Effect of 5NQ on cellular redox status: The naphthoquinone class of compounds is well known for their redox cycling activity. Therefore, we evaluated the effect of 5NQ treatment on cellular redox. Treatment with 5NQ caused time- and dose-dependent increases in mitochondrial ROS in 5NQ-treated lymphocytes, as measured by MitoSOX Red dye. Surprisingly, 5NQ-treated lymphocytes showed time- and dose-dependent decrease in cellular ROS, as measured with H2DCFDA. In addition, we observed a decrease in ThiolTracker violet fluorescence in 5NQ - treated lymphocytes which indicated low levels of cellular GSH in treated cells compared to untreated cells.

b. Effect of 5NQ on cellular redox in presence of thiols: To understand the role of thiols and altered cellular redox status in the observed immunosuppressive activity of 5NQ, we evaluated the effect of 5NQ treatment on cellular redox in the presence of the thiol antioxidant NAC. Pretreatment with NAC inhibited 5NQ-induced alterations in mitochondrial and cellular ROS levels. Moreover, pretreatment with GSH and NAC abrogated the antiproliferative effect of 5NQ on the lymphocytes. Furthermore, incubation of 5NQ with GSH or NAC changed the absorption spectrum of 5NQ indicating a probable physical interaction of 5NQ with the thiol antioxidants.

c. Effect of 5NQ on inflammatory signaling and anti-oxidant response signaling: We evaluated the activation of NF-κB in cellular and nuclear lysates and the phosphorylation status of Akt and S6-kinases, in 5NQ treated, resting, and mitogen-stimulated lymphocytes. Treatment with 5NQ inhibits ConA-induced activation of NF-κB and its nuclear translocation in lymphocytes. It also inhibited the ConA-induced phosphorylation of Akt. However, pretreatment of lymphocytes with NAC reversed the inhibitory effect of 5NQ on NF-κB activation and Akt phosphorylation, thus abrogating 5NQ-mediated suppression of mitogen-induced signaling in lymphocytes. As 5NQ treatment resulted in alterations in cellular redox, we found that lymphocytes treated with 5NQ showed an increase in Nrf-2 expression. Western blot analysis further confirmed a subsequent increase in the expression of downstream targets of Nrf-2, namely heme oxygenase-1 (HO-1) and NAD(P)H quinone dehydrogenase-1 (NQO-1), indicating upregulation of antioxidant response signaling in these cells. However, the upregulation of antioxidant response signaling was

abrogated in presence of NAC. To further study the role of Nrf-2 in mediating the immunosuppressive action of 5NQ, we studied the proliferation of lymphocytes in the presence of the Nrf-2 inhibitor ML385 and found that Nrf-2 inhibition did not reverse the antiproliferative effect of 5NQ. Similar results were obtained when we studied the proliferation of lymphocytes from Nrf-2 KO mice after treatment with 5NQ. Next, we evaluated the effect of 5NQ treatment on mitogen-induced cytokine secretion from Nrf-2 KO lymphocytes. We observed that 5NQ-treated Nrf-2 KO lymphocytes could not restore the mitogen-induced Th1/Th2 cytokine imbalance, that was observed in 5NQ-treated wild-type lymphocytes.

4. **Development of a syngeneic murine model of leukemia and assessment of the efficacy of the lead compound in maintaining the GVL effect of the graft.**

At last, we evaluated the effect of the oral administration of 5NQ on the GVL effect of the donor graft using our allo-HSCT model supplemented with A20 murine leukemia cells[19,20]. All recipients of A20 tumor cells succumbed to the tumor within 3 weeks, with a median survival of 19 days with no significant weight loss. However, all mice developed hind limb paralysis and were euthanized when moribund. The livers of A20 mice showed, on average, 70% tumor infiltration of the hepatic tissue with severe necrosis. Animals transplanted with A20 tumor cells along with donor cells developed severe GVHD within two weeks and were euthanized for necropsy when moribund to check for the presence of tumors. These mice showed clinical symptoms of GVHD development with a significant reduction in body weight and a median survival of 10.5 days, along with the absence of macroscopic tumors nodules in liver at necropsy, however, microscopic analysis showed a low tumor burden (1-2%) in these animals. In contrast, animals treated with 5 mg/kg 5NQ maintained their original body weights, indicative of protection from GVHD, and only 25% of the mice succumbed to the tumor. These mice showed a significant improvement in survival compared with vehicle-treated animals, with a median survival of 23 days. At necropsy, animals treated with 5NQ showed reduced tumor nodules in the liver (1-30%) and spleen, which was further confirmed via histopathological analysis of the liver tissue, which indicates that 5NQ preserved the donor GVL activity. No tumor nodules were observed in the livers of the GVHD mice.

Conclusion: Prophylaxis of GVHD, whilst maintaining GVL activity of donor graft remains a major challenge in successful transplant outcomes. The focus of the study was to screen and identify phytochemicals with immunomodulatory action and develop the lead molecule for GVHD prophylaxis. Accordingly, this study identified two compounds with potent immunomodulatory effects namely Demethylzeylasteral and Juglone or 5-hydroxy-1,4-naphthoquinone. Further, 5NQ was selected as the lead compound as it inhibited proliferation of lymphocytes, whilst maintaining their viability. Our in vitro studies demonstrated the immunomodulatory action of 5NQ. First, transient treatment with 5NQ inhibited mitogen-induced, activation of APCs and $CD4^+$ T-cells and caused inhibition of cytokine secretion in vitro. Second, treatment with 5NQ induced an anergic/exhaustive state in $CD4^+$ T-cells. At last, we show that treatment with 5NQ did not suppress anti-tumor activity of lymphocytes in vitro, thus encouraging us to evaluate its prophylactic efficacy in vivo.

We carried out a detailed oral toxicity study to determine no observed adverse effect level dose (NOAEL) for 5NQ administration. Our acute and sub-acute oral toxicity study of 5NQ established point of departure doses (POD) for single and repeated oral administration of 5NQ. POD for single oral administration was estimated to be 118 mg/kg and POD for repeat oral administration was estimated to be 1.74 mg/kg via BMD analysis and NOAEL was found to be < 5 mg/kg. The established POD values can be used as a reference for pre-clinical efficacy assessments and for deriving the human equivalent reference dose of 5NQ to ascertain its safety for clinical use.

Next, our study demonstrated the prophylactic efficacy of oral 5NQ in a murine model of allo-HSCT based on a complete MHC-I mismatch. Our results showed that 5NQ suppressed GVHD via immunomodulation of innate and adaptive responses. Firstly, oral administration of 5NQ decreased pro-inflammatory cytokines and increased anti-inflammatory cytokines in the serum of animals treated with 5NQ. Secondly, 5NQ treatment inhibited the activation of splenic dendritic cells and $CD4^+$ T-cells and induced $CD4^+$ T-cell anergy and exhaustion. Further, 5NQ-treated animals showed a reduction in the numbers of naïve $CD4^+$ and $CD8^+$ T cells, these subsets have been implicated in GVHD pathogenesis. Additionally, we observed an increase in the central memory subsets of $CD4^+$ and $CD8^+$ T-cells, these subsets play a major role in the GVL activity of the graft. Lastly, treatment

with 5NQ led to protection from GVHD and reduced the tumor burden in our in vivo model for evaluating the GVL activity of the graft.

Lastly, our in vitro mechanistic studies reveal that 5NQ modulated cellular ROS balance and upregulated antioxidant response signaling (Nrf-2/HO-1/NQO1) in lymphocytes, leading to inhibition of NFκB activation. Inhibition of inflammatory signaling by 5NQ can be attributed to its ability to modulate cellular redox and depletion of cellular thiols.

In conclusion, our study reveals that 5NQ administration inhibits antigen presentation, cytokine storm, and activation of CD4 T cells thus demonstrating an immunomodulatory effect of 5NQ at every phase of GVHD pathogenesis. Our study is the first to establish an oral metronomic dose of 5NQ that mitigated GVHD while preserving the GVL effect of the donor graft in mice and this dose can be further used as a reference to devise a suitable dose for human application.

References

1. Thomas, E. D. Stem cell transplantation: Past, present and future. *Stem Cells* (1994) doi:10.1002/stem.5530120602.
2. Henig, I. & Zuckerman, T. Hematopoietic Stem Cell Transplantation—50 Years of Evolution and Future Perspectives. *Rambam Maimonides Med. J.* (2014) doi:10.5041/rmmj.10162.
3. Stem, H. & Sources, C. Hematopoietic Cell Transplantation. 1–16 (2015).
4. Gale, R. P. *et al.* Graft-versus-leukemia reactions after bone marrow transplantation. (1990) doi:10.1182/blood.V75.3.555.bloodjournal753555.
5. Imamura, M., Hashino, S. & Tanaka, J. Graft-versus-leukemia effect and its clinical implications. *Leukemia and Lymphoma* (1996) doi:10.3109/10428199609054857.
6. Passweg, J. R. *et al.* The EBMT activity survey on hematopoietic-cell transplantation and cellular therapy 2018: CAR-T's come into focus. *Bone Marrow Transplant.* **55**, 1604–1613 (2020).
7. Vandenhove, B. *et al.* How to Make an Immune System and a Foreign Host Quickly Cohabit in Peace? The Challenge of Acute Graft-Versus-Host Disease Prevention After Allogeneic Hematopoietic Cell Transplantation. *Front. Immunol.* **11**, 1–18 (2020).
8. Acute Graft-versus-Host Disease Biology, Prevention and Therapy _ Enhanced Reader.pdf.
9. Wölfl, M. *et al.* Current Prophylaxis and Treatment Approaches for Acute Graft-Versus-Host Disease in Haematopoietic Stem Cell Transplantation for Children With Acute Lymphoblastic Leukaemia. *Front. Pediatr.* **9**, (2022).
10. Shouval, R. *et al.* Outcomes of allogeneic haematopoietic stem cell transplantation from HLA-matched and alternative donors: a European Society for Blood and Marrow Transplantation registry retrospective

analysis. *Lancet Haematol.* **6**, e573–e584 (2019).

11. Ruxolitinib in refractory acute and chronic graft-versus-host disease_ a multicenter survey study _ Enhanced Reader.pdf.
12. Mehta, M. *et al.* Prevention of acute graft-versus-host-disease by Withaferin a via suppression of AKT/mTOR pathway. *Int. Immunopharmacol.* **84**, 106575 (2020).
13. *Test No. 423: Acute Oral toxicity - Acute Toxic Class Method*. (OECD, 2002). doi:10.1787/9789264071001-en.
14. Test No. 407: Repeated Dose 28-day Oral Toxicity Study in Rodents. (2008) doi:10.1787/9789264070684-EN.
15. Baralić, K. *et al.* Relevance and evaluation of the benchmark dose in toxicology. *Arh. Farm. (Belgr).* **70**, 130–141 (2020).
16. Slob RIVM, W. Joint project on Benchmark Dose modelling with RIVM. *EFSA Support. Publ.* **15**, 1497E (2018).
17. Hardy, A. *et al.* Update: use of the benchmark dose approach in risk assessment. *EFSA J.* **15**, e04658 (2017).
18. Gohil, D. *et al.* Acute and sub-acute oral toxicity assessment of 5-hydroxy-1,4-naphthoquinone in mice. *https://doi.org/10.1080/01480545.2022.2104306* (2022) doi:10.1080/01480545.2022.2104306.
19. Snyder, K. J. *et al.* Inhibition of Bromodomain and Extra Terminal (BET) Domain Activity Modulates the IL-23R/IL-17 Axis and Suppresses Acute Graft-Versus-Host Disease. *Front. Oncol.* **11**, (2021).
20. Zhang, J. *et al.* The mechanistic study behind suppression of GVHD while retaining GVL activities by myeloid-derived suppressor cells. *Leuk. 2019 338* **33**, 2078–2089 (2019).

Publications in Refereed Journal:

a. Published
Dievya Gohil, Girish Ch. Panigrahi, Saurabh Kumar Gupta, Khushboo A. Gandhi, Poonam Gera, Preeti Chavan, Deepak Sharma, Santosh Sandur & Vikram Gota (2022): Acute and sub-acute oral toxicity assessment of 5-hydroxy-1,4-naphthoquinone in mice, Drug and Chemical Toxicology, DOI:10.1080/01480545.2022.2104306

b. Accepted: NA

c. Communicated: NA

Other Publications:

1. Mehta M, **Gohil D**, Khattry N, Kumar R, Sandur S, Sharma D, Checker R, Agarwal B, Jha D, Majumdar A, Gota V. Prevention of acute graft-versus-host-disease by Withaferin a via suppression of AKT/mTOR pathway. Int Immunopharmacol. 2020 Jul;84:106575. doi: 10.1016/j.intimp.2020.106575. Epub 2020 May 13. PMID: 32416453.

2. Gupta SK, Jadhav S, **Gohil D**, Panigrahi CH, Kaushal R, Gandhi K, Patil A, Chavan P, Gota V. Safety, toxicity and pharmacokinetic assessment of oral Withaferin-A in mice, Toxicology Reports, 2022,9:1204-1212. https://doi.org/10.1016/j.toxrep.2022.05.012.

3. Gupta SK, **Gohil D**, Panigrahi GC, Vaykar S, Rane P, Chavan P, Gota V. Comparison of different autoanalyzers for the determination of lymphocyte and neutrophil counts in mouse blood. Drug Metab Pers Ther. 2021 Dec 1;37(2):219-222. doi: 10.1515/dmpt-2021-0156. PMID: 34854273.

a. Book/Book Chapter: NA

b. Conference/Symposium

1. I presented a poster at the 46th Annual Conference of the Indian Immunological Society, Immunocon, at BARC, Mumbai, India in 2019.
2. I won the "Young Scientist award" for best oral presentation at the 5th IUPHAR World Conference on Pharmacology of natural products at ICMR-National Institute of Nutrition, Hyderabad, India in 2019.
3. I participated in the pre-conference workshop on "Natural product screening and libraries" at the 5th IUPHAR World Conference on Pharmacology of natural products at ICMR-National Institute of Nutrition, Hyderabad, India in 2019.
4. I presented a poster at the 48th Annual meeting of European Society for Blood and Marrow Transplantation (EBMT), held as a virtual event in March 2022.

Signature of Student:
Date:

Doctoral Committee: (KEEP ACTUAL ROWS ONLY)

S. No.	Name	Designation	Signature	Date
1.	Dr. Santosh Kumar Sandur	Chairman	16698:SANTOSH KUMAR SANDUR	21/02/23
2.	Dr. Vikram Gota	Guide/ Convener		
3.		Co-guide (if any)		
4.	Dr. Deepak Sharma	Member		20/02/2023
5.	Dr. Navin Khattry	Member		24/2/23
6.	Dr. Syed Hasan	Member		24/2/23

Forwarded Through:

Dr. Sorab. N. Dalal,
Chairperson, Academic &
Training Programme, ACTREC

(Dr. Sorab N. Dalal)
Chairperson, Academic & Training Programme
Tata Memorial Center, ACTREC,
Kharghar, Navi Mumbai - 410210

17/3/23

Prof. S. D. Banavali,
Dean (Academics)
T.M.C.

PROF. S. D. BANAVALI, MD
DEAN (ACADEMICS)
TATA MEMORIAL CENTRE
MUMBAI – 400 012.

Thesis Overview

THESIS OVERVIEW

This thesis describes the identification of lead compound Juglone through phytochemical drug library screening, followed by an understanding of the molecular mechanisms involved in the immunomodulatory actions of Juglone and its *in vivo* evaluation of immunomodulatory effects and GVHD prophylactic efficacy. The write-up outline includes the sections listed in Table 1.

Table 1: Write-up outline

Sr. no.	**Section**
1	Thesis overview and background
2	Review of Literature
3	Aim and Objectives
4	Materials and Methods
5	Screening of phytochemical drug library for immunomodulatory compounds.
6	Unravelling the molecular mechanisms of immunomodulatory action of Juglone *in vitro.*
7	Evaluation of anti-GVHD potential of Juglone in murine model of GVHD.
8	Assessment of the efficacy of Juglone in maintaining graft versus leukemia (GVL) effect of the graft in syngeneic mice model.
9	Summary and salient findings
10	Conclusion
11	Strengths and Limitations
12	Future Prospects
13	Bibliography

BACKGROUND

Allogeneic hematopoietic stem cell transplantation (allo-HSCT) is the curative treatment available for patients with hematological malignancies. The process involves transplantation of hematopoietic stem cells sourced from a healthy donor to an immunocompromised patient. The success of allo-HSCT is driven by various cellular constituents of donor grafts [1,2]. The immune-competent cell types of the donor graft such as T cells, B cells, and NK cells play an active role in eradicating residual leukemic cells resulting in graft-versus-leukemia activity (GVL). Whereas the alloreactive T-cells can cause graft-versus-host disease (GVHD), a life-threatening complication that arises because donor T-cells recognize host antigens as foreign and mount an immune response against them, thereby destroying host cells and tissues[3–5].

According to the Center for International Blood and Marrow Transplant Research (CIBMTR), about 30,000 HSCTs are performed worldwide every year. However, 40-60% of patients develop acute GVHD within 100 days of transplantation [6–8]. Current prophylactic and treatment regimens include calcineurin inhibitors, posttransplant cyclophosphamide, and corticosteroids. However, about 30% of these patients develop steroid-refractory GVHD for which there is no second-line treatment, and these patients have a poor prognosis with a mortality rate of 60 -80%. However, on September 22, 2021, ruxolitinib, a Janus-associated kinase (JAK) inhibitor, was approved by the US FDA for the treatment of steroid-refractory GVHD [9].

The utility of the existing drug regimens has been limited by their varied degree of response (< 50% of patients with acute GVHD and 40–50% of patients with chronic GVHD depending on initial disease severity) and severe side effects[10], which are essentially attributed to their immunosuppressive action, predisposing the patients to opportunistic

infections. A noteworthy and often unavoidable complication is the diminution of the graft versus leukemia (GVL) effect.

Despite current medical advances, the prevention of GVHD while maintaining the GVL effect of the graft remains a challenging task for clinicians. Therefore, there is a need to develop novel pharmacological agents to combat GVHD, without compromising the GVL effect.

The present study is aimed to screen and develop novel phyto-pharmacological agents with immunomodulatory activities for acute GVHD prophylaxis. Juglone, a naturally occurring naphthoquinone (NQ) derivative, was selected from a phytochemical drug library as the lead molecule and evaluated for its immunomodulatory effects on murine splenic lymphocytes *in vitro*. Furthermore, we evaluated the prophylactic efficacy of 5NQ and its impact on GVL activity in a murine model of allo-HSCT.

Review of Literature

2 REVIEW OF LITERATURE

2.1 Overview of hematopoietic stem cell transplantation

Hematopoietic stem cell transplantation (HSCT) is a medical procedure that replaces damaged or defective hematopoietic stem cells in patients with healthy donor cells[11]. HSCT is a potentially curative treatment for a variety of hematological diseases, including leukemia, lymphoma, myelodysplastic syndrome, aplastic anemia, and certain inherited immune system disorders such as sickle cell anemia and severe combined immunodeficiency[12].

Sources of hematopoietic stem cells (HSCs): The most abundant source of hematopoietic stem cells (HSCs) is bone marrow; however, they are also present in low concentrations in peripheral blood and umbilical cords of newborns. Therefore, HSCT can utilize stem cells from any of these sources. The procedure is referred to as a "bone marrow transplant (BM-HSCT)" if the stem cells are extracted from the bone marrow, a "peripheral blood stem cell transplant (PB-HSCT)" if they are extracted from the peripheral blood, and an "umbilical cord blood transplant (UCB-HSCT)" if they are extracted from the umbilical cord. Under general anesthesia, bone marrow is collected from the posterior iliac crest. However, because this procedure causes donor discomfort, peripheral blood has become a popular source of HSCs[13]. Today, the majority of stem cells used in transplantation come from peripheral blood. Granulocyte colony stimulating factor (G-CSF) is administered to donors five–six days prior to apheresis operation in order to facilitate the movement of stem cells from the bone marrow into the peripheral blood[14,15]. Stem cells can also be extracted from various regions of the umbilical cord, including Wharton's jelly, the cord lining, and the blood vessel region (Figure 1)Figure 1. In UCB-HSCT, Wharton's jelly is the most common

source of stem cells. Although stem cells derived from umbilical cords have been shown to be safe in clinical settings, it is crucial that the patient's UCB be banked at birth. Long-term storage and inadequate stem cell recovery render UCB unattractive as a source of donor cells for HSCT[16]. Table 2 shows the advantages and disadvantages of stem cell transplantation from bone marrow, peripheral blood, and umbilical cord blood.

Table 2: Comparison of HSC sources for transplantation.

	Benefits		**Drawbacks**	
Source of HSC	Donor	Recipient	Donor	Recipient
Bone Marrow		Lower risk of GVHD	Discomfort and pain	HLA matching required
Peripheral Blood	Sedation not required for collection Less distress and pain	Sooner reconstitution and engraftment		Higher risk of GVHD
Umbilical Cord Blood	Non-invasive	Lower risk of GVHD and relapse Stringent HLA matching not required		Inadequate no. of HSCs Delayed engraftment and reconstitution

Abbreviations: HSC: hematopoietic stem cells; GVHD: graft-versus-host disease; HLA: human leukocyte antigen[15,16].

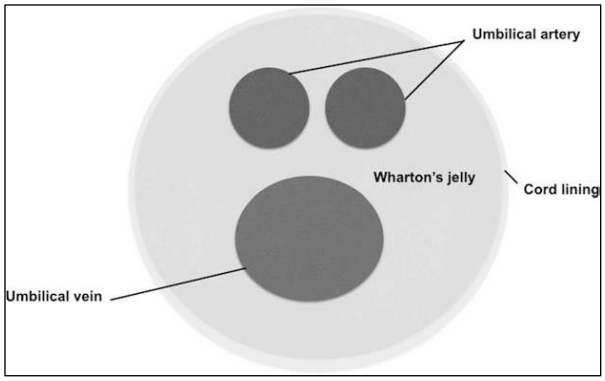

Figure 1: Illustration of cross-section of the human umbilical cord showing different compartments (cord lining, Wharton's jelly, and perivascular region) from where stem cells can be derived[16].

Conditioning regimens: Before undergoing HSCT, patients undergo conditioning treatment with chemotherapy and radiation therapy[17]. The key goals of conditioning regimen are to eliminate the tumor cells in patients and to remove abnormal stem cells in

individuals with hematological disorders. Other goals include the removal of damaged hematopoietic progenitor cells from the bone marrow to replace them with donor stem cells. Moreover, the aim is to suppress the recipient 's immune system to prevent the body from rejecting donor stem cells[17]. Conditioning regimens are categorized into three types based on the duration and degree of cytopenia: myeloablative (high-intensity), reduced-intensity (middle-intensity), and non-myeloablative (low-intensity). Myeloablative conditioning results in prolonged, usually irreversible pancytopenia, which can be fatal unless hematopoiesis is restored via hematopoietic stem cell infusion. Myeloablative conditioning improves disease control and reduces the chance of relapse at the expense of higher toxicity; hence, this conditioning is only utilized in individuals under the age of 55 years who are free of co-morbidities. Since reduced-intensity and non-myeloablative conditioning allow for its use in older and comorbid patients, hematopoietic stem cell transplantation is now routinely used for both malignant and non-malignant purposes. Conditioning therapy is often provided for several days and varies depending on the nature of the chemotherapeutic agent employed, radiation dose, and duration of exposure to accomplish the necessary myeloablation prior to stem cell therapy[17–19].

Types of HSCT: There are two main types of transplantation: autologous transplantation, in which patients' own stem cells are extracted and reintroduced to their bodies after a conditioning regimen, and allogeneic transplantation, in which patients receive stem cells from a relative or unrelated donor[20]. Figure 2 and Table 3 depict the process and differences between autologous and allogeneic transplantation. Human leukocyte antigen (HLA) compatibility between recipients and donors is one of the most significant prognostic factors for allogeneic hematopoietic stem cell transplantation. The HLA-A, -B, -C, -DR, -DQ, and -DP alleles are taken into account during matching. During donor selection, additional parameters including donor age, gender, and recipient-donor cytomegalovirus

compatibility are considered[20]. In approximately 30 percent of patients, an HLA-matched related donor is available and is the preferred donor. Patients lacking an HLA-matched related donor typically undergo transplantation from a matched unrelated donor. Despite the availability of multiple repositories of consenting adult unrelated donors, ethnic minority patients may have difficulty finding a suitable HLA match. It is also possible to use hematopoietic stem cells from cord blood or related donors with matching haplotypes[21]. Haploidentical transplantation can be performed and requires only one HLA haplotype to match the recipient and donor. Since parents, offspring, and half of one's siblings contain the same haplotype, haploidentical transplantation can be made available as a treatment therapy for almost all patients[22]. Allo-HSCT can be divided into three types according to the donor: matched related donor (MRD), matched unrelated donor (MURD), and haploidentical transplantation (parents or siblings as donors).

Recently, guidelines from the American Society for Transplantation and Cellular Therapy (ASTCT) have updated a detailed list of indications for autologous and allogeneic transplantations[23]. Allogeneic transplantation has gained popularity over autologous transplantation and comprises approximately 40% of transplantations worldwide[24] owing to various advantages (Figure 3 and Table 3). Allogeneic transplantation is the standard of care for hematological disorders like acute myeloid leukemia, chronic myeloid leukemia, acute lymphoblastic leukemia, myelodysplastic syndromes, T cell lymphoma, acute promyelocytic leukemia, and sickle cell anemia, whereas; autologous transplantations is the standard of care for solid tumors like germ cell tumors and Ewing’s sarcoma, systemic sclerosis, mantle cell lymphoma, primary central nervous system lymphoma, high-grade B cell lymphoma, Hodgkin’s lymphoma and plasma cell disorders[21,23].

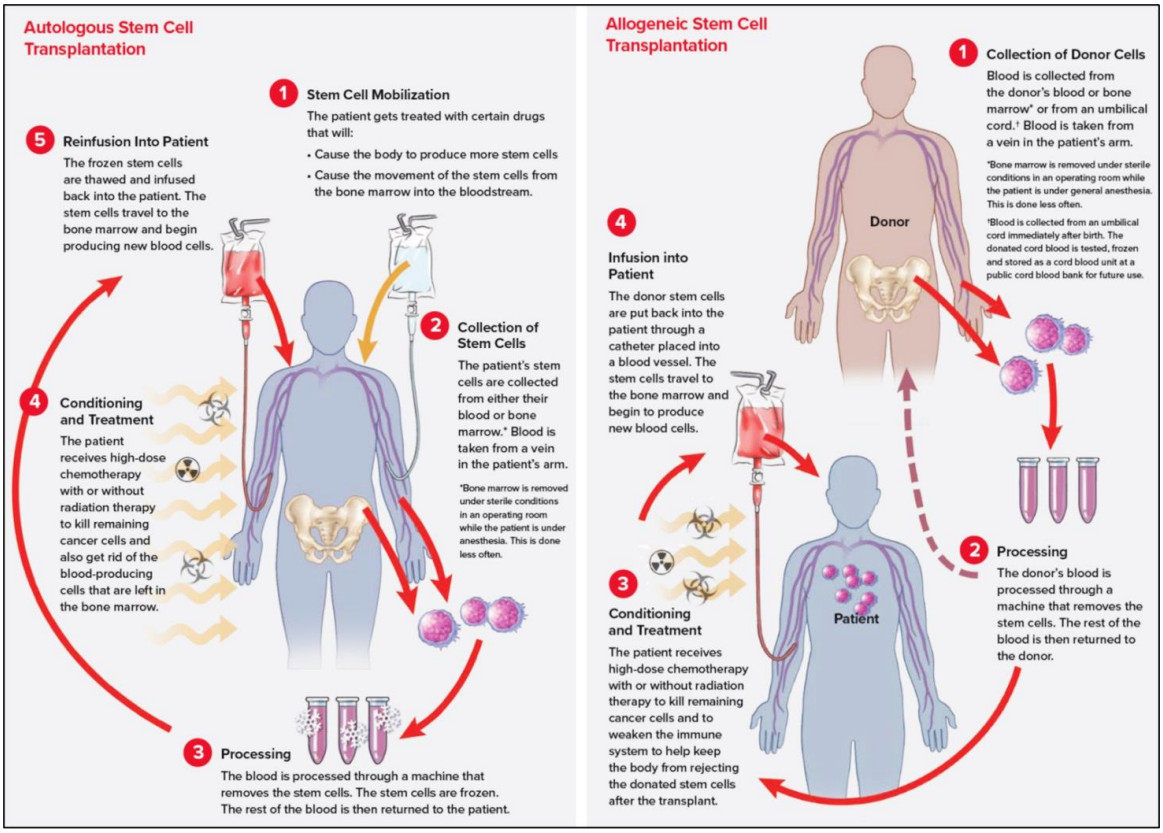

Figure 2: Process of autologous and allogeneic HSCT[25].

For further discussion throughout the thesis, we have concentrated on allogeneic transplantation, as it is the standard of care for various hematological malignancies.

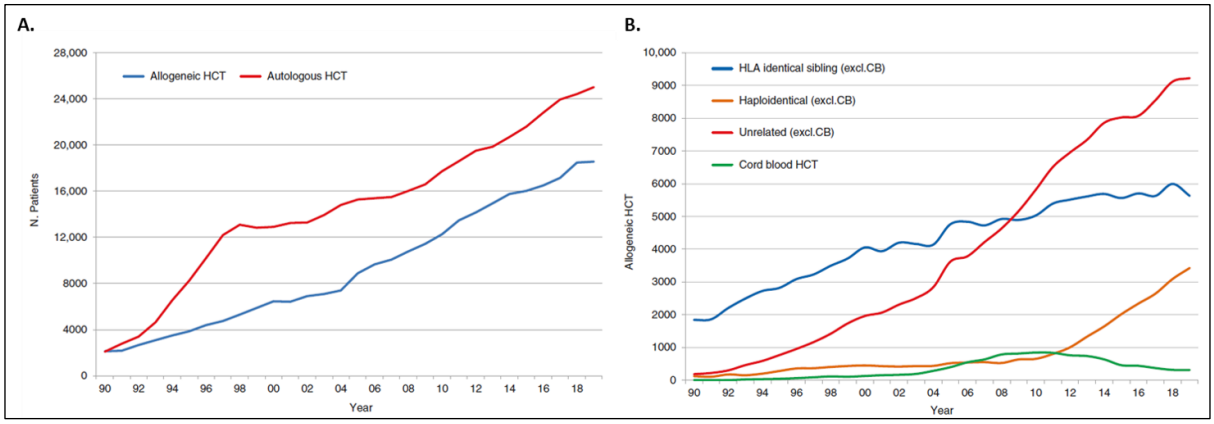

Figure 3: HSCTs performed between 1990 and 2019. (A) Number of patients receiving autologous and allogeneic HSCT. (B) Allo-HSCT with different donor type [24].

Table 3: Advantages and disadvantages of auto and allo-HSCT[26]

	Allogeneic HSCT	**Autologous gene therapy HSCT**
Potential advantages	Strong clinical evidence of benefits, matched sibling donor transplants	Can be performed for all patients, as own cells are the source of donor
		No GVHD development
		Lower chances of graft rejection
Potential disadvantages	Difficult to find appropriate healthy matched donors	Contamination with transformed stem cells or low number of stem cells reduce effectiveness
	Immune suppression required to prevent graft rejection	Limited efficacy due poor transgene stability
	High risk of GVHD development, requiring prolonged immunosuppression	Potential of insertional oncogenesis

Outcomes of allogeneic HSCT: Upon allogeneic transplantation, the infused stem cells migrate to the bone marrow and produce new, healthy blood cells such as white blood cells, red blood cells, and platelets. This is referred to as "engraftment[20]." However, patients undergoing allo-HSCT may experience several complications requiring sustained intensive care (Figure 4). There is a risk of graft rejection following allo-HSCT; consequently, the host immune cells recognize and activate an immunological response against donor cells, which eliminates the donor graft. Patients undergoing allo-HSCT are maintained on immunosuppressants to prevent graft rejection and allow donor cells to engraft[27]. There is a greater danger of viral infections during this period until immune reconstitution begins, thus patients are kept in critical care[28]. One of the most advantageous outcomes of allo-HSCT is the graft-versus leukemia (GVL) effect, according to which, upon immune reconstitution, the donor cells are capable of identifying and destroying residual malignant cells in the patient, resulting in a reduced incidence of relapse[29,30]. Nevertheless, allo-HSCT entails the risk of graft-versus-host disease (GVHD), which occurs when donor cells mount

an immune response against host antigens, causing damage to host tissues and organs, and in extreme cases, death[30,31]. Therefore, while allo-HSCT has the potential benefit of GVL, it also has the potential risk of GVHD.

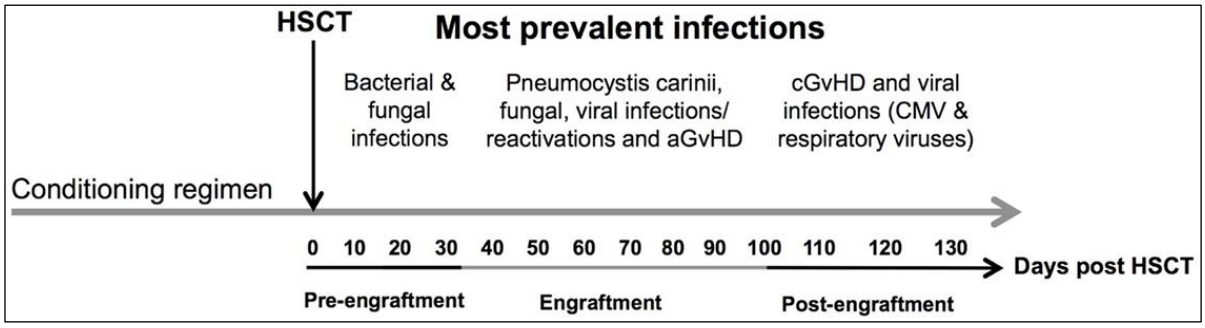

Figure 4: The diagram depicts the most common complications following allo-HSCT based on the three stages of engraftment. Concomitant infectious problems, including bacterial, fungal, and viral infections, are depicted according to their prevalence and correlation with acute and chronic GvHD during three stages of follow-up: (1) pre-engraftment, (2) engraftment, and (3) post-engraftment. Abbreviations: CMV: cytomegalovirus; aGvHD: acute graft-versus-host disease; and cGvHD: chronic graft-versus-host disease[32] .

2.2 Graft-versus-host disease (GVHD)

Graft-versus-host disease (GVHD) is a systemic condition that arises when the immune cells of the graft identify the host as foreign and attack the recipient's tissues and organs. "Graft" refers to transplanted or donated tissue, whereas "host" refers to the recipient's tissues. It is a common adverse reaction to allo-HSCT[30,33,34].

Etiology of GVHD: In In 1996, in a pioneering lecture Dr. Billingham identified three prerequisites for the development of GVHD[35]. They are,

1. The graft should consist of immunologically competent cells
2. The recipient and donor should express different tissue antigens
3. The recipient must be incapable of mounting an immune response against the donor cells[35].

Consequently, the significant determinants of GVHD incidence and severity of GVHD are as follows:

1. Human leukocyte antigen (HLA) disparity between host and donor: The major histocompatibility complex (MHC) encodes highly polymorphic HLAs. Class I HLA (A, B, and C) is expressed in nearly all nucleated cells. Class II HLA (DR, DQ, and DP) are predominantly expressed on B cells, dendritic cells, and monocytes; however, inflammation and/or injury can induce their expression on many other cell types. HLA matching is done for HLA-A, -B, -C, and -DRB1 alleles and the incidence and severity of acute GVHD is proportional to the extent of mismatch between HLA proteins[36,37].

2. Non-HLA factors between the donor and the host: Despite receiving HLA-matched grafts, about 40% of these patients develop acute GVHD because of "minor" histocompatibility antigen (HA) variations between the patient and donor. The minor histocompatibility antigens are not encoded by HLA loci. Some minor HAs, such as HY and HA-3, are expressed on all tissues and have been correlated with incidence of GVHD[38]. Other immunogenetic factors associated with a greater risk of GVHD include single nucleotide polymorphisms in Killer Ig-like receptors (KIR), MHC class I chain-related (MICA)[39], and polymorphisms in immune response genes of cytokines, such as tumor necrosis factor (TNF), interleukin 10 (IL-10), IL-1 gene family, IL-2, IL-6, interferon γ (IFNγ), tumor growth factor β (TGF-β) and their receptors, NOD-like receptors, toll-like receptors, and micro-RNAs[40].

3. Intensity of conditioning regimens: Most frequently, myeloablative conditioning (MAC) or reduced-intensity conditioning (RIC) is utilized for conditioning patients for allo-HSCT. Compared to MAC conditioning, RIC conditioning is associated with a diminished incidence of severe graft-versus-host disease (GVHD) and conditioning-related toxicities.

Although MAC conditioning has been associated to a higher risk of developing GVHD and conditioning related toxicities, but has a lower recurrence rate than RIC conditioning[17–19,41]**.**

4. Source of stem cells: Higher rates of GVHD have been linked to the use of stem cells extracted from peripheral blood rather than from bone marrow or cord blood. Chronic GVHD appears to be more common following peripheral blood stem cell transplantation, further contributing to complications. Cord blood transplantation is associated with a reduced risk of infections, GVHD, and the necessity for strict HLA matching. Disadvantages include delayed engraftment, increased risk of graft rejection, and higher rates of disease recurrence[14,42].

Clinical signs and manifestation of acute and chronic GVHD: In 2018, European Society for Blood and Marrow Transplantation (EBMT), National Institutes of Health (NIH) and Center for International Blood and Marrow Transplant Research (CIBMTR) provided a guideline on standardized terminology criteria for assessment of GVHD. Based on these guidelines, the two major categories of GVHD-acute GVHD and chronic GVHD were further divided into two subcategories. Acute GVHD is subcategorized into classical acute GVHD (occurring within 100 days of transplantation) and late-onset acute GVHD (occurring more than 100 days after transplantation). Clinical features that characterize acute GVHD involve three major organs: the skin (erythematous maculopapular rash), liver (hyperbilirubinemia, cholestatic jaundice), and gastrointestinal (GI) tract (nausea, vomiting, diarrhea, severe pain, and GI bleeding). Chronic GVHD is subcategorized as classic chronic GVHD, which manifests with variable clinical features resembling autoimmune disorders and may be retrained to a particular organ or manifest systemically. The second subcategory of chronic GVHD is called overlap syndrome, which manifests with overlapping features of chronic GVHD and acute GVHD (Figure 5). The

manifestation of chronic GVHD may either be continuous, where acute GVHD gradually becomes chronic, or passive, where acute GVHD resolves completely but is later followed by chronic GVHD[43].

Acute GVHD develops in 30-50% of patients after allo-HSCT[44], whereas 20-80% of patients develop chronic GVHD after allo-HSCT[45].

Epidemiology of GVHD: Acute GVHD develops in up to 50% of patients receiving allo-HSCT from a matched-sibling donor. The incidence of acute GVHD is even higher in unmatched donors. Acute GVHD manifests within 100 days of transplantation with varying severity, and approximately 30% of patients succumb to this disease after allo-HSCT[29]. Chronic GVHD affects 6-80% patients after allo-HSCT. It manifests with symptoms that are milder than acute GVHD and may also develop as a secondary complication after successful treatment of acute GVHD. However, about 10% patients that develop chronic GVHD succumb to the disease[29,46].

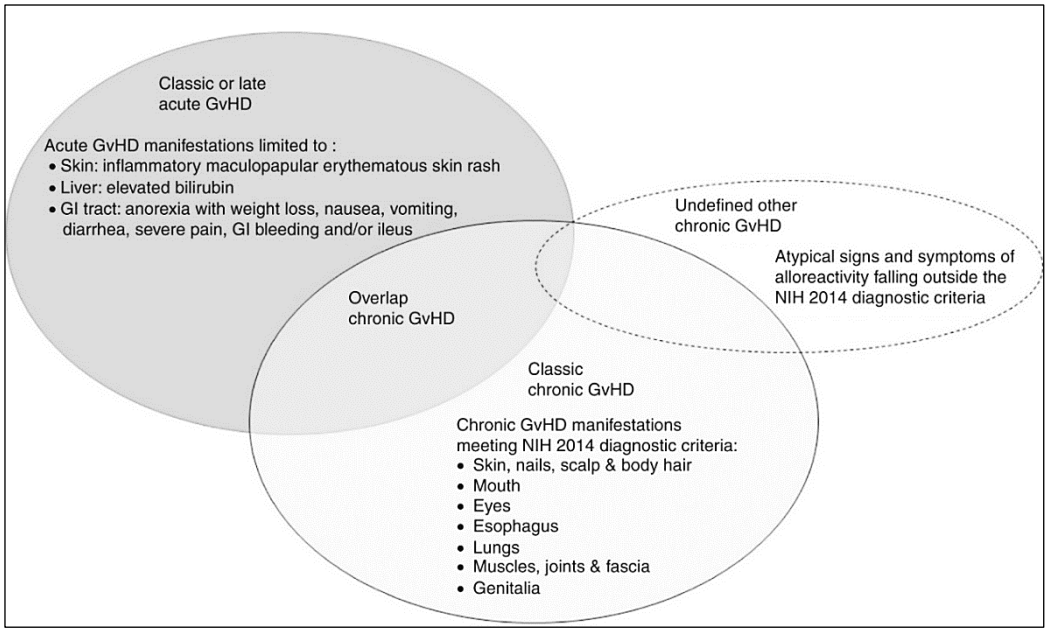

Figure 5:Schematic representation of the types of GVHD[43]

2.3 Rationale for studying acute GVHD

In the absence of effective prophylaxis, 90% patients develop acute GVHD[47]. Moreover, despite the administration of prophylaxis after allo-HSCT, acute GVHD develops in 50% of patients[48]. The overall survival in patients with grade I-II acute GVHD is 70%, and it further reduces to 40% in patients who develop severe grade III-IV GVHD[48]. Prolonged hospitalization, infectious complications, and the need for higher doses of immunosuppressive medication further worsen the quality of life (QOL) at 6 months post-transplantation. Grades II and IV acute GVHD are reported to be associated with worse QOL scores at 12 months post transplantation and is also a major risk factor for development of chronic GVHD[49,50]. Furthermore, acute GVHD weakens the physical abilities of patients and impairs daily living activities, which is further fueled by muscle atrophy and cachexia due to prolonged bed rest, wheelchair use, and other adverse effects of immunosuppressive therapy (osteoporosis, diabetes mellitus, hypertension, etc.)[51].

Our study aimed to identify prophylactic agents for acute GVHD because it occurs soon after transplantation (often within 100 days) and is a key risk factor for chronic GVHD and an increased incidence of secondary infections, both of which contribute to poor outcomes of allo-HSCT.

2.4 Clinical manifestations and grading of acute GVHD: Clinical manifestations of classical acute GVHD involve either one or a combination of three major organs: the skin, liver, and gastrointestinal tract[43,52].

Skin acute GVHD: Affects approximately 80% of individuals with acute GVHD and manifests 14–21 days after allo-HSCT. Maculopapular rash is a common clinical characteristic of acute GVHD of the skin that affects the neck, shoulder, palms, and soles of the feet, and can extend throughout the body, causing irritation and pain. In

severe cases of acute skin GVHD, the rash might ulcerate, resulting in degeneration of basal epithelial layer and lymphocyte infiltration[43,52].

Gastrointestinal (GI) acute GVHD: The most characteristic symptom of acute GVHD of the lower GI tract is diarrhea accompanied by abdominal pain. In severe cases, mucosal ulceration causes bleeding and the passage of blood in stools. The clinical symptoms of acute GVHD in the upper GI tract include anorexia and nausea. The symptoms of the upper and lower GI tract may overlap or occur in isolation, depending on the degree of organ involvement[43,52].

Liver acute GVHD: Hyperbilirubinemia is a classical sign of acute GVHD in the liver. In severe cases, hepatic veno-occlusive disease (HVOD) may develop because of sinusoidal obstruction. Drug toxicity and infections may further augment acute liver GVHD[43,52].

Nonclassic manifestations of acute GVHD: Acute GVHD can potentially affect any organ in the body, including the central nervous system. However, it is difficult to distinguish the symptoms from toxicity due to conditioning regimens. For example, lung acute GVHD symptoms of breathlessness, cough and low blood pressure are difficult to distinguish from the symptoms of lung injury due to radiation conditioning. Similarly, the symptoms of neurological impairment may overlap with the symptoms of neurotoxicity of prophylactic agents[43].

Grading of acute GVHD: In 2018, European Society for Blood and Marrow Transplantation (EBMT), the National Institutes of Health (NIH) and the Center for International Blood and Marrow Transplant Research (CIBMTR), recommended the use of Mount Sinai Acute GvHD International Consortium (MAGIC) criteria for diagnosis and assessment of GVHD severity[43]. According to the MAGIC criteria,

disease in each organ involved (skin, GI and liver) is graded from 0-4, with highest score denoting most severe manifestation (Table 4). Accordingly, the extent of erythema of the skin, bilirubin levels in the liver, diarrhea, and nausea in the lower and upper GI tract were evaluated to assess the involvement of each of these organs. The scores are then utilized to grade GVHD from I -IV using MAGIC criteria, where grade I denotes mild, II denotes moderate, III denotes severe and IV denotes very severe acute GVHD (Table 5). The use of eGVHD APP has gained popularity in aiding clinical professionals in correctly grading GVHD symptoms and prescribing correct treatments[53,54].

Table 4:Acute GVHD organ staging (MAGIC criteria)

Stage	Skin (active erythema only)	Liver (Bilirubin(mg/dl))	Upper GI	Lower GI (stool output/day)
0	No active (erythematous) GVHD rash)	<2	No or intermittent nausea, vomiting or anorexia	Adult: <500ml/day or <3 episodes/day
				Child:10ml/kg/day or <4 episodes/day
1	Maculopapular rash<25% BSA	2-3	Persistent Nausea, vomiting or anorexia	Adult: 500-999ml/day or 3 or 4 episodes/day
				Child: 10-19.9ml/kg/day or 4-6 episodes/day
2	Maculopapular rash 25-50% BSA	3.1-6	NA	Adult: 1,000-1500ml/day or 5-7 episodes/day
				Child: 20-30 ml/kg/day or 71- episodes/day
3	Maculopapular rash >25% BSA	6.1-15	NA	Adult: >1500ml/day or >7episodes/day
				Child: >30ml/kg/day or >10 episodes/day
4	Generalized erythroderma (>50% BSA) plus bullous formation and desquamation >5% BSA	>15	NA	Adult and child: severe abdominal pain with or without ileus or grossly bloody stool (regardless of stool volume)

Abbreviations: BSA: Body surface area; GI: gastrointestinal; GVHD: graft-versus-host disease; NA: not applicable[43].

Table 5: Overall acute GVHD grading (MAGIC criteria).

Grade [a]	**Stage**			
	Skin (active erythema only)	Liver (bilirubin)	Upper GI	Lower GI (stool output/day)
0	0	0	0	0
I	1 or 2	0	0	0
II	3	1	1	1
III	-[b]	2 or 3	-[b]	2 or 3
IV	4	4	-[b]	4

Abbreviations: GI: gastrointestinal; GVHD: graft-versus-host disease; a: overall grade based on target organ with most severe involvement; b: these manifestations are not required for this grading [43].

2.5 Biomarkers for acute GVHD: Historically, a biomarker panel consisting of four proteins, IL-2Rα, TNF receptor 1 (TNFR1), IL-8, and hepatocyte growth factor (HGF), has been used to distinguish between patients with or without GVHD. Organ-specific biomarkers have also been used to assess the severity and prognosis of acute GVHD; for example, higher expression of elafin in plasma can predict skin GVHD, and expression of cytokeratin 18 (CK18) and regenerating islet-derived protein 3α (REG3α) in GI biopsies can distinguish between diarrhea caused by acute GVHD or non-GVHD-related factors. Currently, a biomarker panel consisting of two markers, suppressor of tumorigenesis 2 (ST2, receptor for IL-33), and REG3α, forms the Ann Arbor scoring system. At the onset of acute GVHD, the serum concentrations of ST2 and REG3α are used to generate a score between 1 and 3 that predicts the risk of non-relapse mortality (NRM) and treatment resistance.

2.6 Pathophysiology of acute GVHD: There are three stages in the pathophysiology of acute GVHD: the initiation stage, the activation stage, and the effector stage[55].

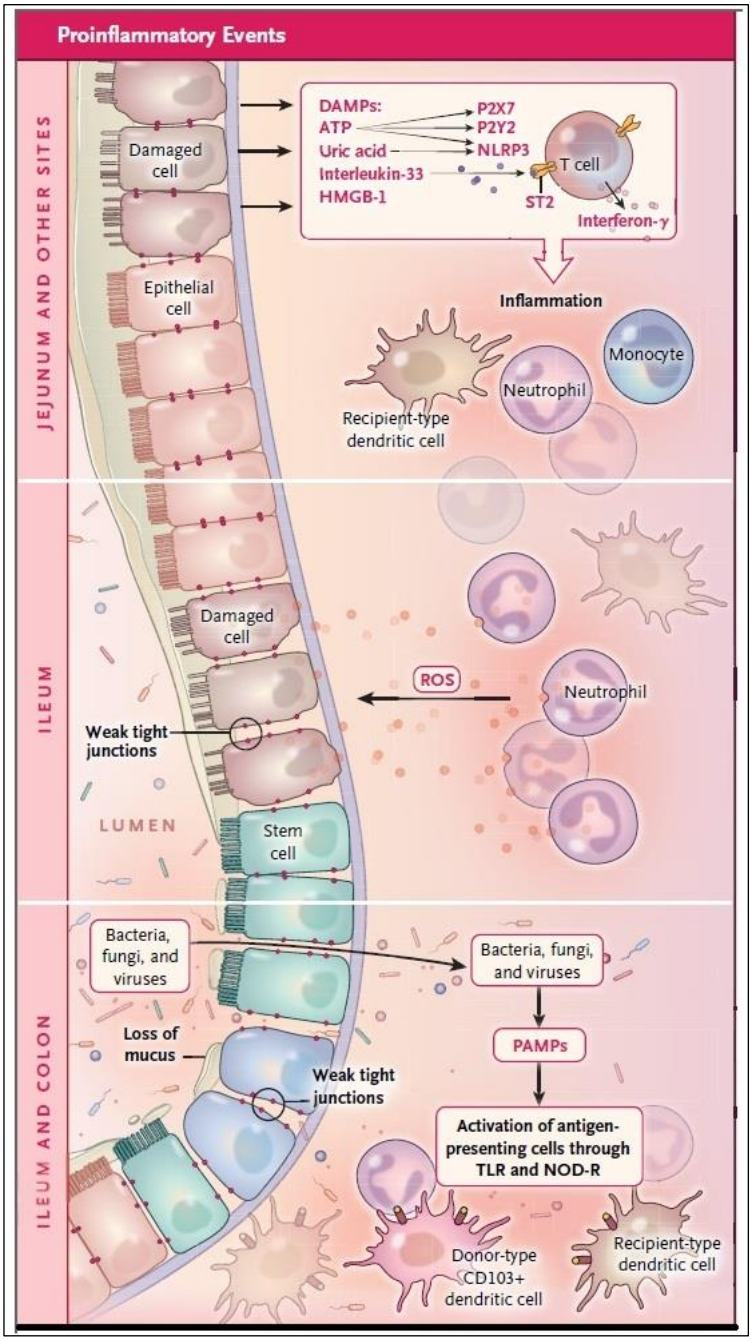

Figure 6: Initiation phase events. PAMPs and DAMPs activate innate immune cells such as monocytes neutrophils and donor derived dendritic cells. Upon activation dendritic cells migrate to mesenteric lymph nodes and activate T cells against these host antigens.

Initiation phase: The epithelial linings of skin, liver and GI tract are the major sites for interaction of commensal and pathogenic bacteria with epithelial cells. Additionally, these organs are highly susceptible targets of radiation and chemotherapy[31]. Thus, administration of conditioning regimen prior to allo-HSCT causes damage to mucosal barriers, leading to disruption of commensal microbiota, cell death and tissue injury in these tissues. This conditioning regimen mediated damage causes release of several pathogen-associated molecular patterns (PAMPs), damage-associated molecular patterns (DAMPs), and inflammatory cytokines, causing innate myeloid cells,

such as neutrophil, granulocytes and monocytes to infiltrate the intestinal tract. PAMPs are molecules derived from destruction of commensal or pathogenic bacteria, fungi or virus and include an array of molecules like lipopolysaccharide (LPS), toll-like receptors (ex. TLR4), nod-like receptors (ex. NOD2), bacterial cell wall proteins and glycoproteins, viral coat proteins and bacterial and viral DNA. Higher levels of LPS, TLR4 and NOD2 have been associated with poor prognosis of acute GVHD. TLRs induce apoptosis of epithelial and endothelial cells via activation of myeloid differentiation factor 88 (MyD88) pathway thus augmenting GVHD. Activation of myeloid and epithelial cells due to exposure to bacterial and viral DNA induces type I interferon (IFN) signaling via retinoic acid-inducible gene-I (RIG-I), which results in is activation of CD8 T cells, leading to cell mediated toxicity of host cells[56]. DAMPs include molecules from the degradation of tissue cells and includes molecules such as uric acid, high-mobility group box 1 (HMGB1), ATP, heat shock proteins, IL-33 and heparan sulfate proteoglycans. Damage to endothelial and epithelial cells leads to release of IL-33 leading to activation of pathways required for immune regulation. PAMPs and DAMPs thus cause infiltration of innate immune cells like granulocytes, monocytes and neutrophils (the first-wave immune responders) at site of tissue injury. Furthermore, PAMPs, DAMPs, inflammatory cytokines and innate immune cells lead to the final outcome of the initiation phase, which is activation of classical antigen presenting cells (APCs) like dendritic cells, macrophages and B cells and non-classic APCs such as mast cells, basophils, endothelial cells and epithelial cells. These activated APCs further migrate to mesenteric lymph nodes where they present host antigen for donor adaptive immune cells, especially $CD4^+$ T cells, leading to their activation and clonal proliferation, thus providing the basis for second phase of GVHD pathogenesis (Figure 6)[30,33,34,55].

Immune regulation factors at play at the initiation phase: The knowledge of the factors that play a role in initiation of acute GVHD, has led to various reformations in the process of allo-HSCT as well as prophylactic strategies. Since the conditioning regimens play a major role in causing host damage, reduction in conditioning related damage may thus alleviate GVHD, this idea led to usage of RIC conditioning for most indications. RIC conditioning has indeed shown lower incidence of GVHD, nevertheless these patients present with higher incidence of tumor relapse[19]. Considering the pivotal role of microbiota and PAMPs, used of antibiotics during conditioning regimen was tested, however, the results showed that use of antibiotics during allo-HSCT leads to destruction of gut microbiota diversity and causes intestinal domination by some species of the microbiota resistant to these antibiotics. For example, intestinal domination of *Enterococcus faecium*, is associated with increased GVHD-related mortality[56]. However, intestinal dominance of certain bacterial species may alleviate GVHD, for example intestinal dominance of genus *Blautia* (order *Clostridiales*) is associated with reduced severity of GVHD. The use of broad-spectrum antibiotics during allo-HSCT can cause loss of this beneficial commensals, and therefore use of broad-spectrum antibiotics is discouraged in clinical practice. These commensals impart their protective effect via production of metabolites like short-chain fatty acids (SCFAs) which protect and activate intestinal stem cells (via IL-22) and induce maintenance of regulatory T cell and the site of inflammation[56]. Certain DAMPs also activate immune regulatory pathways to mitigate conditioning associated damage. For example, cytokine IL-33, which is released by damaged endothelial and epithelial cells, can activate its receptor ST2, which in turn induces immune regulation. ST2 is used as a biomarker for GVHD prognosis[57]. Nonetheless, acute GVHD develops despite these immune regulatory factors at play (Figure 8).

T cell activation phase

Activation of adaptive immune cells, majorly T cells is an important event for development of acute GVHD. Resident T cells in the tissue and lymph nodes are activated by engagement of the T cell receptor (TCR) with MHC antigen peptides expressed by APCs. $CD4^+$ T cells are activated in response to MHC class II differences, and $CD8^+$ T cells are activated in response to MHC class I differences, these T cells are called alloreactive T cells[58]. In clinical settings, as most transplants occur between in HLA-matched sibling donors, minor histocompatibility antigens are the only targets of T cell alloreactivity and can cause acute GVHD[59]. The engagement of TCR with MHC-antigen complex of APC serves as the first signal for T cell activation.

Optimal activation of T cell requires a co-stimulatory signal in addition to engagement of their cognate TCRs (Figure 7). Engagement of the co-stimulatory molecules (CD28 and ICOS, the TNFR superfamily receptors, OX40, and CD137 with their respective binding partners expressed by APCs, cause signal amplification, induces sustained cytokine production, inhibits apoptosis, and supports the metabolism of effector T cells[34,60]. Following activation, T cell undergo proliferation and differentiation into various T cell subsets (effector, memory or regulatory, anergic T cells). This is greatly influenced by a third signal mediated by the cytokines in the inflammatory milieu[61]. Type 1 helper T cell cytokines (IFNγ, IL-1β, IL-2 and TNF) are majorly implicated in augmenting acute GVHD. Activation of immune cells results in transcription of genes related to cytokines, chemokines and their binding receptors. IFNγ has been reported to enhance acute GVHD by boosting the upregulation of chemokines receptors, MHC molecules, adhesion proteins, on monocytes and increasing macrophage sensitivity to stimuli like LPS and accelerating intracellular cascades in response to these stimuli. Contrastingly, studies have shown that IFNγ accelerates donor T cell death and may thus play a role in alleviating acute GVHD.

A similar activity of other cytokines where their effect can either amplify or reduce GVHD have observed. Another example is IL-2, which is an important cytokine that drives T cell proliferation but is also known to play a role in enhancing suppressor T regulatory cells. Therefore, the specific effects of a given cytokine on the severity of GVHD may depend on the timing and duration of the secretion of that cytokine[61]. Specific implications of different cytokines in acute GVHD pathogenesis have been summarized in Table 6.

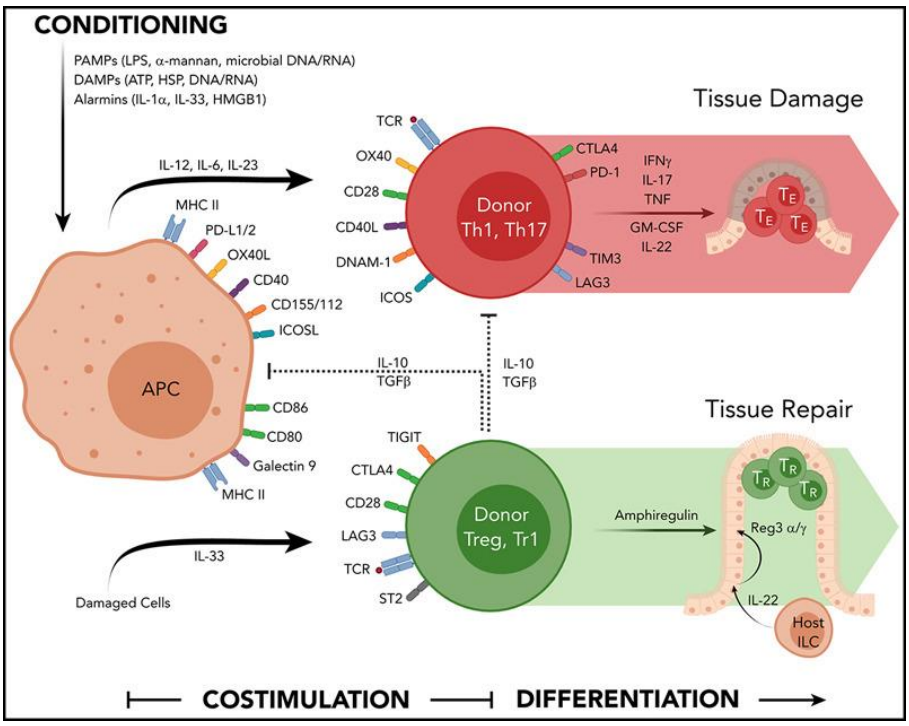

Figure 7: Costimulatory signals and cytokines involved in T cell activation and differentiation in acute GVHD pathogenesis

The importance of T cell in pathogenesis of acute GVHD has been supported by many reports that show that ex vivo T cell depletion in the donor graft resulted in lower incidence and severity of acute GVHD. Nonetheless, these reports also implicated increased relapse rate in these patients thus highlighting the important role of T cells in the GVL activity of the graft[62,63]. Therefore, further studies were conducted to understand the specific T cell subsets that play exclusive roles in GVHD and GVL activity. Accordingly, it was observed that administration of only $CD8^+$ and $CD4^+$ memory T cells did not result in GVHD development in MHC-mismatched murine models of allo-HSCT, however they appeared to mediate GVL responses. GVHD is majorly mediated by naive T cell responses.

Because CD4+ T cells have the capacity to differentiate into Th1 cells, Th2 cells, and Th17 cells, they are crucial in the initiation of GVHD in mice and have been recognized as potential targets for the treatment and prevention of GVHD in clinical settings[64,65]. At the end of the T cell activation phase, T cells migrate to the damaged tissues via chemokine signals and render their effector functions at the site of damage.

Table 6: Important cytokine in GVHD[60].

Proinflammatory Cytokines	**Mechanism of Action**
TNF	Activates dendritic cells and $CD8^+$ T cells Signals cells for apoptosis or
IFNγ	Promotes Cytotoxic T cells function, MHC-II expression Promotes cytokine secretion and Th1differentiation
IL-1	Promotes synthesis of a wide range of other proinflammatory molecules and acute phase proteins in synergy with TNF
IL-2	Promotes T cell proliferation Promotes Treg differentiation
IL-6	Promotes Th17 differentiation and cytotoxic T cell differentiation Stimulates differentiation and activation of macrophages
IL-12	Promotes Th1 differentiation and is secreted by innate immune cells
IL-17	Proinflammatory and anti-inflammatory activity Antagonist to Th1 differentiation
IL-18	Upregulates IL-12 secretion
Anti-inflammatory Cytokines	**Mechanism of Action**
IL-10	Antagonist to inflammatory TNF and Th1 cytokines Restricts proliferation of conventional T cells Majorly secreted by Treg cells
TGFβ	Stimulates T cells to differentiate into Th17 and Treg cells. Antagonist to macrophage activation and Th1 differentiation Inhibition of macrophage activation

Abbreviations: TNF: tumor necrosis factor; TGFβ: transforming growth factor beta; IL: interleukins

Immune regulation at play at the T cell activation phase: Optimal T cell activation requires a stimulation from 3 signals- TCR and MHC engagement, costimulatory signals and cytokine signals. Therefore, several factors bring about regulation of immune response at

each of these 3 signals. Negative regulatory co-stimulatory molecules like cytotoxic T-lymphocyte–associated antigen 4 (CTLA-4, CD152), programmed death 1 (PD-1) (CD279)–PD-L1 (CD274), and B7-H3 (CD276) among others play a role in inhibiting optimal stimulation of T cells. In animal models, blockage of co-stimulation has shown promising results, and is being tested in large clinical trials[60]. Additionally, many immune regulatory cells like T regulatory cells, myeloid derived suppressor cells and others can inhibit T cell activation by secretion of anti-inflammatory cytokines like IL-10 and expression of negative costimulatory molecules[61,66]. Lastly, the end stage of T cell activation that involves migration of these cells to sites of inflammation can be inhibited by suppressing chemokines and integrins that augment migration of activated T cells.

Effector stage

Upon activation, T cells migrate to target sites and mediate tissue cell death by release of soluble activators of apoptosis (or necroptosis) or direct cellular cytotoxicity via expression of Fas ligand and by the release of granzyme B, a serine protease, and perforin, a pore-forming cytolytic protein. The soluble mediators of cell death involve TNF-α, IFN-γ, IL-1, and nitric oxide. This cytotoxic activity is majorly mediated by alloreactive donor $CD8^+$ T cells (or cytotoxic $CD8^+$ T cells; CTLs)[67]. Tissue damage via apoptosis of keratinocytes, intestinal stem cells and related basal Paneth cells, and neuroendocrine cells in GI crypts is most prevalent. Activated alloreactive $CD4^+$ T lymphocytes cause specific cell damage by release of pro-inflammatory cytokines like IFN and TNF. The susceptibility of endothelial and epithelial barriers to T cell mediated destruction may also influence the extent of target tissue damage during the effector phase[68,69].

Immune regulation at play at the T cell effector phase: GVHD is exacerbated by the pro-inflammatory signals described above, but the immune system also contains anti-

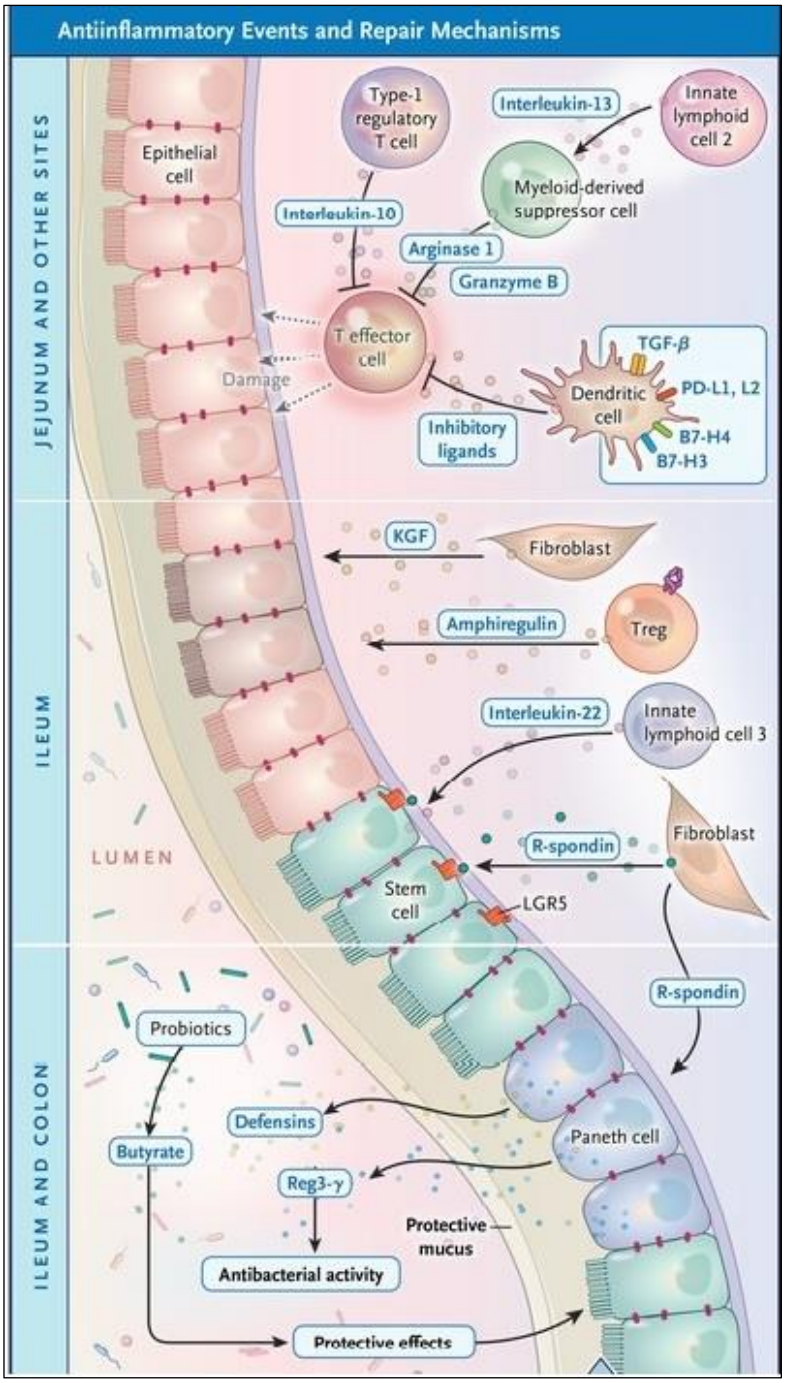

Figure 8: Anti-inflammatory and protective mechanisms that counter balance the inflammation due to conditioning regimen.

inflammatory. components that attempt to suppress these inflammatory responses. Regulatory T cells (Tregs) play a crucial role in immunologic tolerance, in part by releasing anti-inflammatory cytokines like IL-10 and TGFβ. T helper (Th) type 2 (IL-4, IL-10) responses can inhibit potent proinflammatory type 1cytokines, and a Th1 to Th2 transition may be advantageous in aGVHD[65,66]. Invariant natural killer T (iNKT) cells are another cellular subset with putative immunoregulatory functions, which may be important in the pathogenesis of graft-versus-host disease (GVHD)[65]. Moreover, susceptibility of the target tissue may play a role in acute GVHD. Tissues possess an intrinsic, but variable, ability to tolerate or withstand damage from inflammatory immune activity during infection, this phenomenon is called tissue tolerance. It is mediated via factors like expression of inhibitors of apoptosis and microbial-derived metabolites, SCFA, that potentiate anti-inflammatory responses. Thus, the intensity of acute GVHD tissue damage also relies of tissue specific factors (Figure 8)[68].

Summary of acute GVHD pathogenesis: Conditioning with chemo or radiotherapy causes host tissue damage resulting in inflammation and the release of pro-inflammatory cytokines. This increases the capacity of antigen-presenting cells (APCs) to present host antigens to donor T-cells leading to their activation, proliferation, and differentiation. The activated T-cells cause increased release of inflammatory cytokines and promote migration of T-cells to secondary lymphoid organs and target tissues like skin, liver, gut, etc. These activated T-cells cause inflammation-mediated cell death of host tissue and induce apoptosis of host cells via granzyme B and perforin-mediated pathways. Thus, GVHD leads to host tissue damage to an extent of organ failure resulting in death (Figure 9).

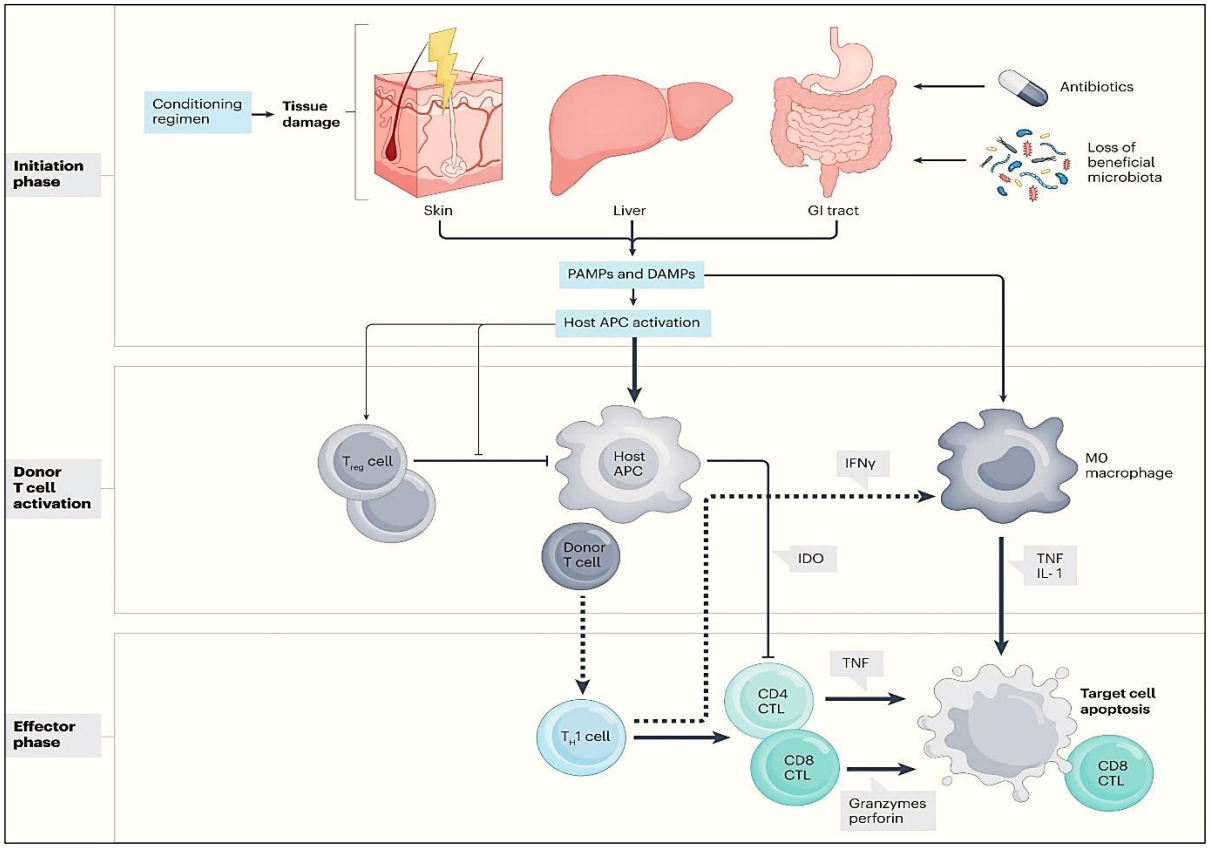

Figure 9: Overview of acute GVHD pathogenesis[30] .

2.7 Prophylaxis of acute GVHD

Clinically, acute GVHD is a complex syndrome which is difficult to treat. Therefore, prevention of this disease is a better option than treatment. Current standard prophylactic regimens for GVHD target T cells, as they are the major culprits for GVHD development

and progression. The prophylactic regimens employ two major strategies, first, use of pharmacological agents that target T cell activation and second, ex vivo manipulation of donor graft via selective T cell depletion to prevent GVHD development[70].

Pharmacological agents: Calcineurin inhibitors cyclosporine (CSA) or tacrolimus (TAC) are the standard of care for GVHD prophylaxis and are commonly administered in combination with either anti-metabolite drug methotrexate (MTX), or mycophenolate mofetil (MMF) (inosine-5'-monophosphate dehydrogenase inhibitor, preferentially depletes guanosine nucleotides in T and B cell, resulting in proliferation) or sirolimus (mTOR inhibitor)[71]. In a randomized phase III trial incidence of GVHD was compared in patients who received the TAC-MTX combination or CSA-MTX and showed that the later combination of CSA-MTX showed lower incidence of grade II-IV acute GVHD. Nevertheless, overall survival remained same in both the arms. Therefore, CSA/TAC in combination with MTX are current standard of care for GVHD prophylaxis[72,73]. Combination of CSA-MMF is preferentially administered to patient undergoing UCB allo-HSCT. This combination is associated with lower incidence of mucositis, when compared to CSA-MTX regimen, however the incidence of grade III-IV GVHD was lower in CSA-MTX group when compared to CSA-MMF group[74]. Combination of CSA-sirolimus has not shown superiority over CSA-MTX and CSA-MMF combinations in randomized phase III trials, and hence is not a popular option for standard prophylactic regimen[72,74].

In 2021, Abatacept (humanised recombinant fusion protein containing extracellular domain of CTLA4 and IgG1), which blocks the costimulatory CD28/CD86 interactions, thus inhibiting T cell proliferation, was approved by FDA for GVHD prophylaxis, becoming the first FDA approved drug for GVHD prophylaxis. Abatacept in combination with CSA-MTX is the new standard of care in GVHD prophylaxis. Although, there was no difference

in incidence of GVHD, use of abatacept in combination with CSA-MTX has been shown to reduce incidence of severe grade III-IV GVHD when compared to CSA-MTX alone in a randomized phase II trial[71].

T cell depletion (TCD): TCD approaches for acute GVHD prophylaxis have been devised due to the significance of T cells in acute GVHD pathophysiology. Two methods of TCD have been employed, ex vivo TCD (donor graft is modified ex vivo before transplantation to the recipient) and in vivo TCD (T cell depleting pharmacological agents are administered to the recipient)[71].

Several strategies of ex vivo TCD have been employed: positive selection of $CD34^+$ cells using electromagnetic methods[75], or $CD34^+$ selection along with specific depletion of $\alpha\beta^+$ T cell receptor (TCR)/ CD19 (enhancing γδ T cell reconstitution), or $CD34^+$ selection along with specific depletion of T naïve cells[76]. These approaches have been shown to lower GVHD incidence, however each of these approaches pose risk of high rate of infections and disease relapse due to delayed immune reconstitution. Moreover, ex vivo TCD is not a very popular approach at many transplant centers as it requires clinical grade laboratories to process the donor graft ex vivo, lax in which may cause serious infections in recipients[71,77,78].

Hence, in vivo TCD approaches are quite popular in most transplant settings and involve administration of T cell depleting pharmacological agents like anti-thymocyte globulin (ATG), post-transplant cyclophosphamide (PTCy) or alemtuzumab along with standard cyclosporine inhibitor regimen[78]. The most extensively used antibodies for in vivo TCD are polyclonal ATGs. Rabbits are immunized with either fresh human thymocytes or the Jurkat T lymphoblastoid cell line to obtain ATGs[79]. PTCy exerts its effects by inducing the functional impairment of alloreactive T cells, whereas it has no cytotoxic effects on

hematopoietic stem cells[80]. Alemtuzumab is a monoclonal anti-CD52 antibody that specifically targets T and B cells, dendritic cells, natural killer cells, monocytes, and macrophages[81]. Amongst these three pharmacological agents, use of ATG and PTCy have shown comparable outcomes in lowering GVHD incidence in phase III randomized trials[78,82]. PTCy regimen in more popular with haploidentical allo-transplants. ATG or PTCy used in combination with standard prophylactic calcineurin inhibitors has shown lower incidence when compared to calcineurin inhibitors alone[82]. In non-randomized studies, alemtuzumab in combination with calcineurin inhibitors was associated with a low incidence of acute GVHD, but these results were not confirmed in prospective randomized trials and further investigations are necessary[83]. Another pharmacological agent that has shown promise in phase III randomized trials is vedolizumab, a monoclonal antibody that selectively antagonizes α4β7 GI integrin receptors, preventing lymphocyte trafficking to the gut. Vedolizumab along with standard prophylactic calcineurin inhibitors have shown to reduce incidence of severe GVHD, however no improvement in overall survival was observed[84].

2.8 Treatment regimens for acute GVHD

First line therapies: Consensus recommendations were recently published by the European Society for Blood and Marrow Transplantation for treatment of acute GVHD[85]. Systemic steroids (6-methylprednisolone) remain the standard first-line treatment for patients with grade II or higher acute GVHD[85]. Patients with grade I GVHD are treated only with topical steroids[86]. Oral beclomethasone is recommended in patients with acute GVHD with GI involvement[87]. Nevertheless, response rates with rates to first-line treatment with prednisone are low, and 50% patients develop steroid-refractory GVHD, which is defined as disease that progresses by day 3 or disease that fails to improve by day 7. Such poor

response rates to systemic steroids emphasizes the need for new therapeutic for acute GVHD[88].

Second- and third-line therapies: Until approval of ruxolitinib in 2020, there were no second-line treatments were available for steroid-resistant or steroid-dependent acute GVHD. treatment with ruxolitinib showed improvement in acute GVHD in twice the number of pateints when compared to those treated with systemic steroids in the phase II randomized trial that led to FDA approval of ruxolitinib as the second line treatment for steroid refractory GVHD. Despite these positive results, in the phase III randomized clinical trial, 38% of ruxolitinib-treated patients did not achieve a complete or partial response by day 28, and the durable response rate at day 56 was 39.6% (indicating that 60.4% of the patients required a third-line immunosuppressive therapy or died)[89,90]. Ruxolitinib-refractory acute GVHD progresses after 5 to 10 days of treatment, fails to improve after 14 days, or loses response at any time after initial improvement. Steroid-resistant and ruxolitinib-resistant acute GVHD treatment is unmet[91]. Various off-label drugs used to counter steroid refractory acute GVHD include, ATG, anti-TNF, MMF, anti-IL-2R, alemtuzumab, sirolimus, extracorporeal photopheresis, methotrexate, mesenchymal stem cells, decidual stromal cells and fecal microbiota transplantation are used as third line of treatment in such patients[91].

2.9 Limitations of current prophylactic and treatment regimens of acute GVHD

Limitation of prophylactic calcineurin inhibitors: Cyclosporine and tacrolimus cause nephrotoxicity, hypomagnesaemia, hyperkalemia, hypertension, tremor, baldness, hypertrichosis, and gingival hyperplasia[92]. Calcineurin inhibitors directly damage endothelium cells, causing transplant-associated thrombotic microangiopathy (TA-TMA), the worst side effect. TA-TMA mostly affects the kidney, causing proteinuria, acute renal

damage, hypertension, intestinal thrombotic microangiopathy, pulmonary hypertension, and neurotoxicity (headache, convulsions, confusion, and hallucinations) leading to withdrawal of the prophylactic regimen resulting in increased risk of acute GVHD development[93]. Calcineurin inhibitors need to be administered for a prolonged period (3-6 months) leading to poor immune reconstitution and increased risk of infections[92]. Administration of methotrexate is associated with severe mucositis and neutropenia[94]. Prophylaxis with Abatacept causes anemia, hypertension, CMV reactivation or infection, pyrexia, pneumonia, epistaxis, reduced CD4 cells, hypermagnesemia, and acute kidney injury. Patients receiving abatacept are required to be administered antiviral prophylaxis for Epstein-Barr virus infection before starting treatment and for 6 months afterward, as well as be monitored for cytomegalovirus infection/reactivation[95]. Therefore, although calcineurin inhibitors offer improvement in incidence of acute GVHD, they are associated with severe toxicities and offer no improvement in overall survival of patients undergoing allo-HSCT, limiting their clinical success.

Limitations of TCD approaches: Although CD34positive selection reduced incidence of GVHD, but it showed no improvement in reduction of recurrence rate when compared to unmodified graft. Moreover, ex vivo TCD are associated with higher risk of infectious complications, particularly of viral origin due to delayed immune recovery of $CD4^+$ cells. Furthermore, fever, chills, erythema, oxygen desaturation, headache, hepatic cytolysis, serum sickness (5–15 days after infusion), and rare systemic allergy can occur following ATG infusion. ATG slows immunological reconstitution and increases risk of viral infection[96]. By far, only PTCy regimen has shown improvement in overall survival with redcued GVHD incidence in all-HSCT recipients. Nevertheless, PTCy, like ATG, delays

immune reconstitution, increasing viral infection and has been linked to early cardiac events (within 100 days following allo-HSCT) in recipients[97].

Limitations of treatment regimens of acute GVHD: High-dose steroids and other immunosuppressive medicines raise the risk of infections as well as cause side effects of prolonged immune suppression and use of steroids. Therefore, these patients are closely monitored for invasive fungal infections, viral infections like CMV re activation, Epstein–Barr virus and influenza and are administered with prophylactic agents for these infections up to day 100 after transplantation, requiring intensive care[98,99]. Patients who have received steroids have a high risk of bacteremia and septic shock and therefore, blood culture is routinely performed and antibiotics like penicillin and streptomycin are routinely administered to these patients[100]. Administration of high-dose steroids may cause other complications like development of diabetes mellitus, osteoporosis, aseptic osteonecrosis, amyotrophy (progressive muscle wasting) and other symptoms of iatrogenic Cushing syndrome[101,102].

Summary and outlook

Despite standard prophylaxis, 50 % patients undergoing allo-HSCT develop acute GVHD, while the ones that are protected from acute GVHD suffer from the side effects of prophylactic agents or present with disease relapse. These outcomes are the bugbears of success of allo-HSCT and novel effective prophylactic regimens remain a medical need in the field of allo-HSCT.

2.10 Rationale of the study

Acute graft versus host disease (aGVHD) is a serious and potentially fatal complication that can arises following allo-HSCT. The current prophylactic and therapeutic approaches

for acute GVHD have limited success in clinical settings due to drug-related toxicity, resistance to steroids, disease recurrence, and heightened risk of infections due to prolonged immunosuppression. Despite extensive preventive measures, 50% of patients still develop acute GVHD, while those who do not experience acute GVHD are at risk of death due to disease relapse. Thus, the greatest challenge in inhibiting acute GVHD is to reduce its severity without diminishing the GVL activity of the donor graft. Consequently, there is a requirement to develop new therapeutics that can regulate the immune responses that promote graft acceptance and reduce the risk of acute GVHD development and disease relapse, to improve the success of allo-HSCT in clinics.

Aim and Objectives

3 AIM AND OBJECTIVES

AIM

To screen and develop novel phyto-pharmacological agents with immunomodulatory activities for acute GVHD prophylaxis using a phytochemical drug library.

OBJECTIVES

1) To screen phytochemical drug library for immunomodulatory compounds.
2) To understand the molecular mechanisms of immunomodulatory action of the lead compound (Juglone) *in vitro.*
3) To evaluate anti-GVHD potential of Juglone *in vivo* in murine model of allo-HSCT.
4) To assess the efficacy of Juglone in maintaining graft-versus-leukaemia (GVL) effect of the graft *in vivo* in syngeneic mice model.

Materials And Methods

4 MATERIALS AND METHODS

4.1 Overview of the workflow (Table 7).

Table 7: Workflow

Objective	**Work plan**	**Outcomes monitored**
1. To screen phytochemical drug library to identify immunomodulatory compounds.	**Primary screening** Drugs dose & time: 10µM, 2 h CFSE assay ELISA	 Leukocyte proliferation IL-2
	Secondary screening (Concentration and time dependent studies) CFSE assay Propidium iodide assay	 Leukocyte proliferation Cytotoxicity
	***Invitro* immunomodulatory activity of 5NQ** Drug dose & time: 1µM, 4 h CFSE assay PI assay Cytometric Bead array (CBA) Flow cytometry for expression of activation and exhaustion markers Anti-tumor activity	 Leukocyte proliferation Cytotoxicity Th1/Th2 and Th17 cytokines Surface expression of MHC-II, CD25, CD69, CD95 (Fas), CD152 (CTLA-4), FoxP3 Cytotoxicity of murine leukemia cell line
2. To understand molecular mechanisms of immuno-modulatory action of Juglone *in vitro.*	**Effect on cellular redox** H2DCFDA assay and CellROX orange assay MitoSOX red assay Thiol tracker violet	 Cellular ROS Mitochondrial ROS Cellular GSH levels

	Effect on inflammatory signaling	
	Immunofluorescence staining	Expression of Nrf-2
	Immunoblotting	Expression of HO1, NQO1, NF-κB, Akt, Phospho-Akt
3. To evaluate anti-GVHD potential of Juglone *in vivo* in murine model of GVHD.	**PART A:** Oral toxicity of 5NQ	
	Acute and sub-acute toxicity studies as per OECD 423 & 407 guidelines respectively)	Survival, hematological, biochemical parameters and histopathology.
	PART B	
	GVHD prophylactic efficacy of oral 5NQ in murine model of allo-HSCT	Improvement in survival, clinical scoring
	Flow cytometry	Innate and adaptive immune cell subsets, hematopoietic recovery, donor engraftment
	Cytometric Bead Array	Th1/Th2 and Th17 serum cytokines
	Histopathology	Histopathological scoring
4. To assess the efficacy of Juglone in maintaining graft versus leukemia (GVL) effect of the graft in vivo in syngeneic mice model.	Murine model of allo-HSCT supplemented with syngeneic leukemia cells	Reduction in hind limb paralysis, improvement in survival histopathology

4.2 Animal housing and maintenance

All animals were provided by the Institutional Laboratory Animal Facility of ACTREC and were maintained under specific pathogen-free conditions. All animal studies were approved by the Institutional Animal Ethics Committee (IAEC), ACTREC, as per the Committee for

the Purpose of Control and Supervision of Experiments on Animals (CPCSEA) guidelines, Government of India (IAEC/10/2021). BALB/cJ (female), C57BL/6J (male), and C57BL/6 mice with Nrf2-/-background were used in this study. All animals were 8–10 weeks of age with weight ranging between 18 to 20 g. They are housed in polypropylene cages containing corn cob as bedding material under standard conditions of 22 ± 2 °C, 55 ± 5% relative humidity, and 12 h light–dark cycles and were provided with a sterile pelleted chow and drinking water *ad libitum*. Animal studies were reported in compliance with the ARRIVE guidelines[103].

4.3 Isolation of splenic leukocytes

Animals were euthanized by CO_2 inhalation. The spleen was aseptically removed from the mice and placed in a sterile petri dish containing RPMI 1640 medium. Single cell suspensions were prepared by transferring the spleen to a 70µM cell strainer, followed by gentle mashing using a plunger. Cells were washed through the strainer with 5 ml PBS and collected in a 15 mL conical tube. The cells were centrifuged at 1200 g for 5 min, followed by washing with PBS. The pellet was dislodged by tapping, and RBC lysis was performed. The cell pellet was resuspended in RPMI 1640 medium supplemented with 10% FBS. Leukocytes were cultured in RPMI 1640 medium supplemented with 10% fetal bovine serum (FBS). Viable cells were counted on a hemocytometer using the trypan blue dye exclusion method. The number of viable cells/ml was calculated using the following formula:

No. cells/mL = average number of cells per WBC chamber x dilution factor x 10^4.

For most of the *in vitro* experiments, 1 x 10^6 splenic leukocytes were seeded per well in 24 well plate. For the transplantation procedure, 15 x 10^6 splenic leukocytes were resuspended in a total of 100µL PBS.

4.4 Isolation of Bone marrow cells

Animals were euthanized and both femurs were aseptically collected. Femurs were flushed with RPMI1640 medium using a 24 G needle and a 5 ml syringe, and a single-cell suspension was prepared using a 70µM cell strainer. The cells were then centrifuged at 1200 g for 5 min. and viable cell counts were determined as previously described. For the transplantation procedure, 5 x 10^6 cells were resuspended in 100µl PBS. For immunofluorescence staining and flow cytometric analysis, bone marrow cells were subjected to ammonium chloride RBC lysis and 5 x 10^6 cells were used for antibody staining.

4.5 RBC lysis of splenic leukocytes

Isolated splenocytes were subjected to RBC lysis to separate leukocytes from RBC cells. RBC lysis was performed using a hypotonic shock by adding sterile distilled water (4.5 mL) for 10 seconds. The isotonicity was restored by adding 0.5 ml 10x PBS[104,105]. The cells were centrifuged at 1200 g for 5 min, followed by washing with PBS. The cells were resuspended in RPMI 1640 medium supplemented with 10% FBS or phosphate-buffered saline (PBS). Viable cell counts were recorded after RBC lysis.

4.6 RBC lysis using ammonium chloride method

Ammonium chloride RBC lysis was performed prior to immunofluorescence staining of the bone marrow cells and peripheral blood samples. The bone marrow cell pellet was re-suspended in 200 µL PBS or 200 µL of blood sample was taken and RBC lysis was carried out using 2 mL of 1x ammonium chloride buffer (155 mM NH_4Cl, 12 mM $NaHCO_3$, 0.1 mM EDTA). The tubes were incubated for 10 min at room temperature. Cells were centrifuged at 1200 g for 2 min, and the cell pellet was resuspended in PBS, followed by

two washes with PBS. Finally, the cells were resuspended in RPMI 1640 medium or staining buffer as per requirement.

4.7 Treatment of leukocytes

For all *in vitro* experiments, leukocytes were transiently treated with 1µM 5NQ for 4 h unless otherwise mentioned. 5NQ was removed from the culture medium by washing leukocytes with PBS. DMSO (0.01% in PBS or RPMI 1640) was used as the vehicle control in all the experiments. Treatment with the antioxidants GSH (10mM), NAC (10mM), and the Nrf-2 inhibitor ML835 (10µM) was given for 2 h before 5NQ treatment. Mitogens concanavalin A (Con A, 2.5µg/mL) or lipopolysaccharide (LPS, 5µg/mL) was used to stimulate leukocytes.

4.8 CFSE dye dilution assay (Proliferation assay)

Leukocytes were stained with CFSE (5µM, 10 min, 37 °C), followed by transient treatment with either vehicle or different concentrations of 5NQ for 4 h. Cells were washed twice with PBS and 1 x 10^6 cells were seeded and stimulated with Con A, LPS, or CD3/CD28 beads for 72 h and incubated at 37 °C in a 95% air, 5% CO_2 atmosphere. After 72 h, the cells were harvested, resuspended in 200µL PBS and analyzed using an Attune NxT flow cytometer (Thermo Fisher Scientific, Inc.). To evaluate the proliferation of $CD4^+$ T cells, leukocytes were harvested after 72 h and stained with CD3ε PE-Cy7 and CD8α APC to gate $CD4^+$ T cells before acquisition on a flow cytometer. Cell proliferation was evaluated using CFSE dilution after 72 h of culture. The fluorescence intensity of unstimulated vehicle-treated cells (parent population) was considered as the control, and daughter cells were defined as cells with reduced fluorescence intensity with respect to the parent population. Proliferation is expressed as the percentage of daughter cells.

4.9 Propidium iodide viability assay

The effect of 5NQ treatment on leukocyte viability was studied using propidium iodide assay. Briefly, 1 x 10^6 leukocytes were transiently treated with vehicle or different concentrations of 5NQ for 4 h. Cells were washed twice and incubated for 24 h at 37 °C in a 95% air and 5% CO_2 atmosphere. After 24 h, cells were washed twice with PBS and 10µg/mL propidium iodide solution was added 5 min before analyzing the cells on the flow cytometer. The percentage of propidium iodide (PI)-positive cells was calculated.

4.10 Protein expression studies

1. *Whole cell lysate preparation and nuclear fractionation* Leukocytes (40 x 10^6) were treated with vehicle or 1µM 5NQ for 3 h, followed by stimulation with Con A for 4 h. NAC treatment was given 2 h prior to 5NQ treatment. The final treatment groups were as follows.

   1. Vehicle control (0.01 % DMSO in complete RPMI 1640 medium)
   2. Con A (vehicle-treated cells stimulated with Con A for 4 h).
   3. 5NQ (treatment with 1µM 5NQ for 3 h)
   4. 5NQ + A (1µM 5NQ for 3 h, followed by stimulation with Con A for 4 h).
   5. NAC (1mM NAC for 2 h)
   6. NAC + A (1mM NAC for 2 h followed by stimulation with Con A for 4 h)
   7. NAC + 5NQ + A (1mM NAC for 2 h followed by treatment with 1µM 5NQ for 3 h followed by stimulation with Con A for 4 h)

   After incubation, the cells were washed with ice-cold PBS and suspended in 0.1 ml lysis buffer [50mM Tris-HCl, 120mM NaCl, 10mM EDTA, 20mM sodium fluoride, 25mM sodium orthovanadate, 0.5% NP40, and protease and phosphatase inhibitor cocktail] (Sigma-Aldrich, St.Louis, MO, USA) and incubated on ice for

30 min with intermittent mixing. The cells were then centrifuged at 7000 g for 15 min. The supernatant was taken as the whole cell lysate and stored at -80˚C till further use. For nuclear fractionation, the pellet was resuspended in 50µl of lysis buffer and briefly sonicated at 20% amplitude for 10-15 seconds (to lyse the nuclei and shear chromatin) and incubated on ice for 30 min with intermittent mixing followed by centrifugation at 7000 g for 15 min. The supernatant was taken as nuclear cell lysate and stored at -80˚C till further use.

2. *Sodium dodecyl polyacrylamide gel electrophoresis:* Whole cell and nuclear cell lysates were separated on 8 and 10% sodium dodecyl sulphate polyacrylamide gel (SDS-PAGE) using Tris-Glycine buffer (25 mM Tris-Cl, 250 mM Glycine and 0.1% SDS pH 8.8) The protein estimation was performed by Bradford method and the samples for gel loading were made in 2x SDS-loading buffer (50mM Tris-Cl pH 6.8, 20% v/v glycerol, 4% SDS, 2% β-mercaptoethanol, and bromophenol blue) and heated at 95 °C for 10 min. Electrophoresis was performed at a constant current of 15 mA in the stacking gel and 25 mA in the resolving gel until the tracking dye bromophenol blue reached the bottom. The gels were then transferred onto PVDF (polyvinylidene difluoride) membranes for western blot analysis.
3. *Western Blotting and development:* Proteins (50 µg for whole cell lysate and 10µg for nuclear cell lysate) from the SDS-PAGE gel were transferred onto a 0.05µM PVDF membrane, which was preactivated in absolute methanol for 1 min, followed by washing with MilliQ water. The gel was equilibrated in 1x transfer buffer and sandwiched between three sheets of Whatman filter, inserted in the transfer assembly tank (Trans-Blot Cell, Bio-Rad), and the transfer was carried out at 300 mA for 1.5 hours under cold conditions. The transfer of proteins was verified by staining the membrane with fast green dye (0.05% in destaining solution) followed

by de-staining until a clear band appeared. This was followed by washing with water, and the membrane was scanned and stored in MilliQ water at approximately 4 °C. The proteins transferred onto the PVDF membrane were probed using specific antibodies, as listed in Table 8. Briefly, the membrane was blocked in blocking buffer - 5% BSA in 1x TBST (Tris-buffered saline with Tween-20) for 1 hour at room temperature on orbital shaker. The membrane was then treated with the primary antibody prepared in 1% BSA in TBST using the recommended and standardized dilution for overnight incubation at 4 °C on an orbital shaker. The membrane was thoroughly washed thrice with 1x TBST for 10 min each at room temperature. The membrane was then incubated with a horseradish peroxidase (HRP)-conjugated secondary antibody in 3% bovine serum albumin (BSA) in 1x TBST for 1 h at room temperature on an orbital shaker. After incubation, the membrane was washed vigorously three times with 1x TBST at room temperature and developed using the Bio-Rad's Clarity Max. The signal was detected and captured in Biorad's Chemidoc analyzer using Image lab software (version 6.0).

4.11 Immunofluorescence Microscopy for Nrf2 expression

Leukocytes were treated with the vehicle or 1µM 5NQ for 4 h at 37 °C in a 5% CO_2 atmosphere. The cells were washed twice with PBS and fixed with fixation buffer (PBS with 1% formaldehyde) for 1 h on ice. Cells were washed again and permeabilized (PBS containing 0.1% Triton X100) for 10 min at room temperature and then incubated with anti-NRF2 rabbit monoclonal IgG primary antibody overnight at 4 °C (1:100 dilution in FACS buffer). The following day, the cells were washed three times with PBS and incubated with Alexa Flour 488 conjugated secondary antibody (1:200 dilution in FACS buffer) for 1 h at room temperature in the dark. Cells were counterstained with Hoechst (10µg/mL) for 30

min, washed twice, mounted on a glass slide, and examined using an LSM 780 Carl Zeiss confocal microscope at 630x with a 1x-3x digital zoom. Sections of 0.5µm of the entire cell were captured, and images were represented as a projection of the entire Z-stack.

Table 8:Antibodies used for immunoblotting

Antibody	Source/ Cat no. and RRID	Blotting conditions
Anti-HO-1 rabbit monoclonal IgG (clone: E9H3A)	Cell Signaling Technology, Cat no. 86806.	Blocking: 5 % BSA Dilution: 1:1000 in 1% BSA
Anti-NQO1 rabbit monoclonal IgG	Cell Signaling Technology, Cat no. 62262.	Blocking: 5 % BSA Dilution: 1:1000 in 1% BSA
Anti-β-actin mouse monoclonal IgG	Santa Cruz, Cat no. sc-47778.	Blocking: 5 % BSA Dilution: 1:2000 in 1% BSA
Anti-NF-κB p65 rabbit monoclonal IgG (clone: D14E12)	Cell Signaling Technology, Cat no. 8242.	Blocking: 5 % BSA Dilution: 1:1000 in 1% BSA
Anti- Phospho-Akt (Ser473) rabbit monoclonal IgG (clone: D9E)	Cell Signaling Technology Cat no. 4060, RRID: AB2315049	Blocking: 5 % BSA Dilution: 1:1000 in 1% BSA
Anti- Akt (pan) rabbit monoclonal IgG (clone: 11E7)	Cell Signaling Technology Cat no. 4685.	Blocking: 5 % BSA Dilution: 1:1000 in 1% BSA
Anti- Histone H3 rabbit monoclonal IgG (clone: D1H2)	Cell Signaling Technology Cat no. 4499.	Blocking: 5 % BSA Dilution: 1:1000 in 1% BSA
Anti-rabbit IgG, HRP-linked Antibody	Cell Signaling Technology, Cat no. 7074.	Dilution: 1:4000 in 3% BSA

4.12 Cell culture of murine leukaemia cells

The murine leukaemia cell lines EL4 (RRID: CVCL0255) and A20 (ATCC, Cat. TIB-208; RRID: CVCL1940) were used in this study. All cell lines were maintained in RPMI 1640 medium supplemented with sodium bicarbonate, L-glutamine, and non-essential amino acids. The cells were cultured at 37 °C in a 5% CO_2 atmosphere supplemented with 10%

FBS and 100units/ml penicillin and 100 mg/mL streptomycin. The medium was changed every alternate day by centrifuging the cells at 500 g for 5 min and resuspending the pellet in a fresh medium.

4.13 Immunofluorescence staining for flow cytometry analysis

For the analysis of cell surface markers, leukocytes were washed twice with FACS buffer (PBS containing 0.1% BSA). To block non-specific staining, cells were resuspended in blocking buffer (PBS with 1% BSA) and incubated for 15-20 mins at 4 °C. Cells were washed once with FACS buffer and incubated with fluorochrome-tagged antibodies for 30 min at 4 °C, followed by washing with FACS buffer. For the analysis of intracellular markers (FoxP3, Nrf-2 and Granzyme B), cells were first stained with antibodies against extracellular markers, as mentioned above, after which the cells were washed twice with FACS buffer and fixed using fixation buffer (FACS buffer with 1% formaldehyde) for 10 min at room temperature or for 1 h on ice. The cells were washed again and permeabilized using permeabilization buffer (FACS buffer containing 0.1% Triton X-100) for 10 min at room temperature (RT), incubated with fluorochrome-tagged antibodies for 45 min at RT, and washed with FACS buffer. Flow cytometry was performed using an Attune NxT Flow Cytometer (Thermo Fisher Scientific Inc.). The list of fluorochrome-conjugated monoclonal antibodies, along with the manufacturer's details and dilutions, are described in Table 9**.** FlowJov10 (RRID:SCR008520) software was used to analyze the flow cytometry data.

4.14 Cytokine analysis

Leukocytes (1 x 10^6) were seeded in 24 well plate after transient treatment with vehicle or 5NQ (0.5 and 1µM for 4h) followed by stimulation with Con A. After 24 h, cell supernatants were collected and centrifuged at 1200 g for 5 min. To estimate serum

cytokine levels, blood from each mouse was collected into microcentrifuge tubes by puncturing the orbital plexus. Blood was allowed to clot for 1 h at 4 °C and the tubes were centrifuged at 600 g for 10 min. The serum was separated and stored at -80 °C until further analysis. Cytokine concentrations (IL-2, IL-4, IL-6, IFN-γ, TNF, IL-10, and IL-17A) were measured in the supernatant or sera using a cytometric bead array (CBA Becton-Dickinson, NJ, USA) ™. The analysis was performed according to the manufacturer's instructions. Briefly, cell supernatants or sera were incubated with mixed capture beads, followed by the addition of the detection antibody, and incubated at room temperature for 3 h according to the manufacturer's instructions. Samples were washed, acquired on a BD FACS Aria, and analyzed using the FCAP array software.

4.15 Murine model of allo-HSCT

A murine model of allo-HSCT based on complete MHC-I mismatch [recipient- female BALB/cJ mice (H-2kD) and donor-male C57BL/6J mice (H-2kB)] was utilized. Female BALB/cJ mice (8–10 weeks old) were acclimatized to individually ventilated cages (IVC) for 1 week before transplantation and maintained in IVC cages until completion of the experiment. Mice were irradiated with a sublethal dose of 6.5 Gy on a linear accelerator. After 24 h, mice were injected with 5×10^6 bone marrow cells and 15×10^6 splenocytes obtained from male C57BL/6 donor mice (8-10 weeks old). The overview of transplantation procedure is presented in Figure 10.

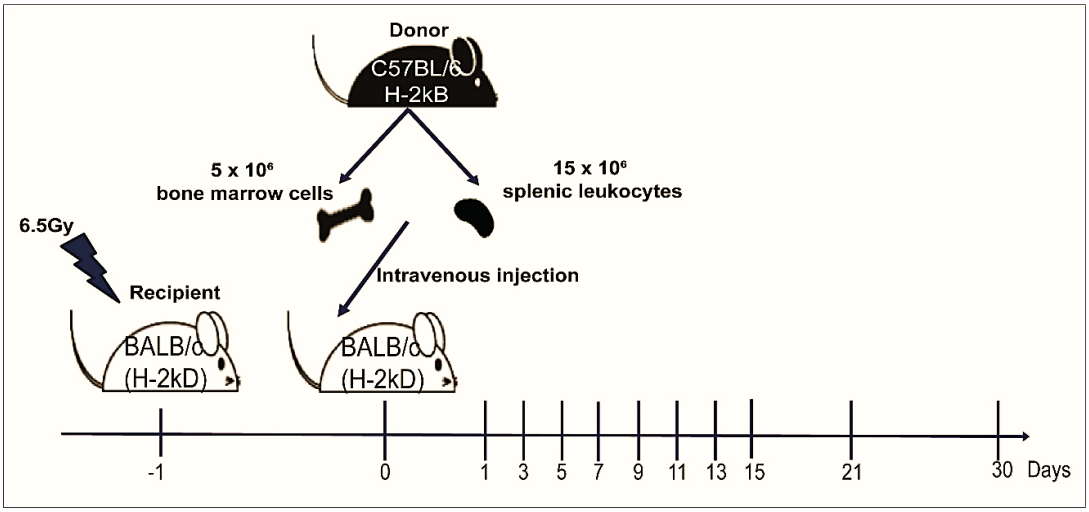

Figure 10: Overview of the workflow for transplantation procedure for induction of GVHD. The murine model is based on MHC class I mismatch, the recipient is BALB/c female mice that express H2kD MHC-I antigen, whereas the donor is C57BL/6 male mice that express H2kB MHC-I antigen. The days before transplantation are numbered with a negative sign, whereas the days after transplantation are numbered with a positive sign. The day of the transplantation is numbered as day 0.

4.16 Data and statistical analyses

For all in *vitro* analyses, statistical analysis was performed only for studies in which each group size had $n \geq 5$ independent values. The *in vivo* studies were designed to generate groups of equal size ($n \geq 5$). GraphPad Prism version 8.2.0 (RRID:SCR_002798) was used for statistical analysis, and the data are presented as the mean ± standard error of mean (SEM). All data were subjected to Kolmogorov–Smirnov normality test, and comparisons of two datasets were made using two-tailed unpaired t-test for parametric data and Mann-Whitney test for non-parametric data. Multiple datasets were compared using one-way ANOVA, and Bonferroni post hoc tests. Two-way analysis of variance (ANOVA) with Bonferroni correction was applied to evaluate the time and concentration or dose dependent differences between groups. Survival data were analyzed using the Mantel-Cox log rank test and graphs were generated using the Kaplan-Meier method. Statistical significance was set at $p < 0.05$.

Table 9: Antibodies used for immunofluorescence staining for flow cytometry

Antibody	**Source**	**(Cat no.)**	**Final dilution**
Anti-mouse CD3ε APC-Cy7 (allophycocyamin)-cyanine7) (145-2C11)	BD Biosciences	557596	0.5:100
Anti-mouse CD3ε PE-Cy7 (phycoerythrin-cyanine7) (17A2)	BioLegend	100220	0.5:100
Anti-mouse CD44 APC-Cy7, (IM7)	BD Biosciences	560568	1:100
Anti-mouse CD4 PerCP-Cy5.5 (peridinin chlorophyll protein-cyanine5.5) (RM4.5)	BD Biosciences	550954	0.5:100
Anti-mouse CD45 PE-Cy7 (phycoerythrin-cyanine7) (30-S11)	BD Biosciences	553081	0.5:100
Anti-mouse CD8α FITC (fluorescein isothiocyanate) (53-6.7)	BD Biosciences	553030	0.5:100
Anti-mouse CD8α APC (53-6.7)	BioLegend	100712	0.5:100
Anti-mouse CD11b FITC (M1/70)	BioLegend	101205	1:100
Anti-mouse H-2Kd PE (SF1-1.1),	BD Biosciences	553566	0.5:100
Anti-mouse H-2Kb FITC (AF6-88.5)	BD Biosciences	562002	0.5:100
Anti-mouse CD25 BV421 (brilliant violet) (PC61)	BD Biosciences	562606	1:100
Anti- mouse FoxP3 AF647 (alexaflour-647) (MF23)	BD Biosciences	560401	5µl/tube
Anti- mouse IA/IE PE (M5/114.15.2)	BD Biosciences	557000	1:100
Anti- mouse CD152 PE (UC10-4F10-11)	BD Biosciences	553720	2:100
Anti- mouse CD62L APC (MEL-14)	BD Biosciences	553152	1:100
Anti- mouse Ly-6C APC (AL-21)	BD Biosciences	560595	1:100
Anti- mouse CD95 APC R700 (Jo2)	BD Biosciences	565130	2:100
Anti- mouse Granzyme B FITC (GB11)	BioLegend	515403	5µl/tube
Anti- mouse Ly-6A/E (Sca-1) FITC (W18174A)	BioLegend	160907	2µl/tube
Anti- mouse CD117 (c-KIT) APC	BioLegend	105812	5µl/tube
Mouse hematopoietic lineage antigens (Lin) cocktail pacific blue [CD3 (17A2), Ly-6G/Ly-6C (RB6-8C5), CD11b (M1/70), CD45R/B220 (RA3-6B2), TER-119/Erythroid cells (Ter-119)	BioLegend	133310	20µl/tube
Anti-NRF2 rabbit monoclonal IgG (clone E5F1A,)	Cell Signaling Technology	20733	1:100

Table 10: Composition of 10X ammonium chloride buffer

Component	**Weight**
NH4Cl (ammonium chloride)	8.02gm
NaHCO3 (sodium bicarbonate)	0.84gm
EDTA (disodium)	0.37gm
Dissolve in 100ml double distilled water. Store at 4˚C Working solution: prepare 1X solution by diluting 10 ml of 10X stock with 90 ml double distilled water.	

Table 11: Composition of lysis buffer for cell lysis

Component	**Stock**	**Volume**
50mM Tris-HCl,	1M Tris-HCl	500 µl
120mM NaCl,	1M NaCl	1.2 ml
10mM EDTA,	0.2 M	500 µl
20mM sodium fluoride,	1 M	200 µl
25mM sodium orthovanadate,	0.5 M	500 µl
0.5% NP40,	-	50 µl
Protease and phosphatase inhibitor cocktail	100X	100 µl
MQ water		6.95 ml

Table 12: Composition of SDS-PAGE gels

Components	**10% resolving**	**8% resolving**	**4% stacking**
MQ Water	3.2 ml	3.7 ml	3 ml
30% Acrylamide	2.67 ml	2.13 ml	0.67 ml
1.5M Tris pH 8.8	2 ml	2 ml	-
1M Tris pH 6.8	-	-	1.25 ml
10% SDS	80 µl	80 µl	50 µl
10% APS	80 µl	80 µl	50 µl
TEMED	8 µl	8 µl	5 µl
Total volume	**10 ml**	**10 ml**	**5 ml**

Table 13: Composition of SDS-Running Buffer

Component	**Weight**
Glycine	14.2 g
Tris	3.03 g
SDS	1 g
Make final volume to 1 L with distilled water	

Table 14: Composition of 1X Transfer buffer

Component	**Weight**
Glycine	14.2 g
Tris	3.03 g
Methanol	200 ml
Make final volume to 1L with distilled water and chill buffer in -20°C until use.	

Objective 1

5 OBJECTIVE 1

5.1 BACKGROUND

Immunomodulation

The term immunomodulation encompasses all interventions that alter the immune response to gain therapeutic benefit. Therapeutic immunomodulation involves adjusting the inherent immune responses to a desired level by immunostimulation, immunosuppression, or induction of immunologic tolerance. The immunostimulatory approach has been widely used in the fields of cancer therapeutics, immunodeficiency disorders, and prevention of infections (vaccination). Immunosuppressive immunomodulation has been applied to control autoimmune disorders and prevent graft rejection after organ transplantation. Induction of immune tolerance has been investigated for autoimmune diseases and the prevention of graft-versus-host disease (GVHD) after allogeneic and haplo-identical hematopoietic stem cell transplantation (HSCT) [106–108].

Immunomodulatory therapy was founded by Dr. Willaim Coley in the 19th century. He reported that the direct injection of streptococcal bacteria into a patient's tumor led to spontaneous regression of cancer.[109] It is now known that Coley exploited various aspects of the immune system to target cancer cells. Although the exact mechanism cannot be identified, we know today that bacterial toxins can induce a strong cytokine response and activate innate immune cells, which can then destroy cancer cells. In 1959, Lloyd et al. showed that the BCG vaccine could be used to treat cancer. Currently, the US Food and Drug Administration (FDA)-approved BCG vaccine for the treatment of bladder cancer, lymphoma, and melanoma [110].

Vaccination is a mode of immunomodulation wherein, there is induction of immunological memory for an infection through specific attenuated pathogens, or DNA from the pathogen, resulting in a prompt protective immune response upon infection.[106,111]. Furthermore,

immunomodulatory therapy has been applied to fight active infections, allergies, and autoimmune diseases, which involves altering the immune response at various levels. The strategy here is mainly to induce an immunosuppressive effect or a tolerogenic response. The major stages of the immune response that can be modulated are 1) antigen processing and presentation to T cells, 2) T cell activation, and 3) T cell proliferation and differentiation. Thus, various drugs and cell mediated therapies used today to counteract above mentioned maladies, modulate or suppress one or more of the above stages of immune activation [106,110,112]. A few examples of drugs that are currently being used in clinical practice are listed in Table 15.

Table 15: Immunomodulators used in clinical practice [106].

Immunomodulatory agent	Mechanism of action	Clinical use
1. Immunomodulators that interfere with antigen presentation		
CTLA-4 Ig (Abatacept, Ipilimumab)	Fusion molecule that binds CD80 and CD86 on the surface of APCs. Blocks co-stimulation of T-cell	Immunotherapy for melanoma, renal cell carcinoma, acute GVHD prevention.
Natalizumab (anti α-4 integrin)	Prevents the interaction between α-4 integrin on the surface of inflammatory cells and VCAM-1 on vascular endothelial cells	Treatment of multiple sclerosis and Crohn's disease.
2. Immunomodulators that interfere with T-cell activation		
Cyclosporine A	Prevents activation of nuclear factor of activated T cells (NFAT). This blocks the activation of T cells	Prevention of organ rejection and GVHD. Rheumatoid arthritis and psoriasis
Tacrolimus (FK506)	Similar to cyclosporine A	Prevention of organ rejection and of GVHD. Atopic dermatitis.
3. Immunomodulators that interfere with T cell proliferation		
Rapamycin (Sirolimus)	Binds to FKBP, inhibits mTOR, resulting in cell cycle arrest between G_1 and S phase.	Prevention of organ rejection, prophylaxis of GVHD and treatment of steroid refractory GVHD.
Mycophenolate mofetil (MMF)	Antimetabolite selectively inhibits purine synthesis in lymphocytes.	Prevention of organ rejection, prophylaxis of GVHD
Methotrexate	dihydrofolate reductase inhibitor	Induction and maintenance therapy during organ transplantation, prevention of GVHD, rheumatoid arthritis and vasculitis
4. Immunomodulation by lymphocyte depletion		
Anti-thymocyte immunoglobulin	Polyclonal immunoglobulin	Aplastic anaemia, acute rejection in renal transplantation
Alemtuzumab (Campath-1H)	Humanized monoclonal antibody directed against CD52	Antineoplastic agent for chronic lymphocytic leukaemia; refractory rheumatoid

		arthritis and vasculitis. GVHD prophylaxis.
5. Other immunomodulatory agents		
Corticosteroids	Pleotropic in action. Steroids bind to glucocorticoid response elements in the promoter regions of cytokine genes. Prevent T-cell recruitment and activation.	Basic immunosuppressants used to treat varied autoimmune diseases, prophylaxis of GVHD.
Infliximab	Chimeric antibody against human TNF-α. Blocks TNF-α action	Used in Crohn's disease (an autoimmune colitis). In allo-HSCT it has been used to treat steroid-refractory GVHD.

Immunomodulation as a strategy to combat GVHD

One of the major challenges in the field of allogeneic HSCT is the prevention of GVHD while maintaining the graft-versus-leukemia (GVL) effects of donor cells. The current understanding of GVHD pathophysiology has helped to establish that immunosuppression is not the best strategy for GVHD prophylaxis, as it increases the risk of secondary infections and leukemia relapse [113–115]. It is well understood that the prevention of GVHD requires alleviation of both innate and adaptive immune responses, along with maintenance of the anti-tumor activity of donor cells. Many novel strategies are currently under preclinical and phase I development. However, these strategies involve modulation of either of the following immune responses:1) reducing donor alloreactivity, 2) inducing peripheral tolerance, and 3) decreasing target organ susceptibility to allogeneic immune responses [116,117].

Phytochemicals - a plethora of possibilities: Plants have been used to treat various diseases since ancient times. Ayurveda, Traditional Indian Medicine and Traditional Chinese Medicine remain the most ancient (4500 BC) practices that have led to the foundation of using plants for therapeutic purposes. Current knowledge of medicinal herbs has been derived from contemporary sciences and has driven the drug discovery process in the modern world [118]. Before the 19th century, extracts from plants were used as herbal

medicines and were administered in the form of powders, decoctions, tinctures, and other formulations. The advent of analytical chemistry has led to the isolation of active compounds from medicinal plants. Isolation of morphine from opium was one of the earliest examples of the isolation of a phytochemical from a plant. This was followed by various other drugs such as, digitoxin, and quinine [118,119].

Phytochemicals are broadly defined as plant secondary metabolites that have potential health benefits. Phytochemicals interact with biological molecules and exhibit antioxidant, anti-inflammatory, anticancer, antimicrobial, antithrombotic, and immunomodulatory activities. Phytochemicals are diverse in their chemical nature and are generally present in small amounts in specific parts of plants. Systematic investigations can help identify the potential pharmacological and health-promoting effects of phytochemicals in humans [120]. Even when new chemical structures are not found during drug discovery in medicinal plants, known compounds with new biological activities can provide important drug leads. In the last four decades, 1881 new drugs have been approved by the US Food and Drug Administration (FDA). According to the study conducted by Newman et al., approximately 53% of the drugs were natural compounds, natural compound derivatives, or natural compound mimics (Figure 11) [119].

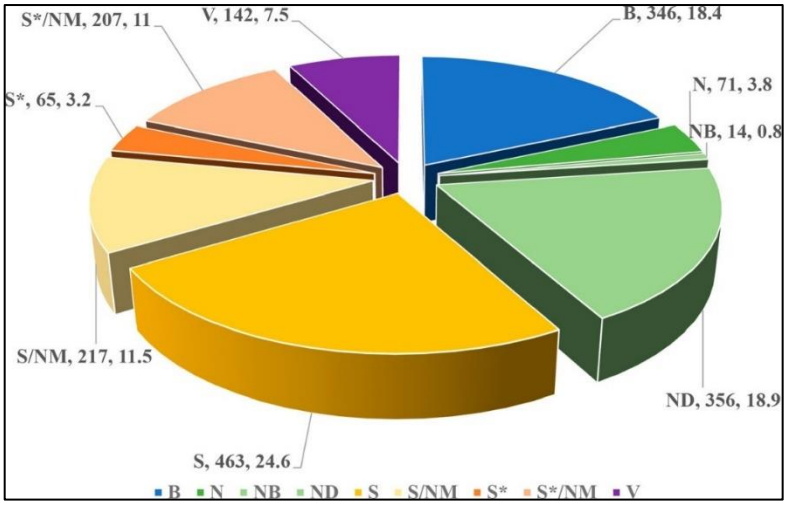

Figure 11: All newly approved drugs, 01JAN81 to 30SEP19; n = 1881. B, biological macromolecule; N, unaltered natural product; NB, botanical drug (defined mixture); ND, natural product derivative; S, synthetic drug; S*, synthetic drug (NP pharmacophore); V, vaccine; S/NM, mimic of the natural product [119].

Examples of phytochemicals used in clinical practice are listed in Table 16.

Table 16: Few clinically useful phytochemicals [121].

Drug	Class of drug	Plant source	Disease	Reference
Apomorphine	Dopamine receptor agonist	*Papaver somniferum*	Parkinsonism	Deleu et al., 2004
Arteether	Sesquiterpene trioxane lactone	*Artemisia annua*	Malaria	van Agtmael *et al*., 1999
Galantamine	Amaryllidaceae alkaloid	*Galanthus woronowii*	Alzheimer's	Heinrich and Lee Teoh, 2004
Nitisinone	Mesotrione	*Callistemon citrinus*	Hepatorenal tyrosinemia	Das, 2017
Paclitaxel	Taxane diterpene	*Taxus brevifolia Nutt.*	Cancer	Wani *et al*., 1971
Tiotropium	Muscarinic receptor antagonist	*Atropa belladonna*	Asthma and COPD	Mundy and Kirkpatrick, 2004

COPD: chronic obstructive pulmonary disease.

Phytochemicals as immunomodulators: A large number of phytochemicals have been studied for their immunomodulatory activities, with promising results. They have been reported to modulate the immune system by enhancing the activity of immune cells, such as natural killer cells, T-cells, and B-cells, while decreasing inflammation. Polyphenols,

flavonoids, and terpenoids are major classes of phytochemicals that have been studied for their immunomodulatory effects. Flavonoids are among the most diverse groups of phytochemicals, with many therapeutic properties, including immunomodulation. A few extensively studied flavonoids include quercetin, epigallocatechin gallate (EGCG), and resveratrol [122–124]. Currently, quercetin is being developed as a supplement or adjuvant therapy for various disease conditions like Covid-19 upper respiratory tract infections [125–127]. Epigallocatechin gallate (EGCG) is a potent antioxidant and anti-inflammatory molecule is currently undergoing clinical trials for the treatment of multiple sclerosis [128]. Resveratrol is a phytoalexin that has shown to possess anti-inflammatory and immunomodulatory effects and has been clinically tested for various neurodegenerative diseases such as Alzheimer's disease [129,130].

β-carotene and lycopene a class of carotenoids with immunomodulatory and antioxidant properties have been shown to modulate the immune system by enhancing the function of T cells and natural killer cells. [131,132]. Curcumin, isolated from *Curcuma longa*, has shown potent immunomodulatory activity in various autoimmune diseases, such as Systemic Lupus Erythematosus (SLE), rheumatoid arthritis, and multiple sclerosis. [133]. Withanolides from *Withania somnifera*, have been used for their anti-inflammatory activities for thousands of years. They are known to inhibit inflammatory mediators such as NF-κB, JAK/STAT, AP-1, PPARγ, Hsp90, Nrf2, and HIF-1, and further inhibit inflammatory cytokines. This ability has proven beneficial in various autoimmune disorders such as inflammatory bowel disease, diabetes, rheumatoid arthritis, and neurodegeneration [134]. Overall, the literature suggests that phytochemicals have demonstrated a significant immunomodulatory potential.

Phytochemicals have been shown to modulate immune responses through one or more mechanisms [108,120,123,135] listed below

1. Regulation of cytokine production
2. Modulation of immune cell activation, proliferation, and differentiation
3. Enhancement of phagocytic activity
4. Inhibition of molecular signals that mediate inflammation.
5. Induction of tolerogenic immune cells

Due to their diverse mechanisms of action phytochemicals serve as promising candidates for the development of immunomodulatory drugs. Further research is needed to fully understand their therapeutic potential as novel immunomodulatory molecules.

Drug library screening is an important tool for drug discovery and development and takes an average of 10-15 years and costs approximately 800 million dollars [136]. Drug research comprises various stages and is powered by the amalgamation of knowledge from a wide range of disciplines, such as chemistry, biology, medicine, pharmacology, mathematics, computing, and molecular modelling. The most laborious and time-consuming step in drug development is lead identification (the first step), followed by lead optimization (involving medicinal and combinatorial chemistry), lead development (including pharmacology, toxicology, pharmacokinetics [absorption, distribution, metabolism, excretion], and drug delivery), and clinical trials (Figure 12) [137].

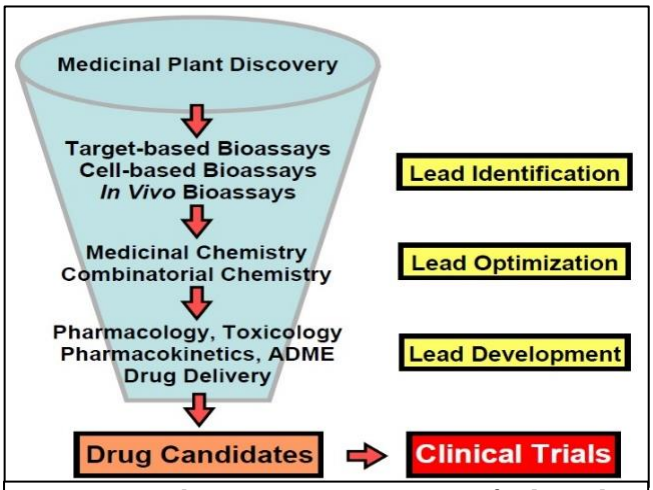

Figure 12: Schematic representation of plant drug discovery and development. Adapted from [433]

The traditional approach of drug development uses ethnopharmacological knowledge about natural compounds and tests their efficacy against various molecular targets; however, this approach has a high risk of failure and thus is not very cost effective. In the

beginning of the 19th century, advancements in molecular modelling and computational approaches led to the design of synthetic drugs and the development of designed drug libraries based on known drug scaffolds. Screening was performed manually, with approximately several hundred samples screened per week against a limited number of targets using receptor-binding assays. Furthermore, the development of automated analyzers and robotics has led to a reduction in screening time for these compounds. The development of high-density microplates, homogeneous assays, high-performance microliter dispensers, and laboratory automation has led to the development of high-throughput screening as a tool for rapid drug discovery and development. The exorbitant costs of high-throughput screening are further reduced via miniaturization of assay formats and fewer handling steps. This resulted in reduction in time required from lead discovery to lead optimization [137–139]. Currently, high-throughput screening of drug libraries has become an integral part of drug discovery and development processes for all pharmaceutical companies. Drug library screening is a constantly developing field with newer technologies such as genomics, proteomics, CRISPR, and machine learning being integrated into it, for the development of clinically effective and safe drugs[140–142].

Drug library screening involves testing large numbers of drug compounds in a systematic and automated manner to identify compounds that exhibit a particular effect in a given system. The compounds can be screened using a variety of assays, such as ligand-receptor binding assay, inhibition or activation of an enzyme or enzyme system, interaction with a particular protein or nucleic acid of interest, cytotoxicity, and effect on signal transduction and responses. Recent advances in genetic engineering have led to the use of genetically modified organisms, such as *D. melanogaster* and *C. elegans,* to identify compounds with therapeutic potency *in vivo*. In recent years, advances in computational methods and

machine learning have begun to play an increasingly important role in drug library screening, allowing the identification of novel drug targets and the design of more effective and selective compounds [143]. The approaches currently employed for drug discovery and development are summarized in Figure 13.

The US National Cancer Institute's (NCI) Natural Product Repository is one of the world's largest and most diverse collections of natural products containing over 230,000 unique extracts derived from plant, marine, and microbial organisms collected from biodiverse regions. This collection of natural products includes perfectionated extracts from various biological sources however, it does not consist of pure isolated compounds from these sources, thus providing an opportunity to identify and characterize novel compounds from these extracts[144]. Today, various biotechnology companies offer different collections of drug libraries or even customize them for academic screening purposes, such as libraries of FDA-approved drugs, disease-specific libraries, pathways, target-specific libraries (tyrosine kinase inhibitors, JAK-STAT inhibitors, cytokine agonists, and antagonists), mitochondria-targeted drug libraries, metabolism-targeted libraries, and natural compound libraries.

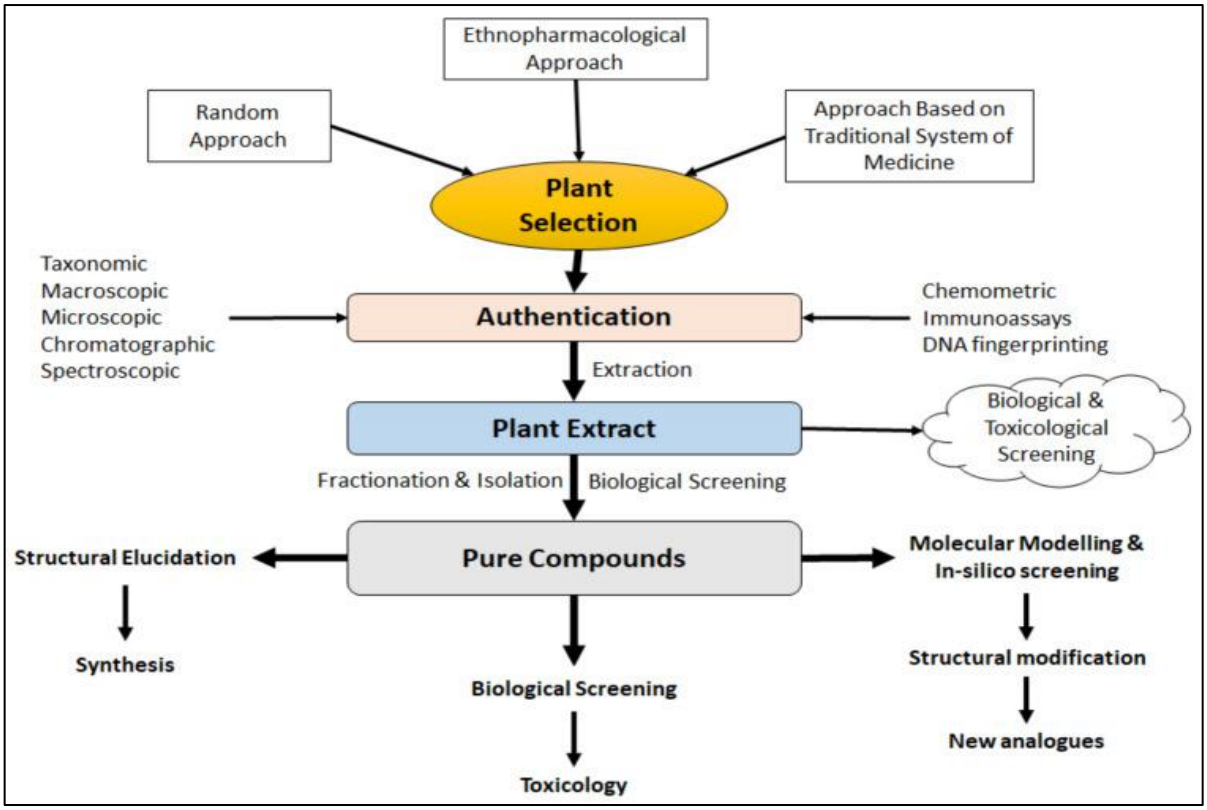

Figure 13: Overall approaches in modern drug discovery and development[145].

These predefined libraries are provided with basic information about their constituents, the source from which each compound was isolated, structure, solubility, target, activity, IC50 value, and biological activity description. In addition, these libraries may contain many rare natural products with extremely high unit prices, making them a cost-effective method for drug screening. Thus, drug libraries provide a platform for lead identification that is time- and cost-effective [143,146].

Screening strategies for immunomodulatory compounds: Strategies used for screening immunomodulatory compounds consist of immune assays to study the activity of various cells of the immune system. Some popular assays used to screen compounds with the potential to affect immune function are listed below.

a. *Evaluation of mitogen (eg. concanavalin A, lipopolysaccharide, phytohemagglutinin) induced proliferation of lymphocytes or a particular subset of*

immune cells (T cells, B cells, etc.). Lymphocyte proliferation has been assessed using 3H-thymidine or bromodeoxyuridine (BrdU) incorporation assays or carboxyfluorescein succinimidyl ester (CFSE) dye dilution assays using imaging or flow cytometric techniques [147–149].

b. *Evaluation of immune cell activation:* Activation of immune cell subsets has been studied by evaluating the expression of specific molecular markers that indicate the activation of these cells. For example, T-cell activation has been studied using CD25, CD69, and lymphoblast formation[148,150].

c. *Evaluation of cytokine secretion:* The secretion of a particular cytokine by an immune cell subset can indicate its activation status. Examples include IL-2 secretion by T cells, IL-12 secretion by dendritic cells, and TNF- and IL-6 secretion by macrophages[150,151].

d. *Evaluation of immune activity via mixed lymphocyte reactions:* Autoimmune and anti-tumour responses have been widely studied using this assay. The immune activity is generally measured using imaging or flow-cytometric techniques [147,148,152].

e. *Expression of molecular markers of inflammation:* With the advancement of genetic engineering, fluorimetry, and luminometry, the expression of proteins can be easily quantified with high accuracy. These techniques have been pivotal in studying the activation of proteins, such as NFκB and JAK-STAT, which play a central role in regulating immune responses. Moreover, these assays have been used to study cytokine secretion following mitogen stimulation. [147,153,154].

Immunomodulatory drugs were screened using *in vitro* and *in vivo* systems. *In vitro* systems mainly include purified macromolecules against which the action of the drug

is to be tested (targets of monoclonal antibodies, receptors, enzymes, etc.) or cell-based assays which include the use of lymphocyte populations acquired from human peripheral blood, murine splenocytes, bone marrow, thymus, blood, or isolated immune cell subsets. Various *in vivo* model systems have also been used to study immunomodulatory functions, including *C. elegans, D. melanogaster*, zebrafish, murine models, and rodent models [155–157].

Strategy for primary and secondary screening of phytochemical drug libraries

Clonal expansion of T cells against allo-antigens is a key event in GVHD pathogenesis. Many innate immune cells play a role in the activation of T-cells against allo-antigens. Therefore, the identification and development of a prophylactic agent for GVHD need to be performed using a cellular system that is representative of different immune cell subsets. Therefore, we used a mixed population of leukocytes isolated from spleen cells of BALB/c mice and studied the activation and proliferation of these cells using mitogen ConA.

To identify immunomodulatory compounds in the primary screening, we evaluated two stages of immune activation of T cells: secretion of IL-2 (the first cytokine to be released upon T-cell activation) and clonal expansion of T-cells upon activation[158]. The IL-2 concentration was analyzed using ELISA, whereas proliferation was studied using the CFSE proliferation assay (Figure 14). Compounds that showed inhibition of both, that is, secretion of IL-2 and lymphocyte proliferation were considered target compounds that were further subjected to secondary screening.

The aim of the secondary screening was to identify compounds that inhibited lymphocyte proliferation at non-toxic concentrations. The rationale for eliminating compounds that are cytotoxic to leukocytes originates from reports showing that transplantation of pan T cell depleted donor grafts showed an increased incidence of tumor relapse and viral infections

in allo-HSCT patients[159,160]. Therefore, an ideal candidate for GVHD prophylaxis is one that can inhibit immune responses to allo-antigens while preserving the anti-tumor activity of leukocytes. Considering the overlapping mechanisms of both phenomena, we decided to select compounds that were non-toxic but simultaneously inhibited lymphocyte proliferation.

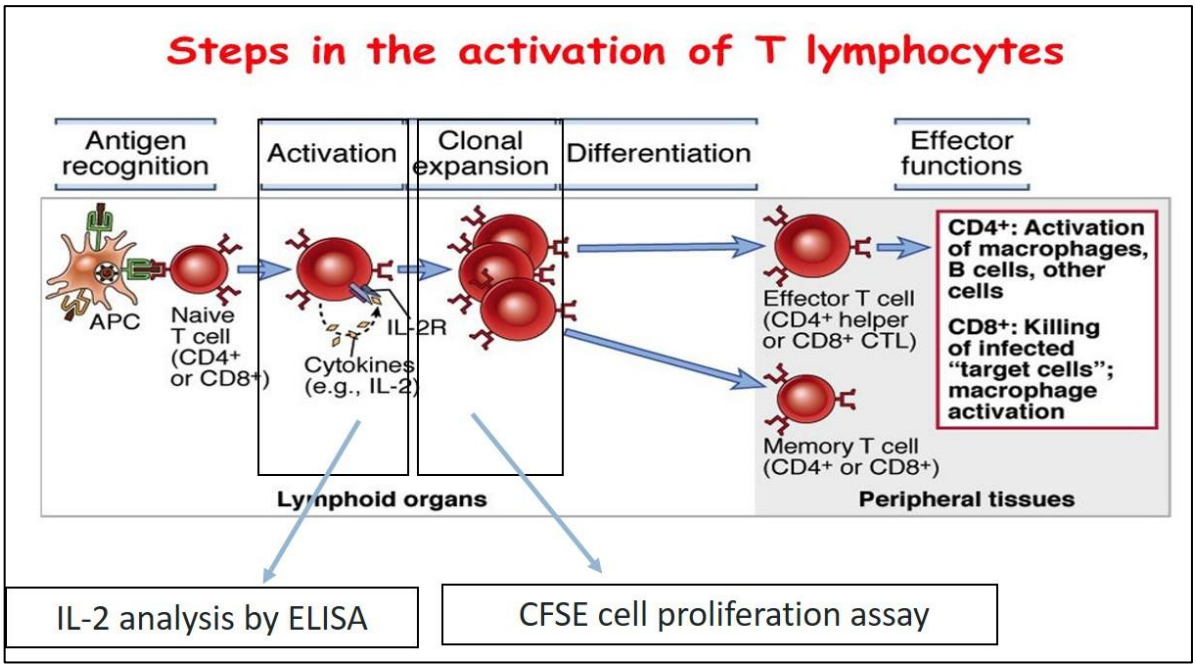

Figure 14: Strategy employed for primary screening of phytochemical drug library[158].

5.2 METHODOLOGY

Phytochemical Drug library: We procured a phytochemical library from TargetMol (Cat no. L6000) containing 134 natural compounds. It is a collection of pure natural compounds from various plant sources which contains a structurally diverse molecules, such as alkaloids, limonoids, sesquiterpenes, diterpenes, pentacyclic triterpenes, sterols, and many rare natural compounds. The natural compounds in the library have known biological activities and can be used for high-throughput screening (HTS) and high-content screening (HCS) for drug development and other fields of research.

Pack size and layout of the phytochemical drug library: The phytochemical library was supplied in a 96 well plate format (two plates), consisting of 100µL of pre-dissolved DMSO solutions of the phytochemicals 10mM each. Thus, 100µL of 10mM of each phytochemical was available for screening purposes (Figure 15).

Figure 15: Representative image of phytochemical drug library

Two 96-well plates were provided. The layout of each plate with the names of the compounds and their CAS nodes is provided in Figure 16 and Figure 17.

Detailed compound information with structure, solubility, target, activity, IC50 value, and biological activity description is provided at appendix 1 excel sheet from drug library information.

TargetMol
A Drug Screening Expert

Natural Compound Library (96-well)

For more information on TargetMol library service, please contact us via info@targetmol.com

Product Details:

Formulation	A collection of 134 Natural Compound supplied as pre-dissolved DMSO solutions
Container	96 Well Format Sample Storage Tube With Cap and Optional 2D Barcode
Shipping	Blue Ice
Standard	100μl,10Mmol/L

Plate layout:D-01

	1	2	3	4	5	6	7	8	9	10	11	12
a	Empty	58-63-9 Inosine	633-65-8 Berberine hydrochloride	138-52-3 Salicoside	88495-63-0 Artesunate	69-65-8 D-Mannitol	471-53-4 Enoxolone	11013-97-1 Methyl hesperidin	35212-22-7 Ipriflavone (Osteofix)	50-70-4 D-Sorbitol	497-76-7 Arbutin	Empty
b	Empty	485-35-8 Cytisine	531-75-9 Esculin	498-00-0 Vanillyl Alcohol	529-44-2 Myricetin	508-02-1 Oleanolic Acid	1405-86-3 Glycyrrhizin (Glycyrrhizic Acid)	539-15-1 Hordenine	477-90-7 Bengenin	1135-24-6 Ferulic Acid	552-41-0 Paeonol	Empty
c	Empty	10236-47-2 Naringin	65-19-0 Yohimbine hydrochloride	520-26-3 Hesperidin	485-71-2 Cinchonidine	568-73-0 Tanshinone I	17912-87-7 Myricetrin	115-53-7 Sinomenine	20702-77-6 Neohesperidin Dihydrochalcone (Nhdc)	18916-17-1 Naringin dihydrochalcone	138-59-0 Shikimic Acid	Empty
d	Empty	19685-09-7 10-Hydroxycamptothecin	491-80-5 Biochanin A	564-20-5 Sclareolide	90-47-1 Xanthone	14375-45-2 Abscisic acid	515-03-7 Sclareol	71939-50-9 Dihydroartemisinin	520-33-2 Hesperetin	77-52-1 Ursolic acid	491-70-3 Luteolin	Empty
e	Empty	485-72-3 Formononetin	961-29-5 Isoliquiritigenin	7085-55-4 Troxerutin	65-86-1 Orotic acid	461-06-3 DL-Carnitine	60-82-2 Phloretin	27200-12-0 Dihydromyricetin	35354-74-6 Honokiol	528-43-8 Magnolol	62499-27-8 Gastrodin	Empty
f	Empty	94-62-2 Piperine	481-74-3 Chrysophanic Acid	56-69-9 5-hydroxytryptophan (5-HTP)	528-48-3 Fisetin	83-49-8 Hyodeoxycholic acid (HDCA)	480-41-1 Naringenin	145572-44-7 Sophocarpine	21967-41-9 Baicalin	607-80-7 Sesamin	5508-58-7 Andrographolide	Empty
g	Empty	484-12-8 Osthole	10338-51-9 Salidroside	84-26-4 Rutaecarpine	464-92-6 Asiatic acid	1180-71-8 Limonin	331-39-5 Caffeic Acid	60-81-1 Phlorizin	13241-33-3 Neohesperidin	67920-52-9 Sodium Danshensu	568-72-9 Tanshinone IIA	Empty
h	Empty	3681-99-0 Puerarin (Kakonein)	16837-52-8 Oxymatrine	518-82-1 Emodin	491-67-8 Baicalein	519-02-8 (+)-Matrine	10605-02-4 Palmatine chloride	35825-57-1 Cryptotanshinone	389-08-2 Nalidixic acid	153-18-4 Rutin	541-15-1 L(-)-Carnitine	Empty

Figure 16: Layout of plate 1 of phytochemical drug library

TargetMol
A Drug Screening Expert

Natural Compound Library (96-well)

For more information on TargetMol library service, please contact us via info@targetmol.com

Product Details:

Formulation	A collection of 134 Natural Compound supplied as pre-dissolved DMSO solutions
Container	96 Well Format Sample Storage Tube With Cap and Optional 2D Barcode
Shipping	Blue Ice
Standard	100µl,10Mmol/L

Plate layout:D-02

	1	2	3	4	5	6	7	8	9	10	11	12
a	Empty	117-39-5 Quercetin	59865-13-3 Cyclosporin A	90-33-5 4-Methylumbelliferone (4-MU)	520-34-3 Diosmetin	525-79-1 Kinetin	520-36-5 Apigenin	1415-73-2 Aloin	29883-15-6 Laetrile	700-06-1 Indole-3-carbinol	480-40-0 Chrysin	Empty
b	Empty	10212-25-6 Cyclocytidine hydrochloride	22888-70-6 Silibinin	517-28-2 Hematoxylin	143-67-9 Vinblastine sulfate	480-18-2 Taxifolin (Dihydroquercetin)	520-18-3 Kaempferol	989-51-5 (-)-Epigallocatechin Gallate	486-35-1 Daphnetin	61281-37-6 Schizandrin B	489-32-7 Icariin	Empty
c	Empty	327-97-9 Chlorogenic Acid	4871-97-0 Curcumol	478-01-3 Nobiletin	38748-32-2 Triptolide (PG490)	6429-04-5 Tetrahydropapaverine hydrochloride	65666-07-1 Silymarin	94-07-5 Synephrine	28957-04-2 Rubescensin A	481-53-8 Tangeretin	33570-04-6 Bilobalide	Empty
d	Empty	498-02-2 Acetovanillone	471-66-9 ALPHA-BOSWELLIC ACID	121-33-5 Vanillin	20554-84-1 Parthenolide	6882-68-4 Sophoridine	75887-54-6 Arteether	19057-60-4 Dioscin	51059-44-0 Wogonoside	529-53-3 Scutellarein	27975-19-5 Isosteviol	Empty
e	Empty	487-11-6 Elemicin	6754-58-1 Xanthohumol	58749-22-7 Licochalcone A	470-37-1 Cinobufagin	107316-88-1 Demethylzeylasteral	113558-15-9 Baohuoside I	118-34-3 Syringin	118525-40-9 Icaritin	26833-87-4 Homoharringtonine	27208-80-6 Polydatin	Empty
f	Empty	3895-92-9 Chelerythrine chloride	6151-25-3 Quercetin Dihydrate	56293-29-9 Aloperine	88495-63-0 Juglone							Empty
g	Empty											Empty
h	Empty											Empty

Figure 17: Layout of Plate 2 of the phytochemical drug library

Dilution and preparation of aliquots of the phytochemical drug library

To avoid repeated freeze-thaw cycles of the phytochemical drug library, we prepared dilutions and aliquots of each drug in a sterile 96 plate. The phytochemical library was handled under aseptic conditions in a laminar airflow hood. All phytochemicals were diluted to 1 mM using sterile cell culture grade DMSO. Two sterile 96 well plates (working stock plates) were used to prepare dilutions. The layout of these working stock plates was

the same as that of the master plate (the phytochemical drug library provided by the manufacturer). Before aliquoting the phytochemicals, the drug library was thawed at 4˚C for 30-40 min. The library was vortexed for 5 min at low speed of 300 rpm to ensure a uniform solution of each phytochemical. For dilution, 90µl of sterile dimethyl sulfoxide (DMSO) was carefully aliquoted into each well of a 96 well plate. Next, 10µl of each phytochemical was added to the respective wells to obtain a working concentration of 1mM for each phytochemical. These working stock plates were used for primary and secondary screening. These plates were freeze-thawed twice during the screening experiments. For primary screening, 10µl solution of the phytochemical solution was added to 1 ml of the culture medium to treat splenic leukocytes.

Primary Screening: Compounds from the phytochemical library were evaluated for two inhibitory effects: inhibition of IL-2 secretion by leukocytes using ELISA and anti-proliferative effect on leukocytes using the CFSE dye dilution assay. The immunomodulatory action of all compounds was evaluated on leukocytes at a concentration of 10µM and exposure for 2 h. Leukocytes were isolated as previously described in chapter 3 and stained with CFSE (5µM), after which 1×10^6 cells were seeded in each well of a 24 well plate. Leukocytes were treated with the compounds of the phytochemical drug library as mentioned above (10µM for 2h) and then stimulated with mitogen ConA and incubated for 72 h. Vehicle-treated leukocytes (0.1%DMSO in RPMI 1640 medium) were used as the control. The compounds were named according to their position in the 96 well plates; for example, 1-A2 refers to the compound in column 2, row A of plate-1, 1-A3 refers to the compound in column 3, row A of plate-1, 1D11 refers to the compound in column 11, row D of plate-1, etc. After incubation, the cells were acquired using a flow cytometer to determine the percentage of daughter cells. Compounds that

inhibited cell proliferation and IL-2 secretion were considered the hit compounds. IL-2 levels in cell supernatants were quantified by ELISA. Briefly, 500µl of the cell supernatant was collected after 24 h of Con A stimulation. The cell supernatant was added in duplicate to estimate IL-2 levels using ELISA. The levels of IL-2 were compared with those of the vehicle leukocytes. Compounds that suppressed IL-2 secretion and lymphocyte proliferation were selected for the secondary screening.

Secondary screening: The aim of the secondary screening was to identify compounds that inhibited proliferation at non-toxic or least toxic doses. The target compounds identified from the primary screen were further evaluated for their dose-dependent toxicity and anti-proliferative effects. Toxicity was evaluated using a propidium iodide viability assay, whereas the anti-proliferative effect was evaluated using a CFSE dye dilution assay. Leukocytes were treated with following drug concentrations and time points for secondary screening.

Concentrations: 0.1, 0.25, 0.5, 1, 2.5, 5, and 10µM.

Time points for the proliferation assay: 2 and 4 h.

Time points for viability assay: 4 h and 24 h

To evaluate the antiproliferative effect, CFSE-stained leukocytes (1×10^6 cells) were seeded in 24 well plate and treated with the target compounds at the above-mentioned doses and times in duplicate. Following treatment, the cells were stimulated with mitogen Con A and incubated for 72 h to determine cell proliferation using a flow cytometer.

To evaluate toxicity, leukocytes (1×10^6 cells) were seeded in 24 well plate and treated with the target compounds at the above-mentioned doses and times in duplicate. Following treatment, cells were harvested, and 10µg/ml propidium iodide solution was added 5 min

before analyzing the cells on the flow cytometer. The percentage of propidium iodide (PI)-positive cells was determined. Compounds that exhibited inhibition of proliferation at least toxic doses were considered lead compounds and were further evaluated for their immunomodulatory effects on leukocytes. An overview of the methodology for photochemical drug library screening and lead compound identification is illustrated in Figure 18.

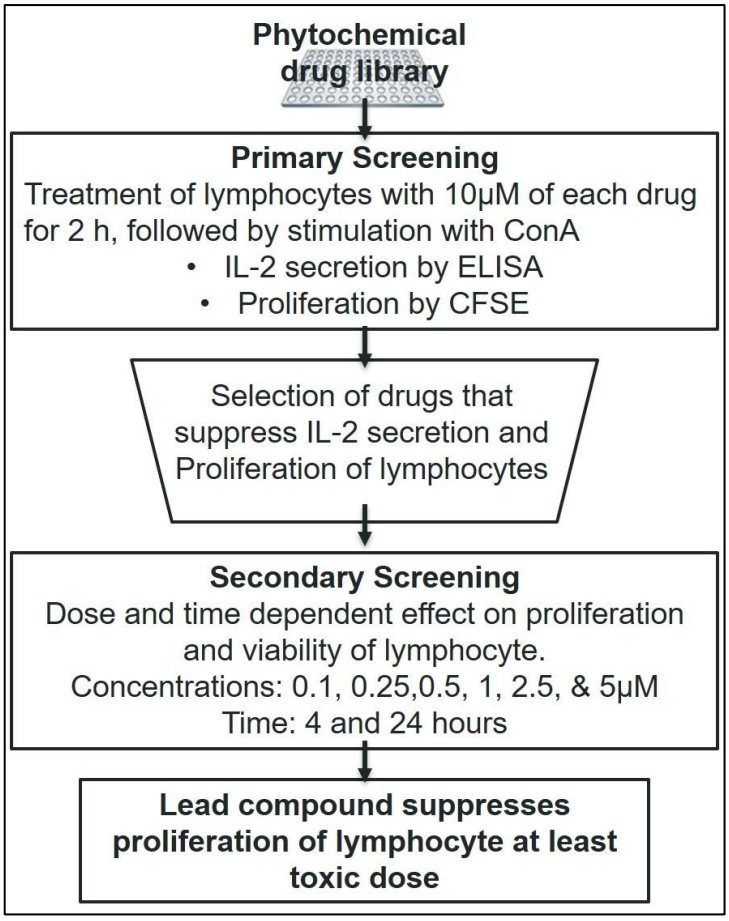

Figure 18: Methodology for phytochemical drug library screening and lead identification

Immunomodulatory effect of Juglone (5NQ) on leukocytes *in vitro*: Based on secondary screening, 5-hydroxy-1,4-naphthoquinone (5NQ) or Juglone was selected as the lead compound as it exhibited immunosuppression without toxicity to leukocytes. Therefore, we evaluated the immunomodulatory effect of transient 5NQ treatment on leukocytes *in*

vitro with respect to its effect on different immune cell subsets and immune responses (Figure 19).

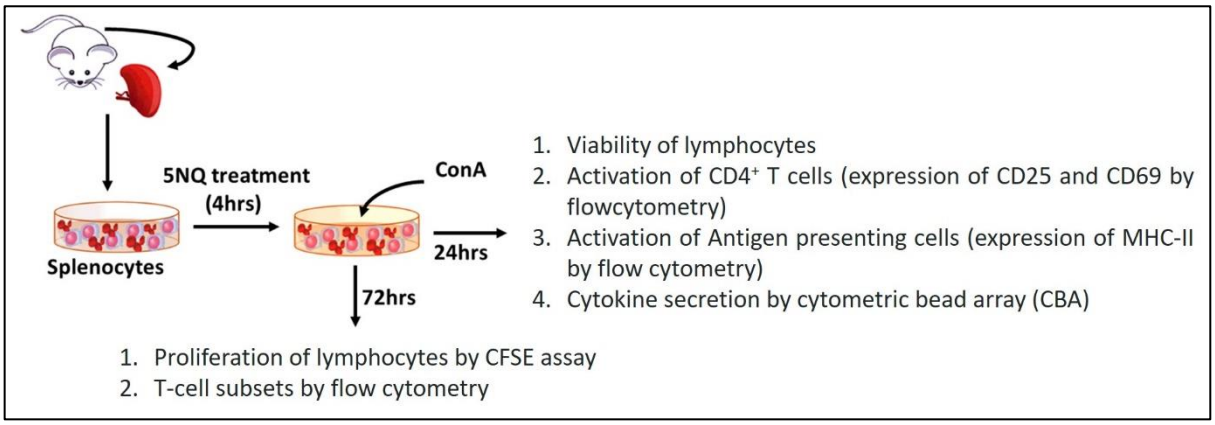

Figure 19: Evaluation of immunomodulatory effect of 5NQ on leukocytes *in vitro*

First, we studied the time- and dose-dependent effects of transient treatment with 5NQ on the proliferation and viability of leukocytes using CFSE and PI assays, as explained above. The effect of transient treatment with 5NQ on lymphocyte proliferation was determined using the CFSE assay.

Briefly, leukocytes were transiently treated with 0.1, 0.25, 0.5,1, and 2.5µM 5NQ for 4 h. The leukocytes were washed with 1x PBS to remove 5NQ from the culture medium. DMSO (0.01% in 1x PBS or RPMI 1640) was used as vehicle control. Cells were stimulated with mitogen Con A (2.5µg/ml) or LPS, 5µg/ml) and incubated for 72 h. After incubation, the cells were acquired using a flow cytometer to determine the percentage of daughter cells. The effect of transient treatment with 5NQ on lymphocyte viability was determined using the PI assay. The leukocytes were transiently treated with vehicle or 5NQ (0.1, 0.25, 0.5, 1, 2.5, 5 and 10 µM) for 4 h. Cells were washed with 1X PBS to remove 5NQ from the culture medium and incubated for 24 h. After 24 h, cells were washed twice with 1X PBS twice and 10µg/ml propidium iodide solution was added 5 min before analyzing the cells

on the flow cytometer. The percentage of propidium iodide (PI)-positive cells was determined.

Second, we evaluated the transient effect of 5NQ treatment on cytokine secretion by leukocytes after Con A stimulation.

Briefly, leukocytes (1 X 10^6) were seeded in 24 well plate after transient treatment with vehicle or 5NQ (0.5 and 1µM for 4h) followed by stimulation with ConA. After 24 h, cytokine concentrations (Th1: IL-2, IFN-γ, TNF; Th2: IL-4, IL-6 IL-10; Th17: IL-17A) were measured in the cell supernatant using a BD™ Cytometric Bead Array (CBA Becton-Dickinson, NJ, USA).

Third, we evaluated the transient effects of 5NQ treatment with 1µM, 4 h on the activation of antigen-presenting cells (APCs).

Briefly, leukocytes were stimulated with Con A after transient treatment with 5NQ and incubated for 72 h. Cells were then harvested and stained with antibodies specific for dendritic cells, macrophages, monocytes, and T cells (Table 17) and acquired on a flow cytometer. The gating strategy is illustrated in Figure 20.

Table 17: Fluorochrome conjugated antibodies used for specific antigen-presenting cells.

Cell type	Markers	Antibody and fluorochrome
Dendritic cells	$CD45^+$ $CD3^-$ $CD11b^-$ $MHC\text{-}II^+$	CD45-PE-Cy7, CD3ε-APC-Cy7, CD11b-FITC, IA/IE-PE, Ly6c-APC
Macrophages	$CD45^+$ $CD3^-$ $CD11b^+$ $MHC\text{-}II^+$ $Ly6c^{hi}$	
Monocytes	$CD45^+$ $CD3^-$ $CD11b^+$ $MHC\text{-}II^+$ $Ly6c^{lo}$	

Fourth, we evaluated the transient effects of 5NQ treatment with 1µM, 4 h on $CD4^+$ T cell activation and $CD4^+$ Treg cell numbers.

Briefly, leukocytes were stimulated with Con A after transient treatment with 5NQ and incubated for 72 h. The cells were harvested and stained with antibodies specific for CD4

T cells, early and late activation markers for CD4 T cells, markers for T-cell anergy and exhaustion, and Treg cells (Table 18) and acquired on a flow cytometer. The gating strategy is illustrated in Figure 21 and Figure 22.

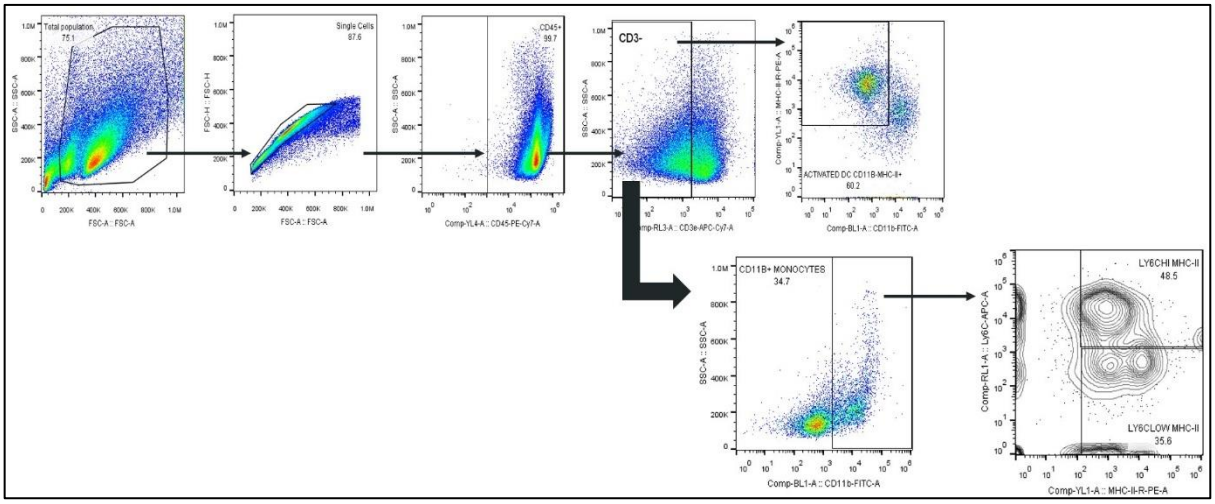

Figure 20: Flow cytometry gating for MHC-II expression on dendritic cells and monocytes

Table 18: Fluorochrome-conjugated antibodies for specific subsets of CD4 T cells.

Cell type	markers	Antibody and fluorochrome
Activated $CD4^+$ T-cells	$CD3\varepsilon^+$ $CD4^+$ $CD25^+$ $CD3\varepsilon^+$ $CD4^+$ $CD69^+$	CD3ε-APC-Cy7; CD4 PerCP-Cy5.5, CD8α FITC, CD25 BV421, FoxP3 AF647; CD152 PE; CD95 APC-R700
Anergic/Exhausted $CD4^+$ T cells	$CD3\varepsilon^+$ $CD8^-$ $CD152^+$ $CD3\varepsilon^+$ $CD8^-$ $CD95^+$	
$CD4^+$ Treg cells	$CD3\varepsilon^+$ $CD4^+$ $CD25^+$ $FoxP3^+$	

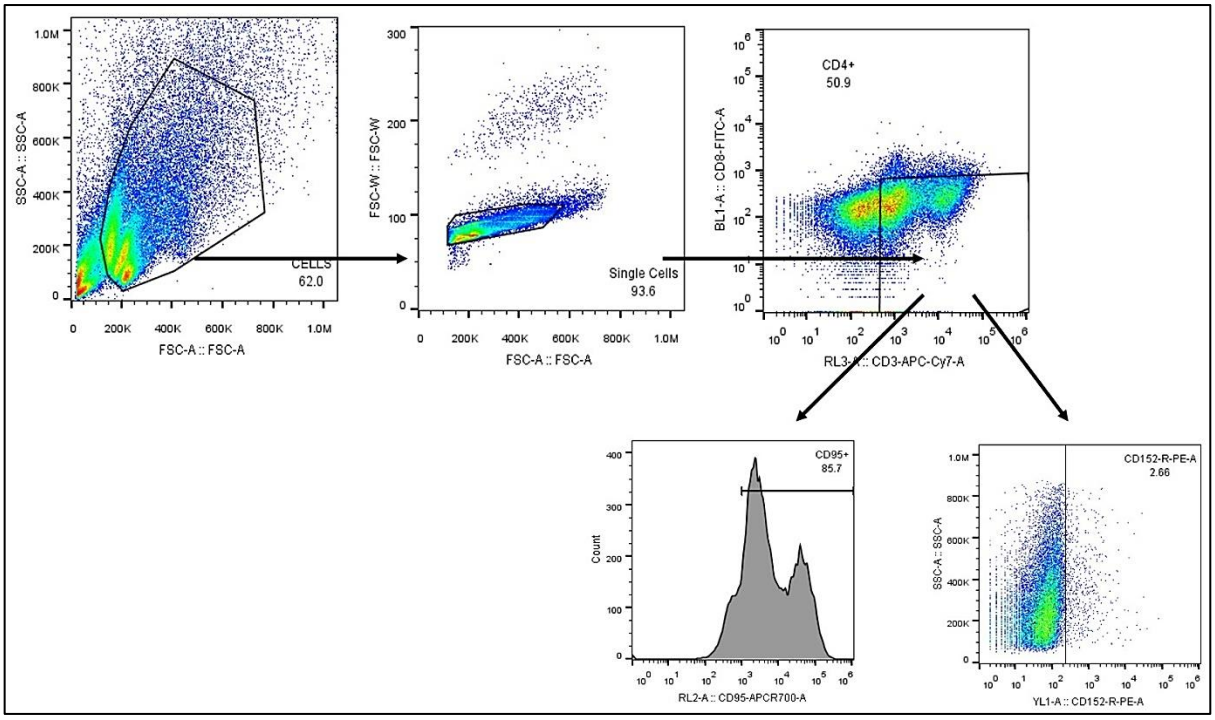

Figure 21: Flow cytometry gating strategy for CD95 and CD152 in $CD4^+$ T cells

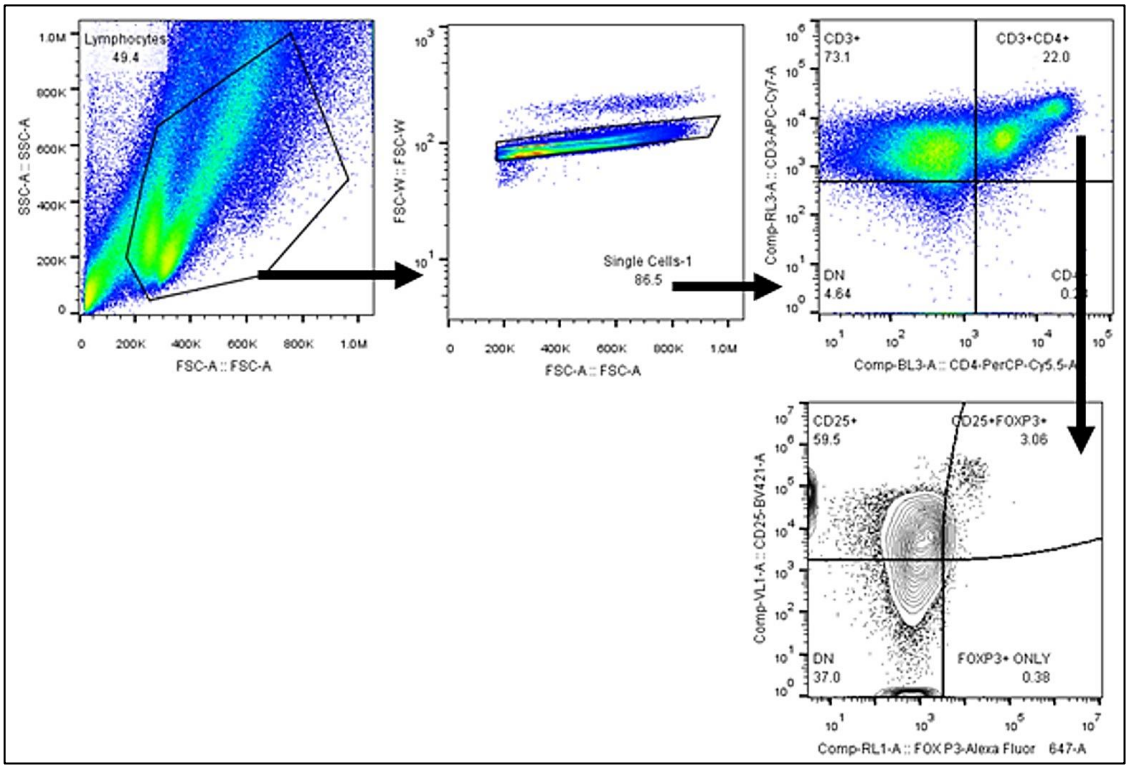

Figure 22: Flow cytometric gating strategy for Treg cells.

We also evaluated the transient effect of treatment with 5NQ (1µM, 4 h) on the anti-tumor activity of leukocytes using an *in vitro* assay (Figure 23).

Briefly, BALB/c splenocytes (6×10^7) were stimulated with 25 Gy-irradiated EL4 or A20 cells (5×10^6), followed by stimulation with 5 µg/ml Con A and incubation for 72 h. Cells were harvested, washed twice to remove debris and dead cells, resuspended in complete RPMI medium, and allowed to rest for 24 h. The following day, viable cell counts were performed, after which the cells were treated with either vehicle (0.1% DMSO, 4 h) or 5NQ (1µM, 4 h). The cells were then incubated with healthy, live, and CFSE labelled EL4 or A20 cells at a 10:1 ratio (leukocytes: leukemia cells) for 24 h. To compensate for cell death due to nutritional stress caused by high seeding density, CFSE labelled A20 and EL4 cells were seeded at the same density as in the mixed lymphocyte group and served as a control. After 24 h, the cells were harvested and stained with propidium iodide immediately before analysis on a flow cytometer. Propidium iodide staining was used to distinguish between live tumor cells (positive for CFSE only) and dead tumor cells (positive for both CFSE and PI).

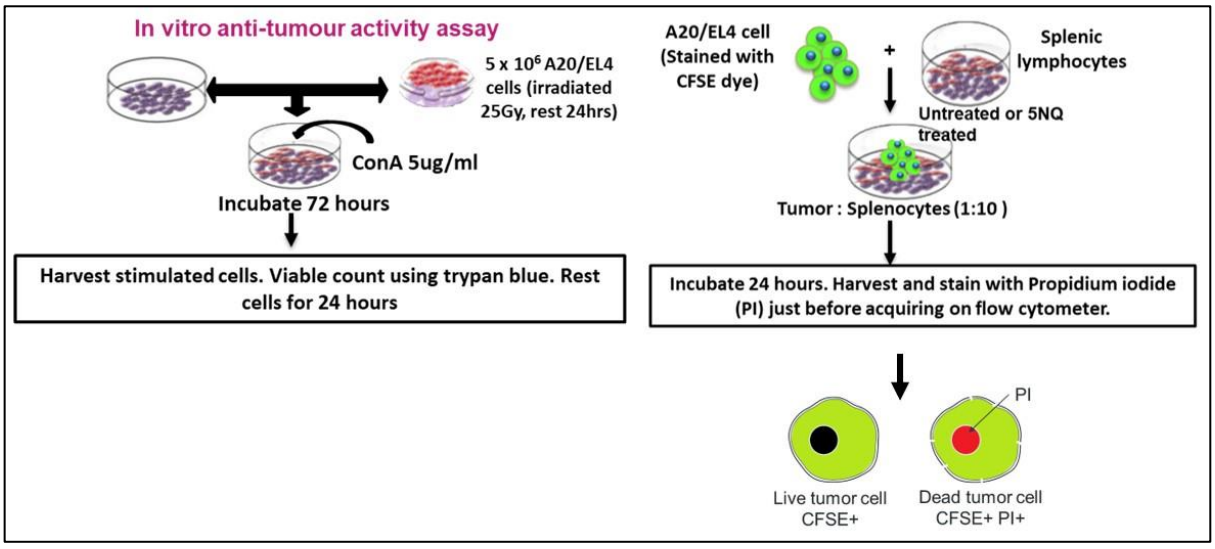

Figure 23: Experimental protocol for evaluating the anti-tumor activity of leukocytes *in vitro*.

5.3 RESULTS

Primary screening: We identified 20 compounds that inhibited proliferation. However, only 9 completely inhibited IL-2 secretion (Table 19, Figure 24). Of these nine compounds, two compounds, 1D2 and 2A3, were known immunosuppressive agents, namely 10-hydroxy-camptothecin and cyclosporin A. The remaining seven compounds were 1-F5 (fisetin), 2-C5 (triptolide), 2-C9 (Rubescensin A), 2-E6 (demethylzeylasteral), 2-E10 (homoharringtonine), 2-F2 (chelerythrine chloride), and 2-F5 (5-hydroxy-1,4-naphthoquinone). The important details provided by the manufacturer regarding these compounds are listed in (Table 20). Further, they were subjected to secondary screening.

Table 19: Compounds that inhibited proliferation and IL-2 secretion

Sr no.	Compound	Name	Inhibition of Proliferation	Inhibition of IL-2 secretion
1	1-D2	10-Hydroxycamptothecin	Yes	Yes
2	1-F5	Fisetin	Yes	Yes
3	2-A3	Cyclosporin A	Yes	Yes
4	2-C5	Triptolide	Yes	Yes
5	2-C9	Rubescensin A	Yes	Yes
6	2-E6	Demethylzeylasteral	Yes	Yes
7	2-E10	Homoharringtonine	Yes	Yes
8	2-F2	Chelerythrine chloride	Yes	Yes
9	2-F5	5-hydroxy-1,4-naphthoquinone	Yes	Yes
10	1-D11	Luteolin	Yes	Partial
11	2-A5	Diosmetin	Yes	Partial
12	2-B5	Vinblastine sulfate	Yes	Partial
13	1-A5	Artesunate	Yes	No
14	1-D8	Dihydroartemisinin	Yes	No
15	1-F11	Andrographolide	Yes	No
16	2-E3	Xanthohumol	Yes	No
17	2-E4	Licochalcone A	Yes	No
18	2-E9	Icaritin	Yes	No
19	2-D7	Artether	Yes	Unknown
20	2-D8	Dioscin	Yes	Unknown

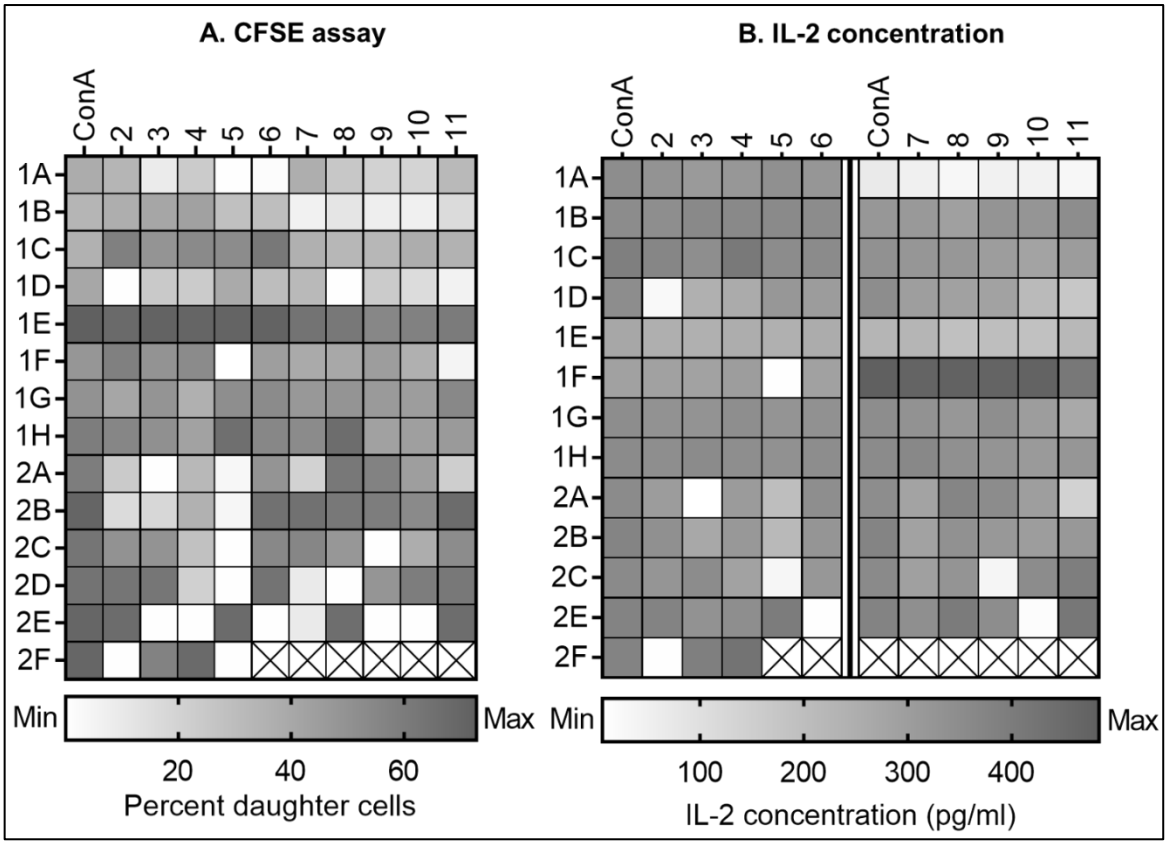

Figure 24: Results of the primary screening. (A) Heatmap showing percentage daughter cells (B) concentration of IL-2 (pg/ml) in cell supernatant, post-treatment with phytochemicals from the drug library, and stimulation with Con A. Vehicle-treated (0.1%DMSO) cells acted as control (denoted as ConA). Boxes with crosses do not represent any data.

Table 20: Details of target compounds from primary screening

Compound	Molecular name	Mol. wt	Bioactivity	Reference
1D2	(S)-10-OH-camptothecin	364.36	Active against hepatoma.	Teicher BA. Biochem Pharmacol. 2007.
1F5	Fisetin	286.24		Kim SC, et al. Biochem Biophys Res Commun. 2015.
2A3	Cyclosporin A	1202.64	Widely used in organ transplantation to prevent rejection.	Handschumacher RE, et al. Science, 1984.
2C5	Triptolide (PG490)	360.40	Herbal immunosuppressive agent.	Qiu D, et al. J Biol Chem, 1999.
2C9	Rubescensin A	364.44	Has potent anti-tumor activity. Targets AE (AML1-ETO) oncoprotein. It induces apoptosis in AE-bearing leukemic cells through activation of intrinsic apoptotic	Ikezoe T, et al. Int J Oncol, 2003.

			pathway and triggering a caspase-3-mediated degradation	
2E6	Demethylzeylasteral	480.59	Strong immunosuppressive agent can be used in the fields of organ transplantation and autoimmune disorders.	1. Liu SL et al. Eur J Drug Metab Pharmacokinet. 2014.
2E10	Homoharringtonine	545.61	Protein synthesis inhibitor with activity in myeloid malignancies It has anti-Y and antileukemic activities, may have the potential ability to treat acute, chronic myeloid leukaemia and Gefitinib-resistant NSCLC.	Jin J, et al. Lancet Oncol. 2013.
2F2	Chelerythrine chloride	383.83	Antiplatelet, anti-inflammatory, antibacterial and antitumor effects. Activates MAPK pathways, independent of PKC inhibition. Inhibits binding of BclXL to Bak or Bad proteins and stimulates apoptosis.	Chan SL, et al. J Biol Chem. 2003.
2F5	Juglone or 5-hydroxy1,4-naphthoquinone	174.15	A natural naphthoquinone irreversibly inhibits peptidyl-prolyl cis/trans isomerases of the parvulin family including human Pin1, yeast Ess1/Ptf1, and *E. coli* parvulin. Juglone also blocks transcription by RNA polymerases I, II, and III and attenuates kidney fibrosis in rats treated with unilateral ureteral obstruction.	Reese S, et al. Fibrogenesis Tissue Repair. 2010.

Secondary screening: In the secondary screening, we conducted time and concentration dependent studies to identify compounds that inhibited lymphocyte proliferation at nontoxic or least toxic concentrations. The results are summarized in Figure 25. Evaluation of lymphocyte viability after treatment with these compounds for 4 h and 24 h showed that none of the compounds were toxic at 4 h time point compared to the vehicle-treated control. A significant decrease in the viability of leukocytes was observed at 24 h for compounds. Homoharringtonine (HH), triptolide (TP) and cherlythrine chloride (CC) showed significant toxicity at concentration of 1µM, whereas demethylzeylasteral (DMZ) and 5-

hydroxy-1,4-naphthoquinone (5NQ) were comparatively safe showing toxicity at concentrations above 2.5µM. With respect to inhibition of lymphocyte proliferation, HH and TP completely inhibited lymphocyte proliferation at the concentration of 0.1µM after 4 h and 24 h exposure. However, these molecules were significantly toxic to leukocytes after 24 h. Lymphocyte proliferation was completely inhibited by CC at the concentration of 5µM, but this concentration was significantly toxic to leukocytes. A dose dependent inhibition of lymphocyte proliferation was observed with DMZ and 5NQ, with 5NQ being slightly potent than DMZ as it inhibited proliferation at the concentration of 0.5µM compared to 1µM for DMZ. As these compounds were not toxic to leukocytes at these concentrations, they emerged as lead compounds in our phytochemical drug library screening (Figure 25). We selected 5NQ for further investigation because of its competitive cost compared with DMZ, as well as its ease of availability.

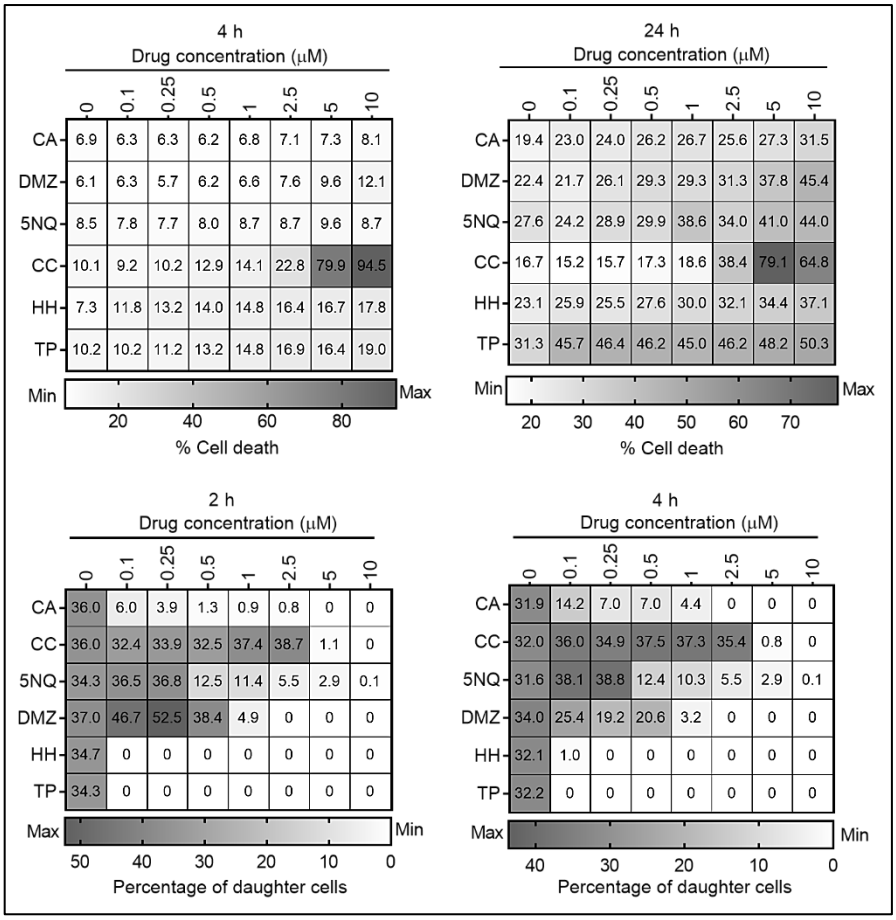

Figure 25: Results of secondary screening of the phytochemical drug library. (A-B) Concentration- and time-dependent effects on lymphocyte viability after treatment with the target compounds. (C-D) Concentration and time-dependent effects on lymphocyte proliferation after treatment with the target compounds and Con A stimulation. Vehicle-treated (0.1%DMSO) cells were used as control (Con A).

Immunomodulatory effect of 5NQ on leukocytes *in vitro*: Based on secondary screening, 5-hydroxy-1,4-naphthoquinone (5NQ) or juglone was selected as the lead compound as it exhibited immunosuppression without toxicity to leukocytes. We evaluated the immunomodulatory effects of 5NQ on murine splenic leukocytes *in vitro*. First, we studied the time and concentration dependent effects of 5NQ on lymphocyte proliferation and toxicity. Transient treatment with 5NQ for 4 h inhibited mitogen (Con A and LPS - lipopolysaccharide) induced proliferation of leukocytes in a dose-dependent manner (Figure 26).

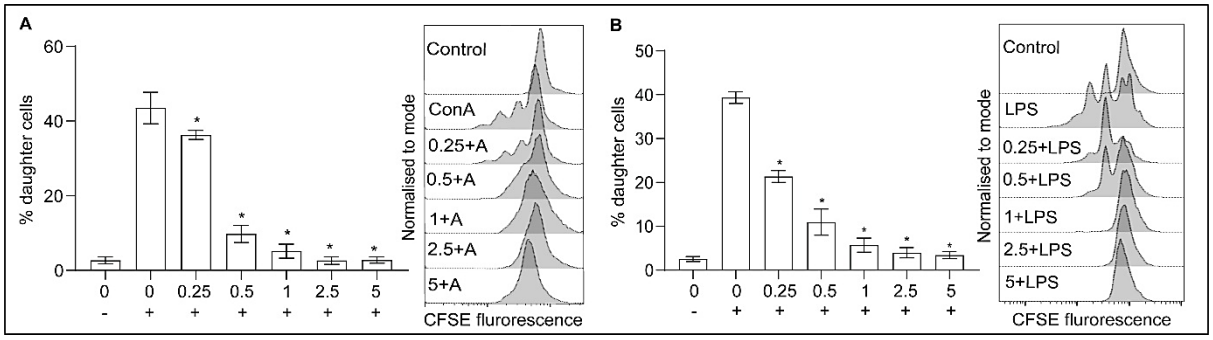

Figure 26: Immunosuppressive effect of 5NQ on murine splenic leukocytes *in vitro.* (A) Lymphocyte proliferation after transient treatment (0.25, 0.5, 1, 2.5, 5µM for 4h) followed by Con A (A) or LPS (B) stimulation. Bar graphs represent percentage of daughter cells after 72 h of stimulation with Con A or LPS, calculated using CFSE dye dilution assay, and representative flow cytograms, indicating inhibition of lymphocyte proliferation (n =5, independent experiments, mean ± SEM). Data were analyzed using one-way ANOVA with Bonferroni correction for multiple comparisons. *****p<0.05, compared to VC + Con A-or VC + LPS-treated groups.

Transient treatment with 1µM 5NQ for 4 h inhibited proliferation without affecting viability, and this dose was used for subsequent experiments (Figure 27).

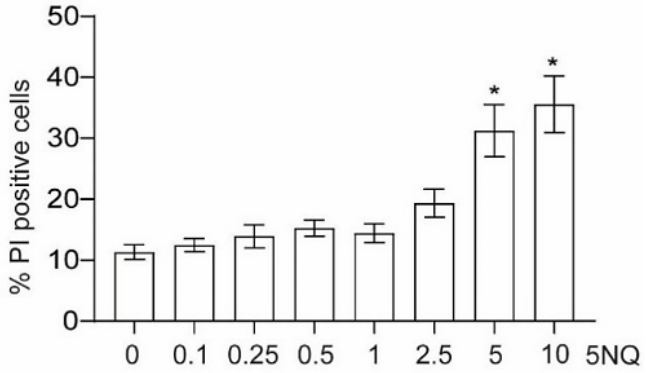

Figure 27: Viability of leukocytes 24 h after transient treatment with different concentrations of 5NQ (0.1, 0.25, 0.5, 1, 2.5, 5 and 10µM, 4 h) quantified using the propidium iodide assay (n = 5, independent experiments, mean ± SEM). Data were analyzed using one-way ANOVA with Bonferroni correction for multiple comparisons; *****p<0.05, compared with VC-treated group.

Second, transient treatment of leukocytes with 5NQ suppressed Con A-induced secretion of IL-2, IL-4, IL-6, IFN-γ, TNF, IL-17A, and IL-10, and restored the Th1/Th2 cytokine imbalance induced by Con A stimulation (Figure 28).

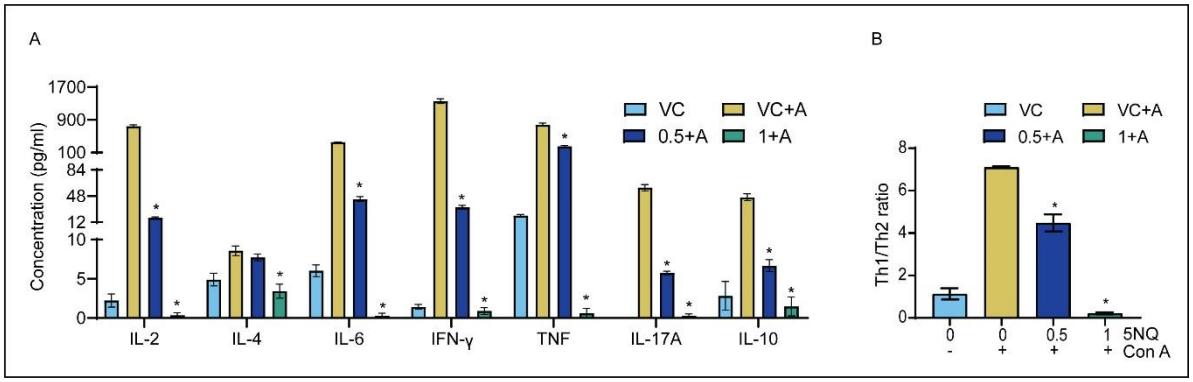

Figure 28: Concentrations of Th1 (IL-2, IFN-γ, TNF) cytokines, Th2 (IL-4, IL-6, IL-10) cytokines, and IL-17A in cell supernatants 24 h after stimulation of transiently treated leukocytes (0.5 and 1μM 5NQ, 4h) with Con A (n = 3 independent experiments; mean ± SEM). (E) Bar graph representing Th1/Th2 cytokine ratio (mean ± SEM). Data were analyzed using one-way ANOVA with Bonferroni correction for multiple comparisons; *****p<0.05, compared to VC + Con A-treated groups.

We further studied the effect on the activation of antigen-presenting cells (APC) and $CD4^+$ T cells and found that transient treatment of leukocytes with 5NQ suppressed the expression of MHC-II on $CD11b^-$ dendritic cells, $CD11b^+$ $Ly6c^{lo}$ macrophages, and $CD11b^+$ $Ly6c^{hi}$ monocytes (Figure 29, A-C) and suppressed the expression of CD69 and CD25 in $CD4^+$ T cells (Figure 29 D). Additionally, we observed an increase in CD95 (Fas) expression in $CD4^+$ T cells following 5NQ treatment (Figure 29 E). Furthermore, we found that transient treatment with 5NQ did not increase the number of $CD4^+$ Tregs in vitro (Figure 29 F). We also evaluated the effect of transient treatment with 5NQ on the anti-leukemic activity of leukocytes using an in vitro model of mixed lymphocyte reaction, with murine leukemia cell lines as stimulator cells. We observed that 5NQ-treated leukocytes exhibited anti-leukemic activity that was comparable to that of their vehicle-treated counterparts.

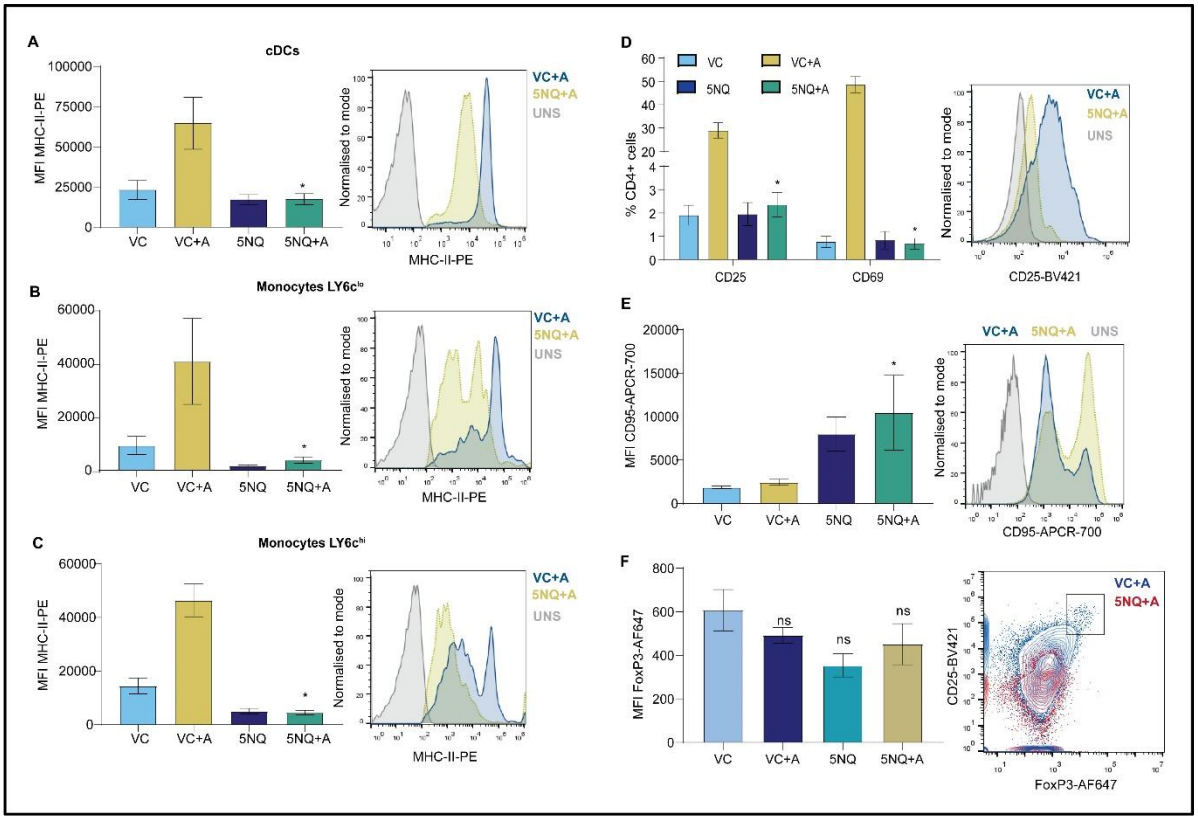

Figure 29: (A-C) Cell surface expression of MHC-II on classical dendritic cells (cDCs) and monocytes was studied at 24h after 5NQ treatment (1µM, 4 h) followed by Con A stimulation, assessed using FACS. (D-F) Cell surface expression of CD25, CD69, and CD95 on $CD4^+$ T cells was studied at 24h after 5NQ treatment (1µM, 4 h) followed by Con A stimulation, assessed using flow cytometry (n = 5, independent experiments), MFI: median fluorescence intensity). Data were analyzed using one-way ANOVA with Bonferroni correction for multiple comparisons; *p<0.05, compared to the VC + Con A-treated group.

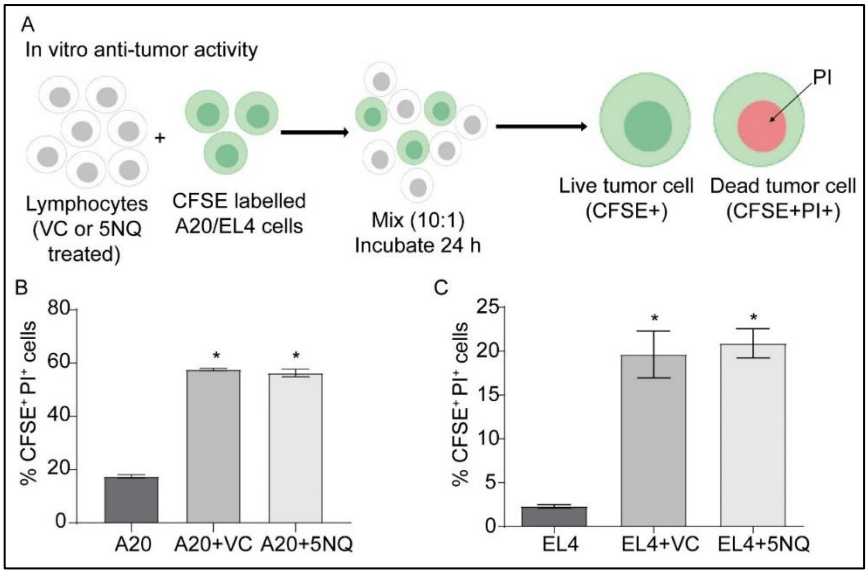

Figure 30: (A) Brief scheme of the in vitro anti-tumor assay. (B-C) Viability of CFSE labelled A20 or EL4 leukemia cells after 24 h incubation with vehicle-treated or 5NQ treated (1µM 4h) leukocytes, assessed using propidium iodide assay (n = 5, independent experiments; mean ± SEM). Data were analyzed using one-way ANOVA with Bonferroni correction for multiple comparisons; *****$p<0.05$, compared to the tumor control group.

5.4 DISCUSSION

Allo-HSCT remains a major curative therapy for various hematological disorders and offers GVL benefits to patient[161]. However, GVHD remains a major hurdle in the success of allo-HSCT and leads to fatality[162,163]. Current prophylactic and treatment options have shown limited success in clinics owing to related toxicities, relapse of malignancy, and/or development of secondary infections due to prolonged immune suppression[163]. Despite the current medical advances in the field of transplantation, prevention of GVHD while maintaining the GVL effects of the graft remains a major unsolved challenge in clinics[164].

In this study, we aimed to identify novel immunomodulatory compounds by screening a phytochemical drug library containing 136 compounds at two levels. Primary screening involved testing the effect of phytochemicals on mitogen (Con A)-induced secretion of IL-2 and lymphocyte proliferation at a fixed concentration of 10 µM and exposure for 2 h. The compounds identified from the primary screening were then subjected to a secondary screening to identify the concentration and time dependent effects of these target compounds on lymphocyte viability and proliferation. Target compounds that inhibited lymphocyte proliferation at non-cytotoxic concentrations were selected as the lead compounds. Finally, the lead compound was evaluated for its concentration and time dependent effects on lymphocyte proliferation and Th1, Th2, and Th17 cytokine secretion. Furthermore, the effect of the lead compound on the activation of antigen-presenting cells and $CD4^+$ T cells and the differentiation of $CD4^+$ T cells was investigated.

Our primary screening strategy was to identify compounds that inhibit IL-2 secretion and lymphocyte proliferation. Our primary screening data identified 20 compounds that could inhibit lymphocyte proliferation; however, among these, only five inhibited IL-2 secretion;

therefore, these compounds (target compounds) were selected and subjected to secondary screening. IL-2 is the first cytokine secreted upon $CD4^+$ T cell activation and plays a major role in the activation and differentiation of both $CD4^+$ and $CD8^+$ T cells[165,166] and therefore is central to inflammatory responses. Hence, we selected target compounds that inhibited both IL-2 secretion (one of the earliest events in the activation of $CD4^+$ T cells) and the clonal expansion of leukocytes (lymphocyte proliferation). To validate our secondary screening results, we used cyclosporin A as a positive control in the secondary screening experiment. The five target compounds that were subjected to secondary screening were 2-C5 (triptolide), 2-E6 (demethylzeylasteral), 2-E10 (homoharringtonine), 2-F2 (chelerythrine chloride), and 2-F5 (5-hydroxy-1,4-naphthoquinone). The aim of secondary screening was to identify compounds that inhibited lymphocyte proliferation at non-toxic concentrations. Our results showed that compounds 5-hydroxy-1,4-naphthoquinone (2F5) and demethylzeylasteral (2-E6) inhibited lymphocyte proliferation at nontoxic concentrations. Triptolide (2-C5), homoharringtonine (2-E10), and chelerythrine chloride (2-F2) exhibited inhibitory effects on lymphocyte proliferation at cytotoxic concentrations and hence were not considered for further evaluation. Chelerythrine chloride inhibited lymphocyte proliferation at a toxic concentration of 5µM, but its inhibitory activity was not observed at concentrations lower than 5µM. Furthermore, chelerythrine chloride is a competitive inhibitor of protein kinase C (PKC) and induces apoptosis by indirectly blocking Bcl-XL. Since the immunosuppressive activity of chelerythrine chloride is caused by the induction of apoptosis, we determined that it is not an ideal candidate for immunomodulator activity. The next compound excluded from further evaluation after secondary screening was triptolide. Triptolide is a diterpene triepoxide isolated from the Chinese medicinal plant *Tripterygium wilfordii*. It is a known anti-inflammatory agent. Triptolide and its derivatives have been reported to exhibit immunosuppressive effects in

murine allo-HSCT models by inhibiting dendritic cell activation and the expansion of alloantigen-specific T cells[167–169]. Our secondary screening results showed that triptolide inhibited lymphocyte proliferation at low concentration (100nM). However, this concentration was found to be highly toxic to the leukocytes. Literature review further suggested that triptolide showed immunosuppression at nanomolar concentrations ranging from 5-100 nM *in vitro* and was toxic at an oral dose as low as 0.5 mg/kg causing hepatic and renal damage[170]. Although triptolide has shown excellent prophylactic effects against GVHD in murine models of allo-HSCT, its clinical translation has been limited because of its toxicity to various organs *in vivo*[170]. Therefore, we were discouraged from selecting triptolide as a lead candidate. Similarly, homoharringtonine inhibited lymphocyte proliferation at 100nM, which was highly toxic to leukocytes. Homoharringtonine is an alkaloid extracted from *Cephalotaxus harringtonia* that is widely used in Chinese folk medicine because of its antiparasitic, anti-inflammatory and antineoplastic effects[171]. Homoharringtonine binds to the A-site in the peptidyl transferase of the ribosome, thus exhibiting cytotoxic effects via inhibition of protein translation[172]. The IC50 of homoharringtonine was reported to be as low as 17nM in P-388 murine leukemic cells. This compound has recently gained attention as a potent treatment option for chronic myelogenous leukemia, acute myeloid leukemia and myelodysplastic syndrome[173,174]. Despite its strong myelosuppressive action demonstrated in clinical trials, the effect of homoharringtonine has only been studied in cancer cells, and knowledge of its effects on normal leukocytes appears to be scarce. Additionally, its immunosuppressive action is based on the induction of apoptosis and is not immunomodulatory; therefore, we eliminated homoharringtonine after secondary screening.

The two lead compounds that emerged were demethylzeylasteral and 5-hydroxy-1,4-naphthoquinone, as they inhibited lymphocyte proliferation at non-toxic concentrations. Demethylzeylasteral is an active component from the plant *Tripterygium wilfordii*. It has been reported to exhibit immunosuppressive effects in rat and canine kidney transplant models[175,176]. Although this compound has shown efficacy in a rodent model of transplantation, its clinical use is limited due to toxicity concerns associated with the active components as well as the cost and difficulties associated with the isolation of demethylzeylasteral[177]. Nevertheless, demethylzeylasteral is an ideal immunomodulator, however, since its prophylactic efficacy has already been evaluated in the transplant setting, we selected 5-hydroxy-1,4-naphthoquinone (5NQ or juglone) as the lead compound. It is an active component of black walnut (*Juglans nigra*). It has been reported to exhibit anti-inflammatory actions in several inflammatory disorders such as ulcerative colitis, inflammation-induced colon carcinogenesis, rheumatoid arthritis, and Alzheimer's disease[178]. It is a potent inhibitor of Pin-1 (prolyl isomerase) which regulates several phosphoproteins and indirectly affects the activity of NF-κB, a major transcription factor that mediates inflammation[179–181]. A study by Seshadri et al. showed that 5NQ causes dose-dependent cytotoxicity in human peripheral blood mononuclear cells (HPBMCs) and causes ROS induced capsapse-3 dependent apoptosis of HPBMCs at a very high concentration of 50μM[182]. Our secondary screening results showed that 5NQ inhibited lymphocyte proliferation at a very low concentration of 1μM and was not cytotoxic to cells at this concentration. Moreover, its anti-inflammatory efficacy has not been evaluated in preclinical allotransplant settings. This encouraged us to assess the immunomodulatory potential of 5NQ *in vitro.* Our results revealed that transient treatment of splenic leukocytes with 5NQ inhibited mitogen-induced activation of APCs and CD4+ T cells, and inhibited mitogen-induced Th1/Th2 cytokine imbalance in vitro. Additionally, transient treatment

with 5NQ induced an anergic/exhaustive state of $CD4^+$ T cells and did not promote their differentiation into Tregs. Therefore, our *in vitro* results provide a preliminary understanding of the immunomodulatory effects of 5NQ and showed that 5NQ modulates immune responses by inhibiting Th1/Th2 imbalance, inhibiting APC activation, and inducing $CD4^+$ T cell anergy. Finally, we showed that treatment with 5NQ did not suppress the anti-tumor activity of leukocytes *in vitro*, thus encouraging us to evaluate its prophylactic efficacy *in vivo.* Most studies reporting the anti-inflammatory effect of juglone have been evaluated using murine or human macrophage cell lines, and limited information is available on the effect of 5NQ on primary leukocytes, mainly T cells[180,183,184]. Our study is among the few that sheds light on the immunomodulatory potential of 5NQ on primary leukocytes and shows that the immunomodulatory effect of 5NQ is exhibited at a much lower concentration than its cytotoxic concentration.

In conclusion, this study identified two potent immunomodulators, demethylzeylasteral and 5-NQ and the latter was further evaluated for its immunomodulatory effects on various immune cell subtypes. The concentration of 5NQ at which the immunomodulatory effect was observed was much lower than its cytotoxic concentration. Lastly, retention of the anti-tumor activity of 5NQ treated leukocytes provided a good basis for evaluation of prophylactic efficacy in murine models of acute GVHD.

Objective 2

6 OBJECTIVE 2

6.1 Background

Juglone

Juglone is a phenolic compound found in the fresh leaves, green husks, roots, bark, and nuts *of Juglans nigra, Juglans regia, Juglans cinera,* and *Carya illinoinensis*, (walnut trees). Chemically it is a naphthoquinone composed of quinone ring with oxygen atoms at positions 1 and 4 and an aromatic ring that has been hydroxylated at position 5. The chemical name of juglone is 5-hydroxy-1,4-naphthoquinone which is abbreviated as 5NQ [185]. The physicochemical characteristics are mentioned in Table 21: Structure and Physicochemical properties of 5NQ.

Table 21: Structure and Physicochemical properties of 5NQ[185].

Chemical name	**1,4-Napthoquinone, 5-hydroxy-(8CI)**
PubChem CID	3806
Synonyms	Akhnot; C.I. 75500; C.I. Natural Brown 7; 5-hydroxy1,4-naphthalenedione;5-hydroxynaphthoquinone; juglone; regianin; walnut extract
Molecular formula	C10H6O3
Molecular weight	174.16
Appearance	Solid
Melting point	155.0 °C
Solubility	Insoluble in water, ~10 mg/ml in EtOH & DMSO
Chemical structure	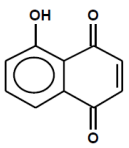

Origin and history

Walnut trees have been revered for their many uses and potential dangers since prehistoric times. Juglone, which is found in the kernels, leaves, and green husks of *Juglans regia*, was

found to be toxic to many other plant species (allelopathic property of juglone), stunting their development[186]. The walnut tree has been cultivated since 4000 B.C., initially for its medicinal and nutritional value, and is now widely harvested for its wood and fruit. The common walnut, or *Juglans regia L.*, is a tree in the family Juglandaceae. It is also known as English walnut and Persian walnut. Walnuts have been used for centuries, in folk medicine and in the pharmaceutical and cosmetic industries, as both food and medicine. Experimental and epidemiological studies have shown that walnuts are beneficial for many chronic diseases, including coronary heart disease, rheumatism, diabetes, obesity, and cancer[178]. In addition, many studies have found a link between dietary intake of walnuts and lower risk of developing cancer. Walnuts are rich in polyphenols, proteins, fiber, sterols, and essential fatty acids. Walnut is the most enriched nut species when only phenolic antioxidant levels are considered[187]. The most well-known naphthoquinone, juglone, is found in the young leaves. The results showed that there were appreciable amounts of juglone, ranging from 13.1 to 1556.0 mg/100 g of leaf dry weight[188]. Juglone was first isolated from walnuts in the 1850s, and scientific evidence of its allelopathic effect was published in 1881[189]. In living plants, juglone is in a non-toxic glycosylated form however, when exposed to soil or air, this allelopathic compound is immediately transformed into an oxidized, highly toxic form. Juglone has been found to have antidepressant, antimicrobial, anti-cancer, anti-fungal, antioxidant, apoptotic, and anti-angiogenic properties[187,188]. Evidence suggests that juglone and its derivatives can prevent food spoilage by making it more resistant to oxygen and reactive species. Seventy-three juglone-related patents were issued in the United States between 1976 and 1999. These patents demonstrate the potential applications of juglone from antiviral naphthoquinone derivatives for AIDS treatment, in skin and hair coloring preparations[190,191].

Biochemistry of naphthoquinones: biological effects of the electrophilic properties of naphthoquinones

Free radicals are reactive chemical entities containing unshared electrons. They consist of radical and non-radical oxygen species formed by the partial reduction of oxygen. Reactive oxygen species (ROS) includes superoxide, ($O_2^{\bullet-}$), hydroxyl ($OH^{\bullet}$), per hydroxyl ($HO_2^{\bullet}$) radicals and hydrogen peroxide (H_2O_2). In biological reactions, cytochrome P450 reductase and other flavoprotein enzymes can reduce the quinone moiety to semiquinone, which can subsequently be reduced to hydroquinone via a sequence of two one-electron reductions[192]. The semiquinone intermediate can further fuel any of the following three reactions. 1) It can be converted to hydroquinone, which is then removed from the cell by de-esterification. 2) The formed hydroquinone can be reconverted to semiquinone via oxidation reactions, 3) The formed semiquinone is converted to superoxide and hydrogen peroxide via a redox cycling chain involving semiquinone and hydroquinone (Figure 31)[192,193]. In conclusion, these two reactions characterize the interactions of quinones with biological systems. First, they function as electron transfer agents, transferring electrons from a reducing agent such as NADPH to oxygen, which produces superoxide that is eventually converted into oxygen and hydrogen peroxide. Second, they form covalent bonds with nucleophilic functional groups, such as thiol (SH), in biological molecules such as electrophiles (Figure 31B)[194]. Therefore, the interactions of naphthoquinones with biological molecules have two major fates: the redox cycling of naphthoquinone to semiquinones leading to ROS production ultimately resulting in cellular oxidative stress and naphthoquinones can directly quench reactive oxygen species by donating hydrogen atoms, inhibiting ROS-producing enzymes, chelating transition metal ions, and regenerating membrane bound antioxidants such as tocopherol (vitamin E)[193,194].

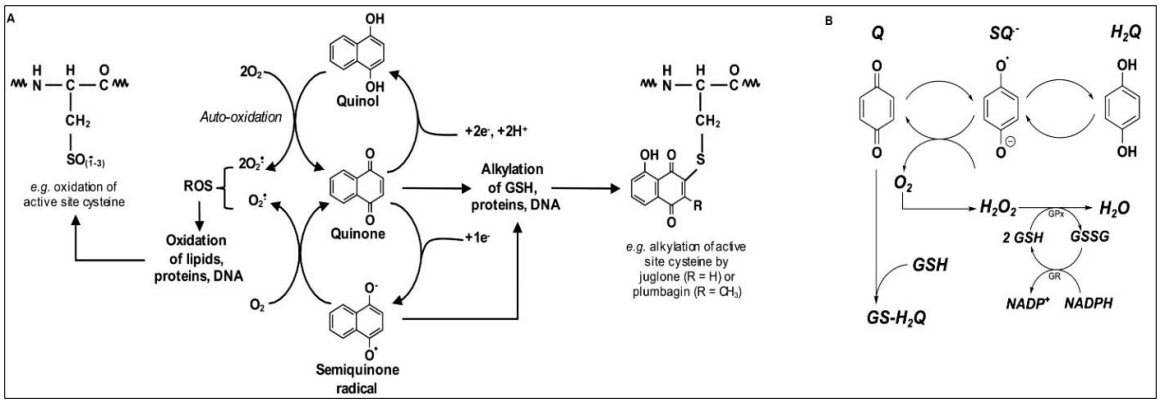

Figure 31: Redox cycling of 1,4-naphthoquinones. (A) Redox cycling of 1,4-naphthoquinones may lead to the generation of reactive oxygen species (ROS), which can oxidize certain cellular macromolecules. (B) The quinone (Q) or semiquinone (SQ^-) forms of 1,4-naphthoquinones can react with nucleophiles, and cellular proteins to form adducts. GSH: glutathione; H_2Q: hydroquinone; GSSG: glutathione disulfide; GS-H_2Q -glutathione-quinone adduct. Figure adapted from[195,196]

Therefore, naphthoquinones can act as pro-oxidants or antioxidants, depending on the exposure conditions, such as the presence of an oxygen-rich environment or the availability of transition metals. Nevertheless, naphthoquinones are redox-active compounds that modulate the activity of cellular proteins via oxidative stress, and their cytoprotective or cytotoxic potential depends on the exposure to naphthoquinones (Figure 32)[197].

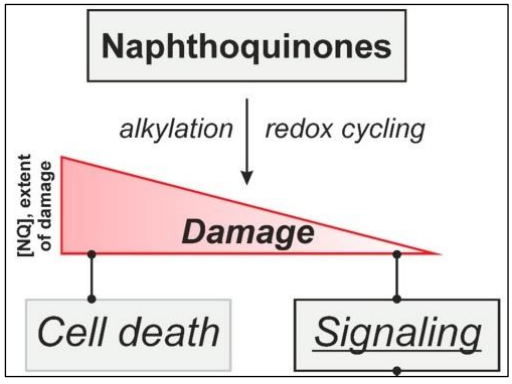

Figure 32: Naphthoquinones (NQ), cause damage that may result in cell death via oxidation or alkylation of cellular target structures. Lower concentrations of NQ elicit cell signaling cascades that prevent cellular damage and activate adaptive stress responses. Figure adapted from[197]

Biological activities of Juglone

Juglone has been reported to have pro-oxidant, antioxidant, anti-inflammatory, anti-cancer, antidiabetic, and anti-microbial activities[178]. The biological effects are concentration dependent, where lower concentrations are cytoprotective, whereas higher concentrations have been cytotoxic[193].

Pro-oxidant effects and Cytotoxicity

Juglone is a known biological toxin because of its allelopathic actions. The potential of juglone as a cytotoxic agent has been extensively studied on various cancer cell lines[198] such as human leukemia cells (HL-60 and doxorubicin-resistant HL-60)[199], the human hepatoma cell line HepG2[200,201], the BALB/c mouse fibroblast cell line 3T3[202], MCF-7 breast cancer cells[203–206], C6 rat glioma cells[207–215], and human keratinocytes[216–218]. DNA damage, inhibition of transcription, and inhibition of p53 have been implicated in juglone-mediated cell death[201,203,210,212]. However, the cytotoxicity of juglone can be attributed to its redox cycling activity or interaction with cellular thiols[202,203,205,212,214]. ROS generated by redox cycling activity can enhance lipid peroxidation and thus facilitate cell death[197,217,219,220]. It also forms adduct which in turn causes glutathione depletion. The thiol group on reduced glutathione is a very good nucleophile and is easily arylated by juglone. The arylation of reduced glutathione by juglone increases cellular toxicity by decreasing the availability of reduced glutathione (GSH).[221,222].

Antioxidant activity

Intramolecular hydrogen bonding between the hydroxyl and keto groups in juglone makes it an active hydrogen atom donor[196]. This chemistry of juglone enables it to directly quench free radicals and reduce oxidative stress. The antioxidant properties of juglone have been evaluated in oxidative stress-linked diseases, such as Alzheimer's disease[223] and fibrotic diseases of the

liver[224] and kidney[225]. Treatment of primary cortical neurons with juglone prevented oxidative and heat stress-induced dephosphorylation of Tau protein *in vitro*[223]. Supplementation with diet rich in walnut to transgenic mice models of Alzheimer's disease showed reduction in oxidative damage[226]. Moreover, juglone has been reported to reduce oxidative stress by inhibiting Smad2 phosphorylation in the kidney and alleviating kidney fibrosis.[225,227] Additionally, in a model of liver fibrosis, juglone increased the activity of superoxide dismutase (SOD), thus reducing oxidative stress. This antioxidative activity has been shown to mitigate inflammatory conditions[224].

Antifungal activity

Concoctions from unripe black walnut hulls have been used since the age of folk medicine to treat fungal infections. It is active against *Candida albicans*, *Trichophyton mentagrophytes*, and *Microsporum canis*, and was as effective as commercially available anti-fungal agents such as zinc undecylenate and selenium sulfide[228,229].

Antibacterial activity

Antibacterial activity of juglone has been widely demonstrated both gram positive and negative bacteria involving *E. coli*, *B. subtilis*, *S. aureus* as well as methicillin resistant *S. aureus* (MRSA)[230–233]. Various mechanisms have been implicated regarding the antibacterial effects, including redox cycling, mitochondrial oxidative stress, and DNA, RNA, and protein synthesis inhibition [229–233].

Juglone as a Pin 1 inhibitor

Peptidyl-prolyl cis/trans isomerase (PIN1) that catalyzes the cis/trans isomerization of peptide bonds preceding prolyl residues regulate protein phosphorylation and cell signaling[234]. Juglone

mediated inhibition of Pin1 has been associated with an improvement in the dephosphorylation of Tau protein in Alzheimer's disease[223,234]. Pin1 activity has been implicated in a variety of inflammatory conditions such as allergy[235], rheumatoid arthritis[236], diabetes[237], and Parkinson's disease[238]. It is responsible for the phosphorylation of NF-κB, leading to its activation; hence, inhibition of Pin1 by juglone is associated with the alleviation of various inflammatory diseases[239–241]. Pin1 was shown to increase nitric oxide production by activating the TNF pathway in neutrophils, causing a heightened inflammatory response in intestinal injury. Juglone inhibited Pin1 activity, thereby reducing neutrophil-induced oxidative stress[242,243]. Pin 1 inhibition has been reported to have antiproliferative effects on cancer cells[239,241].

Effects of juglone on cell signaling pathways

Juglone has been reported to modulate various cell signaling pathways. It activates ERK, JNK, and p38 in the skin, glioblastoma, cervical cancer, melanoma, hepatocellular carcinoma, and smooth muscle cells[200,210,213,215]. Juglone modulates MAP kinases to induce apoptosis. Some investigations have revealed that MAP kinase activation is dependent on ROS generation, suggesting that naphthoquinone redox cycling may be the underlying mechanism. Juglone suppresses the Akt/GSK-3b/Snail pathway and epithelial-mesenchymal transition in prostate cancer cells[244]. Juglone also reduced Akt phosphorylation in trastuzumab-resistant breast cancer cells[205].

Anti-inflammatory effects of juglone

Few studies have highlighted its anti-inflammatory potential. Juglone has been reported to suppress LPS induced activation of RAW.67 and J774.1 macrophages via inhibition of ROS and nitric oxide (NO) production[245]. Additionally, inhibition of Pin1 by juglone at low concentrations (0.5μM) mitigates LPS or TNF-α induced respiratory bursts in human

neutrophils, thus preventing excessive ROS production at the site of inflammation[242,243]. The anti-inflammatory effects of juglone have also been evaluated in murine models of inflammatory conditions. In the DSS-induced colitis murine model, administration of 0.04 mg/kg 5NQ daily with water reduced DSS-induced oxidative stress and tissue damage. The authors further showed that 5NQ administration suppressed the pro-inflammatory cytokines IL-6, TNF-α, and NF-kB via the induction of antioxidant activity through Nrf-2[246]. Additionally, two reports have evaluated its immunomodulatory effects. Treatment with juglone enhanced antitumor immunity by eliminating myeloid-derived suppressor cells (MDSCs) and restoring the Th1/Th17 balance in a murine model of colon carcinoma[247]. In another study, intraperitoneal administration of juglone (3 mg/kg), before immunization with the BCG vaccine, caused an increase in CD8 T cells, showing a potential immunomodulatory effect[248]. In conclusion, anti-inflammatory/ immunomodulatory effects of juglone have been investigated on few types of immune cells namely macrophages[245] and neutrophils[249] However, its effect on T lymphocytes has not been widely studied[248]. Moreover, the anti-inflammatory activity of juglone is mainly mediated through inhibition of Pin1and NFκB inhibition[249–254].

Summary

The above literature suggests that juglone mediates its biological activities through modulation of cellular redox and inhibition of Pin1, which further perturbs the activities of other cellular signaling proteins, such as NF-κB, MAPK, ERK, JNK, p38, p53, and Akt. Moreover, limited studies have described the anti-inflammatory activities of juglone with respect to immune cells. Therefore, we evaluated the effects of juglone (5NQ) on cellular redox reactions, antioxidant response signaling, and inflammatory signaling proteins in murine splenic leukocytes.

6.2 METHODOLOGY

All experiments in this study were conducted using murine splenic leukocytes isolated from the spleen of healthy BALB/c mice (8-10 weeks old).

Evaluation of the effect of 5NQ treatment on cellular redox in leukocytes: The naphthoquinone class of compounds is well known for its redox cycling activity. Therefore, we evaluated the effects of 5NQ treatment on cellular redox reactions.

Measurement of mitochondrial and cellular ROS: To evaluate the effect of 5NQ treatment on mitochondrial and cellular ROS levels, leukocytes were treated with different concentrations of 5NQ (1, 2.5 and 5µM) or vehicle for 1, 2, and 4 h, after which the cells were washed with PBS and stained with MitoSOX red (1µM) and H2DCFDA (1µM) in PBS for 30 min at 37 °C in the dark. The cells were washed thrice and analyzed using a flow cytometer.

To estimate cellular ROS levels using CellROX orange dye, leukocytes were treated with 1µM 5NQ for 2 h, washed, and stained with CellROX orange dye (2.5µM for 30 min at 37 °C) in the dark. The cells were analyzed using a flow cytometer.

For the estimation of mitochondrial and cellular ROS by confocal microscopy, leukocytes were treated with 1µM 5NQ for 2 h, washed, stained with H2DCFDA, MitoSOX red, and CellROX orange dye, as mentioned above, and imaged on a Leica SP8 confocal microscope at a magnification of 630x with a 1x-3x digital zoom. Sections of 0.5µm of the entire cell were captured, and images were represented as a projection of the entire Z-stack. Images were processed using Leica LASX software.

Measurement of intracellular GSH levels: Thiol tracker violet dye was used to determine intracellular glutathione levels in leukocytes after treatment with 1µM 5NQ for 15, 30, 60, 120, and 240 min. The cells were washed twice with PBS and stained with 10µM thiol tracker

violet dye for 30 min at 37 °C in the dark. The cells were then washed and analyzed using flow cytometry.

Evaluation of the effect of pre-treatment of leukocytes with thiol antioxidants on 5NQ mediated effects on cellular redox and leukocyte proliferation: To understand the role of thiols and altered cellular redox status in the observed immunosuppressive activity of 5NQ, we evaluated the effect of 5NQ treatment on cellular redox in the presence of the thiol antioxidant N-acetylcysteine (NAC).

Evaluation of 5NQ mediated cellular redox alterations in presence of N-acetyl cysteine (NAC): Leukocytes were pre-treated with NAC (10mM) for 2 h before 5NQ treatment. Leukocytes were treated with 1µM 5NQ for 4 h unless otherwise mentioned. 5NQ was removed from the culture medium by washing the leukocytes with PBS. DMSO (0.01% in PBS or RPMI 1640) was used as the vehicle control in all the experiments. After 5NQ treatment, cells were washed with PBS and stained with MitoSOX red, H2DCFDA, or CellROX orange dye, as described previously, and analyzed using a flow cytometer.

Evaluation of the effect of thiol antioxidants on the anti-proliferative effect of 5NQ: The effect of thiol antioxidants on the anti-proliferative effect of 5NQ was evaluated using the CFSE dye dilution assay. Leukocytes were stained with CFSE dye. Leukocytes were pre-treated with thiol antioxidants, GSH (10mM) or NAC (10mM) for 2 h, followed by treatment with 1µM 5NQ for 4 h. The cells were then washed with PBS to remove 5NQ from the culture medium. DMSO (0.01% in RPMI 1640) was used as vehicle control. Cells were then stimulated with mitogen concanavalin A (Con A, 2.5µg/ml) and incubated for 72 h. The cells were analyzed using a flow cytometer to measure CFSE fluorescence.

Evaluation of physical interaction of 5NQ with thiol antioxidants GSH and NAC using absorption spectrometry: The absorption spectra of 5NQ were measured using a spectrophotometer in the presence and absence of GSH and NAC. Briefly, 1µM 5NQ was incubated with either GSH (1mM) or NAC (1mM) for 1 h at 37°C, after which absorption spectra were measured at 300-900 nm wavelengths using a spectrophotometer.

Evaluation of the effect of 5NQ treatment on antioxidant response signaling in leukocytes: The effect of 5NQ treatment on the expression of anti-oxidant response proteins Nrf2, HO1, and NQO1 in leukocytes was studied in the presence or absence of NAC and mitogenic stimulation with Con A. Leukocytes were pre-treated with NAC (10mM, 2 h), followed by treatment with vehicle or 1µM 5NQ for 3 h, followed by stimulation with Con A for 4 h. Expression of HO1 and NQO1 was evaluated by immuno-blotting. Nrf2 expression was studied by immunofluorescence microscopy and flow cytometry.

Evaluation of the immunosuppressive effect of 5NQ on leukocytes from Nrf2 knockout mice: We evaluated the effect of 5NQ treatment on cytokine secretion and lymphocyte proliferation in splenic leukocytes from Nrf2 knockout C57BL/6 mice to understand the role of Nrf2 in 5NQ mediated immunosuppressive activity. Briefly, leukocytes were isolated from Nrf2 knockout mice as previously described.

Effect on cytokine secretion: To study the effect of 5NQ treatment on cytokine secretion, 1 x 10^6 leukocytes were seeded in a 24 well plate and treated with either vehicle (0.01% DMSO in RPMI 1640 medium) or 5NQ (0.5 and 1µM, 4h), followed by stimulation with Con A and incubation for 24 h. Cells were harvested by centrifugation at 2500 rpm for 5 min. The supernatants were collected and stored at -80˚C until analysis.

Cytokine concentrations (IL-2, IL-4, IL-6, IFN-γ, TNF, IL-10, and IL-17A) were measured in the supernatant using a BD™ Cytometric Bead Array (CBA Becton-Dickinson, NJ, USA). The analysis was performed according to the manufacturer's instructions. The cell supernatants or sera were incubated with mixed capture beads, followed by the addition of the detection antibody, and incubated at room temperature for 3 h, according to the manufacturer's instructions. Samples were washed, acquired on a BD FACS Aria, and analyzed using the FCAP array software.

Effect on leukocyte proliferation: To study the effect of 5NQ treatment on proliferation of leukocytes from Nrf2 KO mice, leukocytes were stained with CFSE dye. Cells were then treated with 5NQ (0.1, 0.5, 1, 2.5 and 5µM, for 4h) and stimulated with Con A, as previously described. The cells were incubated for 72 h, and CFSE fluorescence was quantified using a flow cytometer.

Effect of 5NQ on leukocyte proliferation in presence of Nrf2 inhibitor: We also evaluated the effect of 5NQ treatment on the proliferation of wild-type leukocytes in the presence of the Nrf2 inhibitor ML385 using the CFSE dye dilution assay. Briefly, the cells were pre-treated with ML385 (10µM) for 2 h, followed by treatment with 5NQ (1µM, 4 h). The cells were washed and stimulated with Con A, as previously described, and incubated for 72 h. CFSE fluorescence was measured by flow cytometry.

Evaluation of the effect of 5NQ treatment on inflammatory signaling in leukocytes: The effect of 5NQ treatment on the activation of inflammatory signaling proteins, such as NF-κB and Akt, was studied in the presence or absence of NAC and mitogenic stimulation with Con A using immuno-blotting. Briefly, leukocytes were pre-treated with NAC (10mM, 2 h), followed by treatment with vehicle or 1µM 5NQ for 3 h, and stimulation with Con A for 4 h.

NF-κB activation was studied by evaluating its expression in the cytoplasmic and nuclear lysates. The expression of phosphorylated and total Akt was evaluated in cytoplasmic lysates.

6.3 RESULTS

Effect of 5NQ on cellular redox status: We evaluated the effect of 5NQ treatment on mitochondrial and cellular ROS levels in leukocytes. Treatment with 5NQ caused a time and concentration dependent increase in mitochondrial ROS in leukocytes, as measured using MitoSOX red dye (Figure 33A and C). Surprisingly, 5NQ treated leukocytes showed time and concentration dependent decrease in cellular ROS, as measured by H_2DCFDA and CellROX orange dye **(**Figure 33A and C**)**. In addition, we observed a decrease in thiol tracker violet fluorescence in 5NQ treated leukocytes which indicated low levels of cellular GSH in treated cells compared with untreated cells (Figure 34).

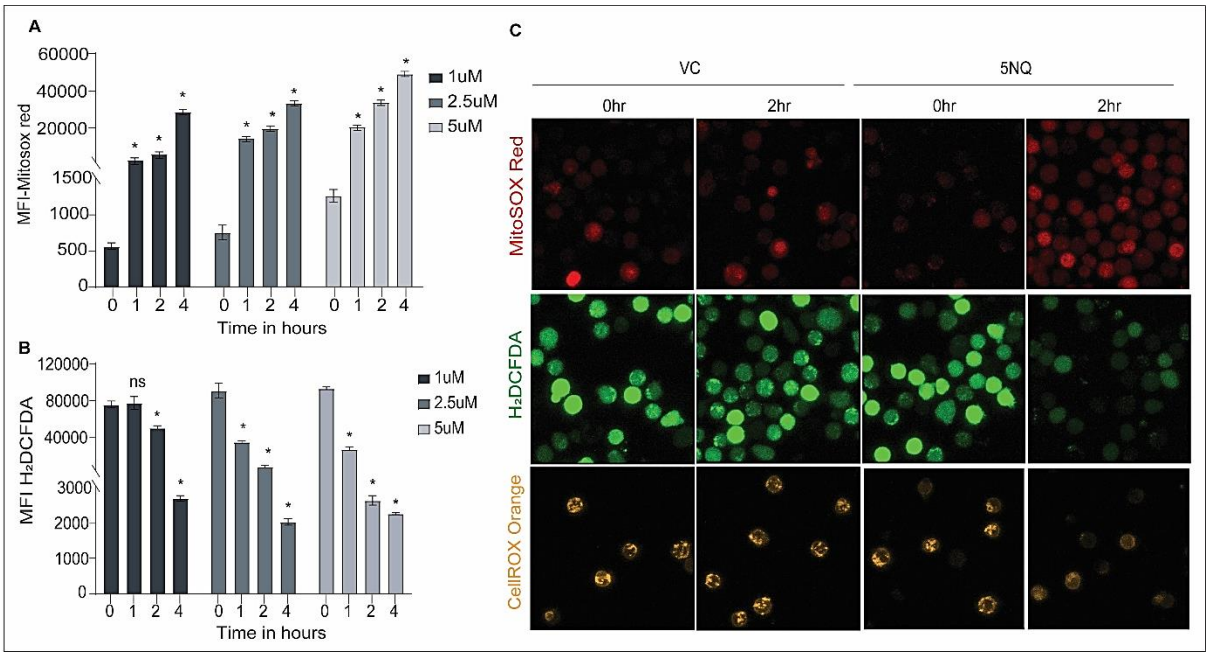

Figure 33: Modulation of cellular redox balance by 5NQ in vitro. (A-B) Bar graph showing median fluorescence intensity (MFI) of MitoSOX red dye and H_2DCFDA. Leukocytes were treated with different concentrations of 5NQ for the indicated times to determine changes in mitochondrial and cellular ROS levels (n = 5 independent experiments; mean ± SEM). (C) Fluorescence microscopy images of leukocytes stained with MitoSOX red, H_2DCFDA, and CellROX orange before and after treatment with vehicle (0.01% DMSO) or 5NQ (1µM, 2 h) (n = 3 independent experiments). Data were

analysed using one-way ANOVA with Bonferroni correction for multiple comparisons; *p<0.05, compared to untreated groups.

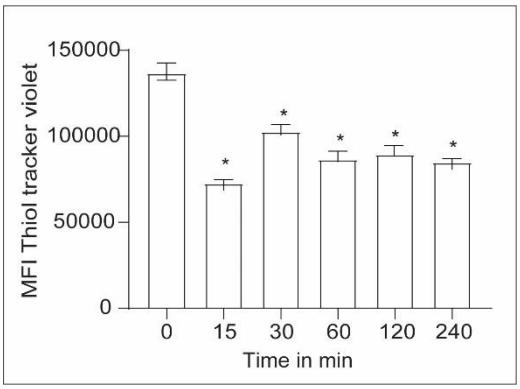

Figure 34: Effect of 5NQ on cellular GSH levels. Bar graph showing MFI for the thiol tracker violet dye used to determine cellular GSH levels in leukocytes treated with 5NQ (1µM) (n = 5 independent experiments; mean ± SEM). Data were analyzed using one-way ANOVA with Bonferroni correction for multiple comparisons; *p<0.05, compared to untreated groups.

Effect of 5NQ on cellular redox in presence of thiols: To understand the role of mitochondrial ROS and altered cellular redox in the observed immunosuppressive activity of 5NQ, we evaluated the effect of 5NQ treatment on cellular redox in the presence of the thiol antioxidant, NAC. Pre-treatment of leukocytes with NAC, inhibited 5NQ induced alterations in mitochondrial and cellular ROS levels (Figure 35A-C). Moreover, pretreatment with GSH and NAC abrogated the anti-proliferative effect of 5NQ on leukocytes (Figure 35D). We further investigated whether 5NQ interacts with thiol antioxidants. Incubation of 5NQ with GSH or NAC changed the absorption spectrum of 5NQ (Figure 36)**,** indicating a probable physical interaction of 5NQ with thiol antioxidants.

Effect of 5NQ on antioxidant response signaling: As 5NQ treatment resulted in alterations in cellular redox, we evaluated the effect of 5NQ on the expression of the redox-sensitive transcription factor Nrf-2 and its downstream targets HO1 and NQO1. We found that leukocytes treated with 5NQ showed an increase in Nrf-2 expression, as observed by confocal microscopy and flow cytometry (Figure 37 A-C). Western blot analysis further

confirmed a subsequent increase in expression of HO-1, a downstream target of Nrf-2, indicating the up-regulation of antioxidant response signaling in these cells. However, pre-treatment of leukocytes with NAC could inhibit 5NQ mediated up-regulation of Nrf-2 and HO-1, thus reversing 5NQ induced up-regulation of antioxidant response signaling in leukocytes (Figure 37D and E).

To further examine the role of Nrf-2 in mediating the immunosuppressive action of 5NQ, we studied leukocyte proliferation in the presence of the Nrf-2 inhibitor ML385 and found that Nrf-2 inhibition did not reverse the anti-proliferative effect of 5NQ (Figure 38A). Similar results were obtained when we studied the proliferation of leukocytes from Nrf-2 KO mice after treatment with 5NQ (Figure 38B). Therefore, to understand the role of Nrf-2 in 5NQ mediated immunomodulation, we studied the effect of 5NQ treatment on mitogen-induced cytokine secretion from Nrf-2 KO leukocytes (Figure 38C). We observed that 5NQ treatment of Nrf-2 KO leukocytes did not restore the mitogen-induced Th1/Th2 cytokine imbalance, as observed in wild-type leukocytes (Figure 38D-E). These results indicate that 5NQ mediates its immuno-modulatory action via alteration of the cellular redox status and thiol depletion, consequently up-regulating the Nrf-2 antioxidant response system.

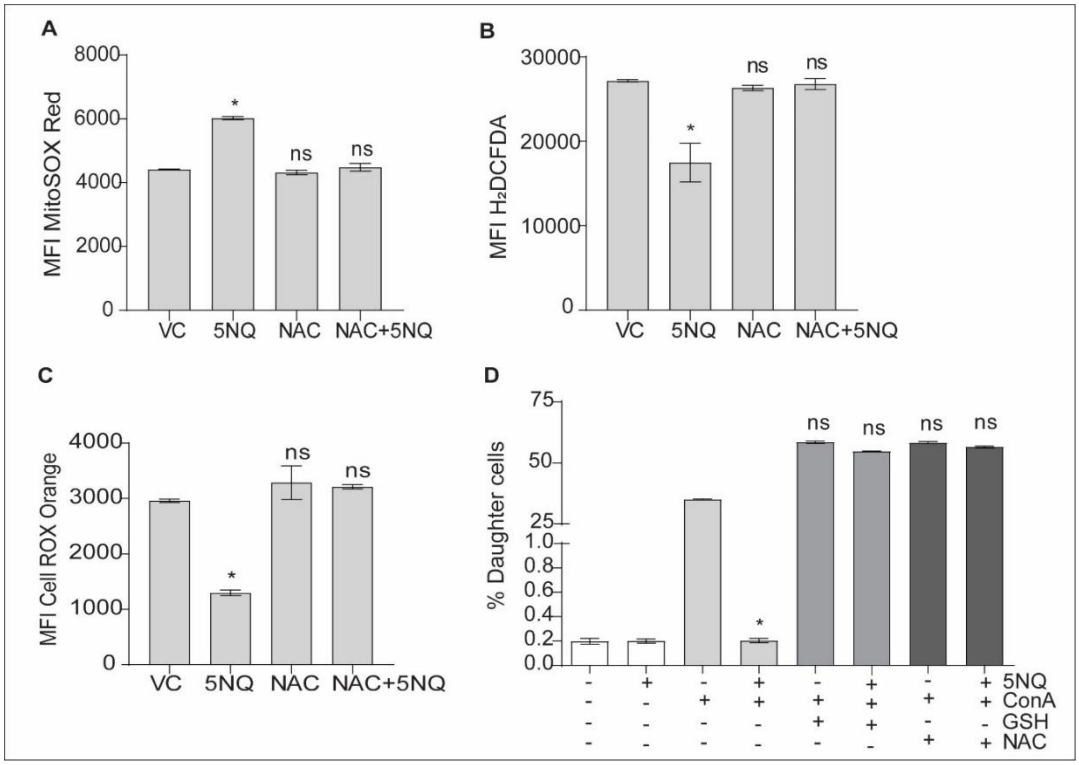

Figure 35: Thiols abrogate the effect of 5NQ on cellular redox reactions. (A-C) Bar graphs showing MFI of MitoSOX red, H2DCFDA, and CellROX orange in leukocytes treated with 5NQ (1µM, 2h) in the presence or absence of N-acetyl cysteine (NAC) (n = 5 independent experiments; mean ± SEM). (D) Effect of 5NQ treatment on leukocyte proliferation in the presence of the thiol antioxidants, NAC and GSH. The bar graph shows the percentage of daughter cells after 72 h of Con A stimulation (n = 5 independent experiments, mean ± SEM). Data were analyzed using one-way ANOVA with Bonferroni correction for multiple comparisons; *p<0.05, compared to untreated, VC, or VC+A-treated groups.

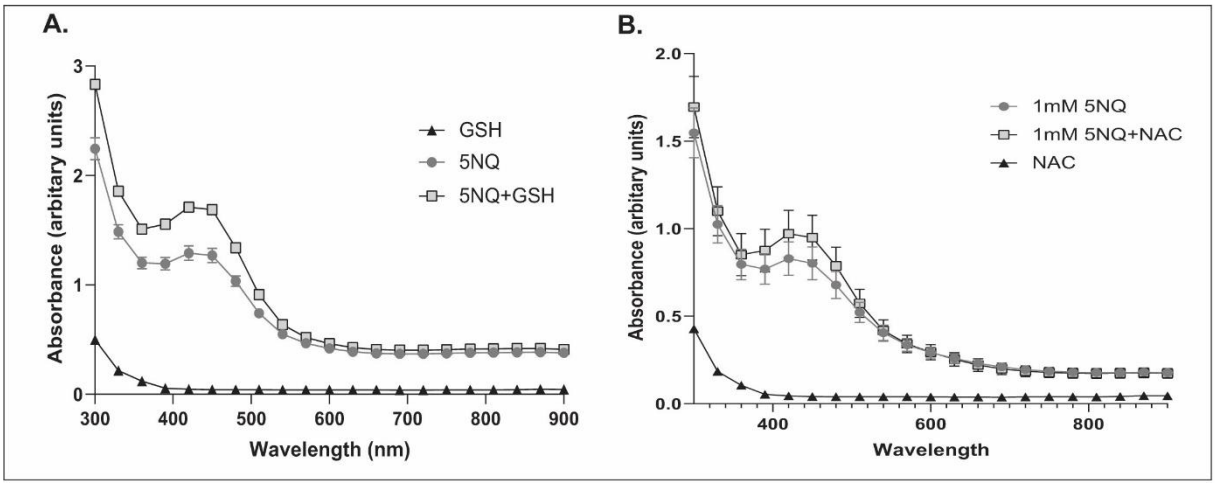

Figure 36: Absorption spectrum of 1mM 5NQ in the presence of (a) GSH and (b) NAC.

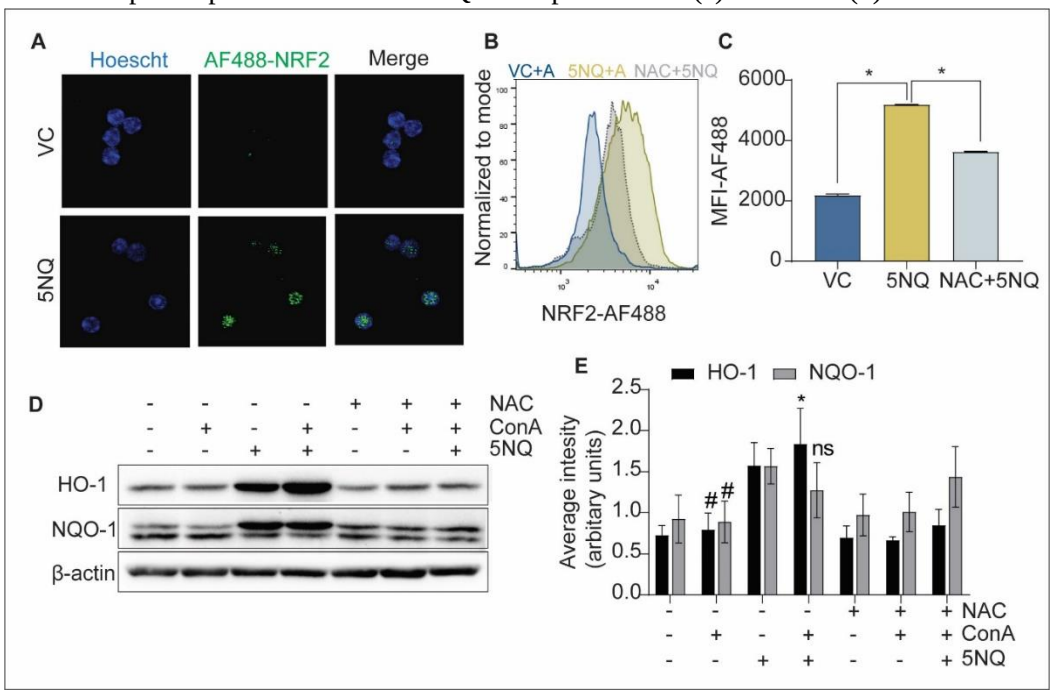

Figure 37: Up-regulation of Nrf-2/HO-1signaling by 5NQ in vitro. (A) Leukocytes were treated with vehicle (DMSO 0.01%) or 5NQ (1µM, 4 h) and stained with Alexa Fluor 488 labelled anti-Nrf-2 antibody and Hoechst 33342. Immunofluorescence images of leukocytes stained with antibodies against Nrf-2 (green) and Hoechst (blue) (n = 3 independent experiments). (B-C) Leukocytes were treated with vehicle (DMSO 0.01%) or 5NQ or pre-treated with NAC (10 mM, 2 h) followed by 5NQ treatment and stained with Alexa Fluor 488 labelled anti-Nrf-2 antibody. Histograms and bar graph showing the median fluorescence intensity (MFI) of Alexa Flour 488 labelled anti-Nrf-2 antibody (n = 5 independent experiments). (D) Western blots showing the expression of HO-1 and NQO-1 after treatment with 5NQ (1µM, 3 h) in the presence or absence of the antioxidant N-acetylcysteine (NAC) and/or stimulation with Con A (2.5µg/ml,4 h). β-actin served as loading control. (E) Semi-quantitative analysis of western blots for HO-1 and NQO-1 (n = 5 independent experiments, mean ± SEM). Data were analyzed using one-way ANOVA with Bonferroni correction for multiple comparisons; *p<0.05, compared to the VC + A-treated group.

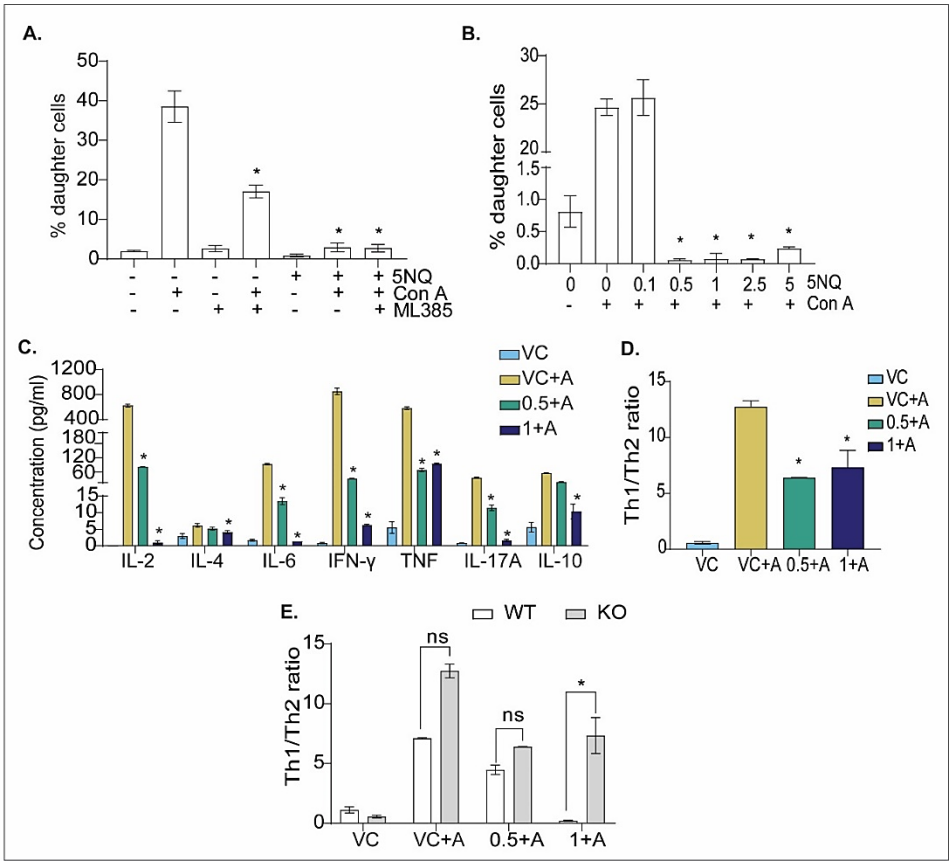

Figure 38: (A) Leukocyte proliferation after 5NQ (1 µM for 4 h) treatment in the presence or absence of the Nrf-2 inhibitor ML385 (10 µM for 2 h) followed by Con A (2.5 µg/ml) stimulation. Bar graphs represent percentage of daughter cells after 72 h of stimulation with Con A, calculated using CFSE dye dilution assay (n = 3 independent experiments; mean ± SEM). (B) Proliferation of Nrf-2 KO leukocytes after transient treatment with 5NQ (0.1, 0.5, 1, 2.5, and 5 µM for 4 h) followed by Con A stimulation. Bar graphs represent percentage of daughter cells after 72 h of stimulation with Con A, calculated using CFSE dye dilution assay (n = 5 independent; mean ± SEM). (C) Concentrations of Th1 (IL-2, IFN-γ, TNF), Th2 (IL-4, IL-6, IL-10) cytokines and IL-17A in cell supernatants at 24 h after stimulation of transiently treated Nrf-2 KO leukocytes with 5NQ (0.5 and 1 µM, 4 h) and stimulated with Con A (n = 3 independent experiments; mean ± SEM). (D) Bar graph representing Th1/Th2 cytokine ratio (mean ± SEM) calculated using concentrations of Th1 and Th2 cytokines in cell supernatants of Nrf-2 KO leukocytes treated with 5NQ (0.5 and 1µM, 4h) and stimulated with Con A. (E) Bar graph comparingTh1/Th2 cytokine ratios (mean ± SEM) calculated using concentrations of Th1 and Th2 cytokines in cell supernatants of wild-type (WT) and Nrf-2 KO (KO) leukocytes treated with 5NQ (0.5 and 1 µM, 4 h) and stimulated with Con A. Data were analyzed using one-way ANOVA with Bonferroni correction for multiple comparisons; *p<0.05, ns: non-significant, data were compared with VC+ Con A group.

Effect of 5NQ on inflammatory signaling: We evaluated the activation of NF-κB in cellular and nuclear lysates and the phosphorylation status of Akt, in 5NQ treated, resting, and mitogen-stimulated leukocytes. Treatment with 5NQ inhibits ConA-induced activation of NF-

κB and its nuclear translocation in leukocytes. It also inhibited ConA-induced phosphorylation of Akt. However, pre-treatment of leukocytes with NAC reversed the inhibitory effect of 5NQ on NF-κB activation and Akt phosphorylation, thus abrogating the 5NQ-mediated suppression of mitogen-induced signaling in leukocytes (Figure 39).

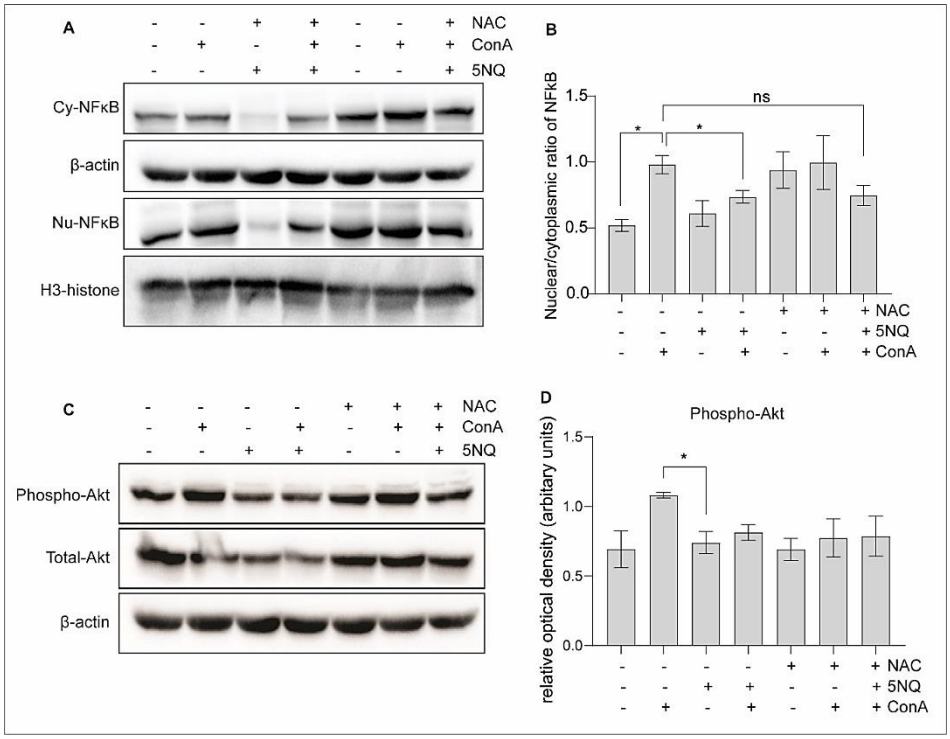

Figure 39: Treatment of leukocytes with 5NQ inhibits inflammatory signaling. (A) Western blots showing the expression of cytoplasmic and nuclear NF-κB in leukocytes after treatment with 5NQ (1µM, 3 h) ± N-acetylcysteine (NAC) and/or stimulation with Con A (2.5µg/ml, 4 h). β-actin served as loading control for cytoplasmic proteins and histone H3 served as loading control for nuclear proteins. (B) Semi-quantitative analysis of the nuclear to cytoplasmic ratio of NF-κB (n = 5 independent experiments, mean ± SEM). (C) Western blotting showing the expression of phosphorylated and total Akt in leukocytes after treatment with 5NQ (1µM, 3 h) in the presence or absence of antioxidant N-acetylcysteine (NAC) and/or stimulation with Con A (2.5µg/ml,4 h). β-actin served as loading control. (D) Semi-quantitative analysis of western blots for phospho-Akt (normalized to total Akt expression) (n = 5 independent experiments, mean ± SEM). Data were analyzed using one-way ANOVA with Bonferroni correction for multiple comparisons; *p<0.05, compared with the VC + A-treated group.

6.4 DISCUSSION

Juglone (5NQ) was selected as the lead molecule based on our phytochemical drug library screening results. The results demonstrated the immunomodulatory effect of juglone on murine splenic leukocytes. Therefore, we performed further experiments to understand the mechanisms underlying the immunomodulatory effects of 5NQ in murine leukocytes.

First, we sought to understand the changes in cellular redox status and signaling in leukocytes after 5NQ treatment to elucidate a plausible mechanism of its immunomodulatory action. Our results showed that 5NQ modulated the cellular ROS balance by selectively increasing mitochondrial ROS in leukocytes. Furthermore, we showed that 5NQ mediated changes in cellular redox were reversed in the presence of thiols. Additionally, we observed a decrease in the cellular GSH levels after treatment with 5NQ. Moreover, the anti-proliferative effect of 5NQ was abrogated in leukocytes pre-treated with thiol antioxidants. Furthermore, the absorption spectra of 5NQ were perturbed in the presence of the thiol-containing antioxidants GSH and NAC, indicating quinone-thiol adduct formation. These results indicate that thiol depletion may be one of the factors contributing to the 5NQ mediated immunomodulatory effects. The naphthoquinone compounds are known to form adducts with thiol-containing proteins and antioxidants, such as GSH and NAC[255,256]. Thiol depletion can have various effects on cellular signaling, the most common being an increase in antioxidant response proteins such as superoxide dismutase (SOD), catalase, thioredoxin (Tx), and Nrf2, which consequently up-regulate the adaptive stress response in these cells, protecting them from further damage and apoptosis[255,256]. However, extensive depletion of thiol antioxidants, which cannot be salvaged by the activated antioxidant response, may lead to cell death[220]. In our study, we observed that transient treatment with 5NQ did not cause cell death at 24 h, indicating that these cells were under adaptive stress. Additionally, it is difficult to explain the

causal relationship between GSH depletion and mitochondrial ROS[195,222]. Juglone or 5NQ is a known narrow-range mitochondrial uncoupling agent, which explains the observed increase in mitochondrial ROS in leukocytes after treatment with 5NQ[257]. The observed increase in mitochondrial ROS may be the primary reason for depletion of GSH nevertheless, the reverse mechanism is also possible, as the naphthoquinone compounds are known to form thiol adducts, leading to depletion of these antioxidants[194,219].

Intriguingly, in our study, we observed that although mitochondrial ROS increased after 5NQ treatment, there was a drastic decrease in cellular ROS, as observed using H_2DCFDA and CellROX orange dye. Therefore, we investigated the expression of Nrf2 and its downstream targets, which are important orchestrators of cellular stress responses. We observed an increase in the antioxidant response signaling protein Nrf2 and its downstream target HO1. This indicates that treatment with 5NQ up-regulates antioxidant response signaling in leukocytes. Nrf-2 and its downstream target HO1 have been shown to mediate anti-inflammatory activities. Nrf2 is a transcription factor up-regulated under oxidative stress conditions. The levels of NRF2 are low in cells under homeostasis conditions, as they are sequestered by KEAP1 (and E3 ubiquitin ligase) and targeted for proteasomal degradation[258]. However, under stress conditions, such as exposure to toxins and ROS, mutations, or metabolic stress, the Nrf2-KEAP1 complex is disrupted, and activated Nrf2 translocates to the nucleus and activates its downstream targets. One of the major factors in the disruption of Nrf2-KEAP1 during oxidative stress is the electrophilic reaction of ROS with cysteine of KEAP1, which inhibits the interaction of Nrf2 with KEAP1, thus stabilizing the newly formed Nrf2 in the cytosol. Activated Nrf2 translocates to the nucleus where it activates the transcription of cytoprotective genes. Furthermore, Nrf2 and NF-κB counteract each other, where Nrf2 directly inhibits the activity of NFκB-mediated transcription of pro-inflammatory cytokines[258]. Moreover,

increased Nrf2 activity has been shown to regulate inflammation via its effects on immune cell differentiation, expansion, survival, and cytokine release. NRF2 activation impairs Th1-driven responses and promotes Th2 mediated responses. Nrf2 activity in stimulated T cells promotes Treg cell differentiation, which alleviates inflammation. Additionally, Nrf2 activity in dendritic cells causes decreased expression of MHC class II and co-stimulatory molecules CD86 and CD80, which eventually leads to suboptimal stimulation of T cells, resulting in a poor inflammatory response. In leukocytes, such as macrophages, NRF2 expression suppresses pro-inflammatory gene expression, which suppresses cytotoxic T cell proliferation and causes T-cell anergy. These outcomes of 5NQ mediated Nrf2 up-regulation have been demonstrated in our results of objective 1, where we observed a reduction in MHC-II expression in leukocytes (macrophages and dendritic cells), as well as T cell anergy in $CD4^+$ T cells[258]. Thus, the upregulation of Nrf2 may play an important role in mediating the immuno-modulatory effects of 5NQ *in vitro.* 5NQ induced up-regulation of Nrf-2 signaling has been reported in DSS-induced colitis and renal ischemia-based murine models of inflammation[259]. However, these studies did not report up-regulation of Nrf-2 in specific lymphocyte populations. 5NQ is a potent inhibitor of Pin1, which is known to interact with Keap-1, thus mediating its degradation and resulting in Nrf-2 activation[260,261]. Furthermore, we observed an increase in HO1, a downstream target of Nrf2. Heme oxygenase1 (HO1) is an important enzyme involved in heme and iron metabolism. Heme is converted to ferrous iron and biliverdin by HO1. Biliverdin is further metabolized to bilirubin. Bilirubin thus formed is known to mediate anti-inflammatory response by binding to HLA proteins which results in inhibition of binding of antigenic peptides to these proteins and their subsequent representation to T cells[262]. Along with this mechanism, HO1 also acts as a transcription factor for the anti-inflammatory cytokine IL-10, thus aiding the alleviation of the inflammatory response[262,263].

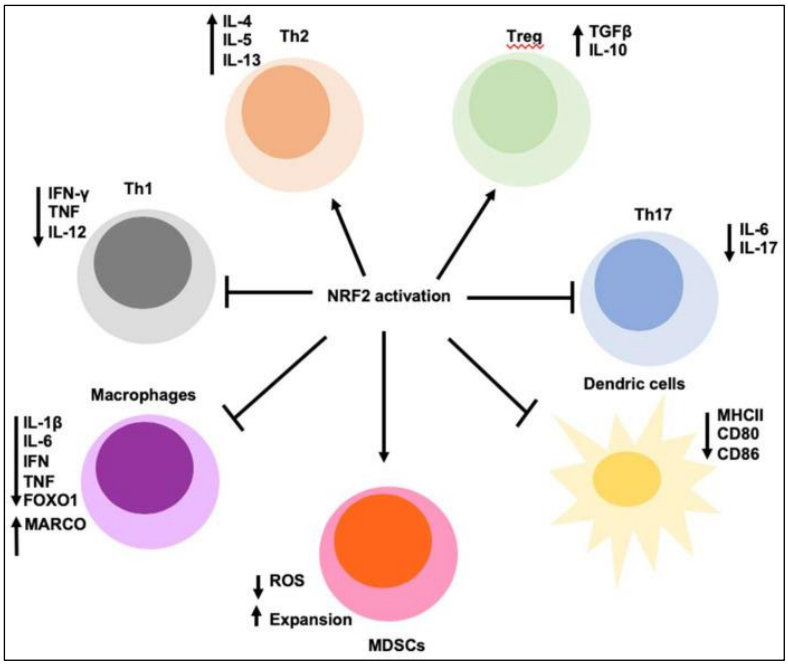

Figure 40: Regulation of inflammation by Nrf2. MDSCs: myeloid-derived suppressor cells, Treg: T regulatory cells.

Furthermore, our finding that treatment with 5NQ increases the expression of Fas (CD95) on $CD4^+$ T cells corroborates the available evidence that an increase in HO1 expression in $CD4^+$ T cells leads to an increase in their activation induced cell death[264].

In conclusion, our results showed that 5NQ modulated the cellular ROS balance and up-regulated antioxidant response signaling (Nrf-2/HO-1) in leukocytes. Thus, treatment with 5NQ induces an adaptive stress response in leukocytes, which can be attributed to an increase in mitochondrial ROS and depletion of the cellular GSH pool. The mechanism of action of 5NQ can be considered a form of hormetic effect, in which exposure to a low amount of stressors (mitochondrial ROS and GSH depletion) triggers an adaptive response (up-regulation of Nrf-2/HO-1), which increases resistance to more severe stress and disease.

To summarize, transient treatment with 5NQ perturbs the cellular redox status and causes GSH depletion, leading to up-regulation of the antioxidant response signaling proteins Nrf2 and HO-1 in leukocytes. These events inhibit the pro-inflammatory proteins NF-κB and Akt,

eventually inhibiting the transcription of pro-inflammatory cytokine genes and increasing the transcription of anti-inflammatory cytokine genes (Figure 41).

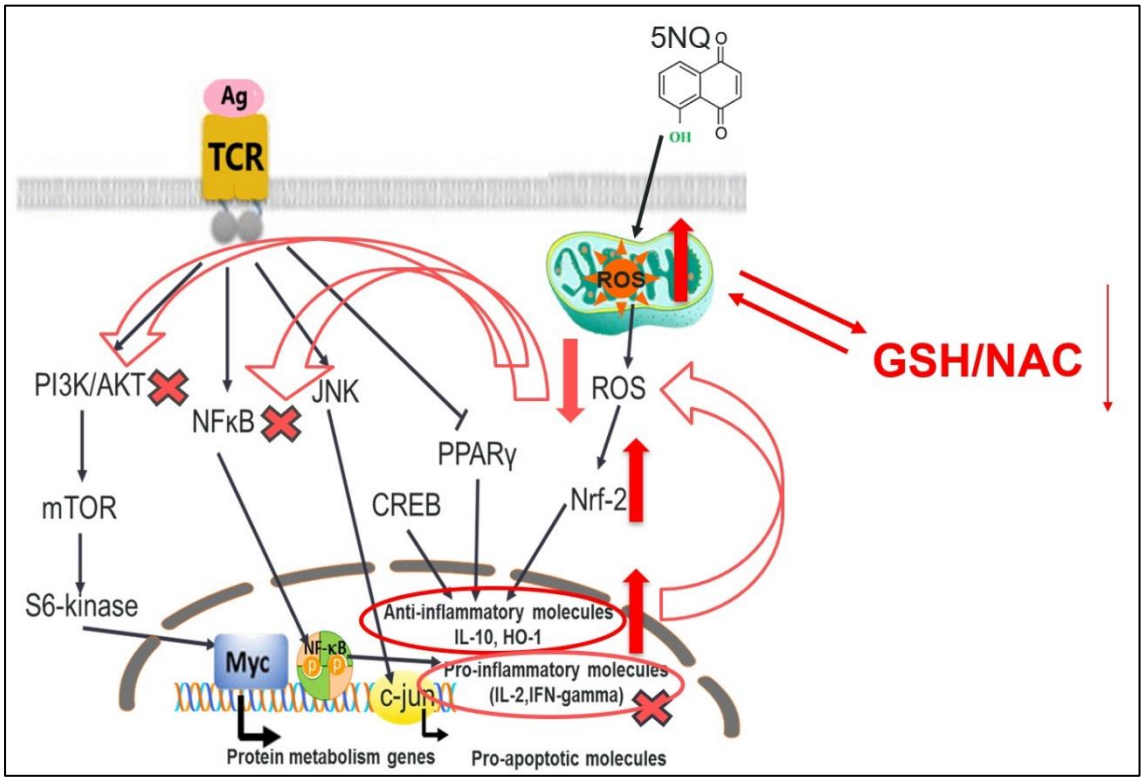

Figure 41: Mechanism of immunomodulatory action of 5NQ in murine leukocytes.

Objective 3

7 OBJECTIVE 3

INTRODUCTION AND OVERVIEW OF OBJECTIVE 3

Objective 3 aimed to evaluate the anti-GVHD efficacy of juglone in a murine model of acute GVHD. However, before we proceeded with the efficacy studies, it was necessary to understand the safety of oral administration of juglone and obtain a reasonable understanding of the related toxicities associated with juglone administration, which may be confounding factors in our efficacy studies.

Therefore, the studies on Objective 3 were conducted in two parts.

Part A: Acute and sub-acute oral toxicity assessment of 5NQ in mice. We studied the oral toxicity of 5NQ in healthy BALB/c mice and estimated the LD_{50} and no observed effect levels of 5NQ. Moreover, we evaluated the effect of the oral administration of 5NQ on haematological and biochemical parameters (liver and kidney function) to assess the sensitivity of these markers to 5NQ administration.

Part B: Evaluation of anti-GVHD efficacy of oral administration of 5NQ in a murine model of allo-HSCT. We studied the prophylactic efficacy of the oral administration of juglone using a murine allo-HSCT model based on complete MHC-I mismatch. A dose-standardization study was conducted to determine an appropriate dosing regimen that offered a survival benefit. We used this dosage of 5NQ to evaluate the effect of its oral administration on the severity of clinical manifestations of GVHD, donor cell engraftment, hematopoietic stem cell recovery, cytokine storm, immune cell milieu, and graft-versus-host disease (GVHD)-associated target tissue damage in a murine model of allo-HSCT.

Objective 3: Part A

7 OBJECTIVE 3: PART A

7.1 BACKGROUND

Pharmacology and toxicity of juglone- a review of literature

The therapeutic potential of 5NQ has been tested in a range of clinical conditions. In vitro, 5NQ exerts its pharmacological effects at different concentrations, depending on the disease model studied. The antibacterial, antifungal, and antiparasitic activities of 5NQ are exhibited at concentrations ranging between 100µM and 500 µM, whereas antiviral, anti-inflammatory, and anticancer activities are observed at concentrations ranging between 3-25 µM.

Pharmacologically, 5NQ is a redox-active molecule that causes the intracellular generation of reactive oxygen species. The redox activity of 5NQ is crucial for its pharmacological effects and affects multiple cellular pathways, leading to the loss of mitochondrial and plasma membrane potential, DNA damage, cellular degeneration, and apoptosis. Although 5NQ is a potent therapeutic agent, there are few reports on its toxicity in normal tissues, and there is no agreement regarding the LD50, preferred solvent, or optimal route of administration. The lack of information regarding the safety and toxicity of 5NQ presents several challenges for its clinical application.

In a 1961 report, the LD50 of 5NQ in mice was determined to be 2.5 mg/kg. However, this study did not disclose any information regarding the route and duration of administration[265]. Single-dose intravenous (IV) toxicity of 5NQ has only been assessed in one investigation, and the study showed an IV LD50 of 4.18 mg/kg in healthy mice[266]. Additionally, by utilizing tritium labelled 5NQ, researchers have conducted a study on the pharmacokinetics and tissue distribution of 5NQ. A single intravenous administration of 5NQ (0.02 mg/kg,

showed that the plasma half-life of 5NQ via the IV route was approximately 2 hours[267]. This biodistribution study reported the highest distribution of 5NQ in the kidneys, followed by that in the liver. This study also reported that intravenous administration of 1 mg/kg 5NQ for 7 days caused significant nephrotoxicity in treated mice[267].

Despite limited understanding of the safety profile of 5NQ, numerous studies have tested its therapeutic effects in murine disease models without proper justification[248,266,268–272]. Many studies that have reported the therapeutic effects of 5NQ in murine disease models have utilized the intraperitoneal route for administration of 5NQ[248,266,270–272] likely due to the ease of conducting experiments with intraperitoneal injections compared to intravenous injections, which have a higher technical failure rate[273]. A majority of these studies have demonstrated that administering 5NQ intraperitoneally to mice, at doses ranging from 1 to 4 mg/kg in 10% DMSO solution, over a period of 10 days, is safe and does not result in any toxicity-related mortality[248,271,274]. Regarding the oral administration of 5NQ, only one study reported that it is safe when 0.05 mg/kg 5NQ (dissolved in carboxymethylcellulose [CMC]) is administered for 60 days. However, these studies did not provide any information regarding the potential adverse effects of 5NQ on normal tissues, if any were observed[270,272].

There is substantial information regarding safety and toxicity of intravenous administration of 5NQ[266,267], however, it is important to consider the challenges associated with both the intravenous and intramuscular routes of administration for clinical use[273,275]. Moreover, the hydrophobicity and low solubility of 5NQ necessitates the use of solvents such as DMSO and methanol for intravenous and intramuscular administration, which are unsuitable for clinical applications[273,275]. However, the oral LD_{50} and toxicity of 5NQ in healthy tissues in mice have not been reported in the literature. Our study aimed to fill this knowledge gap by determining the oral LD_{50} and no observed adverse effect level (NOAEL) of 5NQ in

mice, according to the standard guidelines of the Organization for Economic Cooperation and Development (OECD). Furthermore, along with the traditional approach of determining the NOAEL, we adopted a modern benchmark dose (BMD) modelling approach to determine the point of departure dose (POD) for the daily administration of 5NQ. We also used BMD modelling to identify hematological and biochemical parameters that were sensitive to the oral administration of 5NQ. We also assessed the physicochemical properties of 5NQ using in silico methods to predict the drug-likeness of 5NQ for clinical applications.

ADMET-score

The ADMET score is a scoring function created to assess the suitability of a chemical as a potential drug candidate. ADMET refers to the absorption, distribution, metabolism, excretion, and toxicity of a chemical. Thus, an ideal drug candidate should not only be effective but also have favorable ADMET properties at therapeutic doses. One of the earliest methods used to determine drug likeness was Lipinski's "Rule of Five," which determines whether a molecule is well absorbed orally based on four parameters: molecular weight (≤ 500), octanol/water partition coefficient (*A log P;* ≤ *5*), number of hydrogen bond donors (HBDs; ≤ 5), and number of hydrogen bond acceptors (HBAs; ≤ 10). To be an ideal drug candidate, the chemical must comply with at least two of these parameters[276]. Although Lipinski's "Rule of Five" is still the foundation for many in silico machine learning algorithms, it has limitations when it comes to small molecules derived from natural products. Therefore, additional rules and filters similar to the "Rule of Five" were incorporated into these algorithms to improve their accuracy and performance[277].

ADMETlab 2.0, a comprehensive online platform that provides accurate predictions of ADMET properties and covers all aspects of the ADMET process. The ADMET Evaluation

function module of ADMETlab 2.0 comprises a set of high-quality prediction models that were trained using a multi-task graph attention framework. This module efficiently calculated and predicted 17 physicochemical properties[278], 13 medicinal chemistry measures, 23 ADME endpoints, 27 toxicity endpoints, and 8 toxicophore rules. This provides detailed predictions to aid in the selection of promising lead compounds for further preclinical and clinical development. Figure 42 describes the workflow of ADMETlab 2.0[279].

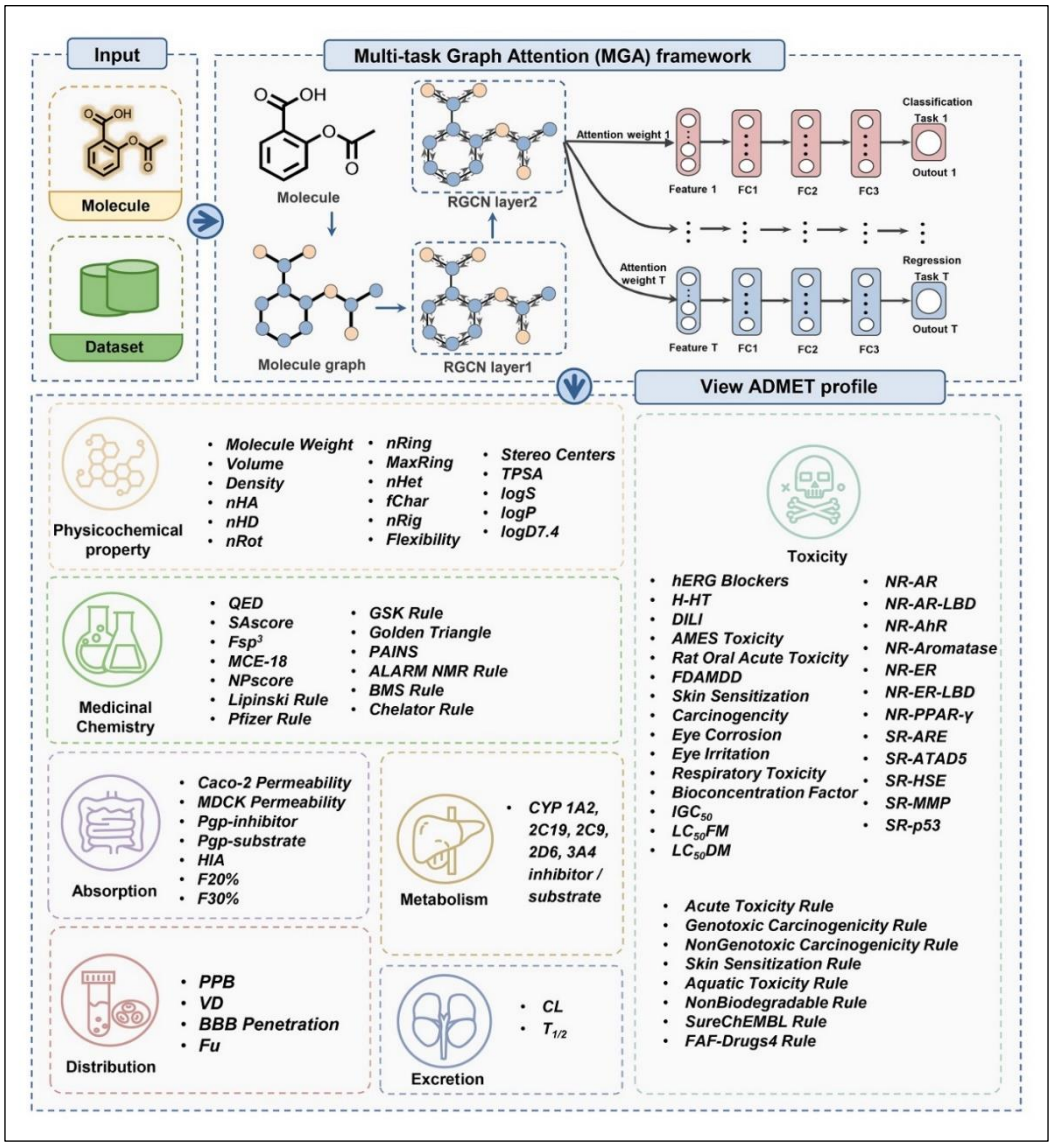

Figure 42: Workflow scheme for ADMETlab 2.0[279].

ADMETlab 2.0 provides predictions for various parameters that are broadly divided into physicochemical properties, medicinal properties, absorption, distribution, metabolism, excretion and toxicity.

Before proceeding with the assessment of acute and sub-acute toxicity of oral 5NQ in mice, ADMETlab 2.0, was used to predict the drug-likeness and probable toxicities of 5NQ in vivo.

OECD guidelines for acute and sub-acute toxicity

The Organization for Economic Cooperation and Development (OECD) Guidelines for the Testing of Chemicals are a compilation of approximately 150 of the most pertinent internationally agreed testing methodologies used by governments, industries, and independent laboratories to identify and characterize potential chemical hazards. These are a set of instruments used primarily in regulatory safety testing and subsequent chemical and chemical product notification, registration, and evaluation. Additionally, they can be utilized for the selection and evaluation of candidate chemicals during the development of new chemicals and products, as well as in toxicology research.

The oral acute toxicity of a chemical can be evaluated using OECD guideline 423 and the oral sub-acute toxicity of a chemical can be evaluated using OECD guideline 407. According to these guidelines, acute toxicity of a chemical is defined as adverse effects occurring following oral administration of a single dose of a chemical or multiple dose administered within 24 hours. The OECD guidelines for oral acute toxicity studies provide guidance on the dose range to be utilized, number of animals to be used per dose, housing conditions, observations that indicate signs of toxicity, endpoints to be monitored, and derivation of LD_{50} of a chemical. The oral acute toxicity study is started using any one of

the doses (5, 50, 300, or 2000 mg/kg). The workflow scheme, with a starting dose of 50 mg/kg, is shown in Figure 43[280]. The test classifies a chemical based on its acute toxicity using a stepwise method, with a minimal number of animals per step. Oral dosing was administered to a group of three animals (generally females). The next stage depends on whether compound-related death occurred in the animals dosed in one phase; accordingly, three more animals were treated with the same dose or another group of animals were treated with a dose lower or higher than the one tested. Accordingly, the procedure classifies the test material into a toxicity class based on the global harmonized classification system (GHS) using preset LD50 cut-off values (Figure 43).

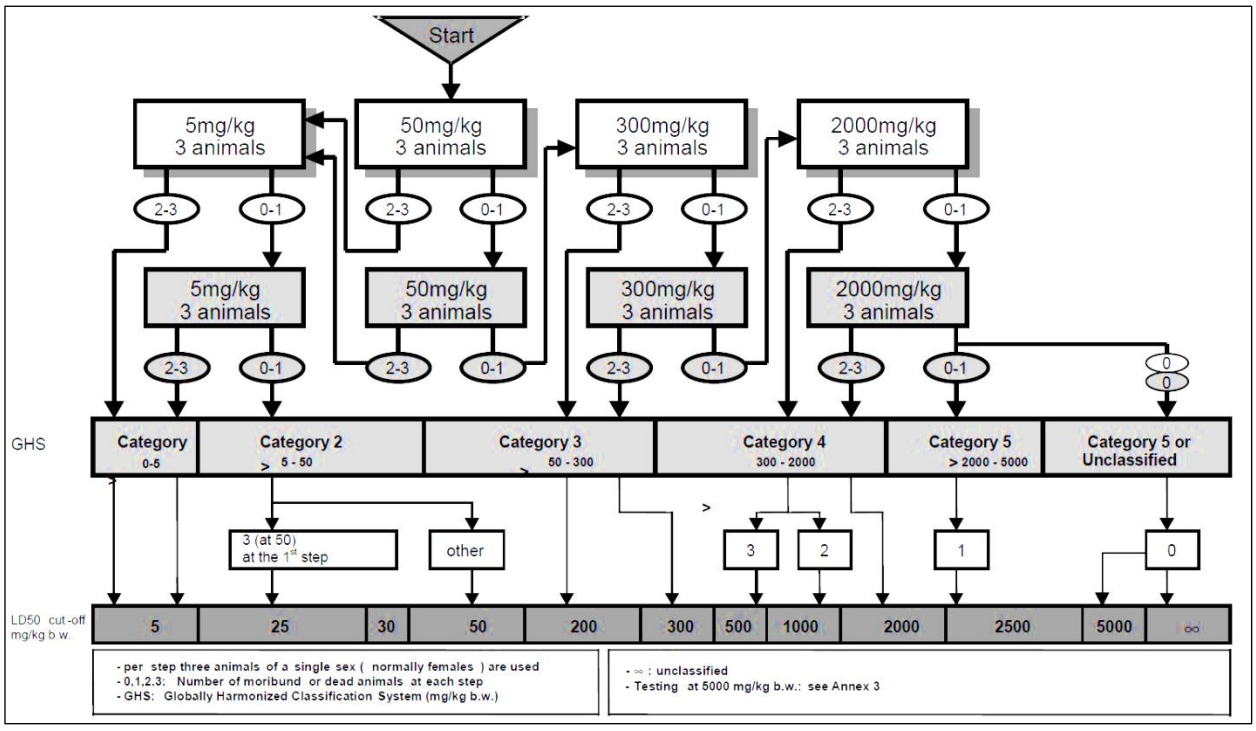

Figure 43: Oral acute toxicity test procedure with a starting dose of 50 mg/kg body weight. Figure adapted from[280]

According to OECD guideline 407, oral sub-acute toxicity or repeated dose 28-day oral toxicity of a chemical is performed once the initial information about the oral acute toxicity is obtained. This test was performed to investigate the possible toxic effects on the nervous,

immune, and endocrine systems, which may arise from repeated exposure to the chemical over a limited period of 28 days. Repeated dose -28day toxicity is generally warranted for chemicals, on which a 90-day study may not be required due to their toxic effects. The results from this test are further used for hazard identification and risk assessment. The procedure involves daily oral administration of 3-5 graduated doses of the chemical to each group for a period of 28 days. During the test the animals are monitored daily for signs of toxicity and are necropsied 24 h after the last dose to study hematological, biochemical and histopathological changes due to the administration of the chemical. The data thus obtained can be used to characterize the dose-response relationships and determine the NOAEL. The guidelines suggest that appropriate doses should be selected for the chemical, taking into account any existing toxicokinetic data. Otherwise, the dose that induces toxic effects but not death can be selected as the highest dose. Other doses should be at least two-fold lower than the highest dose, and the lowest dose should be at least tenfold lower than the highest doses selected. Accordingly, the NOAEL is defined as the highest dose level where no adverse effects are observed due to treatment[281].

Toxicity studies for risk assessment and hazard characterization.

Toxicology studies have been conducted to identify the adverse effects of substances, to characterize the dose–response relationships for the adverse effects, and to set critical standards for their application in humans. The main aim of these studies is to derive a reference dose (RfD) or a reference concentration for human exposure, without the risk of adverse effects[282]. The data for such assessments are primarily obtained from animal studies. Hazard characterization includes a thorough evaluation of all available data to identify and characterize potential health hazards. Dose-response assessment involves analysis of the relationship between exposure to chemicals and health-related outcomes[282].

The data from hazard characterization and dose-response assessment, is used to derive a point of departure dose (POD). The POD obtained is applied along with "uncertainty factors" (to account for limitations and uncertainties in the available data) to determine the RfD for human exposure[283]. To study the dose-response relationships, it is necessary that the doses selected in the study produce different effect sizes, such that information can be obtained for both the lower and higher parts of the dose-response relationship. However, experimental and biological variations in these experiments may affect the responses and cause variations in the observed effects (sampling error). Given the potential for statistical errors in these dose response data, it is important to analyze them using statistical methods to draw accurate conclusions from biological data[284,285]. POD can be determined using two statistical approaches, the NOAEL/LOAEL approach (traditional approach) and the benchmark dose modelling (BMD) approach (modern approach). Each of these approaches is discussed in detail below[283,286,287].

The NOAEL approach

As per the definition, NOAEL is the highest in a study in which no adverse effects are observed. Consequently, the lowest observed-adverse-effect level (LOAEL) is the lowest dose at which adverse effects are observed[287,288]. The estimation of NOAEL and LOAEL is performed by statistically comparing the treated groups with the control group or vehicle-treated group, which may or may not lead to statistically significant differences. Therefore, the estimation of NOAEL and LOAEL is highly dependent on the range of doses selected in a toxicity study, as the NOAEL/LOAEL is restricted to one of the doses included in the study[288]. As the sample size of a study decreases, the ability of a bioassay to distinguish between treatment and control responses also decreases, leading to a higher NOAEL for a compound in studies with smaller numbers of animals per dose group. Furthermore, it

should be noted that NOAELs/LOAELs usually vary among studies owing to variations in the dose range in each study, sample size, effect size, etc., which makes it inapplicable to use these values for the derivation of RfD[287,288]. Moreover, in a study in which a statistically significant response is observed at all the doses in a study, the lowest dose is selected as the LOAEL, and since NOAEL cannot be determined in such studies, it is a common practice to apply an uncertainty factor of up to 10 to the LOAEL to derive the NOAEL in such studies. Such extrapolations are sometimes unjustifiable and hence cannot be used for risk assessment. Another limitation of reporting a NOAEL is that it is possible that at the reported dose levels, the effects may have been too small to be observed, and therefore, a NOAEL may not necessarily be a 'no adverse effect' dose[287]. Crump et al. identified and addressed the limitations of the NOAEL approach in 1984, which led to the development of the BMD approach[289].

The BMD approach

Benchmark dose modelling is a regulatory, scientific, and statistically advanced approach for estimating the point of departure (POD) or guidance dose level for hazard risk assessment[282,288]. Unlike NOAEL, the BMD approach utilizes dose–response data to estimate the shape of the overall dose–response relationship for a particular endpoint. BMD assumes that the magnitude of the response (effect size) to a toxicant relative to background levels remains consistent across different doses and is not dependent on the biological basis of the effect[286,289,290]. Therefore, to calculate the benchmark dose from given dose-response data, one needs to specify the benchmark response (BMR). The BMR is a chemical dose or concentration that produces a predetermined change in the response of an adverse effect, for example, a 5% or 10% increase or decrease in response (such as weight loss or tumor incidence), compared with the background response[284,285,290]. Once the BMR is specified,

the data set is fitted to different dose-response models and a BMD confidence interval (lower and higher confidence intervals) for each of the models, which leads to the generation of a set of BMD confidence intervals. A single set of BMD confidence intervals is then derived from this set using the model averaging method[291–293]. The lower confidence interval (BMDL) thus derived is regarded as POD or equivalent to the NOAEL. BMD analysis can be applied to the dose-response curves of every endpoint studied in toxicity testing[288]. Figure 44 describes the key concepts of BMD modelling using hypothetical continuous dose–response data[283,294]. The two most widely recognized BMD software programs are BMD software developed by the US EPA (https://www.epa.gov/bmds)[282] and PROAST software developed by RIVM (https://www.rivm.nl/proast)[291]. Thus, the BMDL value is not limited to the doses selected in the study and is interpolated from the fitted model of the dose-response curve.

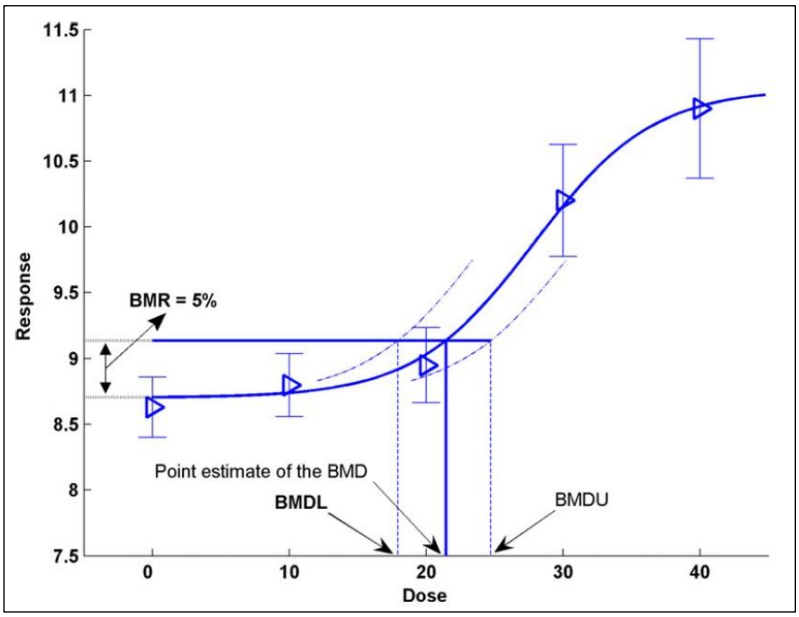

Figure 44:Key concepts of the BMD approach described using hypothetical continuous data. The triangles depict the observed responses and are plotted with their confidence intervals. A solid curve represents the fitted dose-response model. The BMD is determined from the curve using pre-specified BMR (here it is set at 5%). The dashed curves represent the upper and lower 95% confidence levels as a function of the dose. The intersection of these dashed curves with the

horizontal line defines the upper and lower bounds of BMD, that is, the lower bound of BMD (BMDL) and the upper bound of BMD (BMDU). Figure adapted from[283].

In the present study, along with the traditional approach of NOAEL, we evaluated the dose–response relationship of the effects of prolonged administration of 5NQ in healthy mice using benchmark dose (BMD) modelling.

7.2 METHODOLOGY

In silico Absorption, Distribution, Metabolism, Excretion and Toxicity (ADMET) analysis: The ADMETlab2.0 prediction tool was utilized to evaluate the ADMET and physicochemical properties of 5NQ. To begin, the 2D structure of 5NQ in .sdf format was obtained from the PubChem database, which was followed by the generation of isomeric SMILES of 5NQ using the SwissADME online tool. The ADMETlab2.0 employed this SMILES format to conduct an ADMET analysis of 5NQ.

Animal maintenance All animal studies were approved by the Institutional Animal Ethics Committee, ACTREC, as per the Committee for the Purpose of Control and Supervision of Experiments on Animals, Government of India guidelines (IAEC/10/2021). All mice were housed in polypropylene cages, maintained under standard conditions of 22 ± 2°C, 55 ± 5% relative humidity and 12h light–dark cycles, and were provided with a standard pelleted diet and plain drinking water ad libitum. Animal studies were reported in compliance with the ARRIVE guidelines.

Preparation of doses for the acute toxicity study: Dimethyl sulfoxide (DMSO; Cat no. D8418) and 5-hydroxy-1,4-naphthoquinone (5NQ; molecular weight:174.15; Cat no. H47003) were purchased from Sigma Aldrich (St. Louis, MO, USA). 5NQ was supplied in the form of a murky-yellow crystalline solid powder with 97% purity. To prepare the doses

for the acute toxicity study, a clear solution was obtained by dissolving the required amount of 5NQ in DMSO and thoroughly vortexing the solution.

Acute oral toxicity study: An acute oral toxicity study was conducted in accordance with Annex 2c of OECD guideline 423[280]. Female BALB/c mice (8-10 weeks old, 20-22 g) were divided into four groups: vehicle control (DMSO, n = 3), 50 mg/kg (n = 6), 300 mg/kg (n = 6), and 2000 mg/kg (n = 3). Mice were administered a single dose of 5NQ dissolved in 0.1 mL DMSO by oral gavage. The mice were fasted for two hours prior to dosing with 5NQ. After treatment, the animals were observed for the first 30 min to 4 h, and then intermittently every 24 h for 14 days. During this period, behavioral changes were carefully monitored for signs of tremors, convulsions, salivation, diarrhea, difficulty breathing, piloerection, and lethargy. Body weights were recorded at the beginning of the protocol, on the 7th day, and at the end of the study. At the end of the study, the animals were euthanized using CO2 asphyxiation, and their vital organs (liver, lung, heart, kidney, spleen, intestine, brain, and femur) were collected and fixed in 10% formalin solution for histopathological analysis.

Preparation of doses for the sub-acute toxicity study: Given that the sub-acute toxicity study required 5NQ to be administered daily for 28 days, dissolving it in DMSO alone could result in DMSO-related toxicity, which would be a confounding factor. To obtain a clear solution with the required amount of 5NQ, it was first dissolved in a minimum amount of DMSO. A 0.5% carboxymethyl cellulose (CMC) solution prepared in sterile PBS was added to achieve the required concentration, and the concentration of DMSO in the final dose did not exceed 5%.

Sub-acute toxicity study: Repeated dose-28-day oral toxicity study of 5NQ was conducted in accordance with OECD guideline 407[281]. BALB/c mice (five males and five females

per group, n = 10, 8-10 weeks old, weighing 20–22 g) were randomly divided into four groups: vehicle control, received vehicle [5% DMSO in 0.5% CMC, while other groups received 5, 15, and 50 mg/kg body weight of 5NQ. The oral doses for the sub-acute toxicity study were chosen according to the guidelines provided in the dosage section of OECD guideline 407. Accordingly, a dose that caused toxic effects but did not cause severe suffering or mortality after administration of a single dose of the drug was selected as the highest dose. Consequently, 50 mg/kg was chosen as the highest dose and 5 mg/kg as the lowest dose (ten times lower than the highest dose). The intermittent dose was set at 15 mg/kg, which was the geometric mean of the lowest and highest doses. For 28 days, the mice were administered 5NQ via oral gavage at specific doses daily. After oral administration, animals were monitored for the first 30 min and after 4 h. Mortality was monitored every 24 hours. The body weights of the mice were recorded at the beginning of the protocol and once per week. All animals were regularly monitored for any signs of toxicity, and a clinical score was assigned to each animal using a standardized scoring system adapted from a report by JM Vlissingen et al[295]. Five general clinical signs (body weight reduction, posture, vocalization, hypokinesia, and piloerection) were used to score all animals, which may indicate the presence of a severe condition. The weekly food consumption of mice was monitored and recorded, and the average daily intake per mouse was calculated based on the total food consumed per cage. On the 28th day, all animals were subjected to overnight fasting following the last dose. The following day, the mice were anesthetized, and blood was collected through the orbital plexuses for hematological and biochemical analyses. Mice were humanely euthanized by CO2 inhalation, and their vital organs (liver, lung, heart, kidney, spleen, intestine, brain, and femur) were collected and preserved in a 10% formalin solution for histopathological examination.

Analysis of biochemical parameters: Serum levels of alanine aminotransferase (ALT), aspartate aminotransferase (AST), alkaline phosphatase (ALP), total bilirubin (TB), albumin (ALB), total protein (TP), blood urea nitrogen (BUN), creatinine (CRE) and uric acid (UA) were quantified by standard clinical chemistry assays using Siemens Autoanalyzer (Dimension EXL 200, Germany). The serum was separated by allowing the blood samples to clot at room temperature for 1 h and centrifugation at 3000 rpm for 10 min.

Analysis of hematological parameters: Blood was collected in EDTA acid-coated tubes by puncturing the orbital plexus of mice under anesthesia. The red blood cell (RBC) count, hematocrit, hemoglobin, white blood cell (WBC) count, WBC differential, mean corpuscular hemoglobin (MCH), MCH concentration (MCHC), mean corpuscular volume (MPV), platelet count, and platelet volume were analyzed using an ADVIA 2120i (USA) auto-analyzer.

Histopathological examination: Following necropsy, formalin-fixed tissue samples were embedded in paraffin blocks. Ultrathin sections (5µm) were attached to glass slides and subjected to deparaffinization. Tissue sections were stained with hematoxylin and eosin (H&E). The tissues were subjected to histopathological examination by a pathologist who was blinded to the treatment.

Benchmark dose modelling: Dose-response modelling was performed using the EFSA web tool for BMD analysis (https://efsa.openanalytics.eu/), which utilizes the R package PROAST, version 70.0, for related calculations. All parameters determined in the study, including absolute organ weights, hematological and serum parameters (continuous individual data) and survival (quantal data), were modelled according to the software guidelines[291] and the European Food Safety Authority (EFSA) guideline[283]. The minimum

physiological adverse response that can be distinguished from control responses is called the benchmark response (BMR) or the critical effect size (CES)[290]. For BMD modelling of survival data (quantal data), the BMR was set at 10% with a two-sided 90% confidence level as recommended by Scientific Committee of the EFSA[283]. The critical effect size (CES) was defined for each parameter based on the reference values proposed by H.E. Buist and S.Dekkers et al[284,285], for BMD modelling of continuous data (all hematological and biochemical parameters). The software determined the benchmark dose interval (BMDI), which comprised the lower (BMDL) and upper (BMDU) benchmark dose confidence limits, utilizing diverse mathematical models[292,293]. The calculated BMDL values were comparable to those of POD and NOAEL[283]. The Akaike information criteria (AIC) were applied to determine the most suitable dose-response model. Subsequently, the model averaging method with 200 iterations was employed, in accordance with EFSA guidelines, to combine all available models into a single one[283,287,293].

Statistical analysis: The values of body weight, organ weight, serum parameters, and hematological parameters were expressed as the mean ± standard error of mean (SEM). Two-way analysis of variance (ANOVA) with Bonferroni correction was conducted to evaluate the time- and dose-dependent differences between groups, while one-way ANOVA with Bonferroni correction was used to assess significant differences between groups using Prism 8.2.0 software. Statistical significance was set at $p \leq 0.05$.

7.3 RESULTS

In silico ADMET analysis: The Absorption, Distribution, Metabolism, Excretion and Toxicity (ADMET) properties of a molecule define its pharmacological activity. ADMETlab2.0 utilizes the complex molecular structure of a molecule to predict its drug-

likeness, pharmacokinetics, and physicochemical properties. The results of the ADMET analysis of the 5NQ are summarized in (Table 22). ADMET properties are broadly divided into seven categories, which include physicochemical properties, medicinal properties, absorption, distribution, metabolism, excretion, and toxicity. Evaluation of parameters under physicochemical properties revealed that 5NQ possessed optimal values for Topological Polar Surface Area (TPSA), log of aqueous solubility (logS), log of water partition coefficient (logP), and logP (logP at physiological pH 7.4). Predictions under the medicinal chemistry category showed that 5NQ possessed optimal drug-likeness properties according to Lipinski, Pfizer, and GSK rules. Moreover, the predictions highlighted it as a thiol-reactive compound. ADMET analysis further showed that 5NQ possessed optimal absorption properties, as indicated by Caco-2 and MDCK permeability, and Human Intestinal Absorption (HIA) probability. Furthermore, the probability of the distribution parameters indicated that the volume of distribution (VD) of 5NQ was 0.405 L/Kg and its Plasma Protein Binding (PPB) capacity was 72.26%. The distribution profile also suggests that 5NQ may be able penetrate the Blood-Brain Barrier (BBB). Moreover, the bioavailability of 5NQ was estimated to be at least 30%, which suggests that 5NQ has fairly good oral bioavailability. Predictions under the metabolism profile indicated that 5NQ might have a low rate of metabolism, as the probability of 5NQ being a CYP1A2 inhibitor was low at 0.933. Predictions of excretion parameters showed that the clearance rate (CL) of 5NQ was 6.788 mL/min/kg. Additionally, the software predicted that 5NQ would have a shorter half-life (T1/2) of approximately 3h. Notably, toxicity predictions for 5NQ showed that it could be a hepatotoxic agent, as indicated by the high probability of drug-induced liver injury (DILI) and mutagenicity. However, the probability of causing human hepatotoxicity (H-HT) and acute toxicity in rats is low.

Acute toxicity study

Survival: All three animals administered 2000 mg/kg (n = 3) 5NQ died within 48 h. In the 300 mg/kg group, one of three animals died 72 h after drug administration. In accordance with OECD guideline 423, 300 mg/kg 5NQ was administered to three additional animals. In the second cohort, all animals died within 72 h of receiving the drug. All six animals in the 50 mg/kg group survived the 14-day observation period (Figure 45A).

Body weight: Mice in all groups showed no statistically significant differences in body weight (Figure 45B).

Clinical signs: Observations of clinical signs of toxicity were conducted every 24 h. All animals in the 2000 mg/kg group exhibited behavioral changes, including huddling, decreased movement, dyspnea, piloerection, and mild tremors; however, diarrhea was absent. Similar signs were observed in mice treated with 300 mg/kg 5NQ. However, two out of six mice recovered 48 h after drug administration. No behavioral changes were observed in mice in the 50 mg/kg group during the observation period.

Table 22: In silico ADMET prediction for 5NQ.

1.Physicochemical Property		
Property	**Value**	**Comment**
TPSA	51.21	Optimal:0~140
logS	-3.604	Optimal: -4~0.5 log mol/L
logP	0.959	Optimal: 0~3
logD	1.076	Optimal: 1~3
2. Medicinal Chemistry		
SAscore	2.133	SAscore ≥ 6, difficult to synthesize; SAscore <6, easy to synthesize
Lipinski Rule	Accepted	MW ≤ 500; logP ≤ 5
Pfizer Rule	Accepted	logP > 3; TPSA < 75

GSK rule	Accepted	MW ≤ 400; logP ≤ 4
3. Absorption		
Caco-2 Permeability	-4.527	Optimal: higher than -5.15 Log unit
MDCK Permeability	3e-05	Low permeability: < 2×10^6 cm/s Medium permeability: 2–20×10^6 cm/s High passive permeability: > 20×10^6 cm/s
HIA	0.008	Category 1: HIA+ (HIA < 30%); Category 0: HIA- (HIA > 30%); The output value is the probability of being HIA+
$F_{30\%}$	0.023	Category 1: $F_{30\%}$ + (bioavailability < 30%); Category 0: $F_{30\%}$ (bioavailability ≥ 30%); The output value is the probability of being $F_{30\%}$+
4. Distribution		
PPB	72.26%	Optimal: < 90%
VD	0.405	Optimal: 0.04-20L/kg
BBB Penetration	0.724	Category 1: BBB+; Category 0: BBB-; The output value is the probability of being BBB+
Fu	20.00%	Low: < 5%; Middle: 5~20%; High: > 20%
5. Metabolism		
CYP1A2 inhibitor	0.933	The output value is the probability of being inhibitor.
CYP1A2 substrate	0.107	The output value is the probability of being substrate.
CYP3A4 inhibitor	0.042	The output value is the probability of being inhibitor.
CYP3A4 substrate	0.162	The output value is the probability of being substrate.
6. Excretion		
CL	6.788	High: >15 mL/min/kg; moderate: 5-15 mL/min/kg; low: <5 mL/min/kg
$T_{1/2}$	0.339	long half-life: >3h; short half-life: <3h. The output value is the probability of having long half-life.
7. Toxicity		
H-HT	0.058	The output value is the probability of being toxic.
DILI	0.935	The output value is the probability of being toxic.
AMES Toxicity	0.804	The output value is the probability of being toxic.

Rat Oral Acute Toxicity	0.335	The output value is the probability of being toxic.
Skin Sensitization	0.843	The output value is the probability of being sensitizer.
Eye irritation	0.987	The output value is the probability of being irritants.

TPSA: Topological Polar Surface Area; logS: log of aqueous solubility; logP: log of water partition coefficient; logD: logP at physiological pH 7.4; SA score: synthetic accessibility score; HIA: Human Intestinal Absorption; F30%: bioavailability of drug is 30% or higher; PPB: Plasma Protein Binding; VD: Volume of Distribution; BBB: Blood Brain Barrier; Fu: fraction of drug unbound to protein; CYP: cytochrome P450; CL: Clearance; T1/2: half-life; H-HT: Human Hepatotoxicity; DILI: Drug Induced Liver Injury.

Histopathological analysis of the liver: Histopathological examination of liver tissue from mice treated with the vehicle control revealed normal liver architecture and morphology. Histopathological analysis of liver tissues of animals administered a single oral dose of 50 mg/kg or 300 mg/kg showed ballooning of hepatocytes, indicative of hepatocellular degenerative changes, and focal mononuclear cell infiltration was also observed. Animals administered 2000 mg/kg showed severe hepatocellular damage, with disruption of the normal lobular architecture of the liver, degenerative changes in the form of ballooning, mononuclear cell infiltration, and congested vessels along (Figure 45C).

Histopathological analysis of the kidney: Animals in the vehicle control and 50 mg/kg groups showed few dilated and congested vessels in the examined renal tissues. Animals administered a single dose of 300 mg/kg and 2000 mg/kg 5NQ showed clear signs of nephrotoxicity, including focal tubular degeneration, tubular edema, mild mononuclear infiltration, and focal glomerular proliferation along with dilated and congested vessels (Figure 45C).

Toxicity-related histopathological changes were not observed in other tissues such as the lung, heart, brain, intestine, and femur after the administration of a single dose of 5NQ (Figure 46).

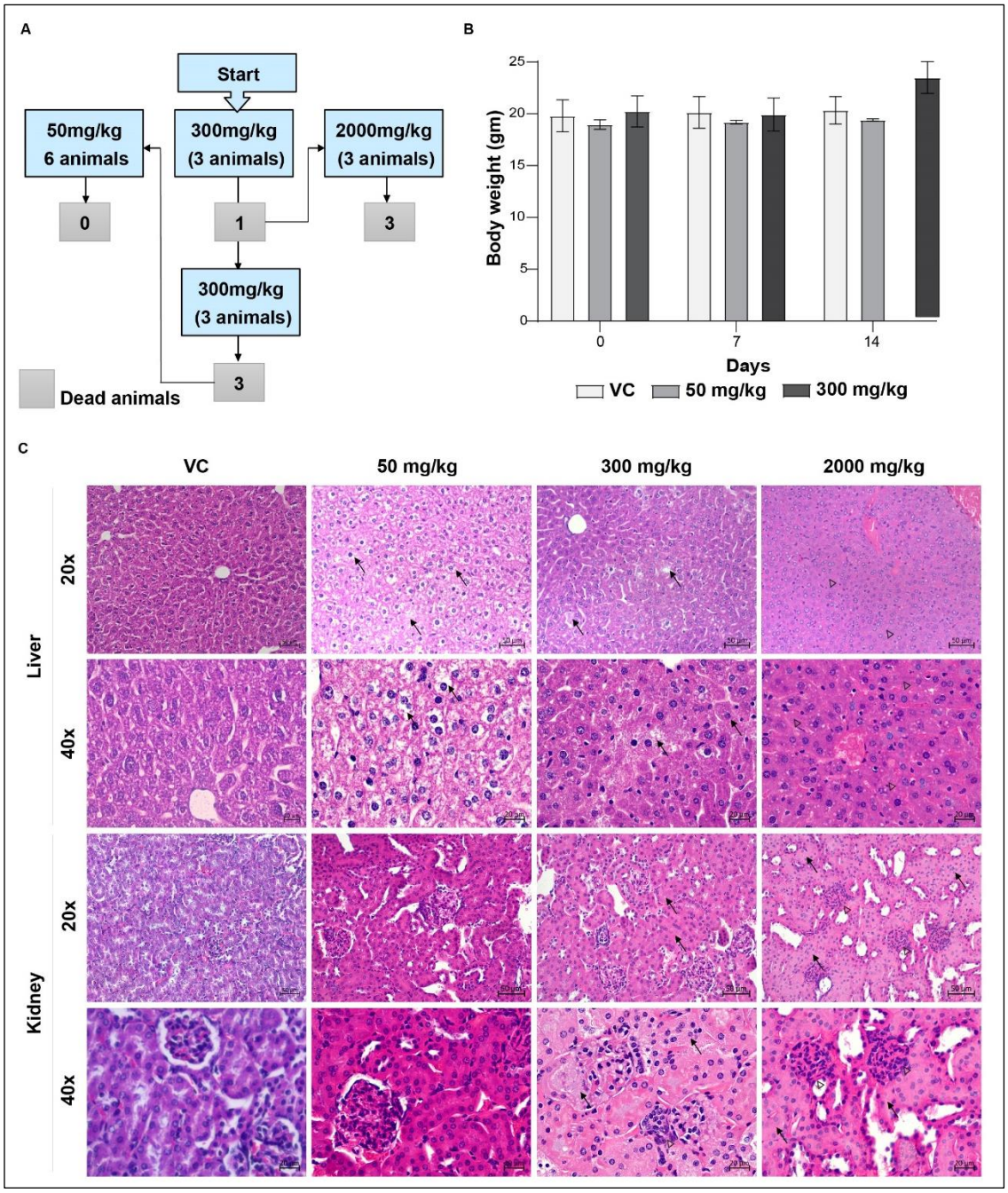

Figure 45:Acute toxicity study (A) Experimental outcome of the oral acute toxicity study (grey boxes indicate the number of dead animals after 5NQ administration). (B) Body weight of animals in all groups at the start of the experiment, that is, on days 0, 7 and day14, no significant difference was observed in the body weight of animals when compared to the vehicle control. Data are expressed as mean ± SEM, n = 3. (C) Representative micrographs of liver and kidney sections stained with H&E, corresponding to mice treated with vehicle control (VC) and with different doses of 5NQ, administered as a single oral dose. Liver: Black arrows indicate focal degeneration of hepatocytes in the form of ballooning, and clear arrowheads indicate complete degeneration of the liver architecture. Kidney: Black arrows indicate tubular edema and degeneration; clear arrowheads indicate glomerular proliferation.

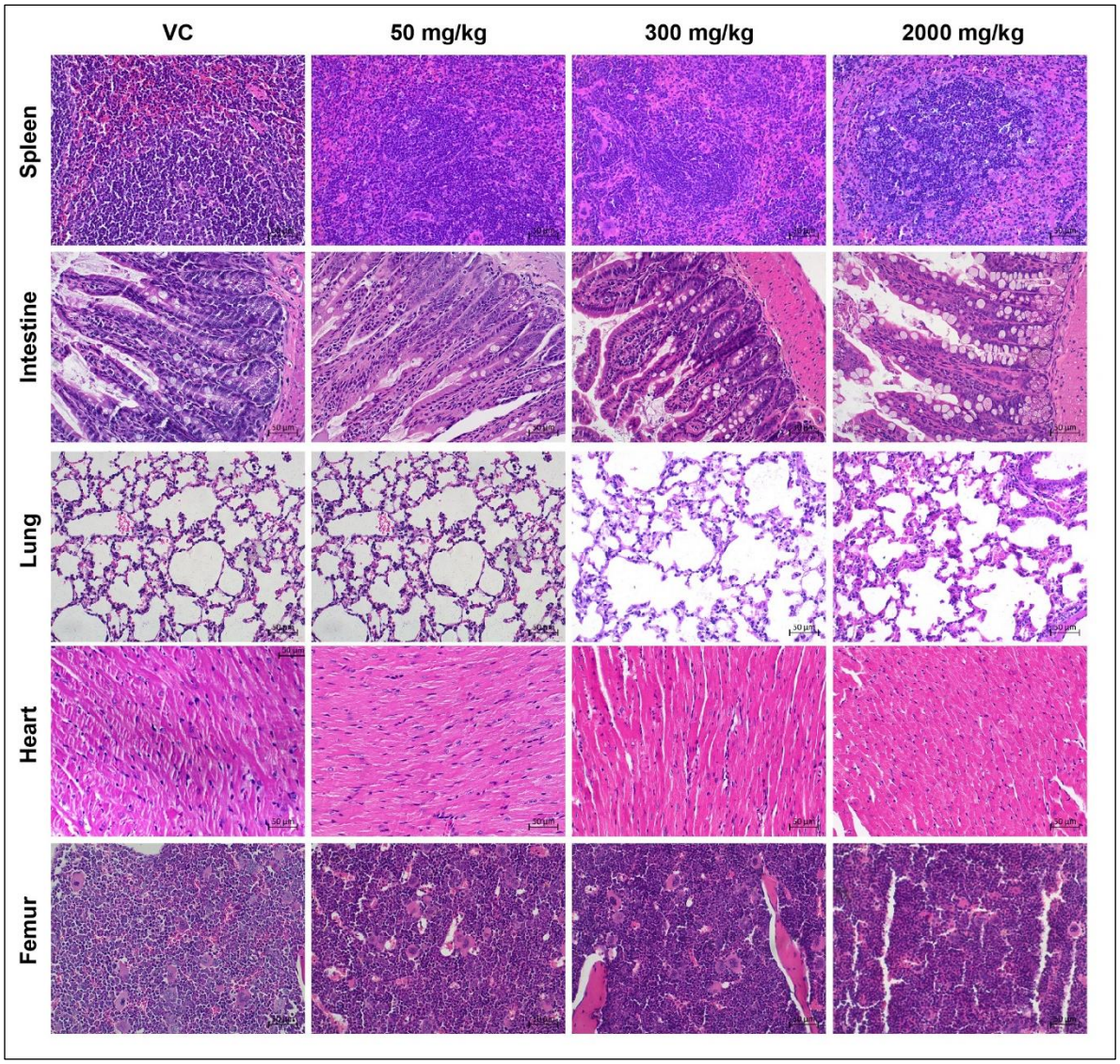

Figure 46: Representative micrographs of spleen, intestine, lung, heart, and femur sections stained with H&E, corresponding to mice treated with vehicle control (VC) and with different doses of 5NQ administered as a single oral dose (20x magnification).

Sub-acute toxicity study

Body weight, clinical score, and food intake: Animals administered 15 and 50 mg/kg showed significant changes in these parameters. Repeated-28-day administration of 15 mg/kg and 50 mg/kg showed a significant reduction in the body weight of the animals (Figure 47A), which also correlated with the decrease in food intake observed in these groups (Figure 47B). No significant differences were observed in the organ-to-body weight ratios of major organs, such as the liver, kidney, spleen, intestine, heart, lung, and brain.

Nevertheless, a notable decrease in the absolute organ weights of the liver, spleen, and kidney was observed in mice administered 5, 15, and 50 mg/kg compared to those in the vehicle control group (Table 23). In the first week, animals administered 15 mg/kg and 50 mg/kg of 5NQ displayed clinical signs of toxicity, and the clinical scores showed a gradual increase in these groups throughout the course of the experiment. The mice that were administered 5 mg/kg 5NQ did not exhibit any signs of toxicity and thus received a low score on the clinical severity scale. (Figure 47D).

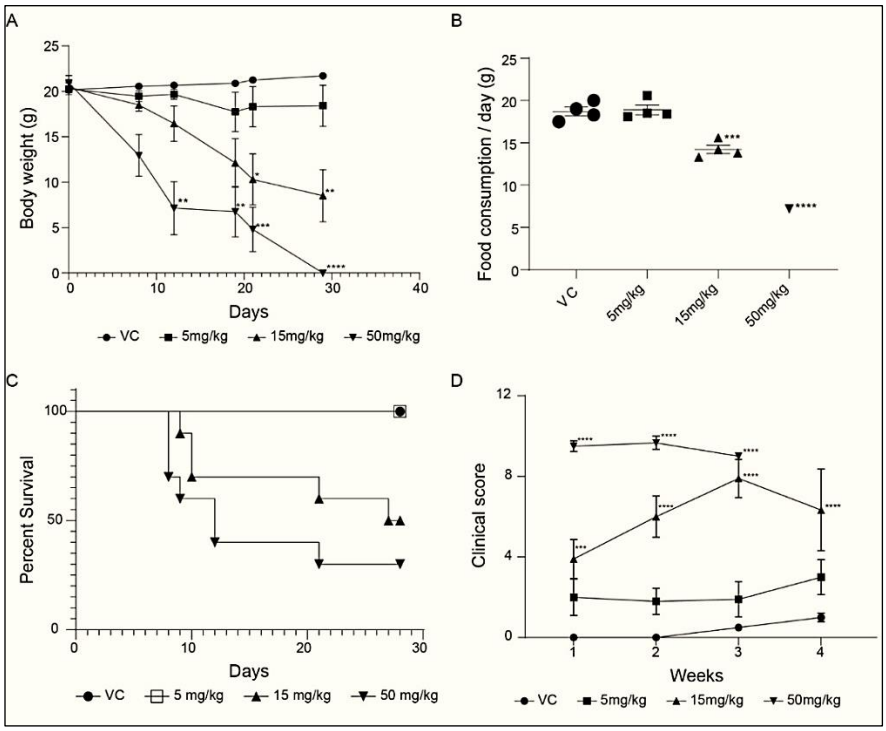

Figure 47: Sub-acute toxicity study (A) Body weight of animals in all groups at start (days 0, 7, 14, 21, and 28). Data are expressed as mean ± SEM (n = 10/group), and two-way ANOVA with Bonferroni correction was applied to evaluate time and dose-dependent differences between groups (*p < 0.05, **p < 0.01, ***p < 0.001, ****p < 0.0001). (B) Average daily food consumption in each group. Total food consumed per cage was recorded and weekly mean intake per mouse was calculated. Each data point represents average food consumption per mouse per day per week. A single data point in 50 mg/kg group represents average food consumption in week one of 5NQ oral dosing. (C) Survival of mice in each group was analyzed using Kaplan-Meier plots and log-rank test (n = 10) was used to compare difference between control & treated groups. (D) Weekly clinical scores of mice in each group are expressed as mean ± SEM (n = 10), and one-way ANOVA with Bonferroni correction was applied to evaluate dose-dependent differences between groups per week (***p < 0.001, ****p < 0.0001).

Survival: Toxicity-related mortality was not observed in the vehicle control or 5 mg/kg groups, and all mice survived the study period. Mice administered 15 mg/kg and 50 mg/kg of 5NQ for 28 days showed a significant decrease in survival, with a median survival of 27 and 12 days, respectively (Figure 47C).

Table 23: Absolute and relative organ weights of mice administered different doses of 5NQ

		Vehicle control	5 mg/kg	15 mg/kg	50 mg/kg	P-value
Liver	Relative	55.72 ± 3.79	64.39 ± 2.54	54.59 ± 2.76	65.42 ± 2.58	ns
	Absolute (g)	1.66 ± 0.12	1.30 ± 0.08*	0.95 ± 0.05**	0.91 ± 0.23**	*0.041, **0.0001
Kidneys	Relative	9.7 ± 1.13	7.85 ± 0.57	7.64 ± 0.50	7.73 ± 0.37	ns
	Absolute (g)	0.30 ± 0.03	0.16 ± 0.01**	0.13 ± 0.01**	0.12 ± 0.01**	** 0.0001
Spleen	Relative	6.56 ± 0.54	5.99 ± 0.54	5.37 ± 0.93	5.75 ± 0.64	ns
	Absolute (g)	0.19 ± 0.01	0.12 ± 0.01**	0.09 ± 0.01**	0.09 ± 0.01**	** 0.0001
Heart	Relative	55.72 ± 0.58	64.39 ± 3.37	54.59 ± 1.41	65.42 ± 2.24	ns
	Absolute (g)	0.19 ± 0.02	0.21 ± 0.08	0.13 ± 0.02	0.12 ± 0.01	ns
Lungs	Relative	12.5 ± 1.59	16.77 ± 1.20	17.9 ± 0.61	12.29 ± 0.28	ns
	Absolute (g)	0.37 ± 0.05	0.33 ± 0.02	0.31 ± 0.01	0.23 ± 0.04	ns
Intestine	Relative	57.19 ± 4.37	74.13 ± 8.67	62.86± 10.73	75.65 ± 6.05	ns
	Absolute (g)	1.7 ± 0.13	1.4 ± 0.10	1.3 ± 0.12	1.4 ± 0.25	ns
Brain	Relative	15.32 ± 0.60	22.46 ± 1.64	23.33 ± 1.53	24.43 ± 5.97	ns
	Absolute (g)	0.46 ± 0.01	0.44 ± 0.02	0.40 ± 0.02	0.44 ± 0.02	ns

Values are mean ± SEM for (n=10/group). The differences between control and treated groups were analysed by ANOVA with Bonferroni correction. The significance levels observed are *p < 0.05 and **p < 0.0001 in comparison to control group values; ns -non significant.

Hematological parameters: Hematological parameters remained unaffected in all the groups, except for high platelet counts observed in the 50 mg/kg group as compared to animals administered vehicle (Table 24).

Table 24: Hematological parameters of mice administered different doses of 5NQ for 28 days.

Parameters	units	Vehicle control	5mg/kg	15mg/kg	50mg/kg	P-value
RBC	10^6/µl	8.68 ± 0.62	8.86 ± 0.54	8.91 ± 1.54	881 ± 0.71	ns
HB	g/dL	11.86±1.20	13.14 ± 1	11.85±3.68	13 ± 1.10	ns
HCT	%	44.01±3.74	44.06±3.10	50.88±8.12	43.35±3.40	ns
MCV	fL	50.64±2.23	49.70±0.61	50.88±2.50	49.25±0.82	ns
MCH	pg	13.64±0.81	14.81±0.41	13.05±2.51	14.78±0.19	ns
MCHC	g/dL	26.90±0.57	29.81±0.58	25.63±4.63	29.98±0.40	ns
RDW	%	12.28±0.97	12.04±0.18	12.10±0.66	12.33±0.50	ns
PLT	10^3/µl	614.17 ± 40.26	733.14 ± 95.39	728.25 ± 117.72	1000.25 ± 219.60**	**0.0021
MPV	fL	7.47 ± 0.23	7.24 ± 0.32	7.30 ± 0.78	6.53 ± 0.25	ns
WBC	10^3/µl	3.48 ± 1.65	6.75 ± 3.19	4.95 ± 1.87	5.07 ± 1.36	ns
Neutrophils	10^3/µl	0.04 ± 0.01	0.05 ± 0.01	0.12 ± 0.04	0.05 ± 0.01	ns
Lymphocytes	10^3/µl	2.46 ± 0.48	4.59 ± 0.87	1.99 ± 0.12	2.95 ± 0.45	ns
Monocytes	10^3/µl	0.84 ± 0.12	1.82 ± 0.32	2.73 ± 1.02	1.98 ± 0.25	ns
Eosinophils	10^3/µl	0.0 ± 0.0	0.0 ± 0.0	0.0 ± 0.0	0.0 ±0.0	ns
Basophils	10^3/µl	0.01 ± 0.01	0.02 ± 0.01	0.01 ± 0.01	0.01 ± 0.01	ns

RBC (red blood cell) count, HB (haemoglobin), HCT (haematocrit), MCV (mean corpuscular volume, MCH (mean corpuscular haemoglobin), MCHC (MCH concentration), RDW (red cell distribution width), PLT (platelet count), MPV (mean platelet volume) WBC (white blood cell) count. Values are mean ± SEM for (n=10/group). The differences between control and treated groups were analysed by ANOVA with Bonferroni correction. The significance levels observed is **p < 0.0021 in comparison to control group values; ns -non significant; ns -non significant.

Serum Biochemistry: The assessment of liver function in mice treated with 15 mg/kg and 50 mg/kg of 5NQ showed significantly elevated levels of AST and ALT, indicating hepatic dysfunction, as compared to the vehicle control mice. In mice administered with 5 mg/kg 5NQ, only AST levels were slightly elevated. The levels of ALP, total bilirubin, and total protein were significantly reduced in mice treated with 50 mg/kg 5NQ compared to those in the control group, indicating impaired liver function. A noticeable increase was found in the uric acid and blood urea nitrogen levels of mice administered 15 mg/kg and 50 mg/kg

of 5NQ, compared to the control mice, suggesting that these animals had mild kidney dysfunction. Administration of 5NQ did not affect serum creatinine levels (Table 25).

Table 25: Serum biochemical parameters of mice administered different doses of 5NQ for 28 days.

Serum parameters	units	Vehicle control	5mg/kg	15mg/kg	50mg/kg	P value
TP	g/dL	5.97 ± 0.8	4.96 ± 1.55	5.98 ± 0.76	4.28±0.31**	**0.0006
ALP	U/L	79.36±15.72	87.13±29.16	80.50±33.32	49.80±19.3*	*0.0071
AST	U/L	66.0 ± 6.99	105.25±47.8*	145.13± 28.98**	182.20 ± 105.10***	*0.019, **0.001, ***0.0001
ALT	U/L	49.96 ± 5.5	57.6 ± 22.7	76.5 ± 34.6*	58.8 ± 21.5	*0.027
UA	mg/dL	2.53 ± 0.43	3.11 ± 1.08	3.62 ± 1.50	1.68 ±0.91*	*0.027
ALB	g/dL	0.8 ± 0.2	1 ± 0.3	1.1 ± 0.2	1 ± 0.3	ns
TB	mg/dL	0.14 ± 0.12	0.03 ± 0.03*	0.04 ± 0.06*	0.11 ± 0.16	*0.047
CRE	mg/dL	0.05 ± 0.07	0.16 ± 0.15	0.08 ± 0.13	0.18 ± 0.15	ns
BUN	mg/dL	51.64 ± 6.22	44.88 ±20.04	66.78±14.0*	55 ± 22.23*	*0.0073

Alanine aminotransferase (ALT), aspartate aminotransferase (AST), alkaline phosphatase (ALP), total bilirubin (TB), albumin (ALB), total protein (TP), blood urea nitrogen (BUN), creatinine (CRE) and uric acid (UA). Values are mean ± SEM for (N=10/group). The differences between control and treated groups were analysed by ANOVA with Bonferroni correction. The significance levels observed are *p < 0.05, **p < 0.001 and ***p < 0.0001 in comparison to control group values; ns -non significant; ns -non significant.

Histopathological analysis of the Liver: All animals that received 50 mg/kg of 5NQ exhibited severe hepatocellular degeneration, characterized by diffuse ballooning of hepatocytes, compared to liver tissue from animals that received the vehicle. In contrast, animals administered 5 mg/kg and 15 mg/kg 5NQ showed mild to moderate hepatocellular degeneration, presenting as focal to diffuse ballooning of hepatocytes, when compared to the vehicle control. These findings are consistent with the elevated levels of AST and ALT observed in animals administered 15 and 50 mg/kg of 5NQ. (Figure 48).

Histopathological analysis of the kidneys: Administration of 15 mg/kg and 50 mg/kg 5NQ to animals resulted in mild to moderate tubular edematous changes and scarce mononuclear infiltration in the renal tissues compared to the vehicle control group, indicating renal damage. However, no histological changes were observed in the renal tissues of animals administered 5 mg/kg 5NQ (Figure 48).

Histopathological analysis of the Spleen: The histological examination of spleen tissues from animals treated with 15 mg/kg and 50 mg/kg of 5NQ revealed a notable increase in the number of megakaryocytes. This finding is consistent with the elevated platelet counts observed in the peripheral blood of animals administered 50 mg/kg 5NQ. In contrast, animals treated with 5 mg/kg 5NQ did not exhibit an increase in the number of megakaryocytes (Figure 49).

No significant histological changes were observed in other tissues, such as lung, heart, brain, intestine, and femur, after repeated administration of 5NQ for 28 days (Figure 49).

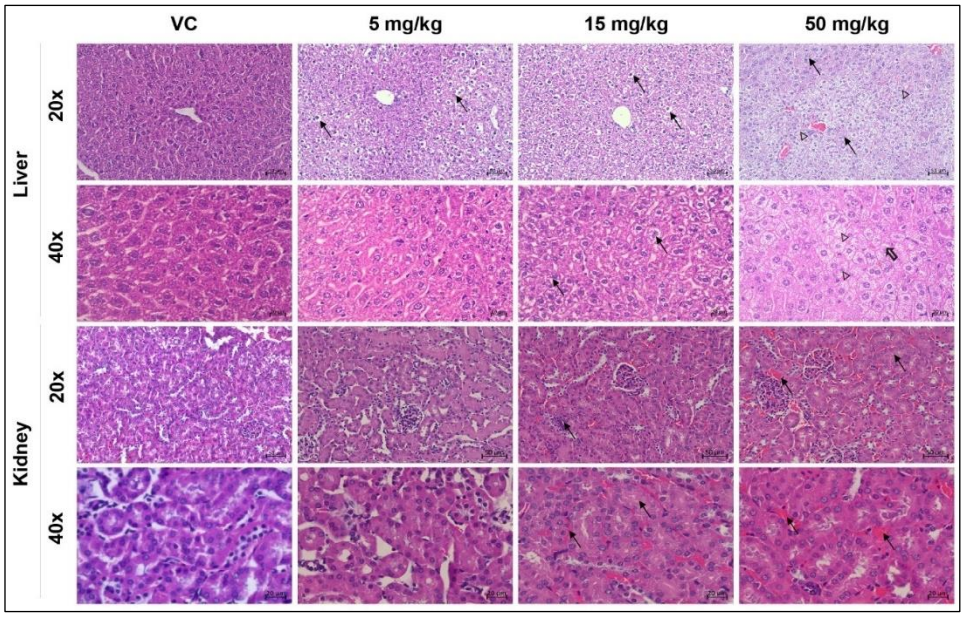

Figure 48: Representative micrographs of H&E stained liver and kidney tissues corresponding to mice treated with vehicle control (VC) and different doses of 5NQ for 28 days. In liver, black arrows indicate ballooning of hepatocytes, whereas clear arrowheads indicate marked diffuse degeneration (20x). At 40x, black arrows point to ballooning of hepatocytes, while clear arrows

indicate loss of lobular architecture and clear arrowheads indicate degeneration of hepatocytes. In the kidneys, black arrows indicate focal tubular edema.

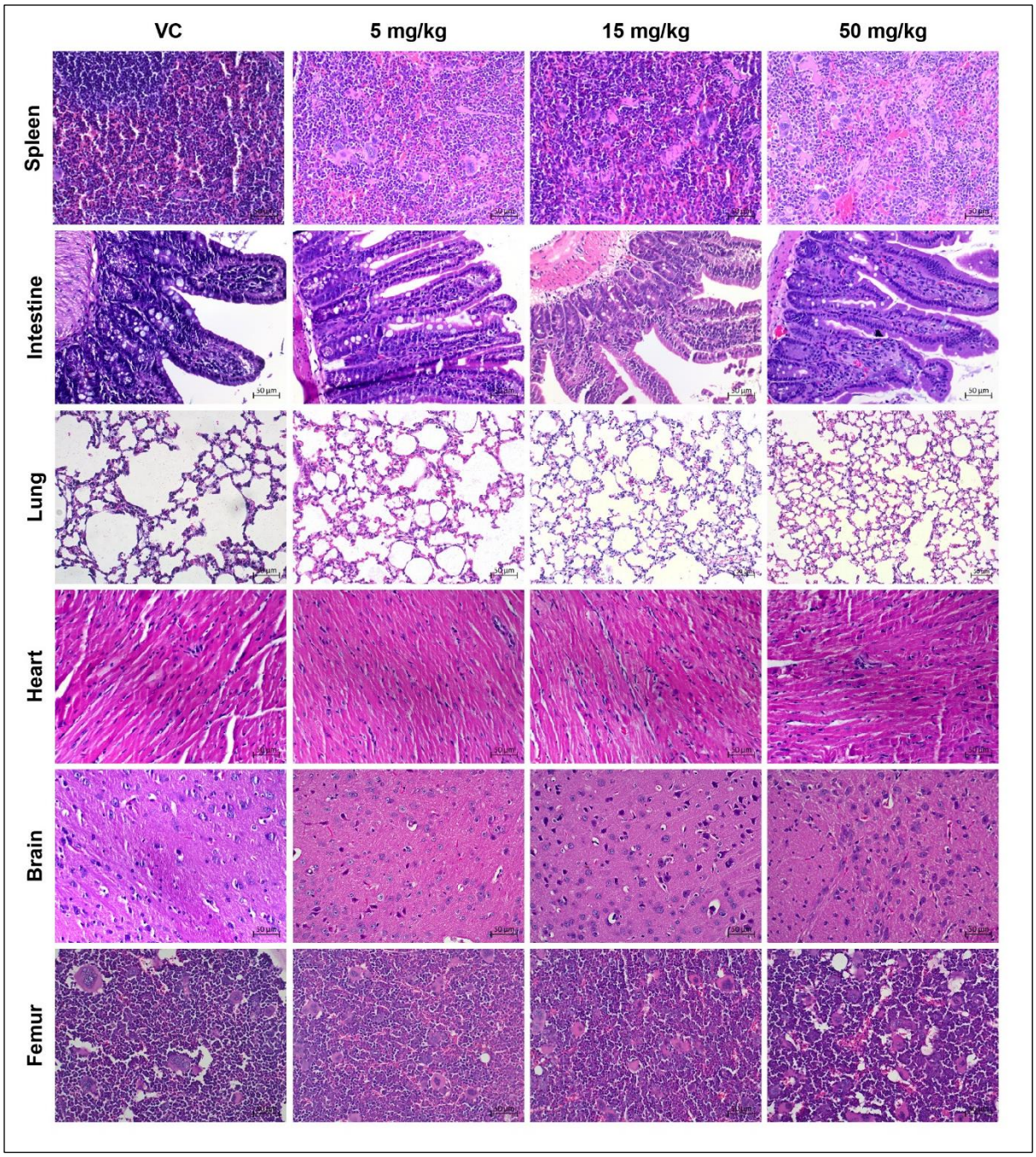

Figure 49: Representative micrographs of spleen, intestine, lung, heart, brain, and femur sections stained with H&E, corresponding to mice treated with vehicle control (VC) and with different doses of 5NQ x 28 days (20x magnification).

Benchmark dose analysis of survival data from the acute toxicity study: Dose-dependent mortality was observed in the acute toxicity study. BMD modelling of this dose-response

survival data resulted in the establishment of a BMDL of 118 mg/kg and BMDU of 247 mg/kg. The BMDL thus obtained can be considered the point of departure dose (POD) for a single administration of 5NQ (Figure 50, Figure 51, Table 26).

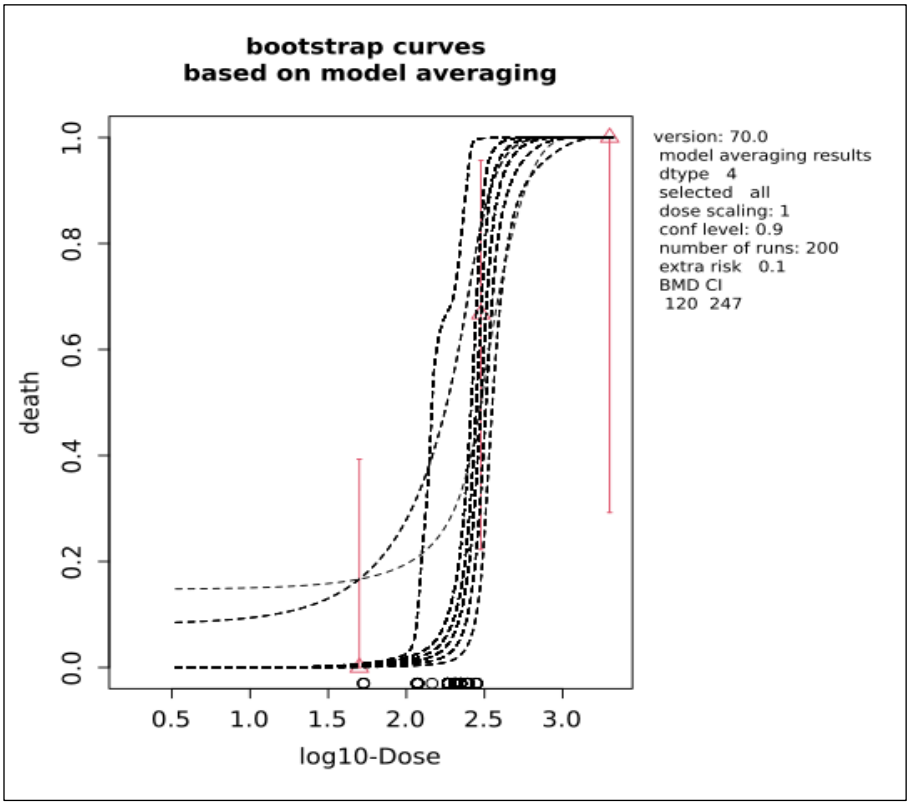

Figure 50: Benchmark dose modelling of survival response in acute toxicity study after administration of single doses of 50, 300, and 2000 mg/kg 5NQ. PROASTweb 70.1 software was used for the calculations, and a model averaging method with 200 iterations was applied. The red triangles represent geometric means. BMD CI- benchmark dose confidence interval

Table 26: Benchmark dose confidence intervals (BMDL and BMDU) obtained using PROASTweb 70.1 software for all fitted models by modelling the survival response after single dose administration of 5NQ in mice (acute toxicity study).

Parameter	Model	No.par	loglik	AIC	accepted	BMDL (mg/kg)	BMDU (mg/kg)	BMD (mg/kg)
% Mortality	null	1	-10.36	22.72		NA	NA	NA
	full	3	-3.82	13.64		NA	NA	NA
	two.stage	3	-4.00	14.00	yes	22.4	155	95.2
	log.logist	3	-3.82	13.64	yes	28.3	295	236.0
	Weibull	3	-3.82	13.64	yes	21.0	296	234.0
	log.prob	3	-3.82	13.64	yes	29.1	268	184.0
	gamma	3	-3.82	13.64	yes	20.1	275	201.0
	LVM: Expon. m3-	3	-3.82	13.64	yes	20.1	290	245.0
	LVM: Hill m3-	3	-3.82	13.64	yes	20.0	285	245.0
BMD CI base on model averaging method						**118 mg/kg**	**247 mg/kg**	

The lower confidence limit of the benchmark dose (BMDL), upper confidence limit of the benchmark dose (BMDU), benchmark dose (BMD) log likelihood (Loglik.), Number of parameters (No.par.), Akaike information criterion (AIC), convergence (conv.) Confidence Interval (CI).

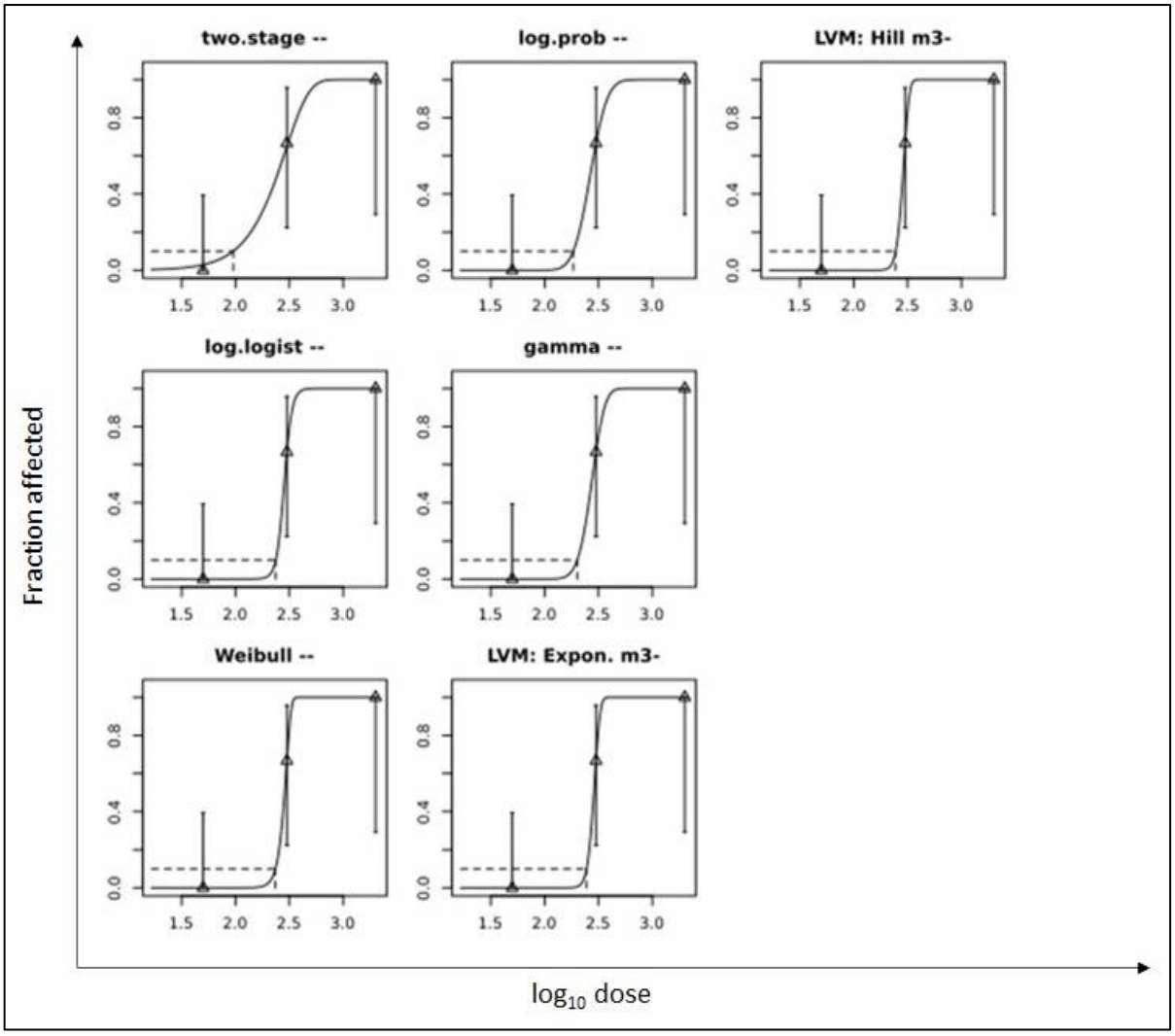

Figure 51: Dose-response models fitted for the survival response observed in the acute toxicity study after administration of single doses of 50, 300, and 2000 mg/kg 5NQ. PROASTweb 70.1 software was used for the calculations.

Benchmark dose analysis of dose-response data from a sub-acute toxicity study A dose-dependent mortality was observed in the sub-acute toxicity study. The model fitting this dose-response data using BMD modelling established a BMDL of 1.74 mg/kg/day (Figure 52, Figure 53, Table 27). The BMDL thus obtained can be considered as the POD dose for repeated administration of 5NQ and equivalent to the NOAEL dose.

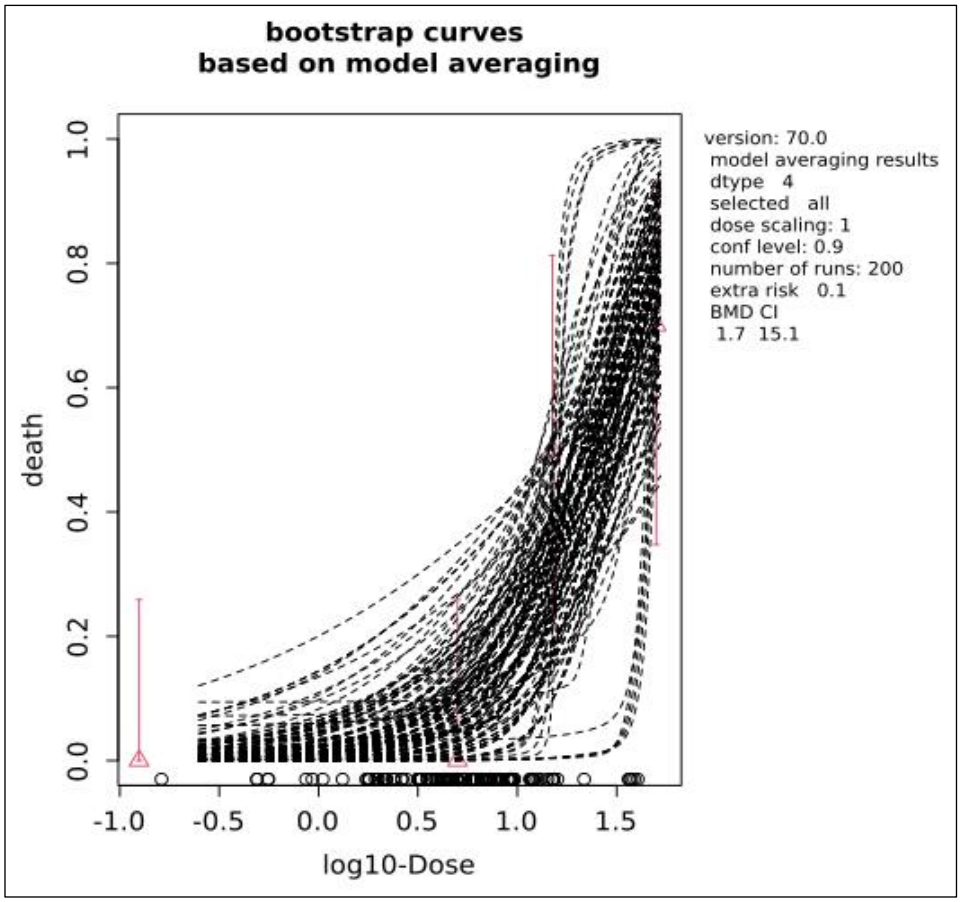

Figure 52: Benchmark dose modelling of the survival response in sub-acute toxicity study after daily administration of 5, 15 and 50 mg/kg 5NQ for 28 days. PROASTweb 70.1 software was used for the calculations, and a model averaging method with 200 iterations was applied. The red triangles represent geometric means. BMD CI- benchmark dose confidence interval

Table 27: Benchmark dose confidence intervals (BMDL and BMDU) obtained using PROASTweb 70.1 software for all fitted models by modelling the survival response after daily administration of 5NQ for 28 days in mice (sub-acute toxicity study).

Parameter	Model	No.par	loglik	AIC	accepted	BMDL (mg/kg/ day)	BMDU (mg/kg/ day)	BMD (mg/kg/ day)
% Mortality	null	1	-24.43	50.86		NA	NA	NA
	full	4	-13.04	34.08		NA	NA	NA
	two.stage	3	-15.02	36.04	Yes	2.470	6.69	3.92
	log.logist	3	-14.60	35.20	Yes	1.280	11.00	5.68
	Weibull	3	-15.00	36.00	Yes	0.611	10.90	4.61
	log.prob	3	-14.45	34.90	Yes	1.690	11.30	6.22
	gamma	3	-14.95	35.90	Yes	0.518	11.40	5.15
	LVM: Expon. m3-	3	-14.79	35.58	Yes	0.781	11.30	5.59
	LVM: Hill m3-	3	-14.73	35.46	Yes	0.845	11.10	5.46
	BMD CI base on model averaging method					**1.74 (mg/kg/ day)**	**15.1 (mg/kg/day)**	**-**

The lower confidence limit of the benchmark dose (BMDL), upper confidence limit of the benchmark dose (BMDU), benchmark dose (BMD) log likelihood (Loglik.), Number of parameters (No.par.), Akaike information criterion (AIC), convergence (conv.) Confidence Interval (CI).

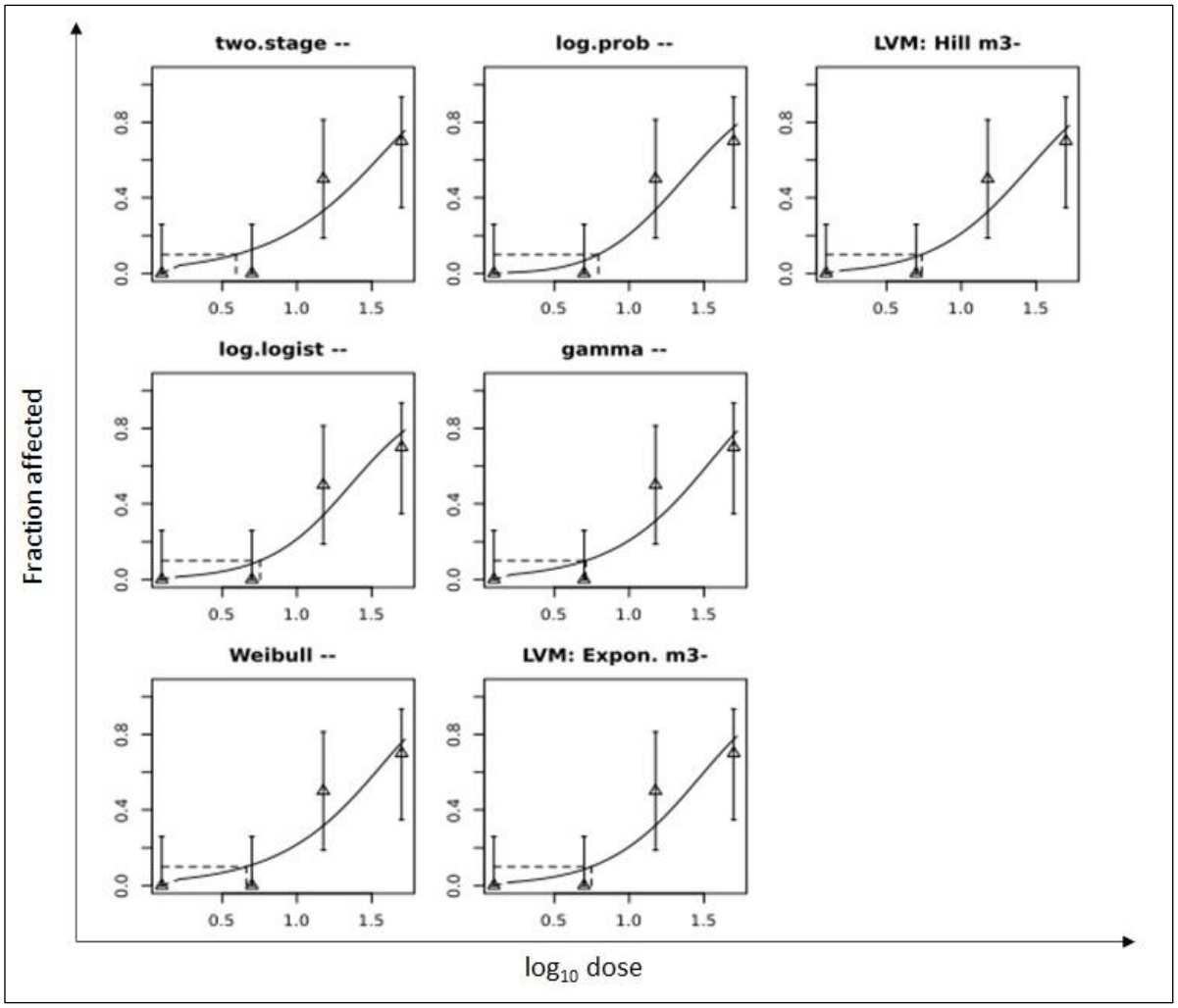

Figure 53: Dose-response models fitted for the survival response observed in the sub-acute toxicity study after daily administration of 5, 15, and 50 mg/kg 5NQ for 28 days. PROASTweb 70.1 software was used for the calculations.

In sub-acute toxicity, the levels of AST, ALT, ALP, total bilirubin, total protein, blood urea nitrogen, and platelets showed a dose-response relationship. Therefore, BMD modelling was performed for each of these dose-response data, and a BMDL was established for each parameter (Table 28). BMD modelling of liver function parameters revealed that AST levels were most sensitive to 5NQ exposure and showed the lowest BMDL of 1.1 x 10-3 mg/kg/day (Figure 54), followed by total bilirubin with BMDL of 0.03 mg/kg/day (Figure 55), followed by total protein with a BMDL of 6.35 mg/kg/day (Figure 56) and uric acid with a BMDL of 1.82 mg/kg/day (Figure 57). Dose-response relationship was also

observed with ALP and ALT levels and these parameters showed significant differences compared to vehicle control levels. However, BMD modelling of these parameters did not show any trend in the data because a BMDL value could not be established for these parameters. Among the hematological parameters, only platelet counts showed a dose - response relationship. BMD modelling of the plate counts established a BMDL of 0.5 mg/kg/day (Figure 58). The BMD modelling results are summarized in Table 29.

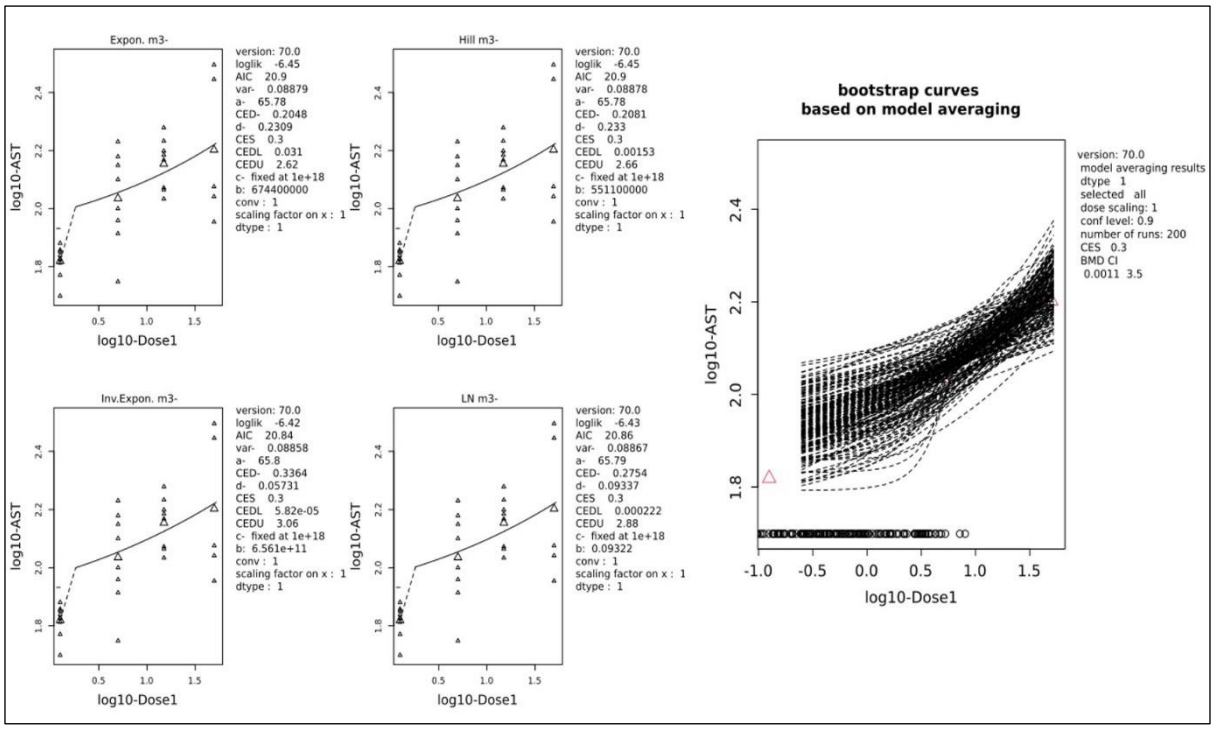

Figure 54: Dose-response modelling for AST levels in mice administered 5, 15, and 50 mg/kg 5NQ daily for 28 days, using an exponential model (Expon.m3-), Hill model (Hill m3-), inverse exponential model (Inv.Expon.m3), Log-normal family model (LN m3-). Bootstrap curves for AST levels based on the model averaging method with 200 iterations (red triangles represent geometric means). PROASTweb 70.1 software was used for the calculations and model averaging.

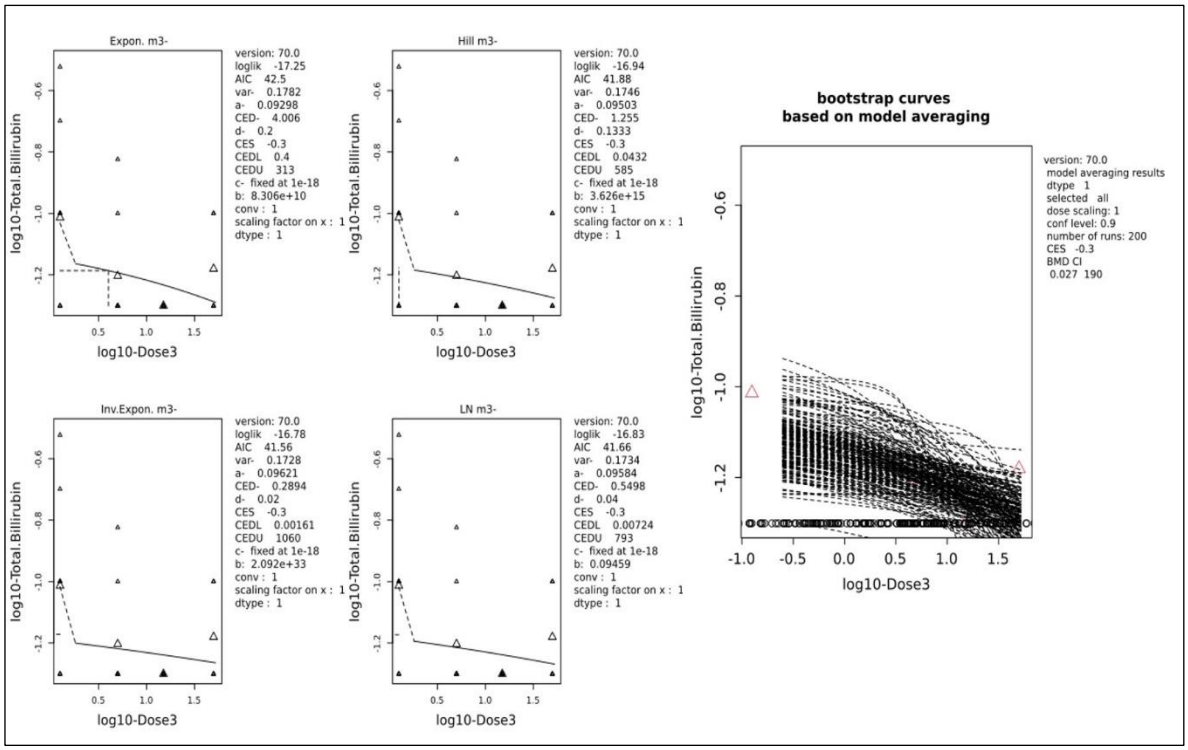

Figure 55: Dose-response modelling for levels of total bilirubin in mice administered 5, 15, and 50 mg/kg 5NQ daily for 28 days, using an exponential model (Expon.m3-), Hill model (Hill m3-), inverse exponential model (Inv.Expon.m3-), and Log-normal family model (LN m3-). Bootstrap curves for AST levels based on the model averaging method with 200 iterations (red triangles represent geometric means). PROASTweb 70.1 software was used for the calculations and model averaging.

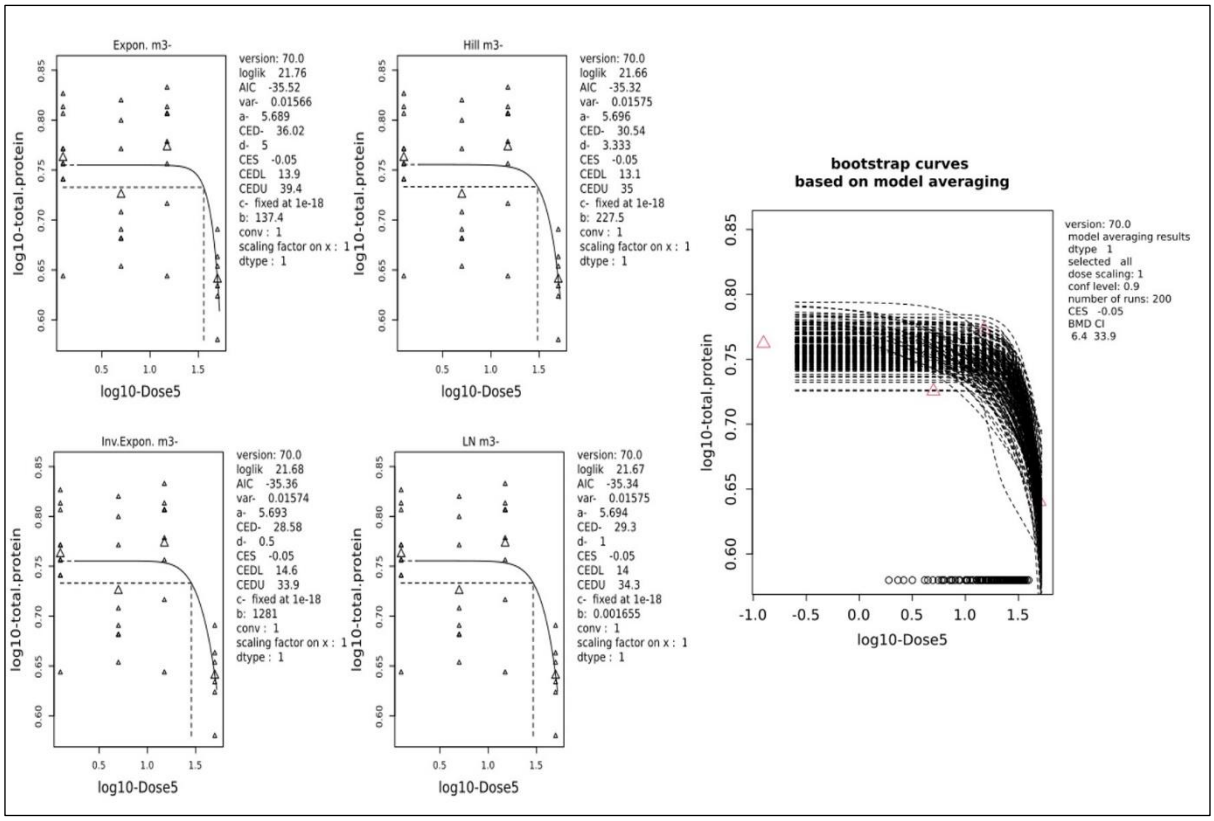

Figure 56: Dose-response modelling for levels of total protein in mice administered 5, 15, and 50 mg/kg 5NQ daily for 28 days, using an exponential model (Expon.m3-), Hill model (Hill m3-), inverse exponential model (Inv.Expon.m3-), and Log-normal family model (LN m3-). Bootstrap curves for AST levels based on the model averaging method with 200 iterations (red triangles

represent geometric means). PROASTweb 70.1 software was used for the calculations and model averaging.

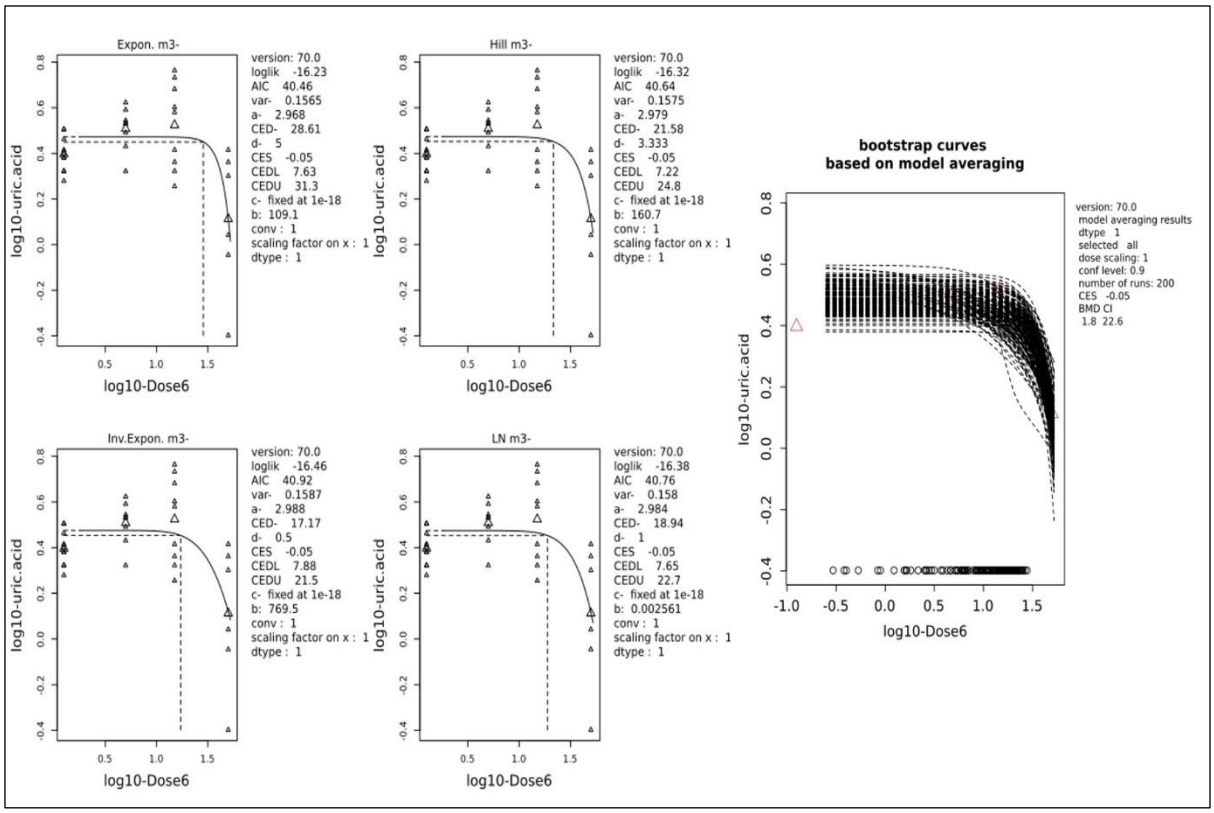

Figure 57: Dose response modelling for uric acid levels in mice administered 5, 15, and 50 mg/kg 5NQ daily for 28 days using an exponential model (Expon.m3-), Hill model (Hill m3-), inverse exponential modnv. Ex,pon.m3-), and Log-normal family model (N m3-). a Bootstrap curve for AST levels based on the model-averaging method with 200 iterations (red triangles represent geometric means). PROASTweb 70.1 software was used for the calculations and model averaging.

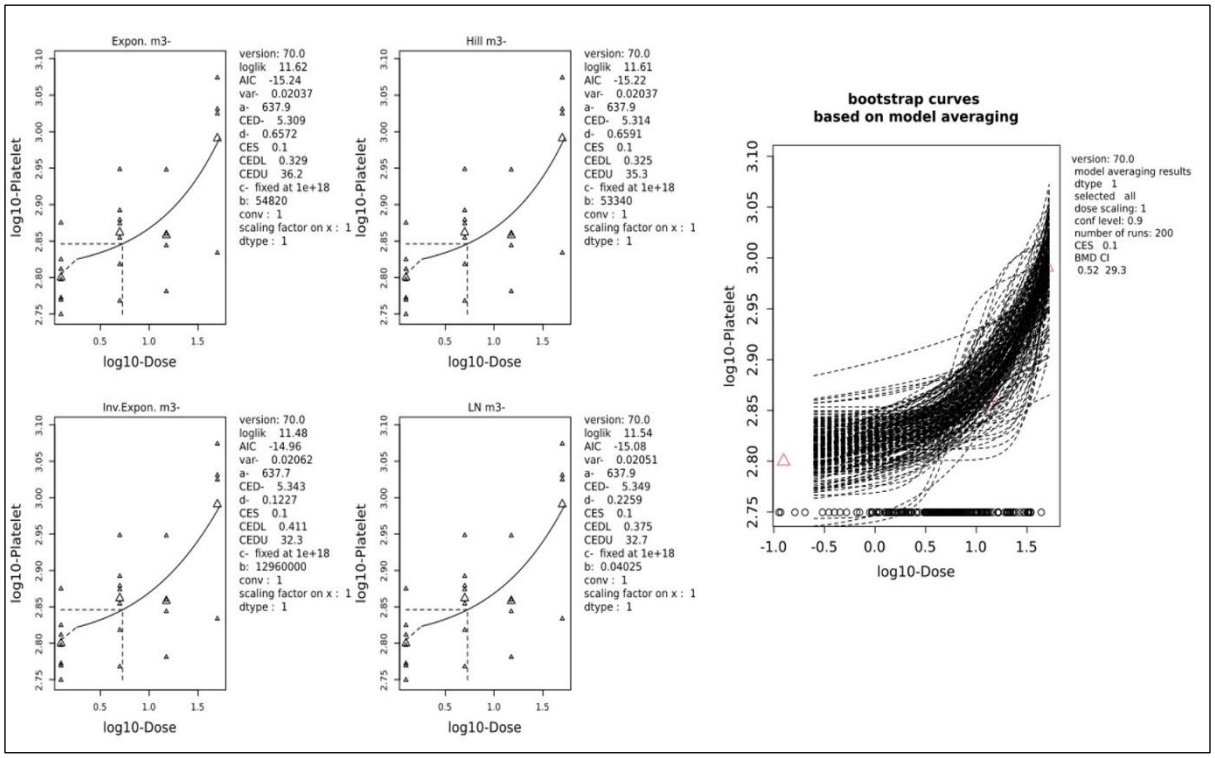

Figure 58: Dose response modelling for platelet counts in mice administered with 5, 15 and 50 mg/kg 5NQ daily for 28 days, using exponential model (Expon.m3-), Hill mode l(Hill m3-), inverse exponential model (Inv.Expon.m3-), Log-normal family model (LN m3-). Bootstrap curves for AST levels based on the model averaging method with 200 iterations (red triangles represent geometric means). PROASTweb 70.1 software was used for the calculations and model averaging.

Table 28: Benchmark dose confidence intervals (BMDL and BMDU)

Parameter	Fitted models	Conv.	Loglik.	No.par	AIC	Model weights	BMDL (mg/kg/day)	BMDU (mg/kg/day)
AST	full model	yes	-6.08	5	22.16		-	-
	null model	yes	-19.73	2	43.46		-	-
	Expon. m3-	yes	-6.45	4	20.90	0.25	0.031	2.62
	Expon. m5-	yes	-6.08	5	22.16		-	-
	Hill m3-	yes	-6.45	4	20.90	0.25	0.0015	2.66
	Hill m5-	yes	-6.08	5	22.16		-	-
	Inv.Expon. m3-	yes	-6.42	4	20.84	0.25	5.82e-05	3.06
	Inv.Expon. m5-	yes	-6.18	5	22.36		-	-
	LN m3-	yes	-6.43	4	20.86	0.25	0.000222	2.88
	LN m5-	yes	-6.08	5	22.16		-	-
						Model averaged	**0.0011**	**3.5**
Total bilirubin	full model	yes	-15.65	5	41.30		-	-
	null model	yes	-20.95	2	45.90		-	-

	Expon. m3-	yes	-17.25	4	42.50	0.18	0.4	313
	Expon. m5-	yes	-16.64	5	43.28		-	-
	Hill m3-	yes	-16.94	4	41.88	0.25	0.04	585
	Hill m5-	yes	-17.17	5	44.34		-	-
	Inv.Expon. m3-	yes	-16.78	4	41.56	0.29	0.00161	1060
	Inv.Expon. m5-	yes	-16.62	5	43.24		-	-
	LN m3-	yes	-16.83	4	41.66	0.28	0.00724	793
	LN m5-	yes	-16.48	5	42.96		-	-
						Model averaged	**0.027**	**190**
Total protein	full model	yes	23.66	5	-37.32	-	-	-
	null model	yes	13.41	2	-22.82	-	-	-
	Expon. m3-	yes	21.76	4	-35.52	0.27	13.9	39.4
	Expon. m5-	yes	21.76	5	-33.52	-	-	-
	Hill m3-	yes	21.66	4	-35.32	0.24	13.1	35
	Hill m5-	yes	21.66	5	-33.32	-	-	-
	Inv.Expon. m3-	yes	21.68	4	-35.36	0.25	14.6	33.9
	Inv.Expon. m5-	yes	21.52	5	-33.04	-	-	-
	LN m3-	yes	21.67	4	-35.34	0.24	14	34.3
	LN m5-	yes	21.60	5	-33.20	-	-	-
						Model averaged	**6.35**	**33.9**
Uric acid	full model	yes	-14.60	5	39.20	-	-	-
	null model	yes	-24.50	2	53.00	-	-	-
	Expon. m3-	yes	-16.23	4	40.46	0.28	7.63	31.3
	Expon. m5-	yes	-16.23	5	42.46	-	-	-
	Hill m3-	yes	-16.32	4	40.64	0.26	7.22	24.8
	Hill m5-	yes	-16.33	5	42.66	-	-	-
	Inv.Expon. m3-	yes	-16.46	4	40.92	0.22	7.88	21.5
	Inv.Expon. m5-	yes	-16.88	5	43.76	-	-	-
	LN m3-	yes	-16.38	4	40.76	0.24	7.65	22.7
	LN m5-	yes	-16.52	5	43.04	-	-	-
						Model average	**1.82**	**22.6**

Platelets	full model	yes	12.38	5	-14.76	-	-	-
	null model	yes	3.79	2	-3.58	-	-	-
	Expon. m3-	yes	11.62	4	-15.24	0.26	0.329	36.2
	Expon. m5-	yes	11.61	5	-13.22	-	-	-
	Hill m3-	yes	11.61	4	-15.22	0.26	0.325	35.3
	Hill m5-	yes	11.61	5	-13.22	-	-	-
	Inv.Expon. m3-	yes	11.48	4	-14.96	0.23	0.411	32.3
	Inv.Expon. m5-	yes	11.44	5	-12.88	-	-	-
	LN m3-	yes	11.54	4	-15.08	0.24	0.375	32.7
	LN m5-	yes	11.52	5	-13.04	-	-	-
						Model average	**0.52**	**29.3**

Benchmark dose confidence intervals (BMDL and BMDU) obtained using PROASTweb 70.1 software for all fitted models by modelling the effect on serum and haematological parameters after daily administration of 5NQ for 28 days (sub-acute toxicity study). The lower confidence limit of the benchmark dose (BMDL), upper confidence limit of the benchmark dose (BMDU), benchmark dose (BMD) log likelihood (Loglik.), Number of parameters (No.par.), Akaike information criterion (AIC), convergence (conv.)

Table 29: Benchmark dose confidence intervals (BMDL and BMDU)

Parameter	CES/BMR	BMDL (mg/kg/day)	BMDU (mg/kg/day)
AST	0.3	1.1×10^{-3}	3.5
Total Bilirubin	0.3	0.03	190
Total Protein	0.05	6.35	33.9
Uric acid	0.05	1.82	22.6
Platelets	0.1	0.52	29.3

Benchmark dose confidence intervals (BMDL and BMDU) obtained using PROASTweb 70.1 software by model averaging method, by modelling the effect on serum biochemical and hematological parameters in mice after daily administration of 5NQ for 28 days (sub-acute toxicity study). Aspartate aminotransferase (AST), critical effect size (CES), benchmark response (BMR), Lower confidence limit of the Benchmark dose (BMDL), upper confidence limit of the Benchmark dose (BMDU).

7.4 DISCUSSION

The therapeutic potential of 5-hydroxy-1,4-naphthoquinone is immense, which makes it a highly attractive pharmacological candidate. The therapeutic effect of 5NQ results from its ability to generate free radicals, which modulate numerous intracellular pathways[296]. Our in silico data suggested that 5NQ has favorable ADME properties, making it a promising drug candidate for further development. However, its estimated toxicity as a mutagenic agent, as well as its potential to cause eye and skin irritation, is a cause of concern. Moreover, as with most quinone compounds, the metabolism of 5NQ is known to produce toxic byproducts, which necessitates the evaluation of its therapeutic effects in light of these potential toxic effects[297]. Consequently, the utilization of 5NQ as a therapeutic agent carries significant risks, making it imperative to comprehensively understand its toxicity profile. The objective of this study was to assess the oral acute and sub-acute toxicity of 5NQ and establish a safe dose for conducting comprehensive preclinical investigations in mouse models to evaluate the therapeutic potential of 5NQ. In addition to utilizing the conventional method of determining the NOAEL (the lowest dose at which no adverse effects were observed), we also employed benchmark dose modelling to establish a point of departure dose for the daily administration of 5NQ and to identify the most sensitive marker of toxicity to 5NQ.

The results of our acute toxicity testing revealed that a single oral dose of 50 mg/kg 5NQ was safe and well tolerated by mice and did not result in mortality. However, histopathological analysis revealed significant degenerative changes in the hepatic and renal tissues of the animals. The results of our acute toxicity study established that 5NQ can be classified as a category 3 substance according to OECD guideline 423 and the Global Harmonized System for the classification of substances and mixtures. This classification

indicates that 5NQ has an acute LD_{50} cutoff dose of > 50 ≤ 300 mg/kg body weight[280]. Additionally, BMD modelling of the survival data of the acute toxicity study established a BMDL of 118 mg/kg, which can be considered as the POD dose for single-dose administration of 5NQ, and mortality can be expected at doses higher than this dose.

A sub-acute toxicity study found that administering 5 mg/kg of 5NQ to mice for 28 days was safe and did not result in any toxicity-related mortality. However, mice administered 5 mg/kg 5NQ experienced significant weight loss over the 4-week period. The observed weight loss could be attributed to the mitochondrial uncoupling activity of 5NQ. Mitochondrial uncoupling disrupts the electron transport chain, resulting in ATP depletion. This causes an increase in fatty acid oxidation to meet the energy requirements of the cell[257]. 5NQ is a narrow-range mitochondrial uncoupler, and higher doses can cause complete mitochondrial uncoupling, leading to ATP depletion, hyperthermia and even death[298]. Mice administered 15 and 50 mg/kg exhibited significant mortality, which may be related to the cellular damage caused by the mitochondrial uncoupling action of 5NQ. Although administration of 5 mg/kg 5NQ did not cause mortality in mice, the observed decrease in body weight indicated the mild toxicity of 5NQ. Based on these observations, we established the NOAEL for the daily administration of 5NQ to be < 5 mg/kg/day. However, there are many limitations in determining POD using the traditional NOAEL approach, which include the limited doses selected in the study, overestimation of POD, and small sample size[283,288]. Therefore, we used the modern and regulatory recommended approach of benchmark dose modelling to determine the POD dose. Our results from the BMD modelling of the survival response in the sub-acute toxicity study established 1.74 mg/kg/day as the POD. This value was 65% lower than that of the lowest dose (5 mg/kg/day) used in this study. Thus, the mathematical approach of BMD and the traditional

NOAEL approach may converge to estimate POD. Nevertheless, the BMD approach is more accurate in estimating POD. This dose can be used to determine the human equivalent reference dose for risk assessment[282].

The metabolism of 5NQ has been studied using rat hepatocytes and has been shown to affect the mitochondria of hepatocytes due to its mitochondrial uncoupling activity[298,299]. Flavoprotein enzymes, such as NADPH-cytochrome P450 reductase and NAD(P)H: quinone oxidoreductase, catalyse the reduction of quinones (such as 5NQ) to semiquinone or hydroquinone radicals[297]. The hydroquinone thus formed is catalyzed to form conjugates with glucuronide or sulfate. This process leads to the detoxification of quinones, with the formation of free radicals such as superoxide as byproducts[297]. In another reaction, 1,4-naphthoquinones such as 5NQ interact with cellular thiols to form hydroquinone conjugates with glutathione (GSH) and N-acetyl cysteine (NAC). These GSH conjugates undergo auto-oxidation thus maintaining the redox activity of these compounds which in further leads to the formation of more free radicals[299]. Therefore, it can be concluded that the biotransformation of 5NQ in the liver and the generation of free radicals as by-products may have a detrimental effect on hepatocytes. To date, no studies have reported the hepatic toxicity associated with 5NQ, despite our understanding of its potential for such effects. Our study is the first to demonstrate dose-dependent hepatic toxicity resulting from the oral administration of 5NQ. Additionally, the abnormal levels of liver function markers ALT, AST, ALP, and total bilirubin, along with the severe hepatic degenerative changes observed through histopathology following repeated oral administration of 5NQ, demonstrated the cytotoxic effect of 5NQ on hepatocytes. Our results not only support our previous in silico study, which indicated a high likelihood of drug-induced liver injury (DILI), but also confirmed these findings. However, the in silico predicted probability of human

hepatotoxicity (HT) and rat oral acute toxicity is extremely low, suggesting that these toxic effects may not manifest during the clinical development of this drug.

Previous studies on the pharmacokinetics and biodistribution of 5NQ have indicated that the kidney tissues accumulate the highest amount of 5NQ regardless of the route of administration[266,267,299]. According to a study conducted by Chen et al. in 2005, the glucuronide and sulfate conjugates formed as a result of biotransformation of 5NQ are primarily excreted through urine and therefore have a significant nephrotoxic effect. The nephrotoxic effect of 5NQ was consistent regardless of the route of administration and can be attributed to the covalent binding of 5NQ or its metabolites (monoglucuronide of 4,8-dihydroxy-1-tetralone) to cytosolic a2u-globulin (a lipocalin class of proteins), which causes hydrocarbon-related nephropathy[297–300]. Additionally, quinone thiol-ethers can cause nephrotoxicity when administered intravenously[301,302]. Our findings of elevated levels of renal function markers, uric acid, and BUN, as well as significant renal tissue damage observed in animals administered 15 mg/kg and 50 mg/kg of 5NQ for 28 days, support the reported nephrotoxic effects of 5NQ.

Our study examined the oral toxicity of 5NQ and found evidence of potential hepatic and renal toxicity. However, these effects were observed at doses higher than those reported in previous studies of parenteral administration of 5NQ[265–267].

Furthermore, the favorable probability of the oral bioavailability of 5NQ predicted in our in-silico study indicates that 5NQ may be a promising candidate for oral administration. Furthermore, our study observed systemic toxicities at relatively low doses, suggesting the good oral bioavailability of 5NQ, which needs to be confirmed in pharmacokinetic studies. It is worth noting that, despite the fact that the administration of 5 mg/kg 5NQ did not result in toxicity-related mortality in mice, we observed mild elevations in AST, a marker of liver

injury, following repeated administration of this dose. Additionally, dose-response modelling of serum AST levels revealed that it was the most sensitive indicator of toxicity of 5NQ, with the lowest benchmark dose level of 1.1×10^{-3} mg/kg/day. Having a recovery group in place would have allowed us to determine the reversibility of this process, which should be considered in future research. Earlier studies have demonstrated that the liposomal preparation of 5NQ, when administered intravenously, enhances its anticancer effectiveness while reducing its systemic toxicity in mice[267]. Therefore, it can be concluded that the safety of oral 5NQ administration can be improved by utilizing appropriate drug delivery systems to harness its therapeutic potential.

Nevertheless, our study provides a reasonable estimate of the safe dose and duration for repeated oral administration of 5NQ, which can aid in determining the dosage for preclinical studies designed to evaluate the therapeutic efficacy of 5NQ in murine models.

Conclusion: In conclusion, we established 118 mg/kg as the POD for a single oral administration of 5NQ and we established 1.74 mg/kg/day as POD for repeated administration of 5NQ. Additionally, serum AST level was identified as the most sensitive marker of 5NQ toxicity. The established POD values can be used as a reference for preclinical efficacy assessments and for deriving the human equivalent reference dose of 5NQ to ascertain its safety for clinical use.

Objective 3: Part B

7 OBJECTIVE 3: PART B

7.5 BACKGORUND

The objective of this section is to evaluate anti-GVHD efficacy of 5NQ *in vivo*. In this segment we provided details regarding the overview of various mouse models used to assess the anti-GVHD potential of drugs with an emphasis on the role of cytokines, innate and adaptive immune cells in the pathogenesis and prevention of acute GVHD.

Murine models of acute GVHD

The use of preclinical animal models has greatly aided our understanding of GVHD and cancer therapy. In HSCT research, most animal models rely on inbred mice, allowing researchers to select specific major histocompatibility complex (MHC) molecules between the host and donor and study the implications of the degree of matching in a controlled setting. Murine models of HSCT are broadly divided with respect to MHC mismatch between recipient and the donor strains, xenogeneic murine models of HSCT are also employed. A systematic review by Schroeder and DiPersio highlighted the key differences and advantages between these models (Table 30).

Mouse models of acute GVHD involve transplantation of bone marrow cells along with donor lymphocytes (splenocytes or lymph node T cells) into irradiated recipient mice. The bone marrow contains stem cells that are important for hematopoietic reconstitution, whereas lymphocytes from the spleen or lymph nodes serve as a source of immune cells that can be manipulated to study the effects of specific immune cells in the development of acute GVHD.

Acute GVHD is caused by a mismatch in MHC antigens, resulting in the immune-mediated rejection of foreign tissues and cells. Although MHC matching is performed in clinical settings, differences in minor histocompatibility antigens (miHAs) can cause acute GVHD (aGVHD). In mice, MHC antigens are represented as H2 and most strains are closely related to H2 antigens. The MHC-mismatched, miHA-mismatched, and xenogeneic murine models are discussed below.

MHC-mismatched models: The most studied murine model based on MHC-mismatch involves C57BL/6 mice (expressing the H2kb MHC-I antigen) as donors and BALB/c mice (expressing the H2kd MHC-I antigen) as recipients. Along with the major MHC mismatches, this model also contains miHA mismatch. The acute GVHD that develops in these mice is primarily dependent on MHC-I mismatch with a limited contribution of miHA mismatch. $CD4^+$ and $CD8^+$ T cells have been reported to play a predominant role in the development of acute GVHD in this murine model[303,304]. The development of acute GVHD in these models is influenced by variations in class I and class II MHC antigens[305,306]. The common parent to F1 strains used in the murine model of HSCT is described in Table 30

MiHA-mismatched models: The murine model based on MiHA-mismatch is more clinically relevant because MHC-mismatched transplants are not commonly performed in humans. The MiHA-mismatched models exhibited lower morbidity compared to MHC-mismatched models while developing severe acute GVHD, thus depicting the clinical scenario[307]. For instance, B10.D2 (H2kd) to BALB/c or DBA/2 (H2kd) mice model suggests that acute GVHD is primarily influenced by $CD4^+$ T cells and to a lesser extent by $CD8^+$ T cells[308,309].

Xenogeneic transplant models: Xenogeneic transplant models have been developed to study acute GVHD mediated by human T cells *in vivo*. As the immune response to xenografts is usually much stronger than that to allografts, the development of these models

necessitates strong immunosuppression. Therefore, initial attempts to develop these models were made using immunocompromised non-obese diabetic severe combined immunodeficiency (NOD/SCID) mice, which lack functional T and B lymphocytes[310]. However, these models show poor engraftment of donor cells due to the functional activity of NK cells in these animals, which may also result in graft rejection. Further, improvement in the experimental settings was achieved, and better engraftment was achieved when RAG2-deficient and IL-2 receptor-γ-deficient mice (BALB/cA- were used as recipients). These mice lack functional T, B, and NK cells, resulting in better engraftment of human cells and consistent development of acute GVHD. Currently, the best strains to develop xenogeneic transplant model is NSG mice (NOD/SCID-RAG2$^{-/-}$IL2rγ$^{-/-}$), which are bred by back crossing mice carrying a homozygous deletion of the common γ-chain of the IL-2 receptor to a NOD/SCID mice[311]. NSG mice lack T, B, and NK cells, and have diminished function of macrophages and dendritic cells. Because T cell recognition of MHC-II is species-restricted, this model predominantly aids in understanding CD4$^+$ T cell-mediated acute GVHD[312].

Table 30: Mouse models of acute GVHD

Donor strain	**Recipient strain**	**Conditioning regimen**	**Genetics**	**Cell type contributing to phenotype**	**Outcome**
C57BL/6 (H2b)	BALB/c (H2d)	900 cGy	Mismatched for MHCI, MHCII and miHAs	CD4$^+$ and CD8$^+$	Lethal disease (10 -21 days)
C3H/HeJ (H2k)	C57BL/6 (H2b)	900 cGy	Mismatched for MHCI, MHCII and miHAs	CD4$^+$ and CD8$^+$	Lethal disease (10 -30 days)
C57BL/6 (H2b)	B6C3F1 (H2k/b)	600 -1050 cGy	Mismatched for MHCI, MHCII and miHAs	CD4$^+$ and CD8$^+$	Lethal disease
C57BL/6 (H2b)	B6D2F1 (H2b/d)	No XRT or 1100 -1300 cGy	Mismatched for MHCI, MHCII and miHAs	CD4$^+$ and CD8$^+$	With XRT: Lethal disease in 30 days otherwise 30-50 days

C57BL/6 (H2b)	B6AF1 (H2b/a)	No XRT	Mismatched for MHCI, MHCII and miHAs	$CD4^+$ and $CD8^+$	Lethal disease depending on T-cell dose
C57BL/6 (H2b)	B10.BR (H2k)	750-900 cGy +/– Cytoxan 120 mg/kg	Mismatched for MHCI, MHCII and miHAs	$CD4^+$ & $CD8^+$	Lethal disease in 14-28 days based on T-cell dose and source
C57BL/6 (H2b)	B6.C-H2bm1 (mutation at MHC I)	950 cGy or sublethal XRT	MHC I mismatch	$CD8^+$	$CD8^+$ T cells infusion lead to systemic disease Death: 30-80 days
C57/Bl6 (H2b)	B6.C - H2bm12 (mutation at MHC II)	950 cGy or sub-lethal XRT	MHC II mismatch	$CD4^+$	$CD4^+$ T cells infusion lead to systemic disease Death: 20-40 days
B10.BR (H2k)	CBA or BALB.K (H2k)	750 cGy	miHA mismatches	$CD8^+$	Systemic disease Symptoms: tail scaling, ear erosions, diarrhea, hunching
B10.D2 (H2d)	DBA/2 (H2d)	800 cGy	miHA mismatches	$CD4^+$ & $CD8^+$	Lethal systemic disease by day 80
B10.D2 (H2d)	BALB/c (H2d)	Sub-lethal 600 -750 cGy or Fractionated 1000 cGy	miHA mismatches	$CD4^+$ & $CD8^+$	Systemic disease
B10 (H2b)	BALB.b (H2b)	775 cGy	miHA mismatches	$CD4^+$ & $CD8^+$	Systemic disease, no cutaneous involvement
C57BL/6 (H2b)	BALB.b (H2b)	800-1000 cGy	miHA mismatches	$CD4^+$	Systemic disease
DBN2 (H2d)	BlO.D2 (H2d)	820 cGy	miHA mismatches	$CD8^+$	Minimal systemic disease with whole spleen cells but increased with purified $CD8^+$ T cells - 50% mortality at day 25
Human PBMCs	NOD/SCID IL2rγ- null (NSG)	No XRT or 200-250 cGy	Mistmatched for MHC I, MHC II and miHAs	$CD4^+$	Death from GvHD in 30- 50 days
Human PBMCs	BALB/cA-$RAG2^{-/-}$ $IL2r\gamma^{-/-}$	350 cGy	Mismatched for MHC I, MHC II and miHAs	$CD4^+$ & $CD8^+$	Systemic disease
Human PB TCs	NOD/SCID 2m-null	250-300 cGy	Mismatched for MHC I, MHC II and miHAs	naive or CD3/CD28 bead expanded	Systemic disease

BM: bone marrow, cGy: centigray, RO: retro-orbital injection, TCD: T-cell depleted, XRT: radiation conditioning, PBMCs: peripheral blood mononuclear cells, PB TCs: peripheral blood T cells[313]

Factors to be considered when selecting a mouse model of GVHD

Acute or chronic GVHD: The choice of an appropriate murine model depends largely on the research question and whether one desires to study acute or chronic GVHD.

Type of intervention being tested and its mechanism of action: If the intervention targets both $CD4^+$ and $CD8^+$ T cells, selecting a model in which acute GVHD is mediated solely by $CD4^+$ T cells may not be optimal. Furthermore, if the intervention aims to modulate cytokines and the selected model is an miHA mismatch, it may not be an optimal choice because this model demonstrates reduced cytokine storm and could result in an overestimation of the intervention's efficacy[313,314].

Clinical manifestations and outcomes to be studied: The severity of GvHD and ability to track specific cell populations are important factors to consider when choosing a model. If the primary outcome of interest is clinical scoring, the C57/Bl6 r BALB/c transplant model may be a good choice, as this model results in severe acute GVHD and complete engraftment of donor cells. Generally, a higher degree of MHC mismatch leads to a more severe GvHD[315,316].

GVHD severity: Several factors influence acute GVHD severity. The dose and type of T cell subsets ($CD4^+$, $CD8^+$, or Treg cells) in the donor bone marrow and the irradiation dose are linked to acute GVHD-related mortality in mice. The myeloablative radiation dose varies according to the mouse strain. Genetic disparities are important in disease, for example, miHAs can affect acute GVHD severity, even in MHC-matched mice[316–320]. GvHD can be affected by environmental pathogens and specific pathogen free (SPF) conditions between laboratories[321,322]. This means that phenotype of the same acute GVHD model can differ based on the radiation dose and delivery rate variability, pathogens load

in animal facilities, and T-cell doses and source of T cells. Therefore, it is crucial to validate the mouse model in the laboratory [313,314].

Factors contributing to differences between mouse and human HSCT

Inbred mice are used in preclinical HSCT studies as they are genetically homozygous, age and sex-matched, fed the same diet, and housed in SPF conditions, allowing researchers to assess disease variables and eliminate extraneous factors. However, the differences between mouse models and clinical conditions must be considered before drawing conclusions. The HSCT response is affected by genetic and MHC diversity, age, health status (BMI, comorbidities), and immunological and microbial exposure. These factors cannot be accounted for in inbred animals[323]. This limitation can be overcome by utilizing outbred animal models. However, they are costly, have small sample sizes, require longer experiments and follow-up periods[324,325].

Age is another factor that affects the mouse model and human outcomes of HSCT. Age-related changes in humans, such as immune senescence, impaired tissue repair, obesity, and thymic dysfunction, increase GVHD severity. Animal models often use young lean mice, which do not accurately reflect the clinical conditions and comorbidities[326–328]. In humans, acute GVHD appears within 100 days of transplantation, but in mice the time frame may differ and are mainly identified by their clinical signs.

Variations in conditioning regimens contribute to discrepancies between acute GVHD and its associated clinical manifestations. The conditioning regimens range from high-dose myeloablative to reduced-intensity, depending on the patient. Most murine transplantation models use complete myeloablative regimens with one or two doses. The prognosis of animal models is affected by the radiation source, mouse strain sensitivity, and genetic

variations. Cesium-137 (radioactive) and X-rays (non-radioactive) are the most common radiation sources, with the latter being more effective in causing myeloablation. Mice are more resistant to radiation than humans, therefore, murine models may not accurately reflect clinical scenarios. Chemotherapeutic agents have rarely been used in mouse models[317–320].

In mice, acute GVHD severity depends on the cytokine storm, MHC-I mismatches, and microbiome composition. Mouse models usually add splenic T cells to grafts to induce acute GVHD. This is not the case in clinical settings. Thus, the graft composition in preclinical models may affect disease pathogenesis. Moreover, applying mouse model findings to human diseases is challenging because the immunosuppressive therapy administered to recipients to prevent acute GVHD is not used in preclinical settings[313,314]. Nevertheless, murine models enable researchers to carefully dissect the mechanism(s) of acute GVHD pathogenesis and make optimal interpretations of results, owing to the fact that these mouse models provide a critical experimental advantage, allowing selective manipulation and evaluation of individual variables. Therefore, the appropriate choice and application of animal models are essential for ensuring the continued progress and translational application of findings in the field of HSCT (Table 31)[313,314].

Table 31: Species variability in hematopoietic stem cell transplantation

Particulars	Murine Model	Human
Prophylaxis	Rare	Immunosuppressive regimens e.g. tacrolimus or mycophenolate mofetil
Conditioning regimens	X-ray: irradiation with single lethal dose / 2 or 3 split doses	Based on patient status, consists of chemotherapy with or without irradiation. Usually with divided doses from lethal to non-myeloablative regimens
Genetic variability	Inbred: well-defined MHC molecules. May be discerned by MHC major or minor mismatch	Outbred: high diversity of MHC alleles thus increased disparity between donor and recipients. May have different degrees of haploidentical HSCT
Donor graft	Bone marrow and T cells are required to induce GVHD	Bone marrow cells as well as GCSF mobilized PBSCs or umbilical blood may also serve as sources of GVHD
Tumor systems	Transplantable, homogenous tumor cell lines. Few spontaneous tumors have been developed	Spontaneous heterogeneous tumors
Age	young mice (< 5 months old)	Mixed age groups - pediatric, adult, or elderly
Obesity	Mean weight is well maintained	Lean/obese patients
Gastrointestinal tract microbiome	More or less homogenous	Complex due to the diversity & heterogeneity
Housing environment	Pathogen-free	Complicated with several opportunistic infections
Type of GVHD	Either acute or chronic	Mixed

GVHD: graft versus host disease, HSCT: hematopoietic stem cell transplantation, MHC: major histocompatibility, PBScs: peripheral blood stem cells, GCSF: granulocyte colony stimulating factor adapted from[314]

Role of cytokines in acute GVHD

Cytokines are the third signal for T-cell activation, which regulate their differentiation and proliferation. Additionally, conditioning regimen related damage can cause the release of cytokines from recipient cells, such as epithelial and endothelial cells, which causes activation of the inflammatory response in these organs. Thus, cytokines play key roles in the initiation and pathogenesis of acute GVHD. In allo-HSCT settings, cytokines are released in response to two major stimuli: activation of toll-like receptors (TLRs) or activation of T cells upon engagement with APCs. Here, we discuss the cytokines produced

by pre-transplant conditioning or T cells, and their role in GVHD pathogenesis. Conditioning regimens induce the release of DAMPs and PAMPs, causing the release of inflammatory cytokines, such as TNF, IL-1, IL-6, IL-33, IL-1, IL-12, IL-23, and type 1 IFN, by recipient cells. The roles of most cytokines are discussed below. Inflammatory signals induced by these cytokines are further exacerbated by the cytokines released by activated T helper cells. Activated T cells mainly differentiate into subsets and secrete specific cytokines. For example, Th1 cells secrete IL-2, IFNγ, and TNF, whereas Th2 cells secrete IL-4, IL-6, IL-10, and Th17 cells, which in turn secrete Th17 cytokines. Eventually, cytokines released by T cells govern the progression of acute GVHD. The role of these cytokines in the initiation and activation phases of GVHD is reviewed below[329–331].

Tumor necrosis factor (TNF): TNF is one of the major influencers of GVHD development after allo-HSCT. Pre-transplant TNF is mainly secreted by the recipient's myeloid cells due to the conditioning regimen[332], whereas, after transplantation, activated donor T cells contribute majorly to TNF levels[333,334]. Pre-transplant TNF-has been shown to affect GVHD severity in murine models. However, in clinics, the success of TNF inhibitors is limited because the administration of prophylactic regimens leads to lower levels of TNF in the recipient. Nonetheless, in murine models of GVHD, TNF levels were highly correlated with the incidence and severity of acute GVHD. TNF enhances proinflammatory responses, and the use of TNF inhibitors, such as etanercept, has shown promising results in alleviating severe GVHD in a phase 2 trial[335].

IL-1β, IL-18, and IL-12: Signaling through nod-like receptors (NLR) and the inflammasome pathway causes secretion of IL-1β, IL-18, and IL-12 by recipient cells after the conditioning regimen[336]. IL-1β, IL-18, and other IL-1 family cytokines, such as IL-33, promote secretion of the proinflammatory cytokine TNF. IL-12 is mainly secreted by DCs

and Langerhans's cells and drives the secretion of IL-18 and IFNγ. IL-18 is secreted by macrophages, dendritic cells (DCs), T lymphocytes, keratinocytes, and intestinal epithelial cells. IL-18, in concert with IL-12, drives Th1 differentiation of activated donor T cells, IFNγ production, and activation of cytotoxic T lymphocytes (CTLs), thus playing an important role in GVHD initiation[337,338].

IL-33: IL-33 is expressed by endothelial cells, epithelial cells, and fibroblast-like cells of various organs and is not a secretory cytokine; rather, it is released as alarmin upon damage to these cells. IL-33 binds to IL-1, Il-12 and IL-18, exacerbating GVHD by increasing TNF and IFNγ production by Th1 helper cells[339].

IFNγ: Th1 cytokines are predominantly produced by Th1, Tc1, B cells, NK cells, and APCs after allo-HSCT. IL-18 and IL-12 promote the secretion of IFNγ, whereas, IL-4, IL-10 and TGF-β inhibit IFN-γ secretion[329]. Preclinical studies have highlighted the contradictory pro-and anti-inflammatory roles of IFN-γ.[340–342] Donor-derived IFNγ signaling in the host parenchyma prevents inflammatory cell infiltration and lung GVHD in mice. In contrast, IFN-γ-mediated activation of IFNγR in the gut epithelial cells causes villi and crypt atrophy[340,343]. Moreover, in clinical practice, IFNγ polymorphisms have not been shown to correlate with GVHD incidence and outcome[344].

IL-2: It is the first cytokine produced by activated $CD4^+$ T cells, drives clonal T cell expansion and Treg differentiation, and promotes NK cell cytolytic activity[345]. In preclinical models, IL-2 inhibition showed a reduction in GVHD incidence and severity; however, it also affected Treg differentiation, thus showing both the positive and negative effects of IL-2 inhibition[346,347].

IL-4: It is predominantly secreted by $CD4^+$ T cells, mast cells, and basophils and promotes Th2 differentiation along with the secretion of other Th1 cytokines such as IL-5, IL-10, and IL-13. IL-4 is an antagonist of the Th1 response and a major Th2 response cytokine[348]. IL-4 shows a protective effect against GVHD development mainly by limiting the production of the Th1 cytokines IFNγ and TNF. However, it does not provide protection from GVHD, as demonstrated in preclinical models[349–351].

IL-6: is a proinflammatory cytokine that is mainly secreted by monocytes, macrophages, mature DC, T and B lymphocytes, and fibroblast cells. It promotes T cell differentiation into CTLs, secretion of proinflammatory IL-17 cytokines, and B cell differentiation into plasma cells.[352] Consistent with this, TGF-β inhibits Treg differentiation. Preclinical studies have shown that inhibition of IL-6 causes a reduction in GVHD severity while preserving the GVL effects of the graft. Phase II studies have shown that tocilizumab alleviates GVHD severity[353,354].

IL-17 and IL-23: IL-17 family of cytokines consists of six isoforms, IL-17A to IL-17F. Isoforms A and F have been the most studied with respect to GVHD. This family of cytokines is secreted by activated $CD4^+$ and $CD8^+$ T-cells[355]. In combination with IL-23, IL-17 promotes the differentiation of activated T cells into Th17 cells, which have been shown to exacerbate GVHD. In contrast, IL-17, IL-6, and TGF-β promoted immunomodulatory effects in the absence of IL-23. Moreover, IL-17A secreted by T cells in mucosal-associated lymphoid tissues protects against gut dysbiosis[356,357]. Therefore, IL-17A plays a protective role in acute GVHD, whereas Th17 cells have been shown to be pathogenic[358].

IL-10 is an immunosuppressive cytokine that affects the action of dendritic cells and macrophages, thus inhibiting T-cell activation. It is primarily secreted by T reg cells, and

some B cells, monocytes, and dendritic cells. IL-10 inhibits Th1 and Th17 mediated secretion of TNF-and IFNγ. Moreover, it promoted Treg proliferation and inhibited Th17 cell proliferation. Exogenous IL-10 has shown better GVHD outcomes in murine models; however, the effects of IL-10 are dose-dependent, and further studies are warranted for its clinical use[359–362].

Innate immune cells in pathogenesis and prevention of acute GVHD

T cell activation requires costimulatory signals from various antigen-presenting cells. Signaling through co-stimulation drives the fate of activated T cells, where it can promote T cell differentiation and proliferation, inhibit T cell differentiation, and promote activation induced cell death (AICD) in these cells[363]. CD28 and CTLA4 are two ligands expressed on T-cells. These ligands interact with CD80 and CD86, which are expressed by APCs. Engagement of CD28 with CD80 and CD86 promotes T cell proliferation; in contrast, engagement of CTLA4 with CD80 and CD86 causes activation-induced cell death of T cells. Therefore, the blockade of CD80 and CD86 on APCs has been shown to alleviate GVHD[364]. Abatacept, a CTLA4 IgG has shown promising results in the prevention of acute GVHD when used in combination with standard prophylaxis in clinics. Abatacept has recently gained FDA approval for GVHD prophylaxis and is the first FDA-approved drug for GVHD prophylaxis[365].

In addition to specific costimulatory signals that govern T cell response, certain innate immune cells have been reported to play an immune regulatory role, leading to the alleviation of GVHD. Induced natural killer cells, tolerogenic dendritic cells, myeloid-derived suppressor cells, and mesenchymal-derived stromal cells exhibit immunosuppressive activities, thus countering inflammation-mediated GVHD[366,367].

T cell subsets in pathogenesis and prevention of acute GVHD

Specific T-cell subsets have been shown to play a role in the prevention or pathogenesis of acute GVHD. Some of the important T cell subsets are discussed below.

Naive, central memory, and effector memory T cells: Naïve T cells (Tn) are $CD62L^{hi}CD44^{lo}$, central memory cells (Tcm) are $CD62L^{hi}CD44^{hi}$, and effector memory cells (Tem) are $CD62^{lo}CD44^{hi}$. Preclinical data suggest that naïve T cells are more potent inducers of GVHD than are central or effector memory cells. Moreover, $CD8^{+}$ Tn cells are particularly sensitive to miHA mismatch and are primarily involved in the pathogenesis of GVHD in matched murine models of allo-HSCT. Memory T cells have been shown to retain GVL activity of grafts[368–373].

Th1 and Tc1 subsets: This subset of T cells is known to secrete the Th1 proinflammatory cytokines IFNγ and TNF, which have been implicated in GVHD pathogenesis. Th1/Tc1 cells are mediators of gut tissue damage and cause high cytotoxicity in this particular tissue, thereby exacerbating GVHD[374,375].

Th17 and Tc17 subsets: These cells show proinflammatory activity and are associated with poor outcomes in patients with GVHD. Clinical studies have reported a higher frequency of Th17 cells in patients with acute GVHD. The number of Th17 cells increases with the progression of acute GVHD, and in the later stages, it drives inflammation by mediating a cytokine storm, potentiating alloreactive T cells, and supporting follicular T helper cells. Moreover, an increase in Th17 cells has been implicated in chronic and steroid-refractory GVHD[374,376].

Th2 and Tc2 subsets: This T cell subset produces Th2 cytokines IL-4, IL-5, IL-10, and IL-13. Preclinical studies have shown that adoptive transfer of Th2/Tc2 induces less severe

GVHD than the Th1/Tc1 subtype of T cells. Their protective effects can be attributed to the secretion of the anti-inflammatory cytokine IL-10. Moreover, these cells showed protection against gut damage in a preclinical GVHD model[377,378].

Treg subset: This subset is characterized by the expression of CD25 and the transcription factor FoxP3. As the name suggests, this particular subset has immunoregulatory action and has been shown to alleviate GVHD when transferred adaptively in preclinical modes. The GVHD preventive effect of these cells can be attributed to their secretion of anti-inflammatory cytokine IL-10. Moreover, these cells compete with naïve T cells for engagement with APCs, causing a reduction in the activation of naïve T cells and thus inhibiting immune responses. Trials are ongoing on the adoptive transfer of Treg cells for the treatment of acute GVHD[379,380].

7.6 METHODOLOGY

Induction of acute GVHD: A murine model of allo-HSCT based on complete MHC-I mismatch [recipient- female BALB/cJ mice (H-2kD) and donor-male C57BL/6J mice (H-2kB)] was utilized. Female BALB/cJ mice (8–10 weeks old) were acclimatized to individually ventilated cages (IVC) for 1 week before transplantation and maintained in IVC cages until completion of the experiment. Mice were irradiated with a sublethal dose of 6.5 Gy on a linear accelerator. After 24 h, mice were injected with 5×10^6 bone marrow cells and 15×10^6 splenocytes obtained from male C57BL/6 donor mice (8-10 weeks old). The overview of transplantation procedure is presented in Figure 59.

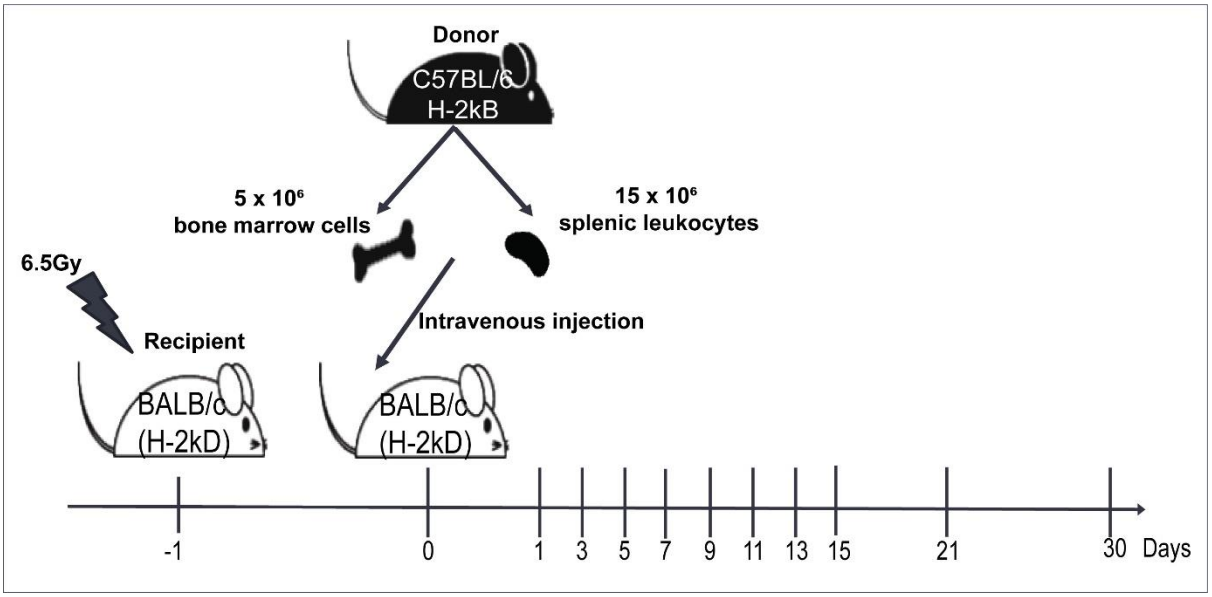

Figure 59: Workflow for transplantation procedure for induction of GVHD. The murine model is based on MHC class I mismatch, the recipient is BALB/c female mice that express H2kD MHC-I antigen, whereas the donor is C57BL/6 male mice that express H2kB MHC-I antigen. The days before transplantation are numbered with a negative sign, whereas the days after transplantation are numbered with a positive sign. Day of the transplantation is numbered as day 0.

Standardization of efficacious prophylactic oral dose of 5NQ: Briefly, transplanted mice were divided into seven groups (n = 6 per group): group I (vehicle control) received vehicle (5% DMSO in 0.5% CMC), whereas groups II, III, and IV received 1, 2.5, and 5 mg/kg 5NQ in vehicle, respectively, daily for 15 days after transplantation. Groups V, VI, and VII received 2.5, 5, and 10 mg/kg 5NQ in the vehicle, respectively, every alternate day for 15 days after transplantation. The first dose was given 24h after transplantation. Survival was monitored daily.

Evaluation of prophylactic efficacy of 5NQ: Transplanted mice were randomly divided into three groups (n = 12 /group): group I (vehicle control) received vehicle (5% DMSO in 0.5% CMC), whereas groups II and III received 2.5 and 5 mg/kg 5NQ in vehicle orally every alternate day for 15 d after transplantation. The first dose was given 24h after transplantation. Body weight was measured before irradiation and weekly after

transplantation along with clinical scoring of GVHD. The overview of the procedure of transplantation and dosing of 5NQ is presented in Figure 60.

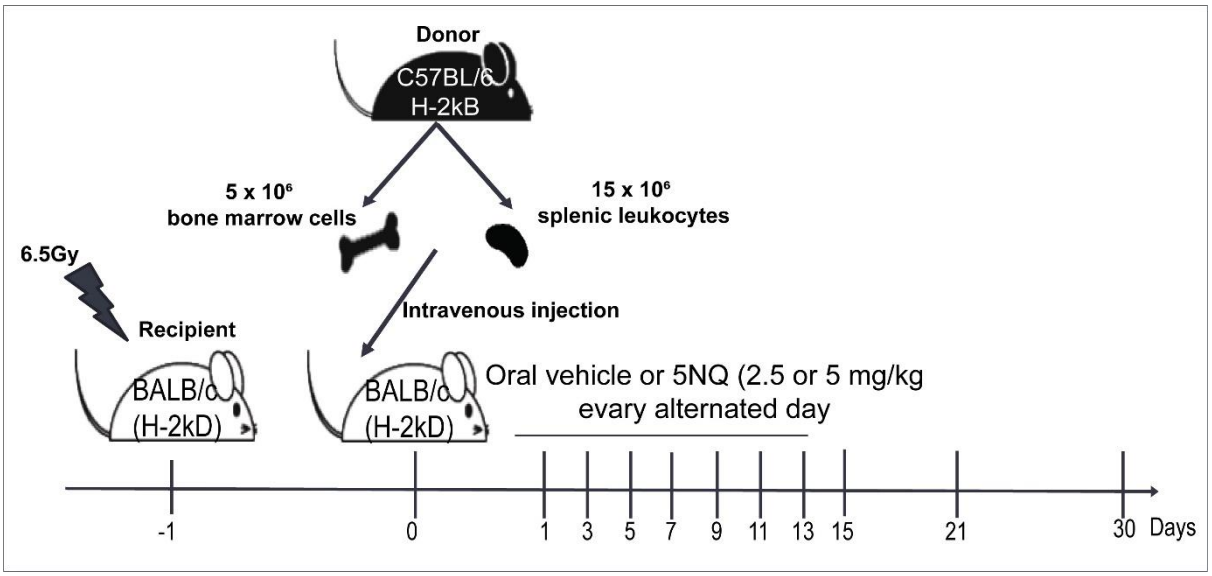

Figure 60: Procedure of transplantation and dosing schedule for 5NQ administration. Vehicle or 5NQ was administered orally every alternate day after transplantation starting from day 1 to day 15

Clinical scoring criteria: Mice were monitored weekly for 30 days after transplantation for signs of GVHD using a previously described scoring system[381]. Briefly, mice were scored based on five criteria: weight loss, posture (hunching), decreased activity, fur ruffling, and skin involvement, giving a total clinical score of 10. Mice were euthanized if a clinical score ≥8 was reached, or weight loss was ≥ 20%.

Comparison of 5NQ efficacy with standard prophylactic regimen of a combination of Cyclosporine (CSA) and Methotrexate (MTX): Recipient BALB/cJ mice were transplanted as described above and randomly divided into four groups (n = 6/group): Vehicle group (VC) received vehicle (5% DMSO in 0.5% CMC), whereas animals in 5NQ group (5NQ) received 5 mg/kg 5NQ in vehicle orally every alternate day for 15 days after transplantation, animals in CSA-MTX group were received intravenous injection of CSA-MTX (0.4 mg/kg/day CSA and 1.5 mg/kg/day MTX) on every alternative day from Day + 1 to Day +9 (a total of five doses) [382,383] ; animals in the CSA-MTX+5NQ group received

a combination of both CSA-MTX and oral 5 mg/kg 5NQ. The first dose was given 24h after transplantation. Body weight was measured before irradiation and weekly after transplantation along with clinical scoring of GVHD.

Evaluation of cytokines and host tissue damage: Mice were divided into two groups (n = 5/group): group I received vehicle and group II received 5 mg/kg 5NQ in vehicle every alternate day for 15 d after transplantation. Serum cytokine levels, host tissue damage, and innate and adaptive donor cell milieu were evaluated 15 d after transplantation. To estimate serum cytokine levels, blood from each mouse was collected into microcentrifuge tubes by puncturing the orbital plexus. Blood was allowed to clot for 1 h at 4 °C and the tubes were centrifuged at 600xg for 10 min. The serum was separated and stored at -80 °C until further analysis. Serum cytokine levels were measured using the BD™ Cytometric Bead Array kit as described previously. For histological analysis, the mice were euthanized after blood collection by CO_2 inhalation, and the liver, spleen, intestine, and abdominal skin were dissected and fixed in buffered formalin. Tissue sections (5µm) were de-paraffinized with xylene and rehydrated with graded ethanol. The sections were stained with hematoxylin and eosin (H&E). To evaluate GVHD-associated tissue damage, tissue sections were screened and scored using a semi-quantitative scoring system by two independent pathologists who were blinded to the treatment received by each animal. Specific parameters scored for the intestines include, villous blunting, crypt regeneration, crypt epithelial cell apoptosis, luminal sloughing of cellular debris, lamina propria inflammatory cell infiltration, and mucosal ulceration[384]. The parameters scored for liver tissue included portal tract expansion by inflammatory cell infiltration, lymphocyte infiltration of bile ducts, bile duct epithelial cell apoptosis, bile duct epithelial cell sloughing, vascular endotheliosis, parenchymal apoptosis, parenchymal micro abscesses, parenchymal mitotic figures, hepatocellular cholestasis, and steatosis[384]. A minimum of 20 high-power fields

and 3 portal tracts were evaluated per tissue section. Specific parameters scored for skin tissue included leukocyte infiltration, epidermal thickening, basal epithelial cell apoptosis, dermal subcutaneous boundary separation[385].The scoring system for each parameter evaluates both the extent and severity of tissue damage, denoted as 0, normal; 0.5, focal and mild, 1 as focal and moderate; and 2, diffuse and severe. The average of these two scores was calculated for each specimen.

Engraftment analysis: Mice were divided into two groups (n = 5/group): group I received vehicle and group II received 5 mg/kg 5NQ in vehicle every alternate day for 15 d after transplantation. Donor cell engraftment was ascertained in the peripheral blood of recipient mice 15 d after transplantation. Blood from each mouse was collected in microcentrifuge tubes (containing the anticoagulant EDTA) by puncturing the orbital plexus. RBC lysis was performed using 2 ml of 1X ammonium chloride buffer (155 mM NH4Cl, 12 mM NaHCO3, 0.1 mM EDTA). The tubes were incubated for 10 min at room temperature. Cells ere centrifuged at 1200 g for 2 min. Cell pellet was resuspended in FACS buffer and were stained using fluorochrome-tagged primary antibodies against the MHC-I antigens H-2Kd PE (SF1-1.1), H-2Kb FITC (AF6-88.5) as described in the materials and methods section.

Evaluation of hematopoietic stem cell recovery: BALB/c Mice were irradiated and transplanted as described previously. Mice were divided into two groups (n = 5/group): group I received vehicle and group II received 5 mg/kg 5NQ in vehicle every alternate day for 15 d after transplantation. Hematopoietic stem cell recovery was ascertained in the bone marrow of recipient mice 15 d after transplantation. The mice were euthanized, and the femurs were collected. Femurs were flushed with RPMI1640 medium using a 24 G needle and a 5 ml syringe and a single-cell suspension was prepared using a 70µM cell strainer. The cells were centrifuged at 1200 × g for 5 min and RBC lysis was carried out as described above. The pellet was resuspended in blocking buffer. Leukocytes were stained and

acquired using a flow cytometer as previously described. Cells were stained with the following antibodies to quantify the percentage of HSCs: mouse hematopoietic lineage antigen (Lin) cocktail Pacific blue [CD3 (17A2), Ly-6G/Ly-6C (RB6-8C5), CD11b (M1/70), CD45R/B220 (RA3-6B2), TER-119/Erythroid cells (Ter-119)], Ly-6A/E (Sca-1) FITC (W18174A), and CD117 (c-Kit) (2B8). Lin-CD45 + Sca-1 + c-KIT + cells were quantified.

***In vivo* immune cell phenotyping:** Effect of oral administration of 5NQ was evaluated on activation of APCs, $CD4^+$ and $CD8^+$ T cells, number of $CD4^+$ and $CD8^+$ T naïve (Tn), central (Tcm) and effector memory cells (Tem), expression of CTLA4 (T cell anergy marker) and number of Treg cells. For immune cell phenotyping, transplanted mice were divided into two groups (n = 5/group): group I received vehicle and group II received 5 mg/kg 5NQ in vehicle every alternate day for 15 d after transplantation. Mice were euthanized 15 days after transplantation, the spleen was dissected, and a single-cell suspension was prepared as described previously. Leukocytes were stained and acquired using a flow cytometer as previously described. Following markers and fluorochrome conjugated antibodies were used for immune cell phenotyping (Table 32).

***Ex vivo* mixed lymphocyte reaction (MLR):** Ex vivo MLR was performed to evaluate the effect of oral administration of 5NQ on lymphocyte proliferation against allogeneic stimulation. Healthy C57BL/6 mice were orally administered either vehicle or 5 mg/kg 5NQ every alternate day for 15 days. The mice were euthanized, and splenic leukocytes were isolated as described previously. Leukocytes from BALB/c mice were mixed in a ratio of 1:10 (stimulator: responders) and incubated under standard cell culture conditions for 72 h. The cells were harvested and stained with an anti-H2k-B FITC antibody for 30 min at room temperature. Cells were fixed and permeabilized as previously described and stained with anti-Ki67 antibody, followed by secondary antibody staining with Alexa Fluor 568.

The cells were acquired using a flow cytometer. Because only responder cells expressed H2k-B MHC-I, the expression of Ki67 in these cells was quantified to assess their proliferation in response to allogeneic stimulation.

Table 32: Fluorochrome-conjugated antibodies used for *in vivo* immune phenotyping study

Cell type	Markers	Antibody and fluorochrome
Activated Dendritic cells	$CD45^+$ $CD3^-$ $CD11b^-$ $MHC\text{-}II^+$	CD45-PE-Cy7, CD3ε-APC-Cy7, CD11b-FITC, IA/IE-PE.
Activated $CD4^+$ T-cells	$CD4^+$ $CD25^+$	CD4 PerCP-Cy5.5, CD25 BV421
Activated $CD8^+$ T-cells	$CD8^+$ $CD25^+$	CD8α FITC; CD25 BV421
CD4+ and CD8+ T naïve, central memory and effector memory cells	Tn: $CD4^+/CD8^+$ $CD62L^{hi}$ $CD44^{lo}$; Tcm: $CD4^+/CD8^+$ $CD62L^{hi}$ $CD44^{hi}$;Tem: $CD4^+/CD8^+$ $CD62L^{lo}$ $CD44^{hi}$	CD4 PerCP-Cy5.5, CD8α FITC, CD44 APC-Cy7, CD62L APC.
Anergic/Exhausted $CD4^+$ and $CD8^+$ T cells	$CD4^+$ $CD25^+$ $CD152^+$ $CD8^+$ $CD25^+$ $CD152^+$	CD4 PerCP-Cy5.5; CD8α FITC; CD25 BV421, CD152 PE
Cytotoxic $CD8^+$ T cells	$CD3e^+$ $CD8^+$ granzyme B^+	CD3ε PE-Cy7, CD8α APC; Granzyme B FITC
Hematopoietic stem cells	Lin^- $CD45^+$ $cKIT^+$ $Sca1^+$	Mouse hematopoietic lineage antigens (Lin) cocktail pacific blue [CD3 (17A2), Ly-6G/Ly-6C (RB6-8C5), CD11b (M1/70), CD45R/B220 (RA3-6B2), TER-119/Erythroid cells (Ter-119)], CD117 (c-KIT) APC, Ly-6A/E (Sca-1) FITC, CD45 PE-Cy7

***Ex vivo* proliferation of leukocytes:** To evaluate the effect of oral administration of 5NQ on leukocyte proliferation in response to mitogen Con A stimulation. Healthy C57BL/6 mice were orally administered either vehicle or 5 mg/kg 5NQ every alternate day for 15 days. The mice were euthanized, and splenic leukocytes were isolated as described previously. Leukocytes were stained with CFSE and stimulated with Con A (2.5 µg/ml) and incubated for 72 h. Proliferation of leucocytes was evaluated by CFSE dye dilution assay.

Ex vivo anti-tumor activity: was performed to evaluate the effect of oral administration of 5NQ on anti-tumor activity of leukocytes. Briefly, healthy C57BL/6 and BALB/c mice were orally administered either vehicle or 5 mg/kg 5NQ every alternate day for 15 days.

The mice were euthanized, and splenic leukocytes were isolated as described previously. Leukocytes were incubated with CFSE labelled syngeneic tumor cells (BALB/c with A20 and C57BL/6 with EL4) in the ratio 1: 10 (tumor cells: leucocytes). To compensate for cell death due to nutritional stress caused by high seeding density, CFSE labelled A20 and EL4 cells were seeded at the same density as in the mixed lymphocyte group and served as a control. After 24 h, the cells were harvested and stained with propidium iodide immediately before analysis on a flow cytometer. Propidium iodide staining was used to distinguish between live tumor cells (positive for CFSE only) and dead tumor cells (positive for both CFSE and PI; similar to protocol described in objective 1).

7.7 RESULTS

Prophylactic efficacy of oral administration of 5NQ in murine model of allo-HSCT

To evaluate the prophylactic efficacy of 5NQ, a dose standardization experiment was conducted to identify the dosage of 5NQ that provided a survival benefit to transplanted mice. We found that oral administration of 2.5 mg/kg and 5 mg/kg every alternate day for 15 days post transplantation significantly improved the survival of these mice (Figure 61). We further validated these doses in a larger cohort of animals and found that mice orally administered 2.5 mg/kg and 5 mg/kg 5NQ showed a significant increase in survival compared to mice treated with vehicle (Figure 62B). The median survival remained undefined for mice administered 5 mg/kg 5NQ, while the median survival for mice administered 2.5 mg/kg 5NQ was 30 days, which was significantly more than 16.5 days of mice administered the vehicle. Mice administered 5 mg/kg and 2.5 mg/kg 5NQ post transplantation showed improved GVHD-associated weight loss (Figure 62C) and mitigated the clinical signs of GVHD as compared to vehicle-treated mice (Figure 62C -

E). Next, we compared the prophylactic efficacy of oral 5NQ with the standard prophylactic regimen of CSA-MTX alone or in combination with CSA-MTX. We observed that oral administration of 5 mg/kg 5NQ improved the overall survival of mice compared with mice treated with the vehicle or CSA-MTX regimen. The median survival remained undefined for mice administered 5 mg/kg 5NQ, while the median survival for mice administered vehicle was 14.5 days and that of CSA-MTX was 21 days. Mice administered with combination of 5NQ and CSA-MTX presented with a median survival of 14 days, with significant reduction in body weight in first 7 days, thus showing probable toxicity of combined treatment (Figure 62F-G).

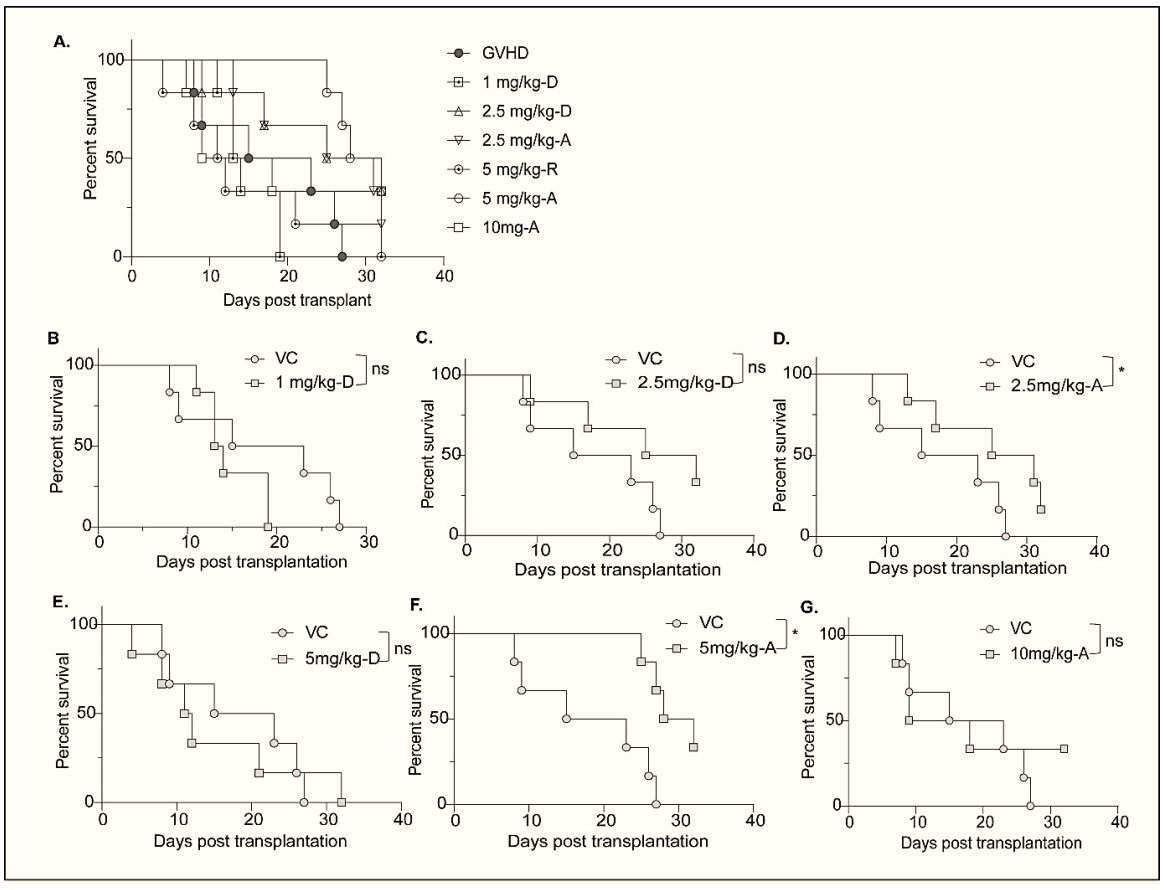

Figure 61: Standardization of oral efficacious dose of 5NQ. Recipient mice were treated with either vehicle (VC, 5% DMSO in 0.5% CMC) or 1, 2.5, 5, or 10 mg/kg 5NQ in vehicle daily (hyphenated as D) or every alternate day (hyphenated as A) from days 1 to 15 (n = 6/group). Mice were monitored for 30 days. (A-G) Survival of transplanted mice treated orally with VC or 5NQ. The Mantel-Cox log-rank test was used to compare survival between the VC and 5NQ treated groups.

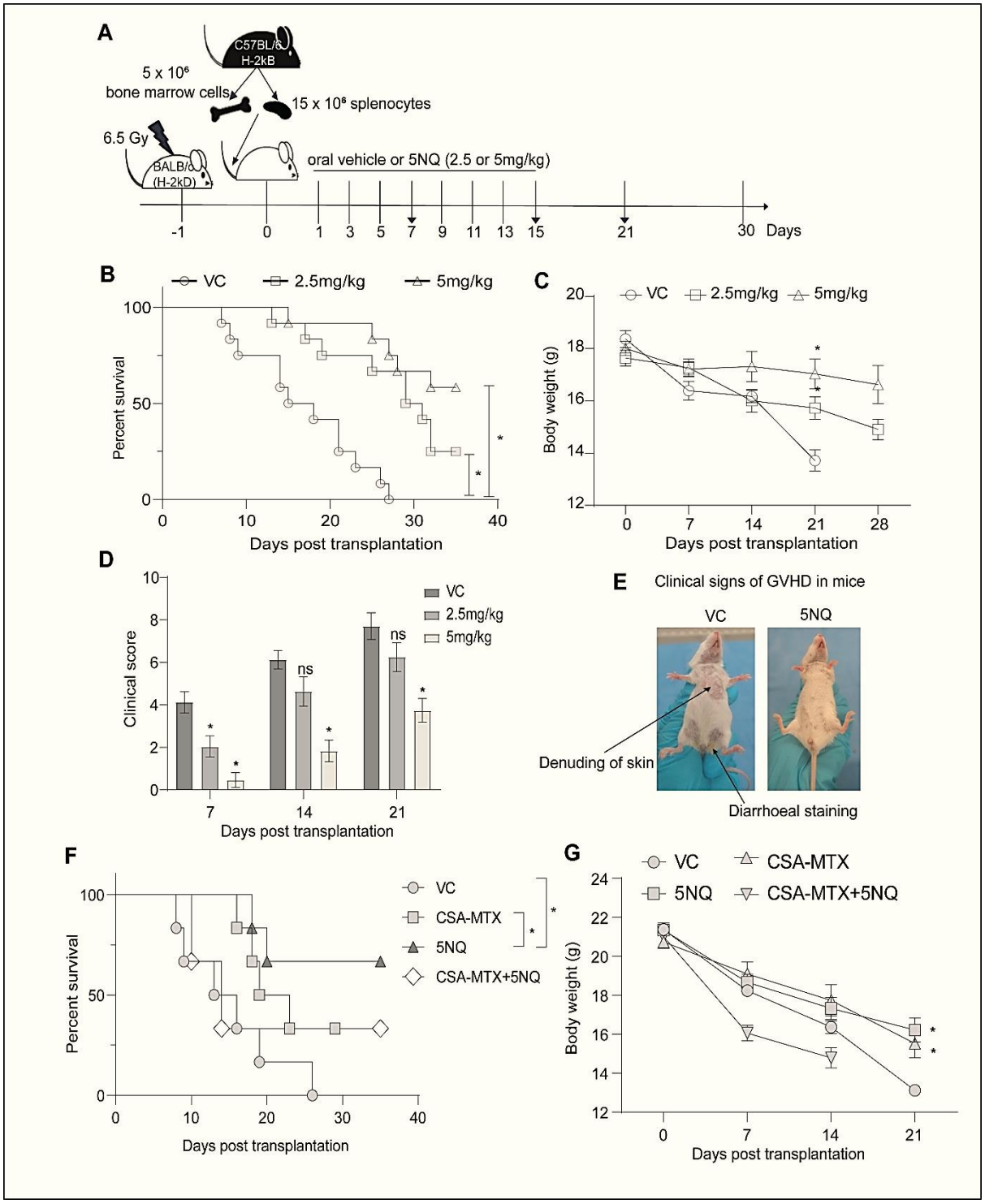

Figure 62: GVHD prophylactic efficacy of oral 5NQ in murine model of allo-HSCT. (A) Overall scheme for allo-HSCT and treatment with 5NQ. Briefly, BALB/c mice received total body irradiation at a dose of 6.5Gy on day -1, followed by transplantation with bone marrow and splenocytes on day 0. Recipient mice were orally administered either vehicle (VC, 0.01% DMSO in 0.5% CMC) or 2.5 mg/kg body weight, or 5 mg/kg body weight 5NQ in vehicle every alternate day from day 1 to day 15 (n = 12 mice/group). Mice were monitored for 30 days. (B) Survival of transplanted mice orally treated with VC or 5NQ. Mantel-Cox log-rank test was used to compare survival between the VC and 5NQ treated groups. (C) Weekly body weights of transplanted mice

(mean ± SEM). (D) Weekly clinical scores of transplanted mice (mean ± SEM). Data were analyzed using Two-way ANOVA with Bonferroni correction to compare time-dependent differences between VC and 5NQ treated groups, *p<0.05, compared to VC treated mice (E) Representative images of mice administered VC or 5NQ. (F) Survival of transplanted mice treated orally with VC or 5NQ or CSA-MTX or a combination of CSA-MTX + 5NQ (n = 6 mice/group). Mantel-Cox log-rank test was used to compare survival between the VC and 5NQ or CSA-MTX and 5NQ treated groups. (G) Weekly body weight of transplanted mice and treated with VC or 5NQ or CSA-MTX or a combination of CSA-MTX + 5NQ (mean ± SEM). Data were analyzed using Two-way ANOVA with Bonferroni correction to compare time dependent differences between VC and 5NQ treated or CSA-MTX and 5NQ groups, *p<0.05.

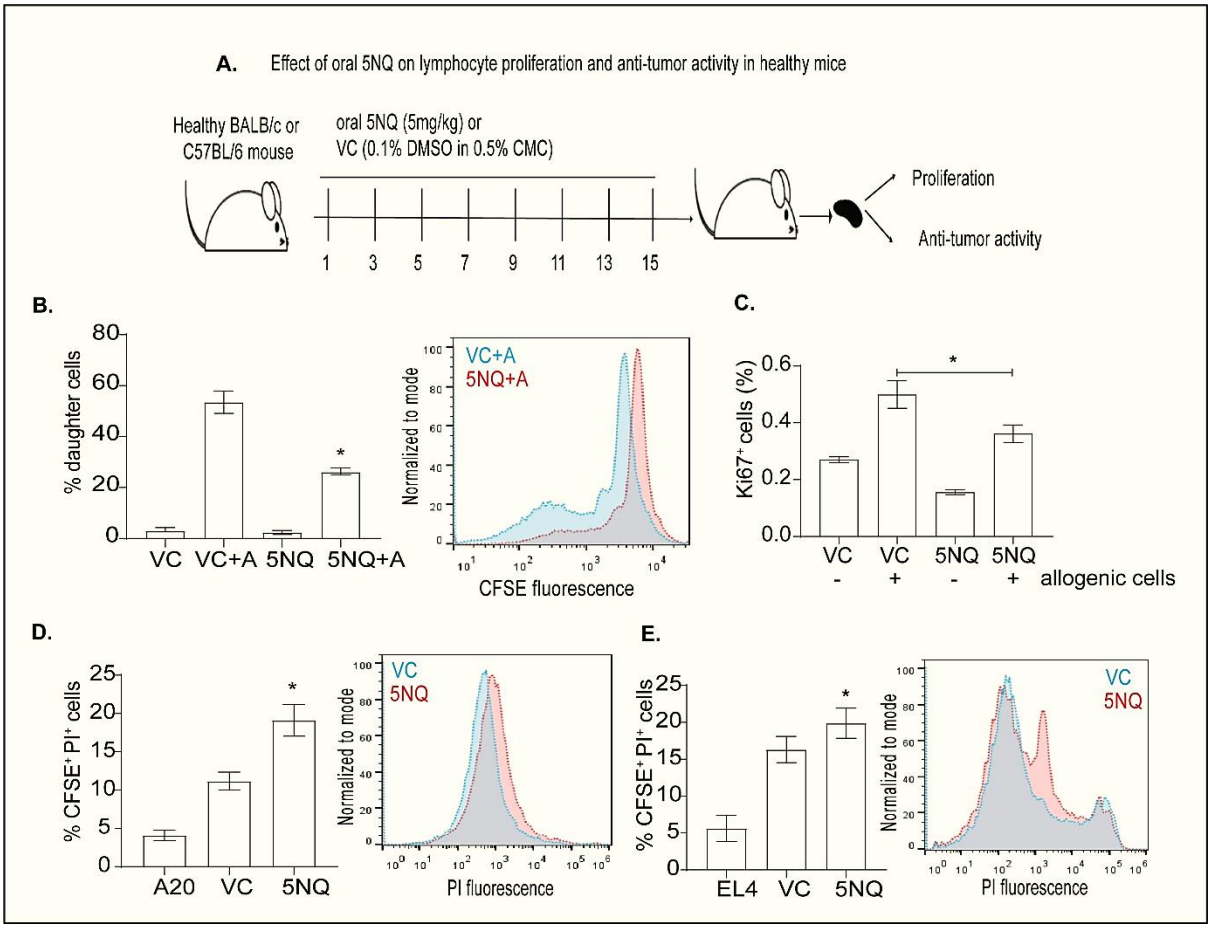

Figure 63: (A) Overall scheme for healthy mice administered 5NQ, followed by ex vivo evaluation of lymphocyte proliferation, alloreactivity and antitumor activity. Briefly, healthy BALB/c mice or C57BL/6 mice (n = 5/group) were orally administered vehicle or 5 mg/kg body weight 5NQ every alternate day for 15 d. Mice were sacrificed 24 h after the last dose. Leukocytes were isolated and stimulated ex vivo with Con A (effect on proliferation), A20, or EL4 leukemia cells (effect on antitumor activity) or allogeneic cells. (B) Ex vivo lymphocyte proliferation. Bar graph shows the percentage of daughter cells after 72 h of Con A stimulation, calculated using the CFSE dye dilution assay (n = 5 independent experiments; mean ± SEM). Data were analyzed using unpaired t-test to compare differences between VC and 5NQ treated groups; *p<0.05, compared to VC treated mice. (C) Bar graph showing H2k-B$^+$ Ki67$^+$ cells after 72 h of allogeneic stimulation of leukocytes from either VC or 5NQ orally treated mice (n = 5 independent experiments). (D-E) Viability of CFSE labelled A20 and EL4 leukemia cells after 24 h incubation with leukocytes from vehicle or 5NQ

administered healthy BALB/c mice, as assessed using propidium iodide assay (n = 5 independent experiments; mean ± SEM). Data were analyzed using one-way ANOVA with Bonferroni correction for multiple comparisons; *p<0.05, compared to the tumor-only group (A20 or EL4).

Immunosuppressive action of 5NQ in healthy mice: We ascertained the immunosuppressive effect of oral administration of 5NQ in healthy donor mice. Oral administration of 5NQ suppressed the proliferation of leukocytes ex vivo compared with that of leukocytes from their vehicle-treated counterparts (Figure 63B).

Effect of oral 5NQ on allo-reactivity of leukocytes from healthy mice: Oral administration of 5NQ suppressed proliferation of leukocytes in response to allogenic stimulation in *ex vivo* MLR assay, as indicated by decrease in the expression of proliferation marker Ki67 (Figure 63C).

Effect of oral 5NQ on ex vivo anti-tumor activity: Leukocytes from oral 5NQ treated mice retained their anticancer activity against syngeneic A20 and EL4 cell lines *ex vivo* (Figure 63D-E).

Oral administration of 5NQ alleviated GVHD in recipient mice via immunomodulation of innate and adaptive donor immune cell responses: Evaluation of serum cytokines at day 14 post transplantation (Figure 64A-G) showed a decrease in IFN-γ (Figure 64D) and TNF (Figure 64E) levels and an increase in serum concentrations of IL-10 (Figure 64F), and IL-17A (Figure 64G) cytokines in recipient mice treated with 5 mg/kg 5NQ orally compared to vehicle treated mice.

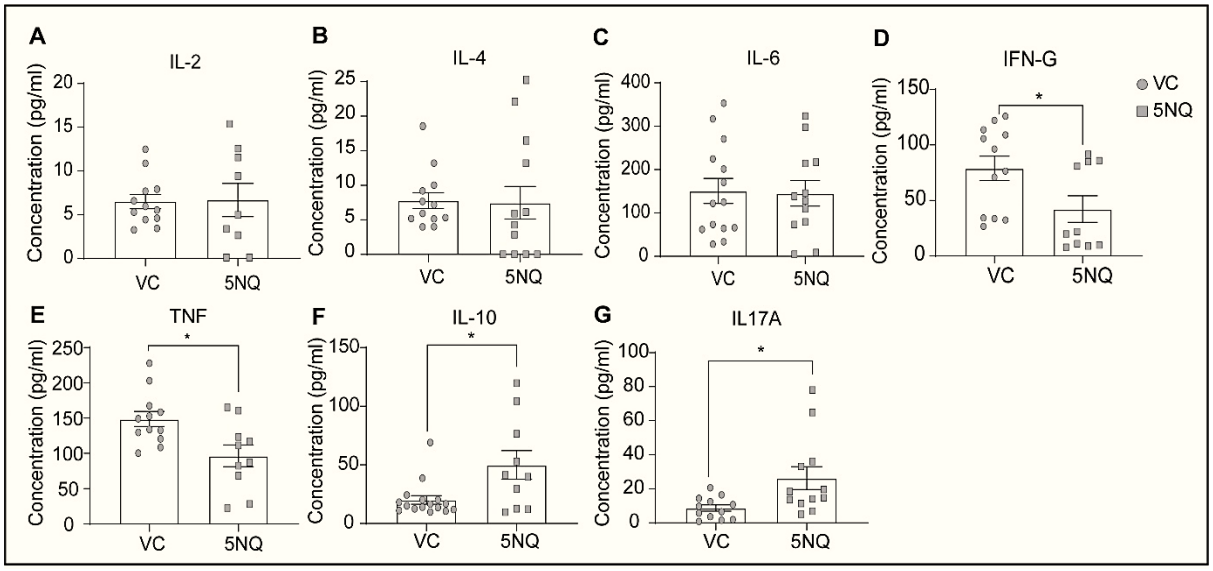

Figure 64: Oral administration of 5NQ suppressed cytokine storm in vivo. (A-G) Concentrations of serum cytokines in vehicle or 5NQ (5 mg/kg) administered mice at day 15 after transplantation (n = 10/group, mean ± SEM). Data were compared using Mann-Whitney test; *p<0.05, compared to VC treated mice.

Additionally, oral administration of 5 mg/kg 5NQ to recipient mice caused a decrease in CD11b^{-}MHC-II^{+} splenic dendritic cell counts (DCs) compared with vehicle-treated mice (Figure 65A) as well as a decrease in MHC-II expression in splenic dendritic cells (Figure 65B).

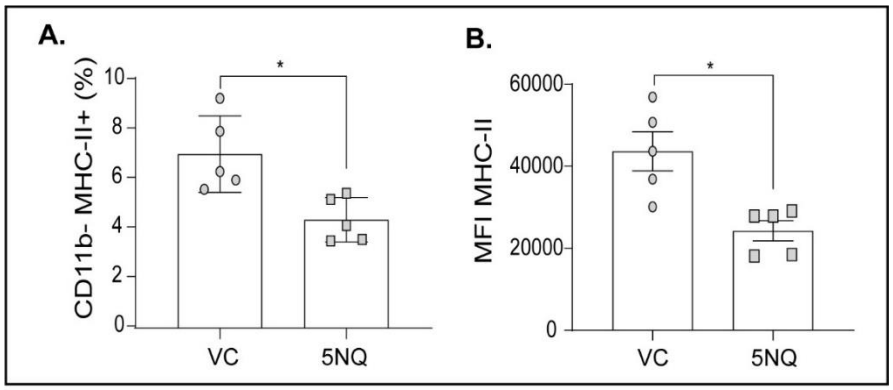

Figure 65: Effect of 5NQ on activation of antigen presenting cells. (A) Quantification of CD11b-MHC-II^{+} classical DCs and (B) flow cytometric analysis of MHC-II expression on CD11b- classical dendritic cells (cDCs) in the spleen of VC and 5NQ treated animals (n = 5/group). Data were compared using an unpaired t-test; *p<0.05.

Furthermore, oral administration of 5NQ decreased the CD4/CD8 ratio in splenic lymphocytes of recipient mice (Figure 66A), that is, there was a significant decrease in $CD4^+$ T cell counts in lymphocytes (Figure 66B) compared to that in vehicle-treated mice.

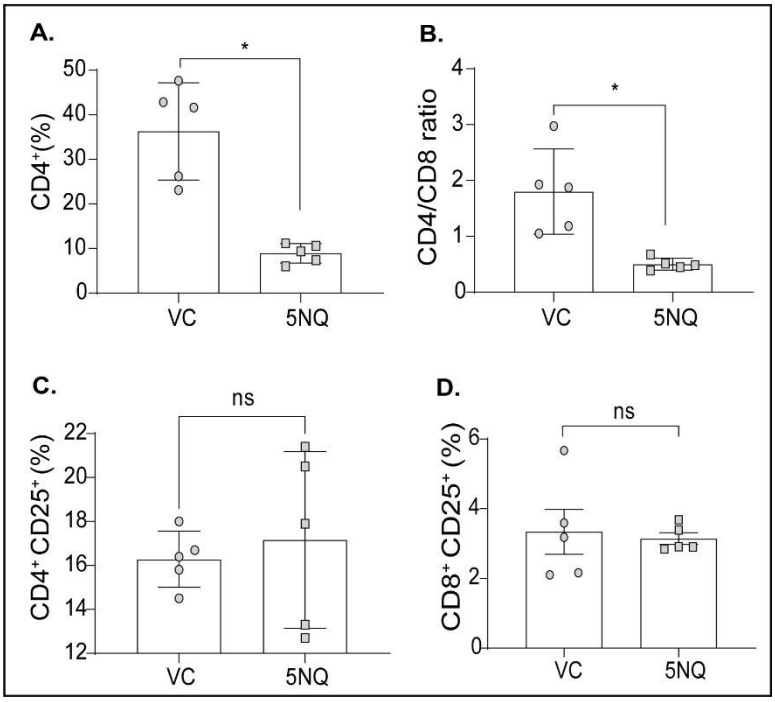

Figure 66: Effect of oral administration of 5NQ on CD4/CD8 ratio and activation of $CD4^+$ and $CD8^+$ T cells. (A) Bar graph of the percentage of $CD4^+$ cells in the spleen of VC and 5NQ treated animals, quantified using flow cytometry. (B) The Ratio of $CD4^+$ and $CD8^+$ cells in the spleen of VC and 5NQ administered animals, quantified using flow cytometry (n = 5/group)

We further observed that $CD4^+CD25^+$ activated T cells showed an increase in the surface expression of CD152 (CTLA4), indicating an increase in the $CD4^+CD25^+CD152^+$ exhausted/anergic T-cell subset in the lymphocytes of recipient mice treated with 5 mg/kg 5NQ orally, compared to vehicle-treated mice (Figure 67 A-C).

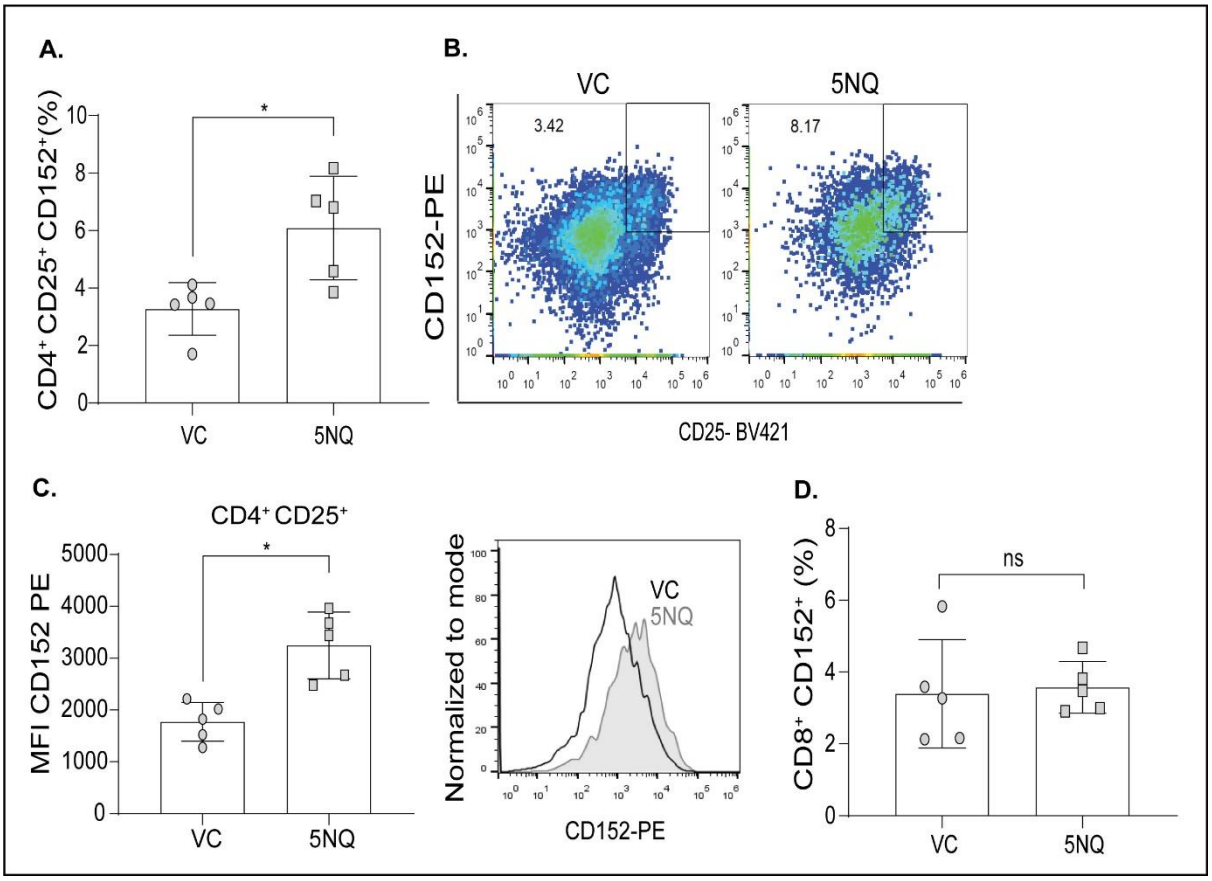

Figure 67: Multi-parameter flow cytometric analysis of leukocytes from the spleen of VC and 5NQ administered mice (n = 5/group). (A-B) $CD4^+$ cells were gated based on expression of CD25 and CD152 (CTLA4), to identify anergic/exhausted $CD4^+$ T cells. Bar graphs represent percentage of $CD4^+CD25^+CD152^+$ cells and (C) median fluorescence intensity (MFI) of PE labelled anti-CD152 antibody. (D) Bar graphs represent the percentages of $CD8^+$ $CD152^+$ cells.

Additionally, oral administration of 5NQ led to an increase in $CD4^+CD62^{hi}CD44^{hi}$ central memory T cells and $CD4^+CD62^{lo}CD44^{hi}$ effector memory T cells and a decrease in $CD4^+CD62^{hi}CD44^{lo}$ mature naïve T cells in the lymphocytes of these mice (Figure 68A). Oral administration of 5 mg/kg 5NQ also caused significant changes in CD8 T-cell subsets, and we observed an increase in $CD8^+CD62^{hi}CD44^{hi}$ central memory T cells in 5NQ treated mice (Figure 68B). However, no significant change was observed in the counts of $CD8^+CD62^{lo}CD44^{hi}$ effector memory cells and $CD8^+CD62^{hi}CD44^{lo}$ mature naïve $CD8^+$ T cells in 5NQ treated mice as compared to those in vehicle-treated mice (Figure 68B). Furthermore, granzyme B expression in $CD8^+$ T cells was evaluated to assess the cytotoxic

potential of these cells in vehicle and 5NQ treated animals. Oral administration of 5NQ significantly reduced the expression of granzyme B in $CD8^+$ T cells compared with that in vehicle-treated mice (Figure 69A). Additionally, there was no difference in the expression of CD152 on $CD8^+$ cells between vehicle and 5NQ treated mice (Figure 67D). Lastly, we did not observe significant differences in the activation of CD4 and CD8 T cells and in the lymphocytes of 5NQ treated mice as compared to those of vehicle-treated mice (Figure 66 C-D).

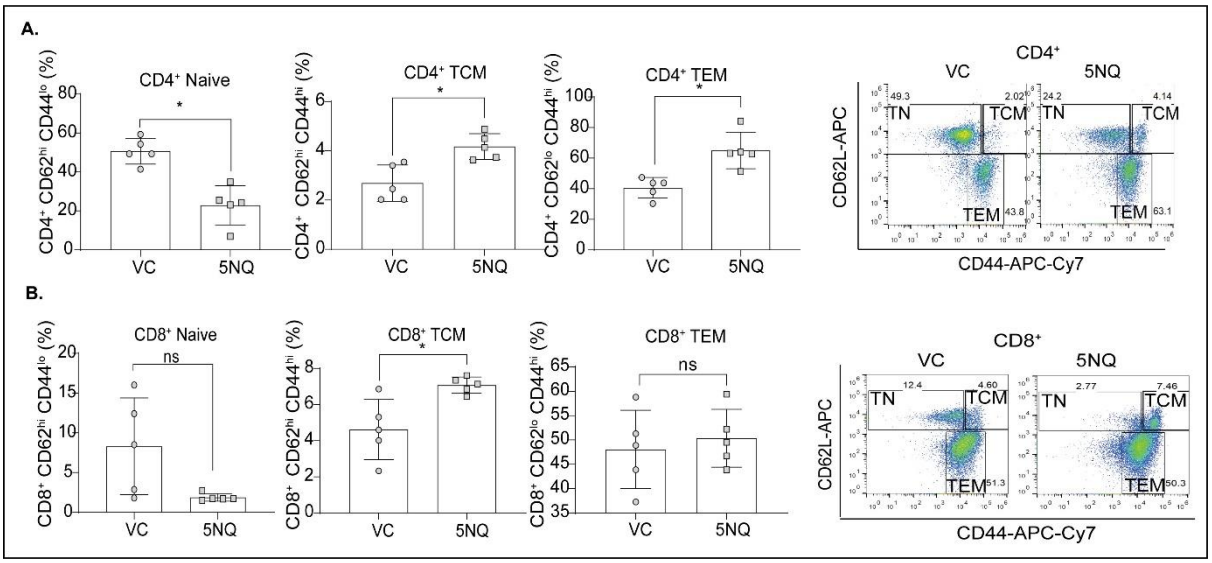

Figure 68: Multi-parameter flow cytometric analysis of leukocytes from the spleen of VC and 5NQ administered mice (n = 5/group). $CD4^+$ and $CD8^+$ T cells were gated based on expression of CD62L and CD44 to identify T naïve (TN), central memory (TCM) and effector memory cells (TEM). Bar graphs show the percentages of $CD4^+$ (A) and CD8+ (B) TN, TCM, and TEM cells. Flow cytograms represent expression of CD62L and CD44 on $CD4^+$ or $CD8^+$ T cells.

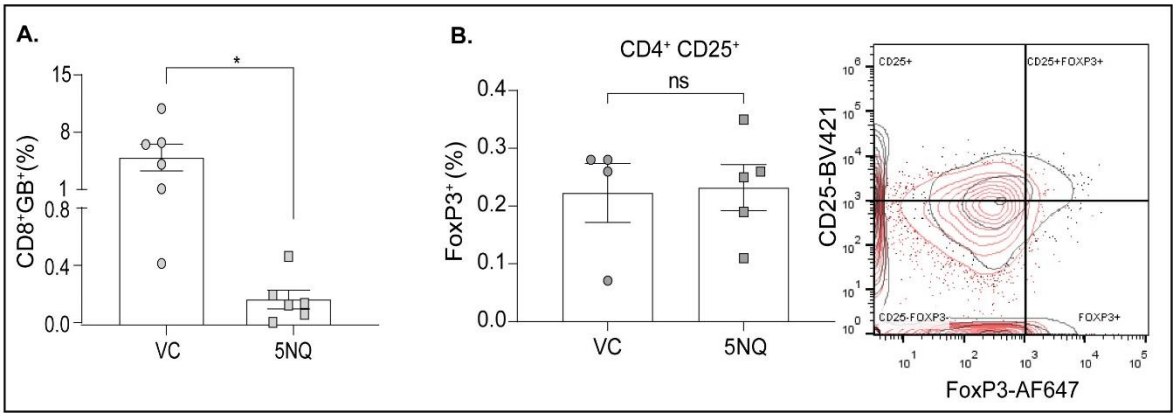

Figure 69: Multi-parameter flow cytometric analysis of leukocytes from the spleen of VC and 5NQ administered mice (n = 5/group). (A) Bar graph represent percentage of $CD8^{+}$granzyme B^{+} T cells. (B)Bar graph showing the percentage of Treg $CD4^{+}CD25^{+}$ $FoxP3^{+}$ cells in the spleens of VC and 5NQ treated animals (n = 5/ group), quantified using flow cytometry. Flow cytogram showing the expression of CD25 and FoxP3 in CD4+ T cells. Data were compared using unpaired t-test; *p<0.05, ns non-significant.

Additionally, no significant differences were observed in $CD4^{+}CD25^{hi}FoxP3^{+}$ T-regulatory (Treg) cells in the lymphocytes of 5NQ treated mice as compared to those of vehicle-treated mice (Figure 69B).

Oral administration of 5NQ did not alter donor chimerism and hematopoietic stem cell (HSC) counts: We evaluated donor chimerism in peripheral blood and assessed the counts of hematopoietic stem cells in bone marrow on day 14 after allo-HSCT in vehicle and 5NQ treated animals. Oral administration of 5NQ did not hamper the engraftment of donor cells, as evidenced by the presence of donor MHC-I ($H2\text{-}kB^{+}$) cells in the peripheral blood of the recipient mice (Figure 70A). Moreover, hematopoietic stem cell counts in 5NQ treated mice were comparable to those observed in healthy mice; however, vehicle-treated animals showed elevated numbers of HSCs compared to 5NQ treated animals, which can be attributed to acute inflammation and hematopoietic injury in these mice (Figure 70B).

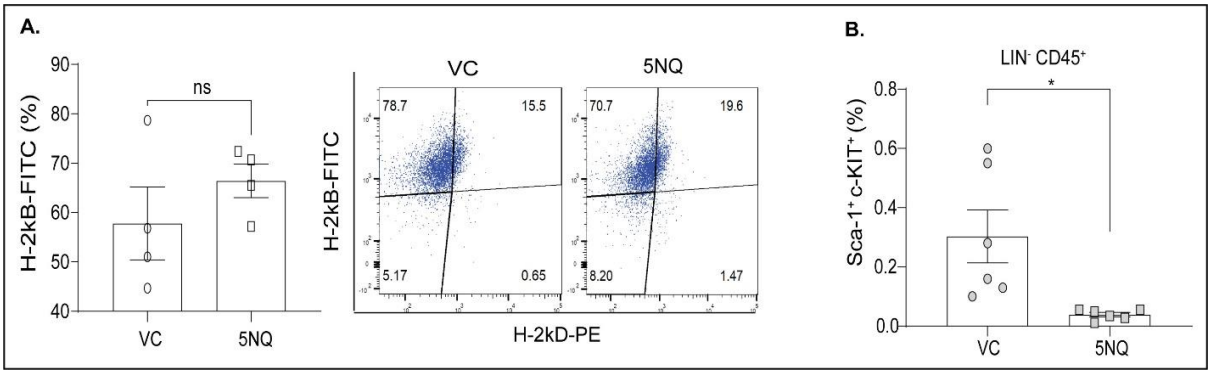

Figure 70: Engraftment analysis and hematopoietic recovery after oral 5NQ. (A)Engraftment of donor cells at day 15 was evaluated using the peripheral blood of transplanted mice (n = 5/group). Peripheral blood lymphocytes were stained using FITC labelled, donor specific anti-H2Kb antibody. Bar graph represents percentage of donor positive cells in peripheral blood of VC or 5NQ administered mice. Flow cytogram representing expression of H2Kb or H2Kd on peripheral blood lymphocytes. (B) Bar graph showing the percentage of hematopoietic stem cells (HSCs, Lin^{-} $CD45^{+}$ $Sca\text{-}1^{+}$ $c\text{-}KIT^{+}$) in the bone marrow of VC and 5NQ treated animals (n = 5/group), quantified using flow cytometry. Data were compared using an unpaired t-test; *$p<0.05$, ns non-significant.

Oral administration of 5NQ protected the recipient mice from GVHD-associated host tissue damage: The primary target organs of GVHD are the intestine, liver and skin; therefore, histopathological evaluation was performed after 15 d of 5NQ administration to determine the severity of GVHD-associated tissue damage in these tissues. Microscopic evaluation of the intestine resulted in a lower pathological score, with a reduction in mucosal ulceration and crypt loss in animals administered 5NQ compared with those treated with vehicle (Figure 71A-B). Microscopic evaluation of and skin tissue showed lower pathological score, with reduction in leukocyte infiltration in skin tissues of 5NQ treated animals compared to those treated with vehicle (Figure 71A and D). Microscopic evaluation of the liver showed no difference in the pathological scores between vehicle and 5NQ treated animals (Figure 71A and C).

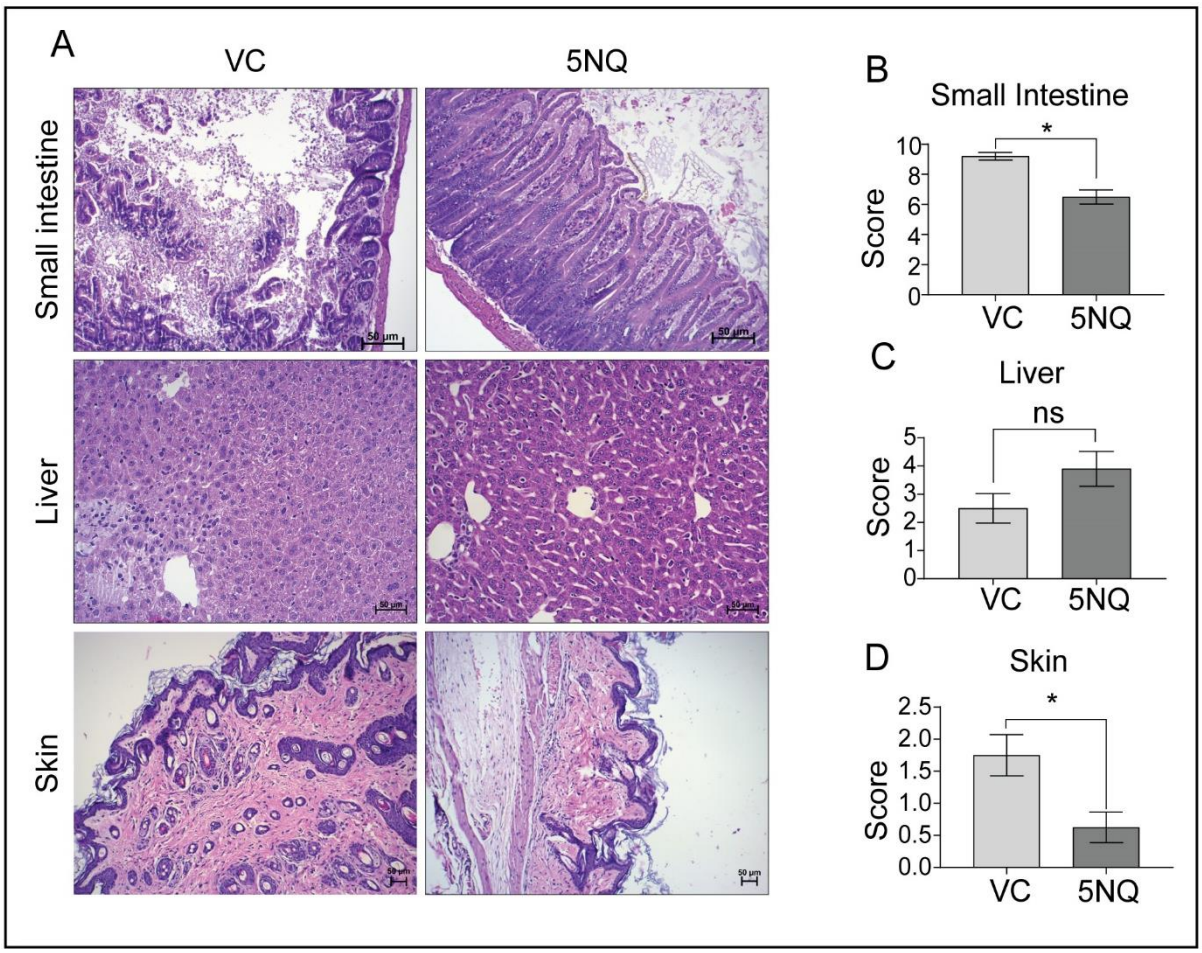

Figure 71: Administration of 5NQ protected against GVHD associated tissue damage. Transplanted mice were administered vehicle or 5NQ every alternate day for 15 d post transplantation. Mice were sacrificed 24 h after the last dose to collect tissues. (A) Representative micrographs of small intestine, liver and skin tissue sections stained with H&E. (B-D) Pathological scores of the small intestine (B), liver (C), and skin (D) tissue sections. Data were compared using an unpaired t-test; *$p<0.05$, ns non-significant.

7.8 DISCUSSION

Studies in objective 3 aimed at evaluating the prophylactic efficacy of oral administration of 5NQ in a murine model of allo-HSCT based on complete MHC-I mismatch. We first standardized the dosing regimen for oral administration of 5NQ in our murine model of allo-HSCT and further validated it in a larger cohort of animals. We evaluated the impact of oral 5NQ administration on various factors, including survival, GVHD-associated weight loss, clinical symptoms, and cytokine levels in the serum, tissue damage in the intestine, liver, and skin, engraftment of donor cells, hematopoietic recovery, and the immune cell composition in the spleen of recipient mice. We also demonstrated the immunomodulatory effects of oral 5NQ in healthy mice. These assessments provide a clear understanding of the prophylactic efficacy and in vivo immunomodulatory activity of oral 5NQ. We employed the most commonly used murine model of allo-HSCT which is based on complete MHC-I mismatch results in development of severe acute GVHD in these mice. Therefore, we anticipate that if the drug under evaluation produces a beneficial prophylactic effect in a complete MHC-I mismatch model, it is likely to be effective in any other model of transplantation based on.

Prophylaxis and treatment of GVHD remains a major challenge in allo-HSCT owing to its complex pathophysiology. The current standard prophylactic regimens mainly target T cells, as they are the major effector cells in the manifestation of GVHD[386–388]. However, the initiation of acute GVHD begins before CD4 effector cells are activated[389,390]. The severity of acute GVHD is greatly influenced by the conditioning regimen-induced oxidative stress and cellular damage[391–394]. Recently, 5NQ has gained attention as a potent immunomodulatory agent[245,246,248,249,252,395–397]. Our study is the first to assess the prophylactic efficacy of oral 5NQ for GVHD using a murine model of allo-HSCT based on a complete MHC-I mismatch. The results of our study reveal multiple mechanisms that

contribute to the efficacy of 5NQ. First, 5NQ exhibited immunosuppressive effects on antigen-presenting cells (APCs) by inhibiting their activation, as evidenced by a decrease in MHC-II expression in dendritic cells, macrophages, and monocytes. A few studies have reported similar effects of 5NQ on APCs. A study by Kim et al. showed that 5NQ can inhibit LPS-induced NLRP3 inflammasome formation in J774.1 macrophages in vitro and thus may have potent anti-inflammatory action[245]; however, this finding was not validated in an in vivo inflammatory disease model. Another recent study in 2021 reported that in a murine model of autoimmune encephalomyelitis, intraperitoneal treatment of mice with 5 mg/kg 5NQ resulted in a decrease in the expression of the costimulatory molecules CD83 and MHC-II in dendritic cells[398]. Considering the pivotal role of host and donor APCs in the activation phase of GVHD pathogenesis, 5NQ's ability to suppress them may be critical for alleviating GVHD.

Second, our study describes the effects of 5NQ treatment on $CD4^+$ and $CD8^+$ T cell activation and differentiation. Upon activation, CD4 T cells upregulate the expression of CD25 and CD69, and subsequent costimulation enables their differentiation into effector, memory, or regulatory subsets[399]. Following mitogenic activation, T cell effector functions are further regulated by the expression of death receptors, such as Fas (CD95) and CTLA4 (CD152). These molecules play a major role in the mitigation of T cell effector functions and induction of peripheral tolerance[400,401]. Our in vitro data showed that 5NQ treatment sensitized $CD4^+$ T cells to activation induced cell death, as evidenced by a reduction in expression of CD25 and CD69, and an increase in the expression of CD95 (Fas) in the presence of Con A. To further understand the mechanism by which 5NQ suppressed GVHD, we evaluated the expression of FoxP3 (expressed by Treg cells), CTLA-4, and Fas in activated $CD4^+$ T cells ($CD4^+CD25^+$). Interestingly, we observed that activation of $CD4^+$

T cells did not cause them to differentiate into Treg cells in vivo because similar numbers of Treg cells were observed in the spleens of vehicle and 5NQ treated mice. This corroborated our in vitro study where 5NQ treated leukocytes did not show an increase in $CD4^+$ T cell differentiation into Treg cells following mitogenic stimulation. This led us to conclude that 5NQ mediated reduction in inflammation and GVHD was not powered by Treg cells. However, we observed an increase in expression of CD95 and CTLA-4 on these activated $CD4^+$ T cells in vivo, indicating an anergic/exhaustive state of these cells. Many extrinsic and intrinsic factors can contribute to the anergic/exhaustive state of activated $CD4^+$ T cells, where suboptimal costimulation by APCs comprises extrinsic factors, whereas intrinsic factors include cell signaling events[400,401]. Induction of T cell anergy/exhaustion is being evaluated as a strategy to prevent GVHD and is still under development. An example of one such drug that exploits $CD4^+$ T cell costimulation is Abatacept (humanized recombinant fusion protein containing extracellular domain of CTLA4 and IgG1), which blocks the costimulatory CD28/CD86 interactions, thus inhibiting T cell proliferation[117,402]. Our study is the first to report this effect of 5NQ on $CD4^+$ T cells.

Furthermore, in our study, oral treatment with 5NQ resulted in modification of $CD4^+$ T helper cell differentiation with a decrease in naïve T cell subset and an increase in central and effector memory $CD4^+$ T cells. Naïve T cells are implicated in GVHD pathogenesis[403,404] whereas it is well known that central memory cells do not play a role in GVHD development[405–407]. Thus, modulation of $CD4^+$ T cell responses by 5NQ is another factor that contributes to its GVHD prophylactic efficacy. A recent study published by Geraghty et al. showed that an increase in splenic CD4:CD8 ratio along with increase in serum IFN-γ and IL-17 were indicative of GVHD in a humanized murine model of

GVHD[381]. Therefore, the observed decrease in splenic CD4:CD8 ratio in animals treated with 5NQ indicated alleviation of GVHD in these animals[381]. Next, we also studied the effect of 5NQ on $CD8^+$ T cells that play a major role in graft versus leukemia immunity and also end stage effector activities[407]. The observed decrease in expression of granzyme B on $CD8^+$ T cells in 5NQ treated animals, indicates a reduction in the cytotoxic potential of these cells which may be responsible for alleviation of GVHD associated tissue damage. It has been observed that a lack of GzmB in $CD8^+$ T cells significantly reduced the lethality and intensity of GVHD after allo-HSCT[408] while enhancing the GVL activity in several tumor models[409]. In addition, we observed decrease in naïve $CD8^+$ T cell population, which may prove beneficial in mitigating GVHD as this subset is known to recognize minor histocompatibility antigens 5-20 times more effectively than the memory subset[410]. Furthermore, the number of $CD8^+$ TCM cells increased after 5NQ treatment in our GVHD model. This proves beneficial in many ways, as this subset of cells are known to play a role in homeostatic proliferation, antitumor immunity and do not play a role in alloreactive responses[411–413]. Moreover, 5NQ treatment did not cause an increase in $CD8^+CD152^+$ cells, indicating that 5NQ treatment did not result in an anergic/exhaustive state of $CD8^+$ cells. Accordingly, 5NQ treatment also preserved the anti-tumor activity of the graft, as demonstrated in the, ex vivo settings in our study, the in vivo results are discussed in the next objective. 5NQ mediated maintenance of GVL activity can be attributed to an increase in $CD8^+$ cells or $CD8^+$ TCM cells but requires further mechanistic investigations.

Third, the oral treatment with 5NQ modulated the cytokine response in the GVHD model by reducing proinflammatory cytokines IFN-γ and TNF and elevating the anti-inflammatory cytokines IL-10 and IL-17A. These results are in accordance with previous studies where, treatment with 5NQ has shown modulation of cytokine secretion in favor of

anti-inflammatory response in different inflammation based murine models[245,246,414]. However, this study is the first to examine this effect using a GVHD based model. Cytokines constitute the third signal for optimal T-cell activation, and cytokines such as IL-6, TNF, and IFN-γ play a major role in promoting the inflammatory response in GVHD settings[415,416]. Cytokines IL-10 and IL-17A have been reported to show beneficial effects in GVHD settings[417,418] and hence 5NQ mediated increase in serum concentrations of IL-10 and IL-17A plays a role in imparting protection against GVHD in our study.

In conclusion, our study revealed that 5NQ administration inhibited antigen presentation, cytokine storm, and activation of $CD4^+$ T cells, thus demonstrating an immunomodulatory effect of 5NQ at every phase of GVHD pathogenesis. Oral administration of 5NQ prevented GVHD development without compromising GVL activity. We found that an alternate day administration of 5NQ was optimal in murine allo-HSCT model.

Objective 4

8 OBJECTIVE 4

8.1 BACKGROUND

GVHD VS GVL - THE ETERNAL STRUGGLE

The success of allo-HSCT is dependent on the GVL effect, which is the ability of the donor immune system to identify and eliminate recipient leukaemia cells[11]. The GVL effect is primarily mediated by donor derived alloreactive T cells and natural killer (NK) cells. However, T cells are also responsible for causing acute and/or chronic graft versus-host disease (GVHD), which is associated with significant morbidity and mortality[33,65]. Depletion of T cells from allografts is associated with increased graft failure and increased rates of leukaemia relapse[77]. Moreover, the immunosuppressive agents used to prevent and treat GVHD compromise the beneficial GVL effects of the donor graft. Preventing GVHD while maintaining the GVL effect remains a challenging yet unresolved phenomenon for successful transplantation[92]. Although, many improvements have taken place in developing novel therapeutics that effectively prevent or treat GVHD, it is equally important to evaluate the effect of these therapies on the GVL occurrence. Therefore, effective outcomes of allo-HSCT requires deeper understanding of the cellular and molecular factors that separate the GVL from GVHD[30].

Factors promoting GVL activity

Tumour reactive macrophages, T cells and NK cells are the major mediators of the GVL response. These cells recognize cues such as abnormal MHC-I expression, minor histocompatibility antigens (miHAs), tumor-associated antigens, or neo-antigens and initiate their cytotoxic activity against these cells. Abnormal MHC-I expression is the primary antigenic clue that triggers the cytotoxic activity of NK cells. HLA-C is now

recognized as the most significant MHC class I subgroup that causes NK cell cytotoxic activity through killer inhibitory receptors (KIRs)[58]. Minor histocompatibility antigens like HA-1 and HA-2 have been shown to potentiate cytotoxic T-lymphocytes (CTLs), leading to GVL response[419]. Nonpolymorphic, non-miHC self-antigens, known as tumor, associated antigens (TAAs), can trigger an antitumor response by activating CTLs, either by qualitative or quantitative expression in tumor cells. Some examples of TAAs include BCR-ABL fusion protein in CML, myeloperoxidase, prostate specific antigen (PSA) in prostate cancer cells. However, in clinics antitumor responses against TAAs is poor due to immune escape mechanisms employed by cancer cells[420].

Cellular and molecular factors that maintain GVL without aggravating GVHD in preclinical models

Granulocyte colony stimulating factor (G-CSF): Preclinical studies have demonstrated that G-CSF mobilized peripheral blood can mediate GVL effects via activation of CTLs or NK T cells. Moreover, G-CSF mobilized graft can alleviate GVHD via reducing systemic levels of LPS and inflammatory cytokines like TNF-α, inducing Th2 response and potentiating tolerogenic antigen presenting cells (APCs)[421,422].

T cells: Various preclinical studies have been designed to assess the subsets of T cells that mediate GVL without causing GVHD. In particular, $CD4^+$ or $CD8^+$ naive (Tn), central memory (Tcm) and effector memory (Tem) cells have been studied with respect to their ability to cause GVHD and mediate GVL effects[374]. In a murine model, transplantation of $CD62^{lo}CD44^{hi}$ effector memory cells, but not naive T cells ($CD62^{hi}CD44^{lo}$) mediated GVL activity without causing GVHD, as these cells retained their cytolytic activity but were unable to proliferate against allo-antigens[369,371,373]. Another study found that $CD4^+$ and

$CD8^+$ central memory T cells did not induce GVHD in a mouse model[368,370]. However, $CD8^+$ Tcm cells were able to induce GVHD but were also crucial for GVL activity[372].

Recent studies have highlighted the role of tissue tolerance in alleviation of GVHD and maintenance of GVL effect. Transplantation of $CD4^+$ T cell depleted graft showed an increase in IFNγ levels in the serum, which caused an up-regulation of PD-L1 on recipient tissues. This resulted in exhaustion of $CD8^+$ CTLs, thus mitigating GVHD associated tissue damage. However, these cells retained GVL activity. Nonetheless, PD-L1 mediated effects on $CD8^+$ T cells is dependent on presence of $CD4^+$ T cells and tissue microenvironment[423].

Regulatory immune cells: Immune cells that regulate inflammation such as Tregs, Bregs, MDSCs, and MSCs, may improve immune homeostasis and protect against GVHD. Tregs have gained much popularity for the GVHD prophylactic effects due to their ability to suppress expansion of alloreactive T cells. Furthermore, these modulations do not impede the GVL activity of conventional T cells, which is mediated by the perforin pathway[366,379,424].

Myeloid-derived suppressor cells (MDSCs) are immune cells that regulate the immune system by secreting the anti-inflammatory cytokine IL-10. This leads to an increase in regulatory T cells and type 2 macrophages. MDSCs can suppress Th1 cells by promoting a Th2 response, which prevents GVHD without affecting GVL activity[425].

Mesenchymal stem cells are another group of immune regulatory cells that can cause increase in ROS, NO, TGF-β and IL-10 which causes suppression of T cell function. Since MSCs do not impede the function of NK cells, they can reduce GVHD while maintaining the GVL effects of the NK cells[426,427].

Breg cells secrete anti-inflammatory cytokines such as IL-10 and TGFβ, which promote immunosuppression by expansion of Treg cells. These cells thus alleviate GVHD without compromising GVL[428].

In summary, these preclinical studies suggest that regulatory cells could alleviate GVHD without compromising the GVL effects however, further studies are required for their application in clinics.

Murine models to study GVL activity

To assess the GVL activity of the graft, a congenic or a syngeneic leukaemia or tumour cell line (that is genetically compatible with recipient mice) is injected along with donor cells during transplantation. The most commonly used tumour cell line-recipient combinations are, A20 cell line for BALB/c recipient[429], EL4 cell line for C57BL/6 recipient, or mouse acute promyelocytic leukaemia cells from PML/RARA transgenic mice for B16 recipient mice[313]. Moreover, human leukaemia or tumour cell lines can also be employed in xenogeneic murine models of allo-HSCT. In most murine models, the leukemic cells are primarily injected after the conditioning regimen and along with donor cells, prevent variation in tumor burdens before therapy. However, only a few models have been developed to simulate the minimal residual disease clinical scenario, where cancer cells are injected 10-15 days prior to the conditioning regimen and followed by the transplantation procedure and administration of the therapeutic intervention[313].

Assessment of the GVL activity of the graft in murine models requires measurement of residual leukemic cells, along with other parameters including survival, therapeutic efficacy, and GVHD scoring in these models. In murine models utilizing A20 leukemic cells, the onset of hind limb paralysis, the presence of tumour nodules in the liver and other

lymphoid tissues, serve as surrogate markers for the leukemic burden in these models[429]. Development of bioluminescent imaging (BLI) has enabled the detection of residual leukaemia cells in real time, without sacrificing the mice. The leukaemia cells are transduced to stably express a fluorescent marker or luciferase. These transgenic leukaemia cells can be injected and detected in real time using bioluminescent imaging[430].

Nonetheless, these models have some limitations in assessing the efficacy of the drug without compromising GVL activity. Tumour cell lines employed in these murine models are highly aggressive, resulting in early mortality and limiting the time available for the therapeutic examination to demonstrate its effects. In preclinical studies, tumor cell lines are injected after conditioning to reduce tumour burden variation. In clinics however, tumours have already developed and adapted to evade immune recognition, making potent graft versus tumour (GVT) effects necessary to prevent relapse. Additionally, human cancers exhibit genetic and cellular diversity that cannot be replicated using genetically stable and homogeneous mouse tumor cell lines. Despite this, evaluating GVL activity in mouse models has provided evidence of the therapeutic intervention's ability to preserve GVL activity of the graft[314].

8.2 METHODOLOGY

Murine model for assessing graft versus leukaemia (GVL) activity of donor graft: To assess the GVL activity of the donor graft, the murine model of allo-HSCT was supplemented with A20 leukemia cells. Briefly, female BALB/c mice (8–10 week old) were irradiated and transplanted with 5×10^6 A20 cells along with bone marrow and splenocyte. A20 is a syngeneic B-cell leukemia cells, originating from BALB/c mice[429]**.**

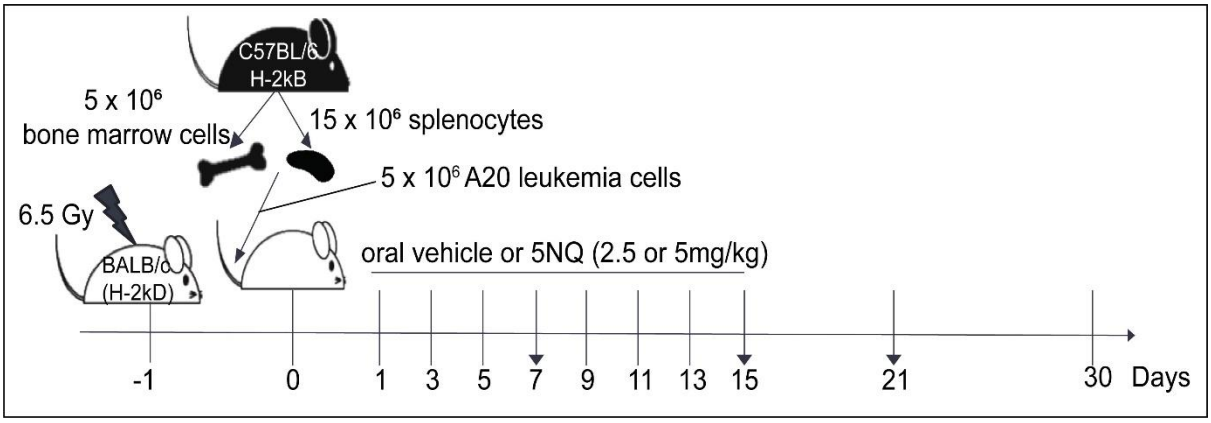

Figure 72: Overview of the workflow for allo-HSCT along with injection of A20 leukemia cells.

Assessment of graft versus leukemia (GVL) activity: The allogeneic graft is immune-competent and can eliminate residual leukemia cells (GVL activity) remaining after myeloablative therapy. We assessed the effect of oral 5NQ treatment on the GVL activity of the graft using the murine model of allo-HSCT supplemented with A20 leukemia cells. Briefly, female BALB/c mice (8–10week-old) were irradiated as mentioned above and either injected with A20 (5×10^6) cells alone or A20 + allogenic bone marrow transplantation (BMT). Animals in the A20+BMT group either received vehicle control (VC) – 5% DMSO dissolved in 0.5% carboxy methylcellulose or 5NQ - 5 mg/kg orally. The final experimental groups were (1) A20, (2) BMT, (3) A20+BMT+VC, (4) A20+BMT+5NQ. GVL activity was assessed as described previously[41,](Snyder et al., 2021; Zhang et al., 2019). Briefly, mice were monitored daily for body weight, clinical signs of GVHD, hind limb paralysis, and survival. Mice were euthanized if they were moribund, developed paralysis in both hind limbs, or had a weight loss of ≥ 20%. Time-to-event outcomes comprised (a) overall survival, defined as the time to death due to leukemia or GVHD, and (b) time to onset of leukemia, defined by the occurrence of hind limb paralysis. Death due to leukemia was defined as the absence of weight loss, development of hind limb paralysis, or macroscopic tumor nodules in the liver or spleen at the time of

necropsy. Death due to GVHD was defined as a significant decrease in weight loss (≥20%), presence of clinical signs of GVHD, and absence of tumor nodules in the liver and spleen. WBC counts were obtained from the peripheral blood[431].

8.3 RESULTS

Oral administration of 5NQ preserved the GVL activity of donor graft *in vivo*

Most therapies that offer protection from GVHD may compromise the graft GVL activity, which is the most beneficial outcome of allogeneic transplantation. Therefore, we evaluated the effect of the oral administration of 5NQ on the GVL effect of the donor graft in GVHD model supplemented with A20 murine B-cell lymphoma cells. Mortality due to tumors was defined by the absence of weight loss, development of hind limb paralysis, and presence of tumor nodules in the liver or spleen at the time of necropsy. Mortality due to GVHD was defined as a significant decrease in weight loss (20-30%), presence of clinical signs of GVHD, and absence of tumor nodules in the liver and spleen. Accordingly, animals from A20 group succumbed to the tumor associated death within three weeks (median survival of 19 days) with no significant reduction in weight loss (Figure 73B and C). However, mice from BMT group developed hind limb paralysis and were euthanized when moribund (Figure 73A and B). All animals in the A20+BMT+VC group, developed severe GVHD within two weeks and were sacrificed when moribund to check for the presence of tumors. These mice showed clinical symptoms of GVHD with a significant reduction in body weight (Figure 73C) and a median survival of 10.5 days, along with the absence of tumors at necropsy (Figure 73B).

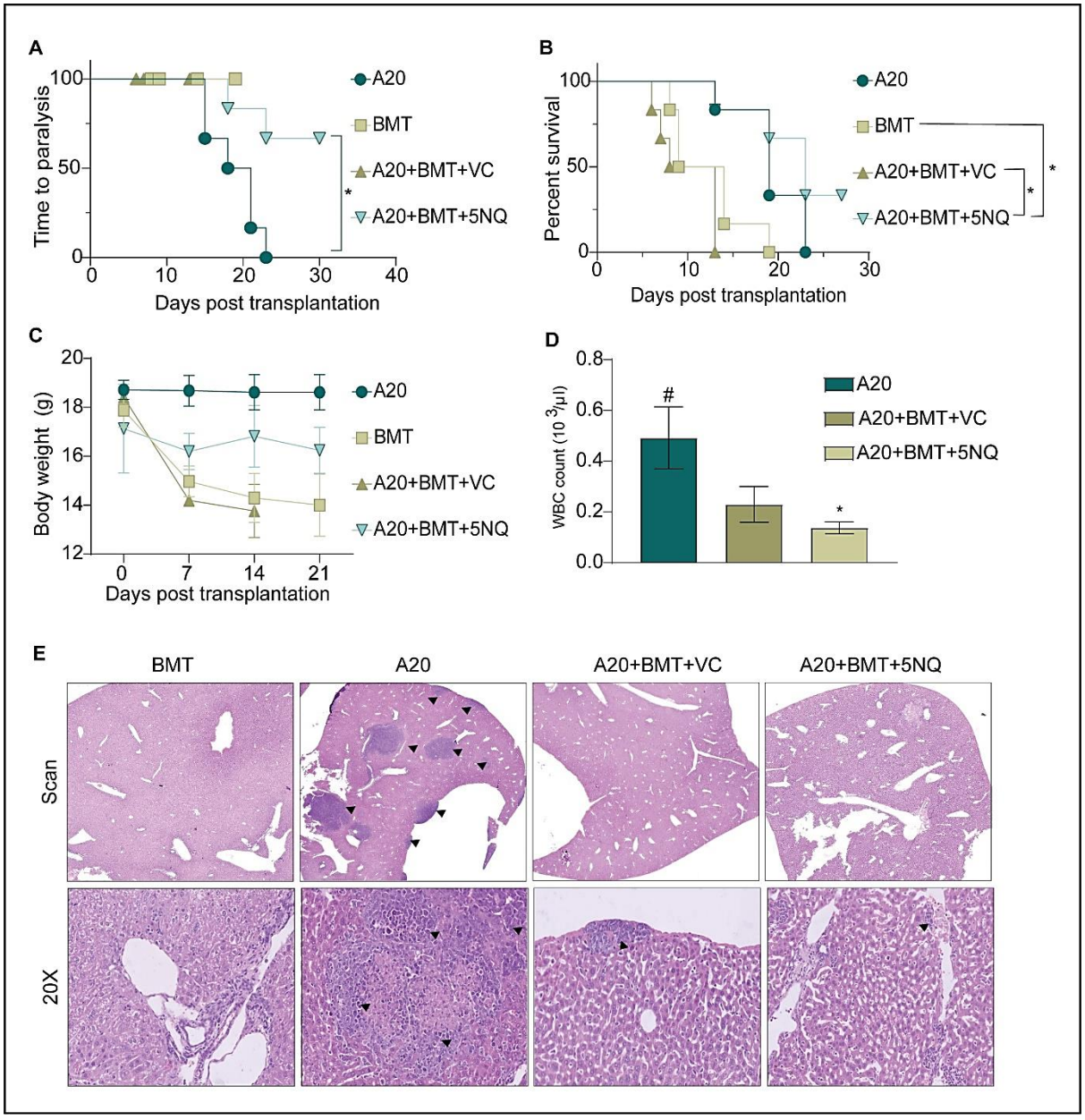

Figure 73: (A) Kaplan–Meier plot for time to onset of leukemia. Mantel-Cox log-rank test was used to compare survival between groups (n = 6/group). (B) Survival of transplanted mice administered orally with VC (A20+BMT+VC) or 5NQ (A20+BMT+5NQ). (C) Body weight of transplanted mice (mean ± SEM). (D) WBC count in peripheral blood (mean ± SEM). Data were analysed using one-way ANOVA, *****$p<0.05$, compared to only tumour (A20 group) control animals (E) Representative micrographs of liver sections stained with H&E, the black arrows indicate tumour infiltration.

In contrast, animals in the A20+BMT+5NQ group, showed significantly lower body weight reduction compared to mice in the BMT and A20+BMT+VC groups, indicative of protection from GVHD (Figure 73C). Only 2 out of 6 mice succumbed to the tumor associated death in this group (Figure 73A). These mice showed a significant improvement

in survival compared with BMT and A20+BMT+VC treated animals, with a median survival of 23 days (Figure 73A and B). Moreover, WBC counts were found to be lower in mice from A20+BMT+5NQ group than in mice injected with A20 cells alone (A20 group) (Figure 73D). At necropsy, animals in the A20+BMT+5NQ group showed reduced tumor nodules in the liver and spleen (Figure 74), which was further confirmed from the liver histopathology (Figure 73E). These findings are suggestive of the protective effect of 5NQ on donor GVL activity. On an average, A20 mice showed 70% tumor infiltration in their liver with severe necrosis. The tumor burden in A20+BMT+VC mice was very low at 1-2% whereas, mice in the A20+BMT+5NQ group showed reduced tumor burden, ranging from to 1-30% involvement of the hepatic tissue (Figure 73E).

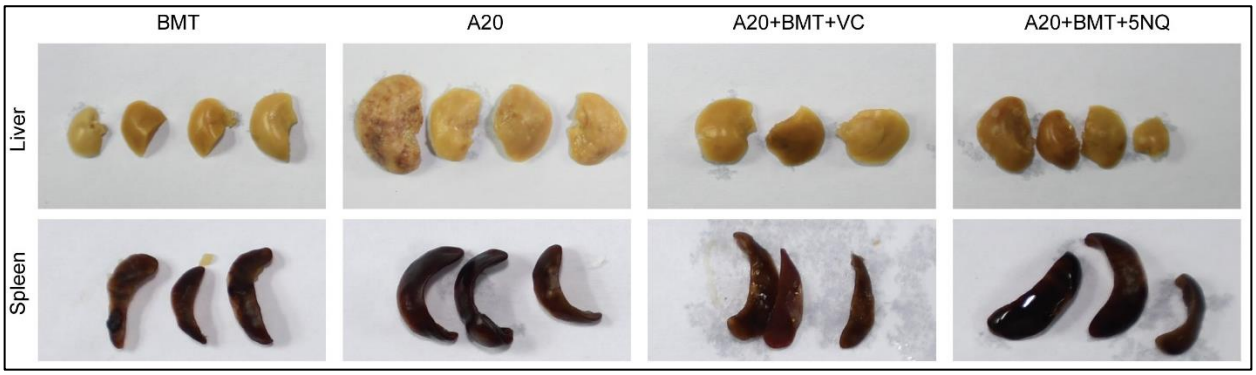

Figure 74: Images of the liver and spleen taken at necropsy, showing a reduction in macroscopic tumor nodules in mice treated with 5NQ.

8.4 DISCUSSION

The present study aimed to evaluate the effect of oral administration of 5NQ on the GVL activity of the donor graft. We for the first time, successfully established an oral dose of 5NQ when given for 15 days following alternate day dosing strategy, alleviated GVHD, without compromising GVL effect of the donor graft in mice. In earlier objectives, we also demonstrated the *in vitro* and *ex vivo* anti-tumor activity of 5NQ on leukocytes. Oral administration of 5NQ resulted in reduced incidence of hind limb paralysis (surrogate

marker for leukemia development), improved survival and lower histological tumor burden in transplanted mice, suggesting the protective effect of 5NQ on the GVL activity of the graft. The conservation of GVL activity can be attributed to an increase in $CD8^+$ cells or $CD8^+$ TCM cells as demonstrated earlier[411,413]. However, further investigations are required to demonstrate the mechanism(s) of 5NQ mediated protection of GVL activity of the graft. Despite the fact that we observed 25% death due to leukemia in mice treated with 5NQ, our study provides a proof of concept regarding the GVL preserving activity of the 5NQ in murine model of allo-HSCT. Our model for assessing the GVL activity of the graft does not reflect the minimal residual disease (MRD) situation encountered in clinics, and better outcomes can be expected in such scenarios.

Summary And Salient Findings

9 SUMMARY AND SALIENT FINDINGS

9.1 Summary

Acute graft-versus-host disease (GVHD) remains a major barrier to successful transplantation. Recent studies have shown that pharmacotherapy for GVHD should target both the innate and adaptive inflammatory immune responses. The development of novel pharmacological therapies for acute GVHD prophylaxis remains an unresolved need in the field of allo-HSCT. In this study, a phytochemical drug library was screened to identify compounds with immunomodulatory activity, and further 5-hydroxy-1,4 naphthoquinone (5NQ) was identified as the lead molecule. Furthermore, the safety of the oral administration of 5NQ was established, and the prophylactic efficacy of oral 5NQ was demonstrated in a murine model of allo-HSCT. Furthermore, the immunomodulatory activity of orally administered 5NQ on the activation of antigen-presenting cells and $CD4^+$ and $CD8^+$ T cell subsets was assessed. Our study demonstrated that oral administration of 5NQ prevented GVHD development by inhibiting the activation of APCs, cytokine storm, and $CD4^+$ T cells and preserved the graft versus leukemia activity of the graft by protecting $CD8^+$ central memory T cells. Furthermore, our study provides a suitable dosage for oral administration of 5NQ, which can be used to devise a clinically relevant dose for human application.

Salient findings

1. **Screening phytochemical drug libraries for immunomodulatory compounds.**
    a. Primary screening using murine splenic leukocytes identified nine compounds that inhibited both IL-2 secretion and lymphocyte proliferation after mitogenic stimulation. These compounds (target compounds) were selected and subjected to secondary screening to identify compounds that exhibited immunomodulatory activity at non-cytotoxic doses.

b. Secondary screening identified two compounds, 5-hydroxy-1,4-naphthoquinone (5NQ, 2F5) and demethylzeylasteral (2-E6), that exhibited potent immunosuppressive activity at non-toxic concentrations in murine leukocytes. Since the prophylactic efficacy of demthylzeylasteral has been previously reported, 5NQ was selected as the lead compound for further investigation.

c. In vitro studies using murine splenic lymphocytes revealed that transient treatment with 5NQ (1µM, 4 h) inhibited the mitogen-induced activation of APCs and $CD4^+$ T cells and inhibited the mitogen-induced Th1/Th2 cytokine imbalance.

d. Transient treatment with 5NQ induced an anergic/exhaustive state in $CD4^+$ T cells, as indicated by the upregulation of CD95 (Fas) expression in these cells.

e. An in vitro mixed lymphocyte reaction assay combining murine leukocytes with syngeneic leukemia cells A20 or EL4 showed that 5NQ treated leukocytes retained their antitumor activity.

2. Understanding the molecular mechanism of the immunomodulatory action of lead compound in vitro.

a. Transient treatment with 5NQ modulated the cellular ROS balance by selectively increasing mitochondrial ROS levels in leukocytes.

b. Transient treatment with 5NQ resulted in depletion of the cellular GSH pool.

c. 5NQ mediated changes in cellular redox were reversed in the presence of thiol antioxidants GSH and NAC. Moreover, the anti-proliferative effect of 5NQ on murine leukocytes was abrogated in the presence of thiols.

d. Transient treatment with 5NQ upregulated Nrf2/HO1 antioxidant response signaling and abrogated inflammatory NF-κB and Akt signaling in murine leukocytes.

3. **Evaluation of anti-GVHD potential of the lead compound using a murine model of GVHD.**

PART A: Acute and subacute oral toxicity assessment of 5NQ in mice.

a. The point of departure dose for the acute oral administration of 5NQ was established to be 118 mg/kg using benchmark dose modeling.

b. The point of departure for repeated administration of 5NQ was established to be 1.74 mg/kg/day using BMD modeling, and the NOAEL was found to be < 5 mg/kg/day. The BMD dose can be used to derive a reference dose of 5NQ for clinical application.

c. Oral administration of 5NQ caused severe hepatic and renal damage at a dose of 50 mg/kg in acute toxicity study, and at higher doses of 15 and 50 mg/kg in sub-acute toxicity study.

d. Serum levels of aspartate aminotransferase (AST) significantly increased upon repeated oral administration and can serve as a marker of 5NQ toxicity.

PART B: Evaluation of the anti-GVHD efficacy of oral administration of 5NQ in a murine allo-HSCT model

a. Oral administration of 5 mg/kg 5NQ every alternate day for 15 days after transplantation significantly reduced GVHD-associated morbidity and mortality and protected against GVHD-associated intestinal and skin tissue damage in transplanted mice.

b. Oral administration of 5NQ protected against GVHD-associated cytokine storm, as evidenced by the reduction in pro-inflammatory cytokines IFNγ

and TNF and increased levels of anti-inflammatory cytokines IL-10 and IL-17A.

c. Oral administration of 5NQ modulated the innate immune response in transplanted mice, showing a significant reduction in dendritic cell activation.

d. The oral administration of 5NQ in transplanted mice resulted in a modulation of $CD4^+$ and $CD8^+$ T-cell responses. A noticeable decrease in the GVHD mediating naïve $CD4^+$ and $CD8^+$ T cells and, cytotoxic $CD8^+$ T cells ($CD8^+$ granzyme B^+) was observed. Whereas a significant increase in central memory $CD4^+$ and $CD8^+$ T and anergic $CD4^+$ T cells observed.

e. Oral administration of 5NQ maintained the hematopoietic recovery and donor cell engraftment in transplanted mice.

4. **Development of a syngeneic murine model of leukemia and assessment of the efficacy of the lead compound in maintaining the GVL effect of the graft.**

   a. Oral administration of 5NQ preserved the GVL activity of the graft and significantly improved the survival of the mice as compared to vehicle treated mice.

Conclusion

10 CONCLUSION

Conclusion

The prophylactic efficacy of juglone against allo-HSCT has been mediated through its immunomodulatory action. It effectively reduced morbidity and mortality associated with GVHD without compromising graft-versus-leukemia activity. The mechanisms proposed are inhibition of dendritic cells and $CD4^+$ T cells activation, (ii) reduction in cytokine secretion and lymphocyte proliferation, and (iii) induction of $CD4^+$ T cells exhaustion as supported by the increased expression of CTLA-4 (CD152) and Fas (CD95). This was also accompanied by a decrease in the naive $CD4^+$ cells and an increase in $CD4^+$ and $CD8^+$ central memory T cells.

Strengths And Limitations

11 STRENGTHS AND LIMITATIONS

Strengths

- ✓ Our study is the first to establish the GVHD prophylactic efficacy of oral 5NQ in preclinical setting.
- ✓ The established dosage framework for orally administered 5NQ through benchmark dose strategy in preclinical efficacy study could pave way to its clinical development.
- ✓ The immunomodulatory action of 5NQ on innate and adaptive immunity after allo-HSCT has been studied through immunophenotyping of specific cell population *in vivo*.

Limitations

- The effect of 5NQ on Nrf-2/HO-1 signaling mediated up-regulation of antioxidant response has been studied only *in vitro* using mixed leukocyte subtypes. Its relevance to specific immune cell subpopulation has not been established *in vivo.*
- In clinical settings, cyclosporin (CSA) is administered for much longer duration of time after allo-HSCT. However, in our efficacy studies we could only use CSA intravenously for a maximum of five doses due to the risk of tail vein phlebitis.
- The prophylactic efficacy of 5NQ was evaluated in a MHC-I mismatch allo-HSCT model but, it could have been more clinically relevant if studied in MHC-matched model of allo-HSCT.

Future Prospects

12 FUTURE PROSPECTS

- The limited therapeutic window of juglone necessitates the development of a formulation that enhances its effectiveness while minimizing its toxicity for clinical use.
- It is necessary to understand the *in vivo* mechanism(s) responsible for the observed immunomodulatory effects of 5NQ on cellular signalling in different immune cell subsets.
- In different murine models of inflammatory diseases, further efficacy studies should be planned with demethylzeylasteral a potent anti-inflammatory agent shortlisted after secondary phytochemical screening.

Bibliography

13 BIBLIOGRAPHY

1. Copelan, E. A., Chojecki, A., Lazarus, H. M. & Avalos, B. R. Allogeneic hematopoietic cell transplantation; the current renaissance. *Blood Rev* **34**, 34–44 (2019).
2. Copelan, E. A. Hematopoietic Stem-Cell Transplantation. *New England Journal of Medicine* **354**, 1813–1826 (2006).
3. Welniak, L. A., Blazar, B. R. & Murphy, W. J. Immunobiology of allogeneic hematopoietic stem cell transplantation. *Annu Rev Immunol* **25**, 139–170 (2007).
4. Ferrara, J. L., Levine, J. E., Reddy, P. & Holler, E. Graft-versus-host disease. *The Lancet* **373**, 1550–1561 (2009).
5. Zeiser, R. & Blazar, B. R. Acute Graft-versus-Host Disease — Biologic Process, Prevention, and Therapy. *New England Journal of Medicine* **377**, 2167–2179 (2017).
6. Penack, O. *et al.* Prophylaxis and management of graft versus host disease after stem-cell transplantation for haematological malignancies: updated consensus recommendations of the European Society for Blood and Marrow Transplantation. *Lancet Haematol* **7**, e157–e167 (2020).
7. Duarte, R. F. *et al.* Indications for haematopoietic stem cell transplantation for haematological diseases, solid tumours and immune disorders: current practice in Europe, 2019. *Bone Marrow Transplant* **54**, 1525–1552 (2019).
8. Niederwieser, D. *et al.* Hematopoietic stem cell transplantation activity worldwide in 2012 and a SWOT analysis of the Worldwide Network for Blood and Marrow Transplantation Group including the global survey. *Bone Marrow Transplant* **51**, 778–785 (2016).
9. Ruxolitinib in refractory acute and chronic graft-versus-host disease_ a multicenter survey study _ Enhanced Reader.pdf.
10. Garnett, C., Apperley, J. F. & Pavlu, J. Treatment and management of graft-versus-host disease: improving response and survival. *Ther Adv Hematol* **4**, 366–378 (2013).
11. Welniak, L. A., Blazar, B. R. & Murphy, W. J. Immunobiology of allogeneic hematopoietic stem cell transplantation. *Annu Rev Immunol* **25**, 139–170 (2007).
12. Passweg, J. R. *et al.* The EBMT activity survey on hematopoietic-cell transplantation and cellular therapy 2018: CAR-T's come into focus. *Bone Marrow Transplant* **55**, 1604–1613 (2020).
13. Miller, J. P. *et al.* Recovery and safety profiles of marrow and PBSC donors: experience of the National Marrow Donor Program. *Biol Blood Marrow Transplant* **14**, 29–36 (2008).

14. Adhikari, J., Sharma, P. & Bhatt, V. R. Optimal graft source for allogeneic hematopoietic stem cell transplant: Bone marrow or peripheral blood? *Future Oncology* **12**, 1823–1832 (2016).

15. Anasetti, C. *et al.* Peripheral-blood stem cells versus bone marrow from unrelated donors. *N Engl J Med* **367**, 1487–96 (2012).

16. Ding, D. C., Chang, Y. H., Shyu, W. C. & Lin, S. Z. Human umbilical cord mesenchymal stem cells: a new era for stem cell therapy. *Cell Transplant* **24**, 339–347 (2015).

17. Jethava, Y. S. *et al.* Conditioning regimens for allogeneic hematopoietic stem cell transplants in acute myeloid leukemia. *Bone Marrow Transplant* **52**, 1504–1511 (2017).

18. Blaise, D. & Castagna, L. Do different conditioning regimens really make a difference? *Hematology Am Soc Hematol Educ Program* **2012**, 237–245 (2012).

19. Valcárcel, D. *et al.* Conventional versus reduced-intensity conditioning regimen for allogeneic stem cell transplantation in patients with hematological malignancies. *Eur J Haematol* **74**, 144–151 (2005).

20. Balassa, K., Danby, R. & Rocha, V. Haematopoietic stem cell transplants: Principles and indications. *Br J Hosp Med* **80**, 33–39 (2019).

21. Sureda, A. *et al.* Indications for allo- and auto-SCT for haematological diseases, solid tumours and immune disorders: current practice in Europe, 2015. *Bone Marrow Transplant* **50**, 1037–1056 (2015).

22. Ruiz-Argüelles, G. J., Ruiz-Delgado, G. J., González-Llano, O. & Gómez-Almaguer, D. Haploidentical Bone Marrow Transplantation in 2015 and Beyond. *Curr Oncol Rep* **17**, (2015).

23. Kanate, A. S. *et al.* Indications for Hematopoietic Cell Transplantation and Immune Effector Cell Therapy: Guidelines from the American Society for Transplantation and Cellular Therapy. *Biology of Blood and Marrow Transplantation* **26**, 1247–1256 (2020).

24. Passweg, J. R. *et al.* Hematopoietic cell transplantation and cellular therapy survey of the EBMT: monitoring of activities and trends over 30 years. *Bone Marrow Transplantation 2021 56:7* **56**, 1651–1664 (2021).

25. Stem Cell Transplantation | Allogeneic Stem Cell Transplantation | LLS. https://www.lls.org/treatment/types-treatment/stem-cell-transplantation/allogeneic-stem-cell-transplantation.

26. Shaw, K. L. & Kohn, D. B. A tale of two SCIDs. *Sci Transl Med* **3**, (2011).

27. Baron, F. & Nagler, A. Novel strategies for improving hematopoietic reconstruction after allogeneic hematopoietic stem cell transplantation or intensive chemotherapy. *Expert Opin Biol Ther* **17**, 163–174 (2017).

28. Pereira, M. R., Pouch, S. M. & Scully, B. Infections in Allogeneic Stem Cell Transplantation. *Principles and Practice of Transplant Infectious Diseases* 209–226 (2019) doi:10.1007/978-1-4939-9034-4_11.

29. Shouval, R. *et al.* Outcomes of allogeneic haematopoietic stem cell transplantation from HLA-matched and alternative donors: a European Society for Blood and Marrow Transplantation registry retrospective analysis. *Lancet Haematol* **6**, e573–e584 (2019).

30. Malard, F., Holler, E., Sandmaier, B. M., Huang, H. & Mohty, M. Acute graft-versus-host disease. *Nat Rev Dis Primers* **9**, (2023).

31. Storb, R. *et al.* Allogeneic hematopoietic cell transplantation following minimal intensity conditioning: predicting acute graft-versus-host disease and graft-versus-tumor effects. *Biol Blood Marrow Transplant* **19**, 792–798 (2013).

32. Ogonek, J. *et al.* Immune reconstitution after allogeneic hematopoietic stem cell transplantation. *Front Immunol* **7**, 223944 (2016).

33. Zeiser, R. Advances in understanding the pathogenesis of graft-versus-host disease. *Br J Haematol* **187**, 563–572 (2019).

34. Zeiser, R. & Blazar, B. R. Acute Graft-versus-Host Disease — Biologic Process, Prevention, and Therapy. *New England Journal of Medicine* **377**, 2167–2179 (2017).

35. Lect., R. B.-H. & 1996, undefined. The biology of graft-versus-host reaction. *cir.nii.ac.jp*.

36. Keever-Taylor, C. A. *et al.* Analysis of risk factors for the development of GVHD after T cell-depleted allogeneic BMT: effect of HLA disparity, ABO incompatibility, and method of T-cell depletion. *Biol Blood Marrow Transplant* **7**, 620–630 (2001).

37. Castilla-Llorente, C. *et al.* Prognostic factors and outcomes of severe gastrointestinal GVHD after allogeneic hematopoietic cell transplantation. *Bone Marrow Transplant* **49**, 966–971 (2014).

38. Martin, P. J. *et al.* Genome-wide minor histocompatibility matching as related to the risk of graft-versus-host disease. *Blood* **129**, 791–798 (2017).

39. Carapito, R. *et al.* Matching for the nonconventional MHC-I MICA gene significantly reduces the incidence of acute and chronic GVHD. *Blood* **128**, 1979–1986 (2016).

40. Xiao, B. *et al.* Plasma microRNA signature as a noninvasive biomarker for acute graft-versus-host disease. *Blood* **122**, 3365–3375 (2013).

41. Bacigalupo, A. *et al.* Reducing transplant-related mortality after allogeneic hematopoietic stem cell transplantation. *Haematologica* **89**, (2004).

42. Ding, D. C., Chang, Y. H., Shyu, W. C. & Lin, S. Z. Human umbilical cord mesenchymal stem cells: a new era for stem cell therapy. *Cell Transplant* **24**, 339–347 (2015).

43. Schoemans, H. M. *et al.* EBMT−NIH−CIBMTR Task Force position statement on standardized terminology & guidance for graft-versus-host disease assessment. *Bone Marrow Transplantation 2018 53:11* **53**, 1401–1415 (2018).

44. Dignan, F. L. *et al.* Diagnosis and management of acute graft-versus-host disease. *Br J Haematol* **158**, 30–45 (2012).

45. Lee, S. J. & Flowers, M. E. D. Recognizing and managing chronic graft-versus-host disease. *Hematology Am Soc Hematol Educ Program* 134–141 (2008) doi:10.1182/ASHEDUCATION-2008.1.134.

46. Jamil, M. O. & Mineishi, S. State-of-the-art acute and chronic GVHD treatment. *Int J Hematol* **101**, 452–466 (2015).

47. Thomas ED, Buckner CD, Banaji M, et al. One hundred patients with acute leukemia treated by chemotherapy, total body irradiation, and allogeneic marrow transplantation. Blood. 1977;49(4):511-533. *Blood* **128**, 2373 (2016).

48. Reshef, R. *et al.* Acute GVHD Diagnosis and Adjudication in a Multicenter Trial: A Report From the BMT CTN 1202 Biorepository Study. *J Clin Oncol* **39**, 1878–1887 (2021).

49. Lee, S. J. *et al.* Quality of life associated with acute and chronic graft-versus-host disease. *Bone Marrow Transplant* **38**, 305–310 (2006).

50. Pallua, S. *et al.* Impact of GvHD on quality of life in long-term survivors of haematopoietic transplantation. *Bone Marrow Transplant* **45**, 1534–1539 (2010).

51. Moon, J. H. *et al.* Early onset of acute GVHD indicates worse outcome in terms of severity of chronic GVHD compared with late onset. *Bone Marrow Transplantation 2010 45:10* **45**, 1540–1545 (2010).

52. Harris, A. C. *et al.* International, Multicenter Standardization of Acute Graft-versus-Host Disease Clinical Data Collection: A Report from the Mount Sinai Acute GVHD International Consortium. *Biology of Blood and Marrow Transplantation* **22**, 4–10 (2016).

53. Schoemans, H. M. *et al.* Accuracy and usability of the eGVHD app in assessing the severity of graft-versus-host disease at the 2017 EBMT annual congress. *Bone Marrow Transplant* **53**, 490–494 (2018).

54. Schoemans, H. M. *et al.* The eGVHD App has the potential to improve the accuracy of graft-versus-host disease assessment: a multicenter randomized controlled trial. *Haematologica* **103**, 1698–1707 (2018).

55. Ferrara, J. L., Levine, J. E., Reddy, P. & Holler, E. Graft-versus-host disease. *Lancet* **373**, 1550–1561 (2009).

56. Fredricks, D. N. The gut microbiota and graft-versus-host disease. *Journal of Clinical Investigation* **129**, 1808–1817 (2019).

57. Vander Lugt, M. T. *et al.* ST2 as a marker for risk of therapy-resistant graft-versus-host disease and death. *N Engl J Med* **369**, 529–539 (2013).

58. Neefjes, J., Jongsma, M. L. M., Paul, P. & Bakke, O. Towards a systems understanding of MHC class i and MHC class II antigen presentation. *Nat Rev Immunol* **11**, 823–836 (2011).

59. Goulmy, E. *et al.* Mismatches of minor histocompatibility antigens between HLA-identical donors and recipients and the development of graft-versus-host disease after bone marrow transplantation. *N Engl J Med* **334**, 281–285 (1996).

60. Hill, G. R. & Koyama, M. Cytokines and costimulation in acute graft-versus-host disease. *Blood* **136**, 418–428 (2020).

61. Kim, S. & Reddy, P. Targeting Signal 3 Extracellularly and Intracellularly in Graft-Versus-Host Disease. *Front Immunol* **11**, (2020).

62. Finke, J. *et al.* Standard graft-versus-host disease prophylaxis with or without anti-T-cell globulin in haematopoietic cell transplantation from matched unrelated donors: a randomised, open-label, multicentre phase 3 trial. *Lancet Oncol* **10**, 855–864 (2009).

63. Wagner, J. E., Thompson, J. S., Carter, S. L. & Kernan, N. A. Effect of graft-versus-host disease prophylaxis on 3-year disease-free survival in recipients of unrelated donor bone marrow (T-cell Depletion Trial): a multi-centre, randomised phase II-III trial. *Lancet* **366**, 733–741 (2005).

64. Latis, E. *et al.* Cellular and molecular profiling of T-cell subsets at the onset of human acute GVHD. *Blood Adv* **4**, 3927–3942 (2020).

65. Jiang, H., Fu, D., Bidgoli, A. & Paczesny, S. T Cell Subsets in Graft Versus Host Disease and Graft Versus Tumor. *Front Immunol* **12**, (2021).

66. Guo, W. W. *et al.* Regulatory T Cells in GVHD Therapy. *Front Immunol* **12**, (2021).

67. Jansen, S. A., Nieuwenhuis, E. E. S., Hanash, A. M. & Lindemans, C. A. Challenges and opportunities targeting mechanisms of epithelial injury and recovery in acute intestinal graft-versus-host disease. *Mucosal Immunol* **15**, 605–619 (2022).

68. Roy, J., Platt, J. L. & Weisdorf, D. J. The immunopathology of upper gastrointestinal acute graft-versus-host disease: Lymphoid cells and endothelial adhesion molecules. *Transplantation* **55**, 572–578 (1993).

69. Zhao, K. *et al.* Interleukin-22 aggravates murine acute graft-versus-host disease by expanding effector T cell and reducing regulatory T cell. *Journal of Interferon and Cytokine Research* **34**, 707–715 (2014).

70. Lv, X. *et al.* Comparative efficacy of 20 graft-versus-host disease prophylaxis therapies for patients after hematopoietic stem-cell transplantation: A multiple-treatments network meta-analysis. *Crit Rev Oncol Hematol* **150**, (2020).

71. Gooptu, M. & Antin, J. H. GVHD Prophylaxis 2020. *Front Immunol* **12**, (2021).

72. Törlén, J. *et al.* A prospective randomized trial comparing cyclosporine/methotrexate and tacrolimus/sirolimus as graft-versus-host disease prophylaxis after allogeneic hematopoietic stem cell transplantation. *Haematologica* **101**, 1417–1425 (2016).

73. Bolwell, B. *et al.* A prospective randomized trial comparing cyclosporine and short course methotrexate with cyclosporine and mycophenolate mofetil for GVHD prophylaxis in myeloablative allogeneic bone marrow transplantation. *Bone Marrow Transplant* **34**, 621–625 (2004).

74. Kharfan-Dabaja, M. *et al.* Mycophenolate mofetil versus methotrexate for prevention of graft-versus-host disease in people receiving allogeneic hematopoietic stem cell transplantation. *Cochrane Database of Systematic Reviews* **2014**, (2014).

75. Roldan, E., Perales, M. A. & Barba, P. Allogeneic Stem Cell Transplantation with CD34+ Cell Selection. *Clin Hematol Int* **1**, 154–160 (2019).

76. Kaynar, L. *et al.* TcRαβ-depleted haploidentical transplantation results in adult acute leukemia patients. *Hematology* **22**, 136–144 (2017).

77. Hobbs, G. S. *et al.* Comparison of outcomes at two institutions of patients with ALL receiving ex vivo T-cell-depleted or unmodified allografts. *Bone Marrow Transplant* **50**, 493–498 (2015).

78. Busca, A. & Aversa, F. In-vivo or ex-vivo T cell depletion or both to prevent graft-versus-host disease after hematopoietic stem cell transplantation. *Expert Opin Biol Ther* **17**, 1401–1415 (2017).

79. Mohty, M. Mechanisms of action of antithymocyte globulin: T-cell depletion and beyond. *Leukemia* **21**, 1387–1394 (2007).

80. Wachsmuth, L. P. *et al.* Post-transplantation cyclophosphamide prevents graft-versus-host disease by inducing alloreactive T cell dysfunction and suppression. *J Clin Invest* **129**, 2357–2373 (2019).

81. Malladi, R. K. *et al.* Alemtuzumab markedly reduces chronic GVHD without affecting overall survival in reduced-intensity conditioning sibling allo-SCT for adults with AML. *Bone Marrow Transplant* **43**, 709–715 (2009).

82. Battipaglia, G. *et al.* Posttransplant cyclophosphamide vs antithymocyte globulin in HLA-mismatched unrelated donor transplantation. *Blood* **134**, 892–899 (2019).

83. Besien, K. Van *et al.* Fludarabine-melphalan conditioning for AML and MDS: alemtuzumab reduces acute and chronic GVHD without affecting long-term outcomes. *Biol Blood Marrow Transplant* **15**, 610–617 (2009).

84. Li, A. C. W., Dong, C., Tay, S. T., Ananthakrishnan, A. & Ma, K. S. K. Vedolizumab for acute gastrointestinal graft-versus-host disease: A systematic review and meta-analysis. *Front Immunol* **13**, (2022).

85. Ponce, D. M. *et al.* Guidelines for the Prevention and Management of Graft-versus-Host Disease after Cord Blood Transplantation. *Transplant Cell Ther* **27**, 540–544 (2021).

86. Bacigalupo, A. *et al.* Steroid treatment of acute graft-versus-host disease grade I: A randomized trial. *Haematologica* **102**, 2125–2133 (2017).

87. Hockenbery, D. M. *et al.* A randomized, placebo-controlled trial of oral beclomethasone dipropionate as a prednisone-sparing therapy for gastrointestinal graft-versus-host disease. *Blood* **109**, 4557–4563 (2007).

88. Malard, F., Huang, X. J. & Sim, J. P. Y. Treatment and unmet needs in steroid-refractory acute graft-versus-host disease. *Leukemia* **34**, 1229–1240 (2020).

89. Jagasia, M. *et al.* Ruxolitinib for the treatment of steroid-refractory acute GVHD (REACH1): a multicenter, open-label phase 2 trial. *Blood* **135**, 1739–1749 (2020).

90. Zeiser, R. *et al.* Ruxolitinib for Glucocorticoid-Refractory Acute Graft-versus-Host Disease. *New England Journal of Medicine* **382**, 1800–1810 (2020).

91. Mohty, M. *et al.* Refractory acute graft-versus-host disease: A new working definition beyond corticosteroid refractoriness. *Blood* **136**, 1903–1906 (2020).

92. Farouk, S. S. & Rein, J. L. The Many Faces of Calcineurin Inhibitor Toxicity—What the FK? *Adv Chronic Kidney Dis* **27**, 56–66 (2020).

93. Young, J. A., Pallas, C. R. & Knovich, M. A. Transplant-associated thrombotic microangiopathy: theoretical considerations and a practical approach to an unrefined diagnosis. *Bone Marrow Transplant* **56**, 1805–1817 (2021).

94. Cutler, C. *et al.* Mucositis after allogeneic hematopoietic stem cell transplantation: A cohort study of methotrexate- and non-methotrexate-containing graft-versus-host disease prophylaxis regimens. *Biology of Blood and Marrow Transplantation* **11**, 383–388 (2005).

95. Watkins, B. *et al.* Phase II Trial of Costimulation Blockade With Abatacept for Prevention of Acute GVHD. *J Clin Oncol* **39**, 1865–1877 (2021).

96. Wagner, J. E., Thompson, J. S., Carter, S. L. & Kernan, N. A. Effect of graft-versus-host disease prophylaxis on 3-year disease-free survival in recipients of unrelated donor bone marrow (T-cell Depletion Trial): A multi-centre, randomised phase II-III trial. *Lancet* **366**, 733–741 (2005).

97. Duléry, R. *et al.* Early Cardiac Toxicity Associated With Post-Transplant Cyclophosphamide in Allogeneic Stem Cell Transplantation. *JACC CardioOncol* **3**, 250–259 (2021).

98. Yuan, Y. *et al.* High incidence of resistant breakthrough invasive fungal infections (IFD) in patients treated for acute gastrointestinal graft-versus-host disease (GI GVHD) following allogeneic haematopoietic cell transplantation. *Bone Marrow Transplant* **57**, 1712–1715 (2022).

99. Clark, C. A., Savani, M., Mohty, M. & Savani, B. N. What do we need to know about allogeneic hematopoietic stem cell transplant survivors? *Bone Marrow Transplant* **51**, 1025–1031 (2016).

100. Averbuch, D. *et al.* European guidelines for empirical antibacterial therapy for febrile neutropenic patients in the era of growing resistance: summary of the 2011 4th European Conference on Infections in Leukemia. *Haematologica* **98**, 1826–1835 (2013).

101. Li, J. X. & Cummins, C. L. Fresh insights into glucocorticoid-induced diabetes mellitus and new therapeutic directions. *Nat Rev Endocrinol* **18**, 540–557 (2022).

102. Seibel, M. J., Cooper, M. S. & Zhou, H. Glucocorticoid-induced osteoporosis: mechanisms, management, and future perspectives. *Lancet Diabetes Endocrinol* **1**, 59–70 (2013).

103. Lilley, E. *et al.* ARRIVE 2.0 and the British Journal of Pharmacology: Updated guidance for 2020. *Br J Pharmacol* **177**, 3611–3616 (2020).

104. Pribush, A., Meyerstein, D. & Meyerstein, N. Kinetics of erythrocyte swelling and membrane hole formation in hypotonic media.

105. Bannikov, G. A. *et al.* Biochemical and enzymatic characterization of purified covalent complexes of matrix metalloproteinase-9 and haptoglobin released by bovine granulocytes in vitro. *Am J Vet Res* **68**, 995–1004 (2007).

106. Gea-Banacloche, J. C. Immunomodulation. *Principles of Molecular Medicine* 893–904 (2006) doi:10.1007/978-1-59259-963-9_92/COVER.

107. Wen, C. C., Chen, H. M. & Yang, N. S. Developing Phytocompounds from Medicinal Plants as Immunomodulators. *Adv Bot Res* **62**, 197–272 (2012).

108. Lebish, I. J. & Moraski, R. M. Mechanisms of immunomodulation by drugs. *Toxicol Pathol* **15**, 338–345 (1987).

109. Vernon, L. F. ImmunoTargets and Therapy Dovepress William Bradley Coley, MD, and the phenomenon of spontaneous regression. 7–29 (2018) doi:10.2147/ITT.S163924.

110. Mulder, W. J. M., Ochando, J., Joosten, L. A. B., Fayad, Z. A. & Netea, M. G. Therapeutic targeting of trained immunity HHS Public Access. *Nat Rev Drug Discov* **18**, 553–566 (2019).

111. Chu, W. S. & Ng, J. Immunomodulation in Administration of rAAV: Preclinical and Clinical Adjuvant Pharmacotherapies. *Front Immunol* **12**, (2021).

112. Alsaffar, R. M. *et al.* Immunomodulation: An immune regulatory mechanism in carcinoma therapeutics. *Int Immunopharmacol* **99**, 107984 (2021).

113. Toubai, T. & Magenau, J. Immunopathology and biology-based treatment of steroid-refractory graft-versus-host disease. *Blood* **136**, 429–440 (2020).

114. Hooker, D. S. *et al.* Improved Therapeutic Approaches are Needed to Manage Graft-versus-Host Disease. *Clin Drug Investig* **41**, 929–939 (2021).

115. Zeiser, R. *et al.* Biology-Driven Approaches to Prevent and Treat Relapse of Myeloid Neoplasia after Allogeneic Hematopoietic Stem Cell Transplantation. *Biology of Blood and Marrow Transplantation* **25**, e128–e140 (2019).

116. Chang, Y. J., Zhao, X. Y. & Huang, X. J. Strategies for Enhancing and Preserving Anti-leukemia Effects Without Aggravating Graft-Versus-Host Disease. *Frontiers in immunology* **9**, 3041 (2018).

117. Vandenhove, B. *et al.* How to Make an Immune System and a Foreign Host Quickly Cohabit in Peace? The Challenge of Acute Graft-Versus-Host Disease Prevention After Allogeneic Hematopoietic Cell Transplantation. *Front Immunol* **11**, 1–18 (2020).

118. Samuelsson, Gunnar. Drugs of natural origin : a textbook of pharmacognosy. 551 (1999).

119. Newman, D. J. & Cragg, G. M. Natural Products as Sources of New Drugs over the Nearly Four Decades from 01/1981 to 09/2019. *Journal of natural products* **83**, 770–803 (2020).

120. Leitzmann, C. Characteristics and Health Benefits of Phytochemicals. *Complement Med Res* **23**, 69–74 (2016).

121. Choudhari, A. S., Mandave, P. C., Deshpande, M., Ranjekar, P. & Prakash, O. Phytochemicals in Cancer Treatment: From Preclinical Studies to Clinical Practice. doi:10.3389/fphar.2019.01614.

122. Ribeiro, D. *et al.* Immunomodulatory Effects of Flavonoids in the Prophylaxis and Treatment of Inflammatory Bowel Diseases: A Comprehensive Review. *Curr Med Chem* **25**, 3374–3412 (2018).

123. Al-Khayri, J. M. *et al.* Flavonoids as Potential Anti-Inflammatory Molecules: A Review. *Molecules* **27**, (2022).

124. Kumazawa, Y., Kawaguchi, K. & Takimoto, H. Immunomodulating effects of flavonoids on acute and chronic inflammatory responses caused by tumor necrosis factor alpha. *Curr Pharm Des* **12**, 4271–4279 (2006).

125. Di Pierro, F. *et al.* Possible Therapeutic Effects of Adjuvant Quercetin Supplementation Against Early-Stage COVID-19 Infection: A Prospective, Randomized, Controlled, and Open-Label Study. *Int J Gen Med* **14**, 2359–2366 (2021).

126. Heinz, S. A., Henson, D. A., Austin, M. D., Jin, F. & Nieman, D. C. Quercetin supplementation and upper respiratory tract infection: A randomized community clinical trial. *Pharmacol Res* **62**, 237–242 (2010).

127. Shohan, M. *et al.* The therapeutic efficacy of quercetin in combination with antiviral drugs in hospitalized COVID-19 patients: A randomized controlled trial. *Eur J Pharmacol* **914**, (2022).

128. Almatrood, S. A. *et al.* Potential Therapeutic Targets of Epigallocatechin Gallate (EGCG), the Most Abundant Catechin in Green Tea, and Its Role in the Therapy of Various Types of Cancer. *Molecules* **25**, (2020).

129. Brenjian, S. *et al.* Resveratrol treatment in patients with polycystic ovary syndrome decreased pro-inflammatory and endoplasmic reticulum stress markers. *American Journal of Reproductive Immunology* **83**, (2020).

130. Moussa, C. *et al.* Resveratrol regulates neuro-inflammation and induces adaptive immunity in Alzheimer's disease. *J Neuroinflammation* **14**, (2017).

131. Chew, B. P. & Park, J. S. Carotenoid Action on the Immune Response. *Journal of Nutrition* **134**, (2004).

132. Milani, A., Basirnejad, M., Shahbazi, S. & Bolhassani, A. Carotenoids: biochemistry, pharmacology and treatment. *Br J Pharmacol* **174**, 1290–1324 (2017).

133. Chamani, S. *et al.* Immunomodulatory effects of curcumin in systemic autoimmune diseases. *Phytotherapy Research* **36**, 1616–1632 (2022).

134. White, P. T., Subramanian, C., Motiwala, H. F. & Cohen, M. S. Natural Withanolides in the Treatment of Chronic Diseases. in *Advances in experimental medicine and biology* vol. 928 329–373 (Adv Exp Med Biol, 2016).

135. Wang, S. *et al.* Immunomodulatory Effects of Green Tea Polyphenols. *Molecules 2021, Vol. 26, Page 3755* **26**, 3755 (2021).

136. Dickson, M. & Gagnon, J. P. Key factors in the rising cost of new drug discovery and development. *Nat Rev Drug Discov* **3**, 417–429 (2004).

137. Pina, A. S., Hussain, A. & Roque, A. C. A. An historical overview of drug discovery. *Methods Mol Biol* **572**, 3–12 (2009).

138. Pereira, D. A. & Williams, J. A. Origin and evolution of high throughput screening. *Br J Pharmacol* **152**, 53–61 (2007).

139. Entzeroth, M., Flotow, H. & Condron, P. Overview of high-throughput screening. *Curr Protoc Pharmacol* **Chapter 9**, (2009).

140. Kurata, M., Yamamoto, K., Moriarity, B. S., Kitagawa, M. & Largaespada, D. A. CRISPR/Cas9 library screening for drug target discovery. *J Hum Genet* **63**, 179–186 (2018).

141. Zielinski, J. M., Luke, J. J., Guglietta, S. & Krieg, C. High Throughput Multi-Omics Approaches for Clinical Trial Evaluation and Drug Discovery. *Front Immunol* **12**, (2021).

142. Mayr, L. M. & Bojanic, D. Novel trends in high-throughput screening. *Curr Opin Pharmacol* **9**, 580–588 (2009).

143. Wilson, B. A. P., Thornburg, C. C., Henrich, C. J., Grkovic, T. & O'Keefe, B. R. Creating and screening natural product libraries. *Nat Prod Rep* **37**, 893–918 (2020).

144. Thornburg, C. C. *et al.* NCI Program for Natural Product Discovery: A Publicly-Accessible Library of Natural Product Fractions for High-Throughput Screening. *ACS Chem Biol* **13**, 2484–2497 (2018).

145. Najmi, A., Javed, S. A., Al Bratty, M. & Alhazmi, H. A. Modern Approaches in the Discovery and Development of Plant-Based Natural Products and Their Analogues as Potential Therapeutic Agents. *Molecules* **27**, (2022).

146. Gong, Z. *et al.* Compound Libraries: Recent Advances and Their Applications in Drug Discovery. *Curr Drug Discov Technol* **14**, (2017).

147. Benjaskulluecha, S. *et al.* Screening of compounds to identify novel epigenetic regulatory factors that affect innate immune memory in macrophages. *Sci Rep* **12**, (2022).

148. Tsai, C.-C. *et al.* Cytomic screening of immuno-modulating activity compounds from Calocedrus formosana. *Comb Chem High Throughput Screen* **11**, 834–842 (2008).

149. The discovery of novel immunomodulatory medicinal plants by combination of historical text reviews and immunological screening assays. *J Ethnopharmacol* **296**, 115402 (2022).

150. Steer, S., Lasek, W., Clothier, R. H. & Balls, M. An in vitro test for immunomodulators? *Toxicol In Vitro* **4**, 360–362 (1990).

151. Langenkamp, A., Messi, M., Lanzavecchia, A. & Sallusto, F. Kinetics of dendritic cell activation: impact on priming of TH1, TH2 and nonpolarized T cells. *Nature Immunology 2000 1:4* **1**, 311–316 (2000).

152. McMillin, D. W. *et al.* Compartment-Specific Bioluminescence Imaging platform for the high-throughput evaluation of antitumor immune function. *Blood* **119**, (2012).

153. Li, Z. *et al.* Screening Immunoactive Compounds of Ganoderma lucidum Spores by Mass Spectrometry Molecular Networking Combined With in vivo Zebrafish Assays. *Front Pharmacol* **11**, (2020).

154. Oh, K. *et al.* A receptor-independent, cell-based JAK activation assay for screening for JAK3-specific inhibitors. *J Immunol Methods* **354**, 45–52 (2010).

155. Khatua, S., Simal-Gandara, J. & Acharya, K. Understanding immune-modulatory efficacy in vitro. *Chem Biol Interact* **352**, (2022).

156. Mohseny, A. B. & Hogendoorn, P. C. W. Zebrafi sh as a model for human osteosarcoma. *Adv Exp Med Biol* **804**, 221–236 (2014).

157. Medetgul-Ernar, K. & Davis, M. M. Standing on the shoulders of mice. *Immunity* **55**, 1343–1353 (2022).

158. Smith-Garvin, J. E., Koretzky, G. A. & Jordan, M. S. T cell activation. *Annu Rev Immunol* **27**, 591–619 (2009).

159. Ash, R. C. *et al.* Bone marrow transplantation from related donors other than HLA-identical siblings: Effect of T cell depletion. *Bone Marrow Transplant* **7**, 443–452 (1991).

160. Goldman, J. M. *et al.* Bone marrow transplantation for chronic myelogenous leukemia in chronic phase. Increased risk for relapse associated with T-cell depletion. *Ann Intern Med* **108**, 806–814 (1988).

161. Horowitz, M. M. *et al.* Graft-versus-leukemia reactions after bone marrow transplantation. *Blood* **75**, 555–562 (1990).

162. Henig, I. & Zuckerman, T. Hematopoietic stem cell transplantation-50 years of evolution and future perspectives. *Rambam Maimonides Med J* **5**, e0028 (2014).

163. Shouval, R. *et al.* Outcomes of allogeneic haematopoietic stem cell transplantation from HLA-matched and alternative donors: a European Society for Blood and Marrow Transplantation registry retrospective analysis. *Lancet Haematol* **6**, e573–e584 (2019).

164. Vandenhove, B. *et al.* How to Make an Immune System and a Foreign Host Quickly Cohabit in Peace? The Challenge of Acute Graft- Versus-Host Disease Prevention After Allogeneic Hematopoietic Cell Transplantation. *Front Immunol* **11**, (2020).

165. Boyman, O. & Sprent, J. The role of interleukin-2 during homeostasis and activation of the immune system. *Nat Rev Immunol* **12**, 180–190 (2012).

166. Spolski, R., Li, P. & Leonard, W. J. Biology and regulation of IL-2: from molecular mechanisms to human therapy. *Nature Reviews Immunology 2018 18:10* **18**, 648–659 (2018).

167. Fidler, J. M. *et al.* Immunosuppressive activity of the Chinese medicinal plant Tripterygium wilfordii. III. Suppression of graft-versus-host disease in murine allogeneic bone marrow transplantation by the PG27 extract. *Transplantation* **74**, 445–457 (2002).

168. Chen, B. J., Liu, C., Cui, X., Fidler, J. M. & Chao, N. J. Prevention of graft-versus-host disease by a novel immunosuppressant, PG490-88, through inhibition of alloreactive T cell expansion. *Transplantation* **70**, 1442–1447 (2000).

169. Chen, X., Murakami, T., Oppenheim, J. J. & Howard, O. M. Z. Triptolide, a constituent of immunosuppressive Chinese herbal medicine, is a potent suppressor of dendritic-cell maturation and trafficking. *Blood* **106**, 2409–2416 (2005).

170. Xi, C., Peng, S., Wu, Z., Zhou, Q. & Zhou, J. Toxicity of triptolide and the molecular mechanisms involved. *Biomed Pharmacother* **90**, 531–541 (2017).

171. Seca, A. M. L. & Pinto, D. C. G. A. Plant Secondary Metabolites as Anticancer Agents: Successes in Clinical Trials and Therapeutic Application. *Int J Mol Sci* **19**, (2018).

172. FRESNO, M., JIMÉNEZ, A. & VÁZQUEZ, D. Inhibition of Translation in Eukaryotic Systems by Harringtonine. *Eur J Biochem* **72**, 323–330 (1977).

173. Quintás-Cardama, A. & Cortes, J. Homoharringtonine for the treatment of chronic myelogenous leukemia. *Expert Opin Pharmacother* **9**, 1029–1037 (2008).

174. Mi, R., Zhao, J., Chen, L., Wei, X. & Liu, J. Efficacy and Safety of Homoharringtonine for the Treatment of Acute Myeloid Leukemia: A Meta-analysis. *Clin Lymphoma Myeloma Leuk* **21**, e752–e767 (2021).

175. Xu, W. *et al.* Immunosuppressive effects of demethylzeylasteral in a rat kidney transplantation model. *Int Immunopharmacol* **9**, 996–1001 (2009).

176. An, H. *et al.* Evaluation of Immunosuppressive Activity of Demethylzeylasteral in a Beagle Dog Kidney Transplantation Model. *Cell Biochem Biophys* **73**, 673–679 (2015).

177. Fan, D., Parhira, S., Zhu, G. Y., Jiang, Z. H. & Bai, L. P. Triterpenoids from the stems of Tripterygium regelii. *Fitoterapia* **113**, 69–73 (2016).

178. Ahmad, T. & Suzuki, Y. J. Juglone in Oxidative Stress and Cell Signaling. *Antioxidants (Basel)* **8**, (2019).

179. Cho, Y. A. *et al.* PIN1 inhibition suppresses osteoclast differentiation and inflammatory responses. *J Dent Res* **94**, 371–380 (2015).

180. Peng, X., Nie, Y., Wu, J., Huang, Q. & Cheng, Y. Juglone prevents metabolic endotoxemia-induced hepatitis and neuroinflammation via suppressing TLR4/NF-κB signaling pathway in high-fat diet rats. *Biochem Biophys Res Commun* **462**, 245–250 (2015).

181. Reese, S. *et al.* The Pin 1 inhibitor juglone attenuates kidney fibrogenesis via Pin 1-independent mechanisms in the unilateral ureteral occlusion model. *Fibrogenesis Tissue Repair* **3**, 1 (2010).

182. Seshadri, P., Rajaram, A. & Rajaram, R. Plumbagin and juglone induce caspase-3-dependent apoptosis involving the mitochondria through ROS generation in human peripheral blood lymphocytes. *Free Radic Biol Med* **51**, 2090–2107 (2011).

183. Kim, N. H. *et al.* Juglone Suppresses LPS-induced Inflammatory Responses and NLRP3 Activation in Macrophages. *Molecules* **25**, (2020).

184. Gaikwad, S., Pawar, Y., Banerjee, S. & Kulkarni, S. Potential immunomodulatory effect of allelochemical juglone in mice vaccinated with BCG. *Toxicon* **157**, 43–52 (2019).

185. NCI. Summary of data for chemical selection - decane. *CAS No. 124-18-5* 21 https://ntp.niehs.nih.gov/ntp/htdocs/chem_background/exsumpdf/apigenin_508.pdf (2002).

186. Jahanban-Esfahlan, Ostadrahimi, Tabibiazar & Amarowicz. A Comprehensive Review on the Chemical Constituents and Functional Uses of Walnut (Juglans spp.) Husk. *Int J Mol Sci* **20**, 3920 (2019).

187. Bi, D. *et al.* Phytochemistry, bioactivity and potential impact on health of Juglans: The original plant of walnut. *Nat Prod Commun* **11**, 869–880 (2016).

188. Croitoru, A., Ficai, D., Craciun, L., Ficai, A. & Andronescu, E. Evaluation and Exploitation of Bioactive Compounds of Walnut, Juglans regia. *Curr Pharm Des* **25**, 119–131 (2019).

189. Ahmad, T. & Suzuki, Y. J. Juglone in Oxidative Stress and Cell Signaling. *Antioxidants (Basel)* **8**, (2019).

190. Use of 5-hydroxynaphthoquinones for dyeing human keratin fibres. (1983).

191. Pannell, L., Spring, S., McMahon, J. B. & Cragg, G. M. Antiviral naphthoquinone compounds, compositions and uses thereof. *J Antibiot (Tokyo)* **115**, 257–266 (1993).

192. Bolton, J. L., Trush, M. A., Penning, T. M., Dryhurst, G. & Monks, T. J. Role of quinones in toxicology. *Chem Res Toxicol* **13**, 135–160 (2000).

193. Bolton, J. L. & Dunlap, T. Formation and biological targets of quinones: Cytotoxic versus cytoprotective effects. *Chem Res Toxicol* **30**, 13–37 (2017).

194. Kumagai, Y., Shinkai, Y., Miura, T. & Cho, A. K. The chemical biology of naphthoquinones and its environmental implications. *Annu Rev Pharmacol Toxicol* **52**, 221–247 (2012).

195. Kelly, R. A. *et al.* Modelling changes in glutathione homeostasis as a function of quinone redox metabolism. *Sci Rep* **9**, (2019).

196. Widhalm, J. R. & Rhodes, D. Biosynthesis and molecular actions of specialized 1,4-naphthoquinone natural products produced by horticultural plants. *Hortic Res* **3**, (2016).

197. Klotz, L. O., Hou, X. & Jacob, C. 1,4-naphthoquinones: from oxidative damage to cellular and inter-cellular signaling. *Molecules (Basel, Switzerland)* **19**, 14902–14918 (2014).

198. Catanzaro, E., Greco, G., Potenza, L., Calcabrini, C. & Fimognari, C. Natural Products to Fight Cancer: A Focus on Juglans regia. *Toxins (Basel)* **10**, (2018).

199. Segura-Aguilar, J., Jönsson, K., Tidefelt, U. & Paul, C. The cytotoxic effects of 5-OH-1,4-naphthoquinone and 5,8-diOH-1,4-naphthoquinone on doxorubicin-resistant human leukemia cells (HL-60). *Leuk Res* **16**, 631–637 (1992).

200. So, K. Y. & Oh, S. H. Prolyl isomerase Pin1 regulates cadmium-induced autophagy via ubiquitin-mediated post-translational stabilization of phospho-Ser GSK3αβ in human hepatocellular carcinoma cells. *Biochem Pharmacol* **98**, 511–521 (2015).

201. Wang, P. *et al.* Juglone induces apoptosis and autophagy via modulation of mitogen-activated protein kinase pathways in human hepatocellular carcinoma cells. *Food and Chemical Toxicology* **116**, 40–50 (2018).

202. Santa-María, I. *et al.* Effect of quinones on microtubule polymerization: A link between oxidative stress and cytoskeletal alterations in Alzheimer's disease. *Biochim Biophys Acta Mol Basis Dis* **1740**, 472–480 (2005).

203. Ji, Y. B., Xin, G. S., Qu, Z. Y., Zou, X. & Yu, M. Mechanism of juglone-induced apoptosis of MCF-7 cells by the mitochondrial pathway. *Genetics and Molecular Research* **15**, (2016).

204. Wang, C. *et al.* Anticancer activity of synthesized 5-benzyl juglone on selected human cancer cell lines. *Anticancer Agents Med Chem* **22**, (2022).

205. Sajadimajd, S., Yazdanparast, R. & Roshanzamir, F. Augmentation of oxidative stress-induced apoptosis in MCF7 cells by ascorbate–tamoxifen and/or ascorbate–juglone treatments. *In Vitro Cell Dev Biol Anim* **52**, 193–203 (2016).

206. Poudel, M., Bhattarai, P. Y., Shrestha, P. & Choi, H. S. Regulation of Interleukin-36γ/IL-36R Signaling Axis by PIN1 in Epithelial Cell Transformation and Breast Tumorigenesis. *Cancers (Basel)* **14**, (2022).

207. Meskelevicius, D., Sidlauskas, K., Bagdonaviciute, R., Liobikas, J. & Majiene, D. Juglone Exerts Cytotoxic, Anti-proliferative and Anti-invasive Effects on Glioblastoma Multiforme in a Cell Culture Model. *Anticancer Agents Med Chem* **16**, 1190–1197 (2016).

208. Atabay, K. D., Yildiz, M. T., Avsar, T., Karabay, A. & Kiliç, T. Knockdown of Pin1 leads to reduced angiogenic potential and tumorigenicity in glioblastoma cells. *Oncol Lett* **10**, 2385–2389 (2015).

209. Fiorito, S. *et al.* Novel juglone and plumbagin 5-O derivatives and their in vitro growth inhibitory activity against apoptosis-resistant cancer cells. *Bioorg Med Chem Lett* **26**, 334–337 (2016).

210. Wu, J. *et al.* Juglone induces apoptosis of tumor stem-like cells through ROS-p38 pathway in glioblastoma. *BMC Neurol* **17**, (2017).

211. Zhang, A. *et al.* Protein sumoylation with SUMO1 promoted by Pin1 in glioma stem cells augments glioblastoma malignancy. *Neuro Oncol* **22**, 1809–1821 (2020).

212. Zhang, J. *et al.* The Anti-Glioma Effect of Juglone Derivatives through ROS Generation. *Front Pharmacol* **13**, 911760 (2022).

213. Wang, J., Liu, K., Wang, X. F. & Sun, D. J. Juglone reduces growth and migration of U251 glioblastoma cells and disrupts angiogenesis. *Oncol Rep* **38**, 1959–1966 (2017).

214. Majiene, D., Kuseliauskyte, J., Stimbirys, A. & Jekabsone, A. Comparison of the effect of native 1,4-naphthoquinones plumbagin, menadione, and lawsone on viability, redox status, and mitochondrial functions of C6 glioblastoma cells. *Nutrients* **11**, (2019).

215. Barciszewska, A.-M., Belter, A., Gawrońska, I., Giel-Pietraszuk, M. & Naskręt-Barciszewska, M. Z. Juglone in Combination with Temozolomide Shows a Promising Epigenetic Therapeutic Effect on the Glioblastoma Cell Line. *Int J Mol Sci* **24**, (2023).

216. Wahedi, H. M., Lee, T. H., Moon, E. Y. & Kim, S. Y. Juglone up-regulates sirt1 in skin cells under normal and UVB irradiated conditions. *J Dermatol Sci* **81**, 210–212 (2016).

217. Klaus, V. *et al.* 1,4-Naphthoquinones as inducers of oxidative damage and stress signaling in HaCaT human keratinocytes. *Arch Biochem Biophys* **496**, 93–100 (2010).

218. Inbaraj, J. J. & Chignell, C. F. Cytotoxic Action of Juglone and Plumbagin: A Mechanistic Study Using HaCaT Keratinocytes. *Chem Res Toxicol* **17**, 55–62 (2004).

219. Kapoor, N., Kandwal, P., Sharma, G. & Gambhir, L. Redox ticklers and beyond: Naphthoquinone repository in the spotlight against inflammation and associated maladies. *Pharmacol Res* **174**, (2021).

220. O'Brien, P. J. Molecular mechanisms of quinone cytotoxicity. *Chemico-Biological Interactions* **80**, 1–41 (1991).

221. Olson, K. R. *et al.* Redox and Nucleophilic Reactions of Naphthoquinones with Small Thiols and Their Effects on Oxidization of H2S to Inorganic and Organic Hydropolysulfides and Thiosulfate. *Int J Mol Sci* **24**, (2023).

222. Diaz-Vivancos, P., De Simone, A., Kiddle, G. & Foyer, C. H. Glutathione - Linking cell proliferation to oxidative stress. *Free Radical Biology and Medicine* **89**, 1154–1164 (2015).

223. Galas, M. C. *et al.* The peptidylprolyl cis/trans-isomerase Pin1 modulates stress-induced dephosphorylation of Tau in neurons. Implication in a pathological mechanism related to Alzheimer disease. *J Biol Chem* **281**, 19296–19304 (2006).

224. Zhou, D. J. *et al.* Hepatoprotective effect of juglone on dimethylnitrosamine-induced liver fibrosis and its effect on hepatic antioxidant defence and the expression levels of α-SMA and collagen III. *Mol Med Rep* **12**, 4095–4102 (2015).

225. Reese, S. *et al.* The Pin 1 inhibitor juglone attenuates kidney fibrogenesis via Pin 1-independent mechanisms in the unilateral ureteral occlusion model. *Fibrogenesis Tissue Repair* **3**, (2010).

226. Pandareesh, M. D., Chauhan, V. & Chauhan, A. Walnut Supplementation in the Diet Reduces Oxidative Damage and Improves Antioxidant Status in Transgenic Mouse Model of Alzheimer's Disease. *J Alzheimers Dis* **64**, 1295–1305 (2018).

227. Djamali, A. Oxidative stress as a common pathway to chronic tubulointerstitial injury in kidney allografts. *Am J Physiol Renal Physiol* **293**, (2007).

228. Vaezi, A. *et al.* In vitro activity of juglone (5-hydroxy-1,4-naphthoquinone) against both fluconazole-resistant and susceptible Candida isolates. *Rev Iberoam Micol* **39**, 50–53 (2022).

229. Wang, K. *et al.* Natural Products for Pesticides Discovery: Structural Diversity Derivation and Biological Activities of Naphthoquinones Plumbagin and Juglone. *Molecules* **28**, (2023).

230. Wan, Y. *et al.* Antibacterial Activity of Juglone Revealed in a Wound Model of Staphylococcus aureus Infection. *Int J Mol Sci* **24**, (2023).

231. Nowicka, B. *et al.* Impact of cytotoxic plant naphthoquinones, juglone, plumbagin, lawsone and 2-methoxy-1,4-naphthoquinone, on Chlamydomonas reinhardtii reveals the biochemical mechanism of juglone toxicity by rapid depletion of plastoquinol. *Plant Physiology and Biochemistry* **197**, (2023).

232. Niaz, F. *et al.* Antibacterial and Antibiofilm Activity of Juglone Derivatives against Enterococcus faecalis: An in Silico and in Vitro Approach. *Biomed Res Int* **2022**, (2022).

233. Fatima, M. *et al.* Quorum Quenchers from Reynoutria japonica in the Battle against Methicillin-Resistant Staphylococcus aureus (MRSA). *Molecules* **28**, (2023).

234. Lee, T. H., Pastorino, L. & Lu, K. P. Peptidyl-prolyl cis-trans isomerase Pin1 in ageing, cancer and Alzheimer disease. *Expert Rev Mol Med* **13**, (2011).

235. Inoue, K. ichiro, Takano, H. & Kumagai, Y. Pin1 blockade in asthma by naphthoquinone? *Journal of Allergy and Clinical Immunology* **121**, 1064 (2008).

236. Jeong, H. G. *et al.* Novel role of Pin1 induction in type II collagen-mediated rheumatoid arthritis. *J Immunol* **183**, 6689–6697 (2009).

237. Wu, Y. *et al.* Anti-Diabetic Atherosclerosis by Inhibiting High Glucose-Induced Vascular Smooth Muscle Cell Proliferation via Pin1/BRD4 Pathway. *Oxid Med Cell Longev* **2020**, (2020).

238. Ghosh, A. *et al.* The peptidyl-prolyl isomerase Pin1 up-regulation and proapoptotic function in dopaminergic neurons: relevance to the pathogenesis of Parkinson disease. *J Biol Chem* **288**, 21955–21971 (2013).

239. Nakada, S. *et al.* Roles of Pin1 as a Key Molecule for EMT Induction by Activation of STAT3 and NF-κB in Human Gallbladder Cancer. *Ann Surg Oncol* **26**, 907–917 (2019).

240. Sun, Q. *et al.* Pin1 promotes pancreatic cancer progression and metastasis by activation of NF-κB-IL-18 feedback loop. *Cell Prolif* **53**, (2020).

241. Wu, K. J. *et al.* Small Molecule Pin1 Inhibitor Blocking NF-κB Signaling in Prostate Cancer Cells. *Chem Asian J* **13**, 275–279 (2018).

242. Boussetta, T. *et al.* The prolyl isomerase Pin1 acts as a novel molecular switch for TNF-α-induced priming of the NADPH oxidase in human neutrophils. *Blood* **116**, 5795–5802 (2010).

243. Liu, M. *et al.* The Prolyl Isomerase Pin1 Controls Lipopolysaccharide-Induced Priming of NADPH Oxidase in Human Neutrophils. *Front Immunol* **10**, (2019).

244. Fang, F. *et al.* Juglone suppresses epithelial-mesenchymal transition in prostate cancer cells via the protein kinase B/glycogen synthase kinase-3β/Snail signaling pathway. *Oncol Lett* **16**, 2579–2584 (2018).

245. Kim, N. H. *et al.* Juglone Suppresses LPS-induced Inflammatory Responses and NLRP3 Activation in Macrophages. *Molecules* **25**, 1–12 (2020).

246. Chen, S., Wu, X. & Yu, Z. Juglone Suppresses Inflammation and Oxidative Stress in Colitis Mice. *Front Immunol* **12**, 1–10 (2021).

247. Wang, H. *et al.* Juglone eliminates MDSCs accumulation and enhances antitumor immunity. *Int Immunopharmacol* **73**, 118–127 (2019).

248. Gaikwad, S., Pawar, Y., Banerjee, S. & Kulkarni, S. Potential immunomodulatory effect of allelochemical juglone in mice vaccinated with BCG. *Toxicon* **157**, 43–52 (2019).

249. Liu, M. *et al.* The Prolyl Isomerase Pin1 Controls Lipopolysaccharide-Induced Priming of NADPH Oxidase in Human Neutrophils. *Front Immunol* **10**, 1–12 (2019).

250. Chao, S. H., Greenleaf, A. L. & Price, D. H. Juglone, an inhibitor of the peptidyl-prolyl isomerase Pin1, also directly blocks transcription. *Nucleic Acids Res* **29**, 767–773 (2001).

251. Nakatsu, Y. *et al.* Development of Pin1 Inhibitors and their Potential as Therapeutic Agents. *Curr Med Chem* **27**, 3314–3329 (2018).

252. Matsunaga, Y. *et al.* Pathological role of pin1 in the development of dss-induced colitis. *Cells* **10**, 4–13 (2021).

253. Nakatsu, Y. *et al.* Physiological and Pathogenic Roles of Prolyl Isomerase Pin1 in Metabolic Regulations via Multiple Signal Transduction Pathway Modulations. *Int J Mol Sci* **17**, (2016).

254. Yu, H., Jiang, G., Hu, W. & Xu, C. Pin1 aggravates renal injury induced by ischemia and reperfusion in rats via Nrf2/HO-1 mediated endoplasmic reticulum stress. *Acta Cir Bras* **37**, (2022).

255. Bolton, J. L., Trush, M. A., Penning, T. M., Dryhurst, G. & Monks, T. J. Role of Quinones in Toxicology†. *Chem Res Toxicol* **13**, 135–160 (2000).

256. Bolton, J. L. & Dunlap, T. Formation and biological targets of quinones: Cytotoxic versus cytoprotective effects. *Chem Res Toxicol* **30**, 13–37 (2017).

257. Lou, P. *et al.* Mitochondrial uncouplers with an extraordinary dynamic range. **140**, 129–140 (2007).

258. He, F., Ru, X. & Wen, T. NRF2, a Transcription Factor for Stress Response and Beyond. *International journal of molecular sciences* **21**, 1–23 (2020).

259. Hua, Y. *et al.* Juglone regulates gut microbiota and Th17/Treg balance in DSS-induced ulcerative colitis. *Int Immunopharmacol* **97**, (2021).

260. Liang, C. *et al.* Mechanical Regulation of Redox Balance via the Induction of the PIN1/NRF2/ARE Axis in Pancreatic Cancer. *Int J Mol Sci* **24**, (2023).

261. Ishii, T., Warabi, E. & Mann, G. E. Stress Activated MAP Kinases and Cyclin-Dependent Kinase 5 Mediate Nuclear Translocation of Nrf2 via Hsp90α-Pin1-Dynein Motor Transport Machinery. *Antioxidants (Basel)* **12**, (2023).

262. Funes, S. C. *et al.* Naturally Derived Heme-Oxygenase 1 Inducers and Their Therapeutic Application to Immune-Mediated Diseases. *Front Immunol* **11**, (2020).

263. Yu, M. *et al.* High expression of heme oxygenase-1 in target organs may attenuate acute graft-versus-host disease through regulation of immune balance of TH17/Treg. *Transpl Immunol* **37**, 10–17 (2016).

264. Mcdaid, J. *et al.* Heme oxygenase-1 modulates the allo-immune response by promoting activation-induced cell death of T cells. *FASEB J* **19**, 1–22 (2005).

265. Westfall, B. A., Russell, R. L. & Auyong, T. K. Depressant agent from walnut hulls. *Science (1979)* **134**, 1617 (1961).

266. Aithal, K. B., Kumar, S., Rao, B. N., Udupa, N. & Rao, S. B. S. Tumor growth inhibitory effect of juglone and its radiation sensitizing potential: In vivo and in vitro studies. *Integr Cancer Ther* **11**, 68–80 (2012).

267. Aithal, B. K. *et al.* Evaluation of pharmacokinetic, biodistribution, pharmacodynamic, and toxicity profile of free juglone and its sterically stabilized liposomes. *J Pharm Sci* **100**, 3517–3528 (2011).

268. Kiran Aithal, B., Sunil Kumar, M. R., Nageshwar Rao, B., Udupa, N. & Satish Rao, B. S. Juglone, a naphthoquinone from walnut, exerts cytotoxic and genotoxic effects against cultured melanoma tumor cells. *Cell Biol Int* **33**, 1039–1049 (2009).

269. Boelkins, J. N., Everson, L. K. & Auyong, T. K. Effects of intravenous juglone in the dog. *Toxicon* **6**, 99–102 (1968).

270. Seetha, A., Devaraj, H. & Sudhandiran, G. Indomethacin and juglone inhibit inflammatory molecules to induce apoptosis in colon cancer cells. *J Biochem Mol Toxicol* **34**, (2020).

271. Wang, P. *et al.* Juglone induces apoptosis and autophagy via modulation of mitogen-activated protein kinase pathways in human hepatocellular carcinoma cells. *Food and Chemical Toxicology* **116**, 40–50 (2018).

272. Seetha, A., Devaraj, H. & Sudhandiran, G. Effects of combined treatment with Indomethacin and Juglone on AOM/DSS induced colon carcinogenesis in Balb/c mice: Roles of inflammation and apoptosis. *Life Sci* **264**, (2021).

273. Wong, J. *et al.* Suspensions for intravenous (IV) injection: A review of development, preclinical and clinical aspects. *Adv Drug Deliv Rev* **60**, 939–954 (2008).

274. Ourique, F. *et al.* DNA damage and inhibition of akt pathway in mcf-7 cells and ehrlich tumor in mice treated with 1,4-naphthoquinones in combination with ascorbate. *Oxid Med Cell Longev* **2015**, (2015).

275. Patel, D., Zode, S. S. & Bansal, A. K. Formulation aspects of intravenous nanosuspensions. *Int J Pharm* **586**, 119555 (2020).

276. Lipinski, C. A. Drug-like properties and the causes of poor solubility and poor permeability. *J Pharmacol Toxicol Methods* **44**, 235–249 (2000).

277. Guan, L. *et al.* ADMET-score – a comprehensive scoring function for evaluation of chemical drug-likeness. *Medchemcomm* **10**, 148 (2019).

278. Fernandes, J. & Gattass, C. R. Topological Polar Surface Area Defines Substrate Transport by Multidrug Resistance Associated Protein 1 (MRP1/ABCC1). *J Med Chem* **52**, 1214–1218 (2009).

279. Xiong, G. *et al.* ADMETlab 2.0: an integrated online platform for accurate and comprehensive predictions of ADMET properties. *Nucleic Acids Res* **49**, W5–W14 (2021).

280. *Test No. 423: Acute Oral toxicity - Acute Toxic Class Method*. (OECD, 2002). doi:10.1787/9789264071001-en.

281. Test No. 407: Repeated Dose 28-day Oral Toxicity Study in Rodents. (2008) doi:10.1787/9789264070684-EN.

282. Conducting a Human Health Risk Assessment | US EPA. https://www.epa.gov/risk/conducting-human-health-risk-assessment.

283. Hardy, A. *et al.* Update: use of the benchmark dose approach in risk assessment. *EFSA Journal* **15**, e04658 (2017).

284. Buist, H. E., von Bölcsházy, G. F., Dammann, M., Telman, J. & Rennen, M. A. J. Derivation of the minimal magnitude of the Critical Effect Size for continuous toxicological parameters from within-animal variation in control group data. *Regulatory Toxicology and Pharmacology* **55**, 139–150 (2009).

285. Dekkers, S., Telman, J., Rennen, M. A. J., Appel, M. J. & De Heer, C. Within-animal variation as an indication of the minimal magnitude of the critical effect size for continuous toxicological parameters applicable in the benchmark dose approach. *Risk Anal* **26**, 867–880 (2006).

286. Slob, W. Benchmark dose and the three Rs. Part II. Consequences for study design and animal use. *Crit Rev Toxicol* **44**, 568–580 (2014).

287. Haber, L. T. *et al.* Benchmark dose (BMD) modeling: current practice, issues, and challenges. *Crit Rev Toxicol* **48**, 387–415 (2018).

288. Baralić, K. *et al.* Relevance and evaluation of the benchmark dose in toxicology. *Arh Farm (Belgr)* **70**, 130–141 (2020).

289. Crump, K. S. Benchmark Analysis. in *Encyclopedia of Quantitative Risk Analysis and Assessment* (John Wiley & Sons, Ltd, 2008). doi:10.1002/9780470061596.risk0253.

290. Slob, W. A general theory of effect size, and its consequences for defining the benchmark response (BMR) for continuous endpoints. *https://doi.org/10.1080/10408444.2016.1241756* **47**, 342–351 (2016).

291. PROAST | RIVM. https://www.rivm.nl/en/proast.

292. Varewyck, M. & Verbeke, T. Software for Benchmark Dose Modelling. *EFSA Supporting Publications* **16**, (2019).

293. Slob RIVM, W. Joint project on Benchmark Dose modelling with RIVM. *EFSA Supporting Publications* **15**, 1497E (2018).

294. Crump, K. S. Calculation of Benchmark Doses from Continuous Data. *Risk Analysis* **15**, 79–89 (1995).

295. Fentener van Vlissingen, J. *et al.* The reporting of clinical signs in laboratory animals. *Laboratory Animals* vol. 49 267–283 Preprint at https://doi.org/10.1177/0023677215584249 (2015).

296. Ahmad, T. & Suzuki, Y. J. Juglone in oxidative stress and cell signaling. *Antioxidants* vol. 8 Preprint at https://doi.org/10.3390/antiox8040091 (2019).

297. Bolton, J. L., Trush, M. A., Penning, T. M., Dryhurst, G. & Monks, T. J. Role of quinones in toxicology. *Chem Res Toxicol* **13**, 135–160 (2000).

298. Saling, S. C., Comar, J. F., Mito, M. S., Peralta, R. M. & Bracht, A. Actions of juglone on energy metabolism in the rat liver. *Toxicol Appl Pharmacol* **257**, 319–327 (2011).

299. Chen, L. J., Lebetkin, E. H. & Burka, L. T. Metabolism and disposition of juglone in male F344 rats. *Xenobiotica* **35**, 1019–1034 (2005).

300. Klotz, L. O., Hou, X. & Jacob, C. 1,4-naphthoquinones: From oxidative damage to cellular and inter-cellular signaling. *Molecules* **19**, 14902–14918 (2014).

301. Sanders, J. M., Griffin, R. J., Burka, L. T. & Matthews, H. B. Disposition of 2-methylimidazole in rats. *J Toxicol Environ Health A* **54**, 121–132 (1998).

302. Monks, T. J. & Lau, S. S. Toxicology of Quinone-Thioethers. *http://dx.doi.org/10.3109/10408449209146309* **22**, 243–270 (2008).

303. Yarkoni, S., Stein, J., Yaniv, I., Askenasy, N. & Claas, F. Antigen-specific priming is dispensable in depletion of apoptosis-sensitive T cells for GvHD prophylaxis. (2014) doi:10.3389/fimmu.2014.00215.

304. van Leeuwen, L., Guiffre, A., Atkinson, K., Rainer, S. P. & Sewell, W. A. A two-phase pathogenesis of graft-versus-host disease in mice. *Bone Marrow Transplant* **29**, 151–158 (2002).

305. Hildebrandt, G. C. *et al.* Donor-derived TNF-alpha regulates pulmonary chemokine expression and the development of idiopathic pneumonia syndrome after allogeneic bone marrow transplantation. *Blood* **104**, 586–593 (2004).

306. Krenger, W., Rossi, S. & Holländer, G. A. Apoptosis of thymocytes during acute graft-versus-host disease is independent of glucocorticoids. *Transplantation* **69**, 2190–2193 (2000).

307. Kaplan, D. H. *et al.* Target antigens determine graft-versus-host disease phenotype. *J Immunol* **173**, 5467–5475 (2004).

308. Korngold, R. & Sprent, J. Lethal graft-versus-host disease after bone marrow transplantation across minor histocompatibility barriers in mice. Prevention by removing mature T cells from marrow. *J Exp Med* **148**, 1687–1698 (1978).

309. Korngold, R. & Sprent, J. Variable capacity of L3T4+ T cells to cause lethal graft-versus-host disease across minor histocompatibility barriers in mice. *J Exp Med* **165**, 1552–1564 (1987).

310. Hoffmann-Fezer, G., Gall, C., Zengerle, U., Kranz, B. & Thierfelder, S. Immunohistology and Immunocytology of Human T-Cell Chimerism and Graft-Versus-Host Disease in SCID Mice. *Blood* **81**, 3440–3448 (1993).

311. Nervi, B. *et al.* Factors affecting human T cell engraftment, trafficking, and associated xenogeneic graft-vs-host disease in NOD/SCID beta2mnull mice. *Exp Hematol* **35**, 1823–1838 (2007).

312. Ito, R. *et al.* Highly sensitive model for xenogenic GVHD using severe immunodeficient NOG mice. *Transplantation* **87**, 1654–1658 (2009).

313. Schroeder, M. A. & DiPersio, J. F. Mouse models of graft-versus-host disease: advances and limitations. *Dis Model Mech* **4**, 318–333 (2011).

314. Stolfi, J. L., Pai, C. C. S. & Murphy, W. J. Preclinical modeling of hematopoietic stem cell transplantation - advantages and limitations. *FEBS J* **283**, 1595–1606 (2016).

315. Cao, T. M., Lo, B., Ranheim, E. A., Grumet, F. C. & Shizuru, J. A. Variable hematopoietic graft rejection and graft-versus-host disease in MHC-matched strains of mice. *Proc Natl Acad Sci U S A* **100**, 11571–11576 (2003).

316. Fanning, S. L., Appel, M. Y., Berger, S. A., Korngold, R. & Friedman, T. M. The immunological impact of genetic drift in the B10.BR congenic inbred mouse strain. *J Immunol* **183**, 4261–4272 (2009).

317. Schwarte, S. *et al.* Radiation protocols determine acute graft-versus-host disease incidence after allogeneic bone marrow transplantation in murine models. *Int J Radiat Biol* **83**, 625–636 (2007).

318. Schwarte, S. & Hoffmann, M. W. Influence of radiation protocols on graft-vs-host disease incidence after bone-marrow transplantation in experimental models. *Methods Mol Med* **109**, 445–458 (2005).

319. Mapara, M. Y. *et al.* Expression of chemokines in GVHD target organs is influenced by conditioning and genetic factors and amplified by GVHR. *Biol Blood Marrow Transplant* **12**, 623–634 (2006).

320. Gendelman, M. *et al.* Host conditioning is a primary determinant in modulating the effect of IL-7 on murine graft-versus-host disease. *J Immunol* **172**, 3328–3336 (2004).

321. Gorski, J. *et al.* Homeostatic expansion and repertoire regeneration of donor T cells during graft versus host disease is constrained by the host environment. *Blood* **109**, 5502–5510 (2007).

322. Gerbitz, A. *et al.* Probiotic effects on experimental graft-versus-host disease: let them eat yogurt. *Blood* **103**, 4365–4367 (2004).

323. Casellas, J. Inbred mouse strains and genetic stability: A review. *Animal* **5**, 1–7 (2011).

324. Kean, L. S., Singh, K., Blazar, B. R. & Larsen, C. P. Nonhuman primate transplant models finally evolve: detailed immunogenetic analysis creates new models and strengthens the old. *Am J Transplant* **12**, 812–819 (2012).

325. Storb, R. *et al.* Mixed hematopoietic chimerism after marrow allografts. Transplantation in the ambulatory care setting. *Ann N Y Acad Sci* **872**, 372–376 (1999).

326. Velardi, E. *et al.* The role of the thymus in allogeneic bone marrow transplantation and the recovery of the peripheral T-cell compartment. *Semin Immunopathol* **43**, 101–117 (2021).

327. Gupta, V. *et al.* Impact of age on outcomes after bone marrow transplantation for acquired aplastic anemia using HLA-matched sibling donors. *Haematologica* **95**, 2119–2125 (2010).

328. Ordemann, R. *et al.* Enhanced allostimulatory activity of host antigen-presenting cells in old mice intensifies acute graft-versus-host disease. *J Clin Invest* **109**, 1249–1256 (2002).

329. Markey, K. A., Takashima, S., Hanash, A. M. & Hill, G. R. Cytokines in GVHD and GVL. *Immune Biology of Allogeneic Hematopoietic Stem Cell Transplantation* 293–322 (2019) doi:10.1016/B978-0-12-812630-1.00017-7.

330. Toubai, T. *et al.* Role of cytokines in the pathophysiology of acute graft-versus-host disease (GVHD): are serum/plasma cytokines potential biomarkers for diagnosis of acute GVHD following allogeneic hematopoietic cell transplantation (Allo-HCT)? *Curr Stem Cell Res Ther* **7**, 229–239 (2012).

331. Kim, S. & Reddy, P. Targeting Signal 3 Extracellularly and Intracellularly in Graft-Versus-Host Disease. *Front Immunol* **11**, (2020).

332. Hill, G. R., Cooke, K. R., Brinson, Y. S., Bungard, D. & Ferrara, J. L. M. Pretransplant chemotherapy reduces inflammatory cytokine production and acute graft-versus-host disease after allogeneic bone marrow transplantation. *Transplantation* **67**, 1478–1480 (1999).

333. Ewing, P. *et al.* Donor CD4+ T-cell production of tumor necrosis factor alpha significantly contributes to the early proinflammatory events of graft-versus-host disease. *Exp Hematol* **35**, 155–163 (2007).

334. Schmaltz, C. *et al.* Donor T cell-derived TNF is required for graft-versus-host disease and graft-versus-tumor activity after bone marrow transplantation. *Blood* **101**, 2440–2445 (2003).

335. Choi, S. W. *et al.* TNF-inhibition with etanercept for graft-versus-host disease prevention in high-risk HCT: lower TNFR1 levels correlate with better outcomes. *Biol Blood Marrow Transplant* **18**, 1525–1532 (2012).

336. Swanson, K. V., Deng, M. & Ting, J. P. Y. The NLRP3 inflammasome: molecular activation and regulation to therapeutics. *Nat Rev Immunol* **19**, 477–489 (2019).

337. Smeltz, R. B., Chen, J., Ehrhardt, R. & Shevach, E. M. Role of IFN-γ in Th1 Differentiation: IFN-γ Regulates IL-18Rα Expression by Preventing the Negative Effects of IL-4 and by Inducing/Maintaining IL-12 Receptor β2 Expression. *The Journal of Immunology* **168**, 6165–6172 (2002).

338. Min, C. K. *et al.* Paradoxical effects of interleukin-18 on the severity of acute graft-versus-host disease mediated by CD4+ and CD8+ T-cell subsets after experimental allogeneic bone marrow transplantation. *Blood* **104**, 3393–3399 (2004).

339. Reichenbach, D. K. *et al.* The IL-33/ST2 axis augments effector T-cell responses during acute GVHD. *Blood* **125**, 3183–3192 (2015).

340. Mauermann, N. *et al.* Interferon-γ regulates idiopathic pneumonia syndrome, a Th17 +CD4+ T-cell-mediated graft-versus-host disease. *Am J Respir Crit Care Med* **178**, 379–388 (2008).

341. Yang, Y. G., Qi, J., Wang, M. G. & Sykes, M. Donor-derived interferon gamma separates graft-versus-leukemia effects and graft-versus-host disease induced by donor CD8 T cells. *Blood* **99**, 4207–4215 (2002).

342. Yang, Y. *et al.* IFN-γ promotes graft-versus-leukemia effects without directly interacting with leukemia cells in mice after allogeneic hematopoietic cell transplantation. *Blood* **118**, 3721–3724 (2011).

343. Burman, A. C. *et al.* IFNgamma differentially controls the development of idiopathic pneumonia syndrome and GVHD of the gastrointestinal tract. *Blood* **110**, 1064–1072 (2007).

344. Robb, R. J. *et al.* Type I-IFNs control GVHD and GVL responses after transplantation. *Blood* **118**, 3399–3409 (2011).

345. Ross, S. H. & Cantrell, D. A. Signaling and Function of Interleukin-2 in T Lymphocytes. *Annu Rev Immunol* **36**, 411–433 (2018).

346. Betts, B. C. *et al.* IL-2 promotes early Treg reconstitution after allogeneic hematopoietic cell transplantation. *Haematologica* **102**, 948–957 (2017).

347. Locke, F. L. *et al.* CD25 Blockade Delays Regulatory T Cell Reconstitution and Does Not Prevent Graft-versus-Host Disease After Allogeneic Hematopoietic Cell Transplantation. *Biol Blood Marrow Transplant* **23**, 405–411 (2017).

348. Nikolic, B., Lee, S., Bronson, R. T., Grusby, M. J. & Sykes, M. Th1 and Th2 mediate acute graft-versus-host disease, each with distinct end-organ targets. *J Clin Invest* **105**, 1289–1298 (2000).

349. Leveson-Gower, D. B. *et al.* Low doses of natural killer T cells provide protection from acute graft-versus-host disease via an IL-4-dependent mechanism. *Blood* **117**, 3220–3229 (2011).

350. Foley, J. E. *et al.* Ex vivo rapamycin generates donor Th2 cells that potently inhibit graft-versus-host disease and graft-versus-tumor effects via an IL-4-dependent mechanism. *J Immunol* **175**, 5732–5743 (2005).

351. Nakamura, K. *et al.* IL-4-producing CD8(+) T cells may be an immunological hallmark of chronic GVHD. *Bone Marrow Transplant* **36**, 639–647 (2005).

352. Scheller, J., Chalaris, A., Schmidt-Arras, D. & Rose-John, S. The pro- and anti-inflammatory properties of the cytokine interleukin-6. *Biochim Biophys Acta* **1813**, 878–888 (2011).

353. Tawara, I. *et al.* Interleukin-6 modulates graft-versus-host responses after experimental allogeneic bone marrow transplantation. *Clin Cancer Res* **17**, 77–88 (2011).

354. Kennedy, G. A. *et al.* Addition of interleukin-6 inhibition with tocilizumab to standard graft-versus-host disease prophylaxis after allogeneic stem-cell transplantation: a phase 1/2 trial. *Lancet Oncol* **15**, 1451–1459 (2014).

355. Gaffen, S. L. Structure and signalling in the IL-17 receptor family. *Nat Rev Immunol* **9**, 556–567 (2009).

356. Das, R., Chen, X., Komorowski, R., Hessner, M. J. & Drobyski, W. R. Interleukin-23 secretion by donor antigen-presenting cells is critical for organ-specific pathology in graft-versus-host disease. *Blood* **113**, 2352–2362 (2009).

357. Ratajczak, P. *et al.* Th17/Treg ratio in human graft-versus-host disease. *Blood* **116**, 1165–1171 (2010).

358. Wu, Y. & Yu, X. Z. IL-17A ≠ Th17 in GvHD. *Cell Mol Immunol* **15**, 282–283 (2018).

359. Zhang, P. & Hill, G. R. Interleukin-10 mediated immune regulation after stem cell transplantation: Mechanisms and implications for therapeutic intervention. *Semin Immunol* **44**, (2019).

360. Tawara, I. *et al.* Donor- but not host-derived interleukin-10 contributes to the regulation of experimental graft-versus-host disease. *J Leukoc Biol* **91**, 667–675 (2012).

361. Rowe, V. *et al.* Host B cells produce IL-10 following TBI and attenuate acute GVHD after allogeneic bone marrow transplantation. *Blood* **108**, 2485–2492 (2006).

362. Taylor, P. A., Lees, C. J. & Blazar, B. R. The infusion of ex vivo activated and expanded CD4(+)CD25(+) immune regulatory cells inhibits graft-versus-host disease lethality. *Blood* **99**, 3493–3499 (2002).

363. Chen, L. & Flies, D. B. Molecular mechanisms of T cell co-stimulation and co-inhibition. *Nat Rev Immunol* **13**, 227–242 (2013).

364. Blazar, B. R., Taylor, P. A., Panoskaltsis-Mortari, A., Gray, G. S. & Vallera, D. A. Coblockade of the LFA1:ICAM and CD28/CTLA4:B7 pathways is a highly effective means of preventing acute lethal graft-versus-host disease induced by fully major histocompatibility complex-disparate donor grafts. *Blood* **85**, 2607–2618 (1995).

365. Ngwube, A., Rangarajan, H. & Shah, N. Role of abatacept in the prevention of graft-versus-host disease: current perspectives. *Therapeutic advances in hematology* **14**, 20406207231152644 (2023).

366. Highfill, S. L. *et al.* Bone marrow myeloid-derived suppressor cells (MDSCs) inhibit graft-versus-host disease (GVHD) via an arginase-1-dependent mechanism that is up-regulated by interleukin-13. *Blood* **116**, 5738–5747 (2010).

367. Rutella, S., Danese, S. & Leone, G. Tolerogenic dendritic cells: cytokine modulation comes of age. *Blood* **108**, 1435–1440 (2006).

368. Chen, B. J., Cui, X., Sempowski, G. D., Liu, C. & Chao, N. J. Transfer of allogeneic CD62L- memory T cells without graft-versus-host disease. *Blood* **103**, 1534–1541 (2004).

369. Dutt, S. *et al.* Naive and memory T cells induce different types of graft-versus-host disease. *J Immunol* **179**, 6547–6554 (2007).

370. Chen, B. J. *et al.* Inability of memory T cells to induce graft-versus-host disease is a result of an abortive alloresponse. *Blood* **109**, 3115–3123 (2007).

371. Zheng, H. *et al.* Effector memory CD4+ T cells mediate graft-versus-leukemia without inducing graft-versus-host disease. *Blood* **111**, 2476–2484 (2008).

372. Zheng, H., Matte-Martone, C., Jain, D., McNiff, J. & Shlomchik, W. D. Central memory CD8+ T cells induce graft-versus-host disease and mediate graft-versus-leukemia. *J Immunol* **182**, 5938–5948 (2009).

373. Bleakley, M. *et al.* Leukemia-associated minor histocompatibility antigen discovery using T-cell clones isolated by in vitro stimulation of naive CD8+ T cells. *Blood* **115**, 4923–4933 (2010).

374. Jiang, H., Fu, D., Bidgoli, A. & Paczesny, S. T Cell Subsets in Graft Versus Host Disease and Graft Versus Tumor. *Front Immunol* **12**, (2021).

375. Hill, G. R., Betts, B. C., Tkachev, V., Kean, L. S. & Blazar, B. R. Current Concepts and Advances in Graft-Versus-Host Disease Immunology. *Annu Rev Immunol* **39**, 19–49 (2021).

376. Iclozan, C. *et al.* T helper17 cells are sufficient but not necessary to induce acute graft-versus-host disease. *Biol Blood Marrow Transplant* **16**, 170–178 (2010).

377. Jung, U. *et al.* Ex vivo rapamycin generates Th1/Tc1 or Th2/Tc2 Effector T cells with enhanced in vivo function and differential sensitivity to post-transplant rapamycin therapy. *Biol Blood Marrow Transplant* **12**, 905–918 (2006).

378. Tawara, I. *et al.* Combined Th2 cytokine deficiency in donor T cells aggravates experimental acute graft-vs-host disease. *Exp Hematol* **36**, 988–996 (2008).

379. Di Ianni, M. *et al.* Tregs prevent GVHD and promote immune reconstitution in HLA-haploidentical transplantation. *Blood* **117**, 3921–3928 (2011).

380. Edinger, M. *et al.* CD4+CD25+ regulatory T cells preserve graft-versus-tumor activity while inhibiting graft-versus-host disease after bone marrow transplantation. *Nat Med* **9**, 1144–1150 (2003).

381. Geraghty, N. J. *et al.* Increased splenic human CD4 + :CD8 + T cell ratios, serum human interferon-γ and intestinal human interleukin-17 are associated with clinical graft-versus-host disease in humanized mice. *Transpl Immunol* **54**, 38–46 (2019).

382. Kumar Gupta, S. *et al.* Withaferin-A alleviates acute graft versus host disease without compromising graft versus leukemia effect. *Int Immunopharmacol* **121**, 110437 (2023).

383. Mehta, M. *et al.* Prevention of acute graft-versus-host-disease by Withaferin a via suppression of AKT/mTOR pathway. *Int Immunopharmacol* **84**, (2020).

384. Cooke, K. R. *et al.* Tumor necrosis factor-α production to lipopolysaccharide stimulation by donor cells predicts the severity of experimental acute graft-versus-host disease. *Journal of Clinical Investigation* **102**, 1882–1891 (1998).

385. Hogenes, M. C. H. *et al.* Histological Assessment of the Sclerotic Graft-versus-Host Response in the Humanized RAG2-/-γc-/- Mouse Model. *Biology of Blood and Marrow Transplantation* **18**, 1023–1035 (2012).

386. Wölfl, M. *et al.* Current Prophylaxis and Treatment Approaches for Acute Graft-Versus-Host Disease in Haematopoietic Stem Cell Transplantation for Children With Acute Lymphoblastic Leukaemia. *Front Pediatr* **9**, (2022).

387. Martinez-Cibrian, N., Zeiser, R. & Perez-Simon, J. A. Graft-versus-host disease prophylaxis: Pathophysiology-based review on current approaches and future directions. *Blood Rev* **48**, 100792 (2021).

388. Acute Graft-versus-Host Disease Biology, Prevention and Therapy _ Enhanced Reader.pdf.

389. Zeiser, R., Socié, G. & Blazar, B. R. Pathogenesis of acute graft-versus-host disease: from intestinal microbiota alterations to donor T cell activation. *Br J Haematol* **175**, 191–207 (2016).

390. Ramadan, A. & Paczesny, S. Various forms of tissue damage and danger signals following hematopoietic stem-cell transplantation. *Front Immunol* **6**, 1–20 (2015).

391. Cetin, T. *et al.* Oxidative stress in patients undergoing high-dose chemotherapy plus peripheral blood stem cell transplantation. *Biol Trace Elem Res* **97**, 237–247 (2004).

392. Shen, H. *et al.* An acute negative bystander effect of γ-irradiated recipients on transplanted hematopoietic stem cells. *Blood* **119**, 3629–3637 (2012).

393. Tkachev, V. *et al.* Programmed death-1 controls T cell survival by regulating oxidative metabolism. *J Immunol* **194**, 5789–5800 (2015).

394. Wahid, S. F. A. *et al.* Comparison of reduced-intensity and myeloablative conditioning regimens for allogeneic hematopoietic stem cell transplantation in patients with acute myeloid leukemia and acute lymphoblastic leukemia: a meta-analysis. *Stem Cells Dev* **23**, 2535–2552 (2014).

395. Khalil, R. G., Ibrahim, A. M. & Bakery, H. H. Juglone: "A novel immunomodulatory, antifibrotic, and schistosomicidal agent to ameliorate liver damage in murine schistosomiasis mansoni". *Int Immunopharmacol* **113**, 109415 (2022).

396. Maruo, S. *et al.* Inhibitory effect of novel 5-O-acyl juglones on mammalian DNA polymerase activity, cancer cell growth and inflammatory response. *Bioorg Med Chem* **19**, 5803–5812 (2011).

397. Wang, H. *et al.* Juglone eliminates MDSCs accumulation and enhances antitumor immunity. *Int Immunopharmacol* **73**, 118–127 (2019).

398. Ge, Z. Z., Wu, Y. B., Xue, Z. Y., Zhang, K. & Zhang, R. X. The therapeutic effects of the peptidyl-prolyl cis/trans isomerase Pin1 inhibitor juglone on animal-model experimental autoimmune encephalomyelitis. *J Physiol Pharmacol* **72**, (2021).

399. Geginat, J. *et al.* The CD4-centered universe of human T cell subsets. *Semin Immunol* **25**, 252–262 (2013).

400. Paulsen, M. & Janssen, O. Pro- and anti-apoptotic CD95 signaling in T cells. *Cell Communication and Signaling* **9**, 1–9 (2011).

401. Schwartz, R. H. T cell anergy. *Annu Rev Immunol* **21**, 305–334 (2003).

402. Koura, D. T. *et al.* In vivo T cell costimulation blockade with abatacept for acute graft-versus-host disease prevention: a first-in-disease trial. *Biol Blood Marrow Transplant* **19**, 1638–1649 (2013).

403. Teschner, D. *et al.* Depletion of naive T cells using clinical grade magnetic CD45RA beads: a new approach for GVHD prophylaxis. *Bone Marrow Transplant* **49**, 138–144 (2014).

404. Dekker, L., Sanders, E., Lindemans, C. A., de Koning, C. & Nierkens, S. Naive T Cells in Graft Versus Host Disease and Graft Versus Leukemia: Innocent or Guilty? *Front Immunol* **13**, (2022).

405. Anderson, B. E. *et al.* Memory CD4+ T cells do not induce graft-versus-host disease. *J Clin Invest* **112**, 101–108 (2003).

406. Chen, B. J., Cui, X., Sempowski, G. D., Liu, C. & Chao, N. J. Transfer of allogeneic CD62L- memory T cells without graft-versus-host disease. *Blood* **103**, 1534–1541 (2004).

407. Jiang, H., Fu, D., Bidgoli, A. & Paczesny, S. T Cell Subsets in Graft Versus Host Disease and Graft Versus Tumor. *Front Immunol* **12**, 1–15 (2021).

408. Graubert, T. A., Russell, J. H. & Ley, T. J. The Role of Granzyme B in Murine Models of Acute Graft-Versus-Host Disease and Graft Rejection. *Blood* **87**, 1232–1237 (1996).

409. Bian, G. *et al.* Granzyme B-mediated damage of CD8+ T cells impairs graft-versus-tumor effect. *Journal of immunology (Baltimore, Md. : 1950)* **190**, 1341–1350 (2013).

410. Bleakley, M. *et al.* Leukemia-associated minor histocompatibility antigen discovery using T-cell clones isolated by in vitro stimulation of naive CD8+ T cells. *Blood* **115**, 4923–4933 (2010).

411. Zheng, H., Matte-Martone, C., Jain, D., McNiff, J. & Shlomchik, W. D. Central memory CD8+ T cells induce graft-versus-host disease and mediate graft-versus-leukemia. *J Immunol* **182**, 5938–5948 (2009).

412. Wherry, E. J. *et al.* Lineage relationship and protective immunity of memory CD8 T cell subsets. *Nat Immunol* **4**, 225–234 (2003).

413. Klebanoff, C. A. *et al.* Central memory self/tumor-reactive CD8+ T cells confer superior antitumor immunity compared with effector memory T cells. *Proc Natl Acad Sci U S A* **102**, 9571–9576 (2005).

414. Seetha, A., Devaraj, H. & Sudhandiran, G. Effects of combined treatment with Indomethacin and Juglone on AOM/DSS induced colon carcinogenesis in Balb/c mice: Roles of inflammation and apoptosis. *Life Sci* **264**, 118657 (2021).

415. Kim, S. & Reddy, P. Targeting Signal 3 Extracellularly and Intracellularly in Graft-Versus-Host Disease. *Front Immunol* **11**, 1–10 (2020).

416. Hill, G. R. & Koyama, M. Cytokines and costimulation in acute graft-versus-host disease. *Blood* **136**, 418–428 (2020).

417. Tawara, I. *et al.* Interleukin-6 modulates graft-versus-host responses after experimental allogeneic bone marrow transplantation. *Clinical Cancer Research* **17**, 77–88 (2011).

418. Wu, Y. & Yu, X. Z. IL-17A ≠ Th17 in GvHD. *Cellular & Molecular Immunology 2018 15:3* **15**, 282–283 (2016).

419. Bleakley, M. & Riddell, S. R. Molecules and mechanisms of the graft-versus-leukaemia effect. *Nat Rev Cancer* **4**, 371–380 (2004).

420. Parham, P. & McQueen, K. L. Alloreactive killer cells: hindrance and help for haematopoietic transplants. *Nat Rev Immunol* **3**, 108–122 (2003).

421. Hartung, G. *et al.* Enhanced antileukemic activity of allogeneic peripheral blood progenitor cell transplants following donor treatment with the combination of granulocyte colony-stimulating factor (G-CSF) and stem cell factor (SCF) in a murine transplantation model. *Bone Marrow Transplant* **32**, 49–56 (2003).

422. Morris, E. S., MacDonald, K. P. A. & Hill, G. R. Stem cell mobilization with G-CSF analogs: A rational approach to separate GVHD and GVL? *Blood* **107**, 3430–3435 (2006).

423. Hill, G. R. & Koyama, M. Cytokines and costimulation in acute graft-versus-host disease. *Blood* **136**, 418–428 (2020).

424. Yu, Y. *et al.* Prevention of GVHD while sparing GVL effect by targeting Th1 and Th17 transcription factor T-bet and RORγt in mice. *Blood* **118**, 5011–5020 (2011).

425. Demosthenous, C. *et al.* The Role of Myeloid-Derived Suppressor Cells (MDSCs) in Graft-versus-Host Disease (GVHD). *J Clin Med* **10**, (2021).

426. Blanco, B. *et al.* Immunomodulatory effects of bone marrow versus adipose tissue-derived mesenchymal stromal cells on NK cells: implications in the transplantation setting. *Eur J Haematol* **97**, 528–537 (2016).

427. Braun, L. M. & Zeiser, R. Immunomodulatory Therapies for the Treatment of Graft-versus-host Disease. *Hemasphere* **5**, e581 (2021).

428. Mercadante, A. C. T. *et al.* Oral Combined Therapy with Probiotics and Alloantigen Induces B Cell–Dependent Long-Lasting Specific Tolerance. *The Journal of Immunology* **192**, 1928–1937 (2014).

429. KJ, K., C, K.-L., RM, M., DH, S. & R, A. Establishment and characterization of BALB/c lymphoma lines with B cell properties. *J Immunol* **122**, 549–554 (1979).

430. Edinger, M. *et al.* CD4+CD25+ regulatory T cells preserve graft-versus-tumor activity while inhibiting graft-versus-host disease after bone marrow transplantation. *Nat Med* **9**, 1144–1150 (2003).

431. Zhang, J. *et al.* The mechanistic study behind suppression of GVHD while retaining GVL activities by myeloid-derived suppressor cells. *Leukemia 2019 33:8* **33**, 2078–2089 (2019).

432. Snyder, K. J. *et al.* Inhibition of Bromodomain and Extra Terminal (BET) Domain Activity Modulates the IL-23R/IL-17 Axis and Suppresses Acute Graft-Versus-Host Disease. *Front Oncol* **11**, (2021).

433. Balunas, M. J. & Kinghorn, A. D. Drug discovery from medicinal plants. *Life Sci* **78**, 431–441 (2005).

DRUG AND CHEMICAL TOXICOLOGY
https://doi.org/10.1080/01480545.2022.2104306

Taylor & Francis
Taylor & Francis Group

RESEARCH ARTICLE

Acute and sub-acute oral toxicity assessment of 5-hydroxy-1,4-naphthoquinone in mice

Dievya Gohil[a,b], Girish Ch. Panigrahi[a,b]*, Saurabh Kumar Gupta[a,b]*, Khushboo A. Gandhi[a], Poonam Gera[c,d], Preeti Chavan[e], Deepak Sharma[b,f], Santosh Sandur[b,f] and Vikram Gota[a,b]

[a]Clinical Pharmacology Laboratory, ACTREC, Tata Memorial Centre, Navi Mumbai, India; [b]Homi Bhabha National Institute, Anushaktinagar, Mumbai, India, Mumbai, India; [c]ICGC Lab, ACTERC, Tata Memorial Centre, Navi Mumbai, India; [d]Biorepository, ACTREC, Tata Memorial Centre, Navi Mumbai, India; [e]Department of Clinical Biochemistry, ACTREC, Tata Memorial Centre, Navi Mumbai, India; [f]Radiation Biology & Health Science Division, Bio-science Group, Bhabha Atomic Research Centre, Mumbai, India

ABSTRACT

5-hydroxy-1,4-naphthoquinone (5NQ) or juglone is a bioactive molecule found in walnuts and has shown therapeutic effects in various disease models. Limited information is available regarding the toxicity of 5NQ, thereby limiting the clinical development of this drug. In the present study, oral acute (50, 300 and 2000 mg/kg) and sub-acute toxicity (5, 15 and 50 mg/kg) was assessed in mice to evaluate the safety of 5NQ. The acute toxicity study identified 118 mg/kg as the point-of-departure dose (POD) for single oral administration of 5NQ using benchmark dose modeling (BMD). Repeated administration of 5NQ at doses of 15 and 50 mg/kg/day caused reduction in food consumption and body weight of mice along with alterations in liver and renal function. Histopathological assessment revealed significant damage to hepatic and renal tissues at all doses in the acute toxicity study, and at higher doses of 15 and 50 mg/kg in the sub-acute toxicity study. We observed dose dependent mortality in sub-acute toxicity study and the no observed adverse effect level (NOAEL) was established as < 5 mg/kg/day. Modeling the survival response in sub-acute toxicity study identified 1.74 mg/kg/day as the POD for repeated administration of 5NQ. Serum levels of aspartate aminotransferase (AST) were most sensitive to 5NQ administration with a lower limit of BMD interval (BMDL) of 1.1×10^{-3} mg/kg/day. The benchmark doses reported in the study can be further used to determine a reference dose of 5NQ for human risk assessment.

ARTICLE HISTORY
Received 21 February 2022
Revised 8 July 2022
Accepted 17 July 2022

KEYWORDS
Juglone; NOAEL; benchmark dose; point of departure dose; PROAST

Introduction

5-hydroxy-1,4-naphthoquinone (5NQ) or Juglone is a phenolic compound found abundantly in fresh leaves and green husk of several species of walnut trees belonging to the Juglandaceae family (*Juglans nigra, Juglans regia, Juglans cinera und Carya illinoinensis*). It is also found in smaller quantities in the roots, bark and nuts of the walnut tree (Bello *et al.* 2018, McCoy *et al.* 2018, Jahanban-Esfahlan *et al.* 2019). As the name suggests, 5NQ belongs to the naphthoquinone class of drugs and contains an aromatic ring hydroxylated at the 5-position and a quinone ring with oxygen at positions 1 and 4. Table 1 describes the physico-chemical characteristics of 5NQ (NCI 2002, Juglone | C10H6O3 - PubChem 2021). The therapeutic potential of 5NQ has been tested in a range of clinical conditions. It exhibits anti-bacterial(Wang, Cheng, *et al.* 2016, Wang, Liu, *et al.* 2016, Wang, Wang, *et al.* 2016), anti-fungal (Gumus *et al.* 2020) and anti-parasitic (Jha *et al.* 2015, Moghadaszadeh *et al.* 2021) activity at concentrations ranging between 0.1 and 0.5 mM. It shows anti-viral (Cui and Jia 2021), anti-inflammatory (Seshadri *et al.* 2011, Gaikwad *et al.* 2019, Kim *et al.* 2020) and anti-cancer activity (Aithal *et al.* 2012, Catanzaro *et al.* 2018, Wang *et al.* 2018) at concentrations ranging between $3-25\,\mu$M. Notably, 5NQ is a redox active molecule and has a strong ability to generate reactive oxygen species (ROS) (Klotz *et al.* 2014, Ahmad and Suzuki 2019, Majiene *et al.* 2019, Mesalam *et al.* 2020). This redox activity of 5NQ is responsible for its pharmacological actions and affects various cellular pathways (Wang *et al.* 2018, Kao *et al.* 2021), causing loss of mitochondrial and plasma membrane potential (Ji *et al.* 2010, Anaissi-Afonso *et al.* 2018, Majiene *et al.* 2019, Mesalam *et al.* 2020), DNA damage (Kiran Aithal *et al.* 2009, Ourique *et al.* 2015), cellular degeneration and apoptosis (Seshadri *et al.* 2011). Despite being a potent therapeutic agent, clinical application of 5NQ faces many challenges as few reports are available for its toxicity in normal tissues, lethal dose (LD_{50}), favorable solvent and route of administration.

Westfall and team (1961), reported a LD_{50} of 2.5 mg/kg in mice, however, no information about the route of administration or duration of dosing was specified (Westfall *et al.* 1961). To our knowledge, the study by Aithal and group (2012), is

CONTACT Vikram Gota vgota76@gmail.com Clinical Pharmacology Laboratory, ACTREC, Tata Memorial Centre, Kharghar, Navi Mumbai 410210, India
*These authors contributed equally.

Supplemental data for this article can be accessed at https://doi.org/10.1080/01480545.2022.2104306.

	QR code	MOLENAME	Row	Col			
1	1137106768	Inosine	A	2	268.23	A purine nucleoside that has hypoxanthine linked by the N9 nitrogen to the C1 carbon of ribose. It is an intermediate in the degradation of purines and purine nucleosides to uric acid and in pathways of purine salvage. It also occurs in the anticodon of certain transfer RNA molecules.	Xanthine Oxidase inhibitor
2	1137106769	Berberine hydrochloride	A	3	371.80	An alkaloid from Hydrastis canadensis L., Berberidaceae. It is also found in many other plants. It is relatively toxic parenterally, but has been used orally for various parasitic and fungal infections and as antidiarrheal.	Antibiotic
3	1137106770	Salicoside	A	4	286.28	Salicin is a phenol β-glycosid produced from willow bark that shows anti-inflammatory effects.	COX inhibitor
4	1137106771	Artesunate	A	5	384.42	Artesunate is a part of the artemisinin group of agents with an IC50 of < 5 μM for small cell lung carcinoma cell line H69. Artesunate is a semi-synthetic derivative of artemisinin that is water-soluble and may therefore be given by injection. Artesunate is used primarily as treatment for malaria; but artesunate has also been shown to be >90% efficacious at reducing egg production in Schistosoma haematobium infection.	Others
5	1137106772	D-Mannitol	A	6	182.17	D-Mannitol is an osmotic diuretic agent and a weak renal vasodilator.	Dehydrogenase substrate
6	1137106773	Enoxolone	A	7	470.68	Enoximone is a selective phosphodiesterase inhibitor with vasodilating and positive inotropic activity that does not cause changes in myocardial oxygen consumption. It is used in patients with congestive heart failure. Trials were halted in the U.S., but the drug is used in various countries.	Dehydrogenase inhibitor
7	1137106774	Methyl hesperidin	A	8	624.59	Methyl Hesperidin is a flavanone glycoside (flavonoid) (C28H34O15) found abundantly in citrus fruits. Its aglycone form is called hesperetin.	Akt inhibitor; PKC inhibitor
8	1137106775	Ipriflavone (Osteofix)	A	9	280.32	Ipriflavone (7-Isopropoxyisoflavon) is used to inhibit bone resorption.	Immunologic Factors
9	1137106776	D-Sorbitol	A	10	182.17	D-Sorbitol is a sugar alcohol that is commonly used as a sugar substitute.	Others
10	1137106777	Arbutin	A	11	272.25	Arbutin(β-Arbutin) is a glycoside; a glycosylated hydroquinone extracted from the bearberry plant in the genus Arctostaphylos; inhibits tyrosinase and thus prevents the formation of melanin.	Tyrosinase inhibitor
11	1137106789	Cytisine	B	2	190.25	Cytisine is an alkaloid that is found naturally in several plant genera such as Laburnum and Cytisus of the family Fabaceae. Recent studies have shown it to be a more effective and significantly more affordable smoking cessation treatment than nicotine replacement therapy. Also known as baptitoxine or sophorine, cytisine has been used as a smoking cessation treatment since 1964, and is relatively unknown in regions outside of central and Eastern Europe. Cytisine is a partial nicotinic acetylcholine agonist with a half-life of 4.8 hours. Recent Phase III clinical trials using Tabex (a brand of Cytisine marketed by Sopharma AD) have shown similar efficacy to varenicline, but at a fraction of the cost.	AChR agonist

12	1137106788	Esculin	B	3	340.28	Extracted from Aesculushippocastanumlinn;Suitability:Hot ethanol,methanol,pyridine,ethyl acetate and acetic acid;Store the product in sealed,cool and dry condition	Others
13	1137106787	Vanillyl Alcohol	B	4	154.16	Vanillyl alcohol is derived from vanillin. It is used to flavor food.	Others
14	1137106786	Myricetin	B	5	318.24	Myricetin is produced from the parent compound taxifolin through the (+)-dihydromyricetin intermediate and can be further processed to form laricitrin and then syringetin, both members of the flavonol class of flavonoids. Dihydromyricetin is frequently sold as a supplement and has controversial function as a partial GABAA receptor potentiator and treatment in Alcohol Use Disorder (AUD).	ROS inhibitor
15	1137106785	Oleanolic Acid	B	6	456.72	Oleanolic Acid is a naturally occurring triterpenoid found in garlic and Phytolacca Americana. Exhibits strong anti-HIV activity. Mechanism of action is the induction of iNOS and of Cyclooxygenase 2	Others
16	1137106784	Glycyrrhizin (Glycyrrhizic Acid)	B	7	822.93	Actions Biologically active constituent in the sweet root of Glycyrrhiza species (licorice). Antiviral. Packaging 25,100 g in poly bottle	Dehydrogenase inhibitor
17	1137106783	Hordenine	B	8	165.23	Extracted from Germinated barley seeds; Suitability:Ethanol,chloroform and ether;Store the product in sealed,cool and dry condition	Others
18	1137106782	Bengenin	B	9	328.27	Bergenin, a polyphenol, is a potent antinarcotic agent with antioxidant action.	NO agonist; TNF-alpha inhibitor; IL inhibitor; NF-κB inhibitor
19	1137106781	Ferulic Acid	B	10	194.19	Ferulic Acid is a hydroxycinnamic acid and a type of organic compound found in the Ferula assafoetida L. or Ligusticum chuanxiong.	FGFR inhibitor
20	1137106780	Paeonol	B	11	166.17	Paeonol (Peonol), a phenolic compound extracted from Chinese herbs Paeonia suffruticosa (moutan cortex) and Cynanchum paniculatum, inhibits MAO with an IC50 of about 50 μM.	MAO inhibitor
21	1137106792	Naringin	C	2	580.53	Naringin is a flavanone glycoside, which exerts a variety of pharmacological effects such as antioxidant activity, blood lipid lowering, antiY activity, and inhibition of cytochrome P450 enzymes.	CYP inhibitor
22	1137106793	Yohimbine hydrochloride	C	3	390.90	Yohimbine hydrochloride is an alpha 2-adrenoreceptor antagonist, blocking the pre- and postsynaptic alpha-2 adrenoreceptors and causing an increased release of noradrenaline and dopamine.	Adrenergic Receptor antagonist
23	1137106794	Hesperidin	C	4	610.56	Hesperidin is a flavanone glycoside found abundantly in citrus fruits.	Others
24	1137106795	Cinchonidine	C	5	294.39	Cinchonidine is an alkaloid found in Cinchona officinalis. It is used in asymmetric synthesis in organic chemistry. It is a stereoisomer and pseudo-enantiomer of cinchonine.	Others
25	1137106796	Tanshinone I	C	6	276.29	Tanshinone I is a pigment isolated from the herbal medicine Salvia miltiorrhiza Bunge. Tanshinone I displays cytotoxicity against human macrophages and IFN-g production in KLH-primed lymph node cells.	Phospholipase inhibitor
26	1137106797	Myricetrin	C	7	464.38	Myricitrin, a flavonoid compound isolated from the root bark of Myrica cerifera, which exerts antinociceptive effects.	PKC inhibitor

27	1137106798	Sinomenine	C	8	329.4	Sinomenine, a pure alkaloid extracted from the chinese medical plant Sinomenium acutum, is used for the treatment of rheumatism and arthritis.	Others
28	1137106799	Neohesperidin Dihydrochalcone (Nhdc)	C	9	612.58	Neohesperidin dihydrochalcone(Nhdc), sometimes abbreviated to neohesperidin DC or simply NHDC, is an artificial sweetener derived from citrus.	Others
29	1137106800	Naringin dihydrochalcone	C	10	582.55	Naringin Dihydrochalcone(Naringin DC) is a new-style sweetening agent and an artificial sweetener derived from naringin.	Others
30	1137106801	Shikimic Acid	C	11	174.15	Actions Biosynthetic precursor of aromatic amino acids,as well as many alkaloids and other aromatic metabolites.	Others
31	1137106813	10-Hydroxycamptothecin	D	2	364.36	(S)-10-Hydroxycamptothecin is a clinical therapy agent against hepatoma.	Topoisomerase inhibitor
32	1137106812	Biochanin A	D	3	284.26	Biochanin A, an O-methylated isoflavone from Trifolium pratense, inhibits protein tyrosine kinase (PTK) of epidermal growth factor receptor with IC50 values of 91.5 μM.	FAAH inhibitor; EGFR inhibitor
33	1137106811	Sclareolide	D	4	250.38	Sclareolide is a sesquiterpene lactone natural product derived from various plant sources including Salvia sclarea, Salvia yosgadensis, and cigar tobacco. It is a close analog of sclareol, a plant antifungal compound.	Others
34	1137106810	Xanthone	D	5	196.21	Xanthone is an organic compound and can be prepared by the heating of phenyl salicylate. In 1939, xanthone was introduced as an insecticide and it currently finds uses as ovicide for codling moth eggs and as a larvicide.	Antifungal
35	1137106605	Abscisic acid	D	6	264.32	Abscission-accelerating plant growth substance isolated from young cotton fruit, leaves of sycamore, birch, and other plants, and from potatoes, lemons, avocados, and other fruits.	Others
36	1137106808	Sclareol	D	7	308.51	Sclareol, a labdane-type diterpene isolated from clary sage (Salvia sclarea), exerts growth inhibition and cytotoxic activity against a variety of human Y cell lines. Extracted from Salvia SclareL. inflorescence,stem and leaf;Store?the?product?in?sealed,?cool?and?dry?condition	Others
37	1137106807	Dihydroartemisinin	D	8	284.35	Dihydroartemisinin (DHA) is a semi-synthetic derivative of artemisinin and isolated from the traditional Chinese herb Artemisia annua.	Others
38	1137106806	Hesperetin	D	9	302.27	Hesperetin is a bioflavonoid and, to be more specific, a flavanone.	TGF-beta/Smad inhibitor; Histamine Receptor antagonist
39	1137106805	Ursolic acid	D	10	456.70	Ursolic acid(Bungeolic acid) is a natural pentacyclic triterpenoid carboxylic acid, exerts anti-tumor effects and is an effective compound for Y prevention and therapy.	Others
40	1137106804	Luteolin	D	11	286.24	Luteolin is a falconoid compound, which exhibits antiY properties.	TNF-alpha inhibitor; IL inhibitor; NF-κB inhibitor
41	1137106816	Formononetin	E	2	268.27	Formononetin is a phytoestrogen from the root of Astragalus membranaceus and an O-methylated isoflavone.	Others

42	1137106817	Isoliquiritigenin	E	3	256.25	Isoliquiritigenin, an anti-tumor flavonoid from the root of Glycyrrhiza glabra, inhibits aldose reductase with an IC50 of 320 nM.	Aldose reductase inhibitor
43	1137106818	Troxerutin	E	4	742.67	Troxerutin, a natural bioflavonoid isolated from Sophora japonica., has been reported to have many benefits and medicinal properties.	Others
44	1137106819	Orotic acid	E	5	156.10	Orotic acid (OA) is an intermediate in pyrimidine metabolism. Orotic acid(6-Carboxyuracil) is a heterocyclic compound and an acid.	DHOase inhibitor
45	1137106820	DL-Carnitine	E	6	161.20	Constituent of striated muscle and liver. It is used therapeutically to stimulate gastric and pancreatic secretions and in the treatment of hyperlipoproteinemias.	Others
46	1137106821	Phloretin	E	7	274.28	Phloretin is a dihydrochalcone, a type of natural phenols. It can be found in apple tree leaves and the Manchurian apricot.	SGLT inhibitor
47	1137106822	Dihydromyricetin	E	8	320.25	Dihydromyricetin (Ampelopsin, Ampeloptin) is a natural antioxidant flavonoid from Ampelopsis grossedentata.	GABAR agonist
48	1137106823	Honokiol	E	9	266.32	Honokiol is the active principle of magnolia extract that inhibits Akt-phosphorylation and promotes ERK1/2 phosphorylation.	Akt inhibitor; MEK inhibitor
49	1137106824	Magnolol	E	10	266.32	Magnolol is isomeric to honokiol (sc-202653). Magnolol is an anxiolytic,anti-thrombotic and antibacterial. . Inhibitor of nitric oxide (NO) and TNF-α production in LPS-activated macrophages by the suppression of inducible nitric oxide synthase(iNOS; NOS	NF-κB inhibitor; p53 activator; PPAR inhibitor
50	1137106825	Gastrodin	E	11	286.28	Gastrodin, an anti-inflammatory polyphenol extracted from Chinese natural herbal Gastrodia elata Blume., benefits neurodegenerative diseases. Extracted from Orchids Gastrodia; Suitability:Water,methanol,ethanol;Store the product in sealed,cool and dry condition	Others
51	1137106837	Piperine	F	2	285.35	Piperine (1-Piperoylpiperidine) is the alkaloid responsible for the pungency of black pepper and long pepper, which has also been used in some forms of traditional medicine and as an insecticide.	CYP inhibitor
52	1137106836	Chrysophanic Acid	F	3	254.24	Extracted from Rheum palmatum L.;Suitability:Boiling ethanol,benzene,chloroform,ether,acetic acid and acetone;Store the product in sealed,cool and dry condition	EGFR inhibitor; mTOR inhibitor
53	1137106835	5-hydroxytryptophan (5-HTP)	F	4	220.23	5-Hydroxytryptophan (5-HTP), also known as oxitriptan (INN), is a naturally occurring amino acid and chemical precursor for the treatment of depression. Extracted from Griffonia simplicifolia;Suitability:Water;Store the product in sealed,cool and dry condition	Others
54	1137106834	Fisetin	F	5	286.24	Extracted from Rhus succedanea L;Store the product in sealed, cool and dry condition.	Sirtuin activator
55	1137106833	Hyodeoxycholic acid (HDCA)	F	6	392.58	Extracted from Pigs bile;Suitability:alcohol;Store the product in sealed,cool and dry condition	Farnesoid X receptor antagonist
56	1137106832	Naringenin	F	7	272.26	Extracted from Amacardi-um occidentale L.;Suitability:Ethanol,ether and benzene;Store the product in sealed,cool and dry condition.	CYP inhibitor
57	1137106831	Sophocarpine	F	8	246.35	Extracted from Sophora flavescens Ait.;Suitability:Methanol,ethanol,chloroform,acetone and benzene;Store the product in sealed,cool and dry condition	Others

58	1137106830	Baicalin	F	9	446.37	Baicalin, one the effective compositions of scutellaria baicalensis, possesses multiple properities such as antioxidant, anti-tumor, anti-HIV, treating cardiovascular disease and so on.	GABAR Agonist
59	1137106829	Sesamin	F	10	354.36	Extracted from Sesamum indicum L.;Suitability:Chloroform,benzene,acetic acid,acetone;Store the product in sealed,cool and dry condition	Others
60	1137106828	Andrographolide	F	11	350.44	Andrographolide(Andrographis) is an irreversible antagonist of NF-κB and prevents in vitro T cell activation; displays antiviral, antiinflammatory, antiapoptotic, and antihyperglycemic properties.	NF-κB inhibitor
61	1137106840	Osthole	G	2	244.29	Osthole(NSC 31868, Osthol), a coumarin-like derivative extracted from Chinese herbs, has been shown to stimulate osteoblast proliferation and differentiation, anti-inflamatory.	Others
62	1137106841	Salidroside	G	3	300.30	Salidroside is a bioactive phenolic glycoside compound isolated from Rhodiola crenulata.	Others
63	1137106842	Rutaecarpine	G	4	287.32	Actions Delayed rectifier K+ channel blocker. Inhibits platelet aggregation; vasoldilator	Others
64	1137106843	Asiatic acid	G	5	488.70	ActionsAsiatic acid is commonly used in wound healing. Asiatic acid has antioxidant,anti-inflammatory and neuroprotective properties.Packaging500 mg in glass bottleApplicationStarting material for asiatic acid derivative synthesis for use as: Anticance	p38 MAPK inhibitor
65	1137106844	Limonin	G	6	470.52	Limonin is a limonoid, and a bitter, white, crystalline substance found in citrus and other plants. It is also known as limonoate D-ring-lactone and limonoic acid di-delta-lactone. Chemically, it is a member of the class of compounds known as furanolactones.	HIV Protease inhibitor
66	1137106845	Caffeic Acid	G	7	180.16	Extracted from Solidago decurrens,large-fruited Chinese hawthorn;Suitability:Hot water and cold ethanol;Store the product in sealed,cool and dry condition	Others
67	1137106846	Phlorizin	G	8	436.42	Phlorizin, a natural product and dietary constituent found in a number of fruit trees, is a 2'-glucoside of phloretin, Phlorizin is a competitive and classic inhibitor of hSGLT1(Ki=300 nM) and hSGLT2(Ki= 39 nM).	Hsglt
68	1137106847	Neohesperidin	G	9	610.56	Flavanone glycoside with antioxidant and neuroprotective properties. Unlike other citrus flavanones,it does not inhibit oral carcinogenesis in a rat model.	Others
69	1137106848	Sodium Danshensu	G	10	220.16	Extracted from Salvia miltiorrhiza Bge.;Suitability:Methanol,water;Store the product in sealed,cool and dry condition	CYP inhibitor
70	1137106849	Tanshinone IIA	G	11	294.35	Tanshinone IIA(Tanshinone B) is the most abundant diterpene quinone in Danshen, Salviae miltiorrhizae Radix, a widely prescribed traditional herbal medicine that is used to treat cardiovascular and inflammatory diseases.	Others
71	1137106861	Puerarin (Kakonein)	H	2	416.38	Puerarin (Kakonein), an isoflavones found in the root of Radix puerariae, is a 5-HT2C receptor and benzodiazepine site antagonist.	5-HT2C receptor antagonist
72	1137106860	Oxymatrine	H	3	264.37	Alkaloid isolated from Sophora flavescens. Antifribotic. Neuroprotective.1 Traditional chinese medicine used in the treatment against hepatitis B virus.2	Autophagy
73	1137106859	Emodin	H	4	270.24	Emodin is a naturally occurring anthraquinone present in the roots and barks of numerous plants; exerts antiproliferative effects in Y cells that are regulated by different signaling pathways.	Dehydrogenase inhibitor

74	1137106858	Baicalein	H	5	270.24	The flavonoid component of Nepalese and Sino-Japanese crude drugs.1,2 Baicalein,a major flavone of Scutellariae baicalensis,inhibits the 12-lipoxygenase (12-LOX) pathway of arachidonic acid metabolism,which inhibits Y cell proliferation and induce	CYP inhibitor
75	1137106857	(+)-Matrine	H	6	248.37	Matrine is an alkaloid found in plants from the Sophora genus. It has a variety of pharmacological effects, including anti-Y effects, and action as a kappa opioid receptor and ?-receptor agonist.	Opioid Receptor agonist
76	1137106856	Palmatine chloride	H	7	387.87	Palmatine chloride an isoquinoline alkaloid, is an important medicinal herbal extract with diverse pharmacological and biological properties.	Others
77	1137106855	Cryptotanshinone	H	8	296.37	Cryptotanshinone is a STAT3 inhibitor with IC50 of 4.6 μM in a cell-free assay, strongly inhibits phosphorylation of STAT3 Tyr705, with a small effect on STAT3 Ser727, but none against STAT1 nor STAT5.	STAT inhibitor
78	1137106854	Nalidixic acid	H	9	232.24	Nalidixic acid is a synthetic 1,8-naphthyridine antimicrobial agent with a limited bacteriocidal spectrum.	Topoisomerase inhibitor
79	1137106853	Rutin	H	10	610.52	Rutin, a flavonol glycoside found in many plants including buckwheat; tobacco; forsythia; hydrangea; viola, etc., which possesses healthy effects for human.	AKR
80	1137106852	L(-)-Carnitine	H	11	161.20	L-carnitine is constituent of striated muscle and liver. It is used therapeutically to stimulate gastric and pancreatic secretions and in the treatment of hyperlipoproteinemias.	Fatty acid carrier
81	1137105805	Quercetin	A	2	302.24	Quercetin, a natural flavonoid present in vegetables, fruit and wine, is a stimulator of recombinant SIRT1 and also a PI3K inhibitor with IC50 of 2.4-5.4 μM. Phase 4.	Sirtuin inhibitor
82	1137105806	Cyclosporin A	A	3	1202.64	Cyclosporin A is an immunosuppressive agent, binds to the cyclophilin and then inhibits calcineurin with IC50 of 7 nM, widely used in organ transplantation to prevent rejection.	Others
83	1137105807	4-Methylumbelliferone (4-MU)	A	4	176.17	A coumarin derivative possessing properties as a spasmolytic, choleretic and light-protective agent. It is also used in ANALYTICAL CHEMISTRY TECHNIQUES for the determination of NITRIC ACID.	HAS inhibitor
84	1137105808	Diosmetin	A	5	300.26	Diosmetin is an O-methylated flavone, a chemical compound that can be found in the Caucasian vetch[1] It has been found to act as a weak TrkB receptor agonist.	Trk receptor agonist
85	1137105809	Kinetin	A	6	215.21	Kinetin is a type of cytokinin, a class of plant hormone that promotes cell division.	Others
86	1137105810	Apigenin	A	7	270.24	Apigenin is a potent P450 inhibitor for CYP2C9 with Ki of 2 μM.	CYP inhibitor
87	1137105811	Aloin	A	8	418.39	Aloin, a natural anthracycline from Aloe vera, is a tyrosinase inhibitor	tyrosinase inhibitor
88	1137105812	Laetrile	A	9	457.43	Laetrile is a glycoside initially isolated from the seeds of the tree Prunus dulcis, also known as bitter almonds.	Others
89	1137105813	Indole-3-carbinol	A	10	147.17	Indole-3-Carbinol is a naturally occurring, orally available cleavage product of the glucosinolate glucobrassicanin, a natural compound present in a wide variety of plant food substances including members of the family Cruciferae with antioxidant and potential chemopreventive properties.	NF-κB inhibitor; p53 activator

90	1137105814	Chrysin	A	11	254.24	Chrysin is a naturally occurring flavone chemically extracted from the blue passion flower (Passiflora caerulea).	Others
91	1137105825	Cyclocytidine hydrochloride	B	2	261.66	Cyclocytidine is the prodrug of cytarabine, which is a pyrimidine nucleoside analog that inhibits the DNA synthesis and used mainly in the treatment of leukemia.	DNA/RNA Synthesis inhibitor
92	1137105824	Silibinin	B	3	482.44	Silibinin, the main flavonoid extracted from the milk thistle Silybum marianum, displays hepatoprotective properties in acute and chronic liver injury.	Others
93	1137096174	Hematoxylin	B	4	302.28	Hematoxylin is a natural product.	Others
94	1137105823	Vinblastine sulfate	B	5	909.06	Vinblastine sulfate can inhibit the formation of microtubule, it also inhibit nAChR(IC50=8.9 uM).	Microtubule Associated inhibitor; MRP inhibitor
95	1137105822	Taxifolin (Dihydroquercetin)	B	6	304.25	Taxifolin is a flavonoid in many plants such as Taxus chinensis, Siberian larch, Cedrus deodara and so on.	Adrenergic Receptor antagonist; NGF inhibitor; TNF-alpha inhibitor
96	1137105821	Kaempferol	B	7	286.23	Kaempferol is a natural flavonol, a type of flavonoid, that has been isolated from plant sources	Others
97	1137105820	(-)-Epigallocatechin Gallate	B	8	458.38	Epigallocatechol Gallate(EGCG) is an antioxidant polyphenol flavonoid that inhibits telomerase and DNA methyltransferase. EGCG blocks the activation of EGF receptors and HER-2 receptors.	telomerase; DNA methyltransferase inhibitor
98	1137105819	Daphnetin	B	9	178.14	Daphnetin, a natural coumarin derivative, is a protein kinase inhibitor, inhibits EGFR, PKA and PKC with IC50 of 7.67 μM, 9.33 μM and 25.01 μM, respectively, also known to exhibit anti-inflammatory and anti-oxidant activities.	EGFR inhibitor; PKC inhibitor
99	1137105818	Schizandrin B	B	10	400.46	Schisandrin B(Wuweizisu-B) is a dibenzocyclooctadiene derivative isolated from Fructus Schisandrae, has been shown to produce antioxidant effect on rodent liver and heart.	ATM/ATR inhibitor
100	1137105817	Icariin	B	11	676.68	Icariin(Ileariline) is a major constituent of flavonoids from the Chinese medicinal herb Epimedium brevicornum; exhibits multiple biological properties, including anti-inflammatory, neuroregulatory and neuroprotective activities.	PDE inhibitor
101	1137105828	Chlorogenic Acid	C	2	354.32	Chlorogenic acid(NSC-407296; 3-O-Caffeoylquinic acid) is one of the most abundant polyphenols in the human diet, has been reported to inhibit Y cell growth and a major anti-inflammatory constituent of lonicerae flos extract.	Others
102	1137105829	Curcumol	C	3	236.35	Curcumol is a pure monomer isolated from Rhizoma Curcumaeis with antitumor activities. Extracted from Curcuma zedoaria(Berg.)Rose;Store the product in sealed,cool and dry condition	JAK inhibitor
103	1137105830	Nobiletin	C	4	402.40	Nobiletin is an inhibitor of ERK with in a concentration-dependent manner .	MMP inhibitor
104	1137105831	Triptolide (PG490)	C	5	360.40	Triptolide is a diterpene triepoxide, immunosuppresive agent extracted from the Chinese herb Tripterygium wilfordii.	Others
105	1137105832	Tetrahydropapaverine hydrochloride	C	6	379.88	Tetrahydropapaverine, one of the TIQs and an analogue of salsolinol and tetrahydropapaveroline, has been reported to have neurotoxic effects on dopamine neurons.	Hydroxylase inhibitor

106	1137105833	Silymarin	C	7	482.44	Silymarin (Silybin B), a polyphenolic flavonoid extracted from the seeds of Silybum marianum or milk thistle, is used in the prevention and treatment of liver diseases and primary liver Y.	Others
107	1137105834	Synephrine	C	8	167.21	Sympathetic alpha-adrenergic agonist with actions like PHENYLEPHRINE. It is used as a vasoconstrictor in circulatory failure, asthma, nasal congestion, and glaucoma.	Adrenergic Receptor antagonist
108	1137105835	Rubescensin A	C	9	364.44	Oridonin has potent anti-tumor activity. Oridonin targets AE (AML1-ETO) oncoprotein. Exposure to oridonin induces apoptosis in AE-bearing leukemic cells through the activation of intrinsic apoptotic pathway and triggering a caspase-3-mediated degradation	Others
109	1137105836	Tangeretin	C	10	372.38	Tangeretin, a flavonoid from citrus fruit peels, has been proven to play an important role in anti-inflammatory responses and neuroprotective effects in several disease models, and was also selected as a Notch-1 inhibitor.	Notch-1 inhibitor
110	1137105837	Bilobalide	C	11	326.30	Bilobalide, a bioactive from Gingko biloba,is active on hypoxia induced alterations	Others
111	1137105849	Acetovanillone	D	2	166.17	Apocynin is a selective NADPH-oxidase inhibitor with IC50 of 10 μM.	Others
112	1137105848	ALPHA-BOSWELLIC ACID	D	3	456.70	Boswellic acidsare a series of pentacyclictriterpenemolecules that are produced by plants in the genusBoswellia.	Others
113	1137105847	Vanillin	D	4	152.15	Vanillin is mainly used as a flavouring agent, primarily in foods and beverages such as chocolate and dairy products, but also to mask unpleasant tastes in medicines or livestock fodder. It is also an intermediate in the manufacture of certain pharmaceuticals and agrochemicals. - See more at: http://www.evolva.com/vanillin/#sthash.JhsWbxT7.dpuf	Others
114	1137105846	Parthenolide	D	5	248.32	(-)-Parthenolide is a sesquiterpene lactone which occurs naturally in the plant feverfew(Tanacetum parthenium) and also promotes the ubiquitination of MDM2 and activates p53 cellular functions.	E3 Ligase activator
115	1137105845	Sophoridine	D	6	248.36	Sophoridine, a natural antiY drug, has been used in China for decades. A series of novel N-substituted sophoridinic acid derivatives were synthesized and evaluated for their cytotoxicity with 1 as the lead. The structure-activity relationship indicated that introduction of an aliphatic acyl on the nitrogen atom might significantly enhance the antiY activity. Among the compounds, 6b bearing bromoacetyl side-chain afforded a potential effect against four human tumor cell lines (liver, colon, breast, and lung). The mechanism of action of 6b is to inhibit the activity of DNA topoisomerase I, followed by the S-phase arrest and then cause apoptotic cell death, similar to that of its parent 1. We consider 6b promising for further antiY investigation.	DNA topoisomerase I inhibitor
116	1137105844	Arteether	D	7	312.4	Arteether, a new antimalarial drug	CXCL; CCL inhibitor
117	1137105843	Dioscin	D	8	869.04	Dioscin is a saponin extracted and isolated from Polygonatum Zanlanscianense Pamp, showing antitumor activities.	Others

118	1137105842	Wogonoside	D	9	460.39	Wogonoside acts as a positive allosteric modulator of the benzodiazepine siteof the GABAA receptor.	GABAA
119	1137105841	Scutellarein	D	10	286.24	Scutellarein Reduces Inflammatory Responses by Inhibiting Src Kinase Activity	Src inhibitor
120	1137105840	Isosteviol	D	11	318.45	Stevioside, a common natural sweetener, belongs to tetracyclic diterpene glycosides. The pharmacology researches have suggested that stevioside and its hydrolysis products, steviol, isosteviol and steviolbioside, have many biological activities, such as reducing blood glucose, lowering blood pressure, anti-inflammation, anti-tumor, anti-diarrhea, antibacterium, immunoregulation, etc	NF-κB; TNF-α; IL-6; COX-2; Potassium Channel inhibitor
121	1137105852	Elemicin	E	2	208.25	Elemicin is a constituent of several plant species' essential oils. It has anticholinergic effects in humans	5-HT2A agonist
122	1137105853	Xanthohumol	E	3	354.40	Xanthohumol, a prenylated chalcone from hop, inhibits COX-1 and COX-2 activity and shows chemopreventive effects. Phase 1. It has been showed the properties of antioxidation, anti-Y and anti-virus	COX inhibitor
123	1137105854	Licochalcone A	E	4	338.40	Licochalcone A exhibits potent antimalarial activity via and might be developed into a new antimalarial drug. Licochalcone A had anti-tumor activity in all cell lines tested and enhanced the effect of paclitaxel and vinblastine chemotherapy. Licochalcone A induced apoptosis in MCF-7 and HL-60 cell lines, as demonstrated by cleavage of PARP, the substrate of ICE-like proteases. Licochalcone A exhibits a strong antileishmanial activity ,that appropriate substituted chalcones might be a new class of antileishmanial drugs.	caspase
124	1137105855	Cinobufagin	E	5	442.55	Cinobufagin is a specific Na+/K+-ATPase inhibitor. About as active as ouabain.	ATPase inhibitor
125	1137105856	Demethylzeylasteral	E	6	480.59	Demethylzeylasteral has strong immunosuppressive activity, can be used in the fields of organ transplantation and autoimmune disorders. The risk of elevated serum concentrations of estradiol due to the inhibition of estradiol glucuronidation by Demethylzeylasteral. Demethylzeylasteral increases both activation and inactivation time constants of Ca(2+) currents, can inhibit significantly the sperm acrosome reaction initiated by progesterone.	UGT inhibitor
126	1137105857	Baohuoside I	E	7	514.52	Baohuoside I exhibits anti-inflammatory activity and anti-osteoporosis activities. Baohuoside I exerts its antimetastatic effect through the downregulation of CXCR4 expression . Baohuoside I has anti-Y activity, used for a variety of Ys in vitro ,by inhibiting tumor growth and inducing apoptosis by inhibiting β-catenin-dependent signaling pathways.	CXCR inhibitor
127	1137105858	Syringin	E	8	372.40	Syringin has antitumour, antiproliferative, immunomodulatory and platelet aggregation inhibiting effects. Syringin can prevent Abeta(25-35)-induced neuronal cell damage. It has anti-inflammatory and antinociceptive effects, may be attributed to its in vivo transformation to sinapyl alcohol.	NOS inhibitor

128	1137105859	Icaritin	E	9	368.38	Icaritin has hormone regulation activity and cardiovascular function improvement activity. Icaritin has antiY activity, can induce S phase arrest and apoptosis, inhibit ENKL cell proliferation. Icaritin has anti-multiple myeloma activity, mainly mediated by inhibiting IL-6/JAK2/STAT3 signaling. Icaritin at low concentration (4 or 8 μmol/L) can promote rat chondrocyte proliferation and inhibit cell apoptosis, while the effect of Icaritin on rat chondrocyte at high concentration was reversed.	JAK; STAT inhibitor
129	1137105860	Homoharringtonine	E	10	545.61	Homoharringtonine is an alkaloid inhibitor of protein synthesis with activity in myeloid malignancies. It might have clinical activity in some patients with myelodysplastic syndrome . Homoharringtonine enhances the paracellular permeability of Caco-2 cell monolayers by modulating the protein expression and localization of claudin isoforms. Homoharringtonine has anti-Y and antileukemic activities, may have the potential ability to treat acute, chronic myeloid leukaemia and Gefitinib-resistant NSCLC.	STAT inhibitor
130	1137105861	Polydatin	E	11	390.39	Polydatin is the glycoside of Resveratrol (sc-200808) originally isolated from the Chinese herb Polygonum cuspidatum. The compound has been shown to inhibit platelet aggregation and elevate the ratios of LDL-C/HDL-C and TC/HDL-C. Myocardial cell, white blood cell, vascular smooth muscle cell, and endothelial cell studies report that Polydatin can inhibit ICAM-1 expression, elevate Ca2+, weaken white blood cell-endothelial cell adhesion, and activate KATP channels.	ICAM-1 inhibitor
131	1137105873	Chelerythrine chloride	F	2	383.83	Cell-permeable inhibitor of protein kinase C (IC50 = 660 nM); competitive with respect to the phosphate acceptor and non-competitive with respect to ATP. Has a wide range of biological activities, including antiplatelet, anti-inflammatory, antibacterial and antitumor effects. Activates MAPK pathways, independent of PKC inhibition. Inhibits binding of BclXL to Bak (IC50 = 1.5 μM) or Bad proteins and stimulates apoptosis.	PKC inhibitor
132	1137105872	Quercetin Dihydrate	F	3	338.27	Quercetin, a polyphenolic flavonoid found in a wide variety of plant-based foods, such as apples, onions, berries, and red wine, is utilized in many different cultures for their nervous system and antiY effects.	Others
133	1137105871	Aloperine	F	4	232.36	Aloperine is an isolated alkaloid in sophora plants such as Sophora alopecuroides L, and exhibits anti-inflammatory, antibacterial, antiviral, and anti-tumor properties.	Others
134	1137105872	Juglone(5-hydroxy1,4-naphthoquinone	F	5	174.17	Juglone is a natural naphthoquinone found in the black walnut (J. nigra) and other plants in the Juglandaceae family. Juglone also irreversibly inhibits peptidyl-prolyl cis/trans isomerases of the parvulin family, including human Pin1, yeast Ess1/Ptf1, and E. coli parvulin (Ki = 55.9 nM). Juglone also blocks transcription by RNA polymerases I, II, and III (IC50s = 2-7 μM) and attenuates kidney fibrosis in rats treated with unilateral ureteral obstruction, both through Pin1-independent mechanisms.	Pin1 inhibitor